8-2018

Scattering of Few Photon Fields by Two Level Systems in a One Dimensional Geometry

William Konyk
University of Arkansas, Fayetteville

Scattering of Few Photon Fields by Two Level Systems in a One Dimensional Geometry

A dissertation submitted in partial fulfillment
of the requirements for the degree of
Doctor of Philosophy in Physics

by

William Konyk
Miami University
Bachelor of Science in Physics, 2009

August 2018
University of Arkansas

This dissertation is approved for recommendation to the Graduate Council.

Julio Gea-Banacloche Ph.D.
Dissertation Director

Reeta Vyas Ph.D.
Committee Member

Surendra Singh Ph.D.
Committee Member

Abstract

Recent experimental progress has realized strong, efficient coupling of effective two level systems to waveguides. We study the scattering of multimode photons from such emitters coupled losslessly to the confined geometry of a one dimensional waveguide. We develop novel techniques for describing the scattered state of both single and multi-photon wavepackets and explore how such wavepackets interact with arrays of emitters coupled to a one dimensional waveguide. Finally, we apply these techniques and analyze the capability of two particular systems to act as a quantum conditional logic gate.

Acknowledgements

First, I thank Julio Gea-Banacloche, my advisor, for his support, encouragement, and guidance. I am grateful that he was willing, while department chair, to take on the responsibility of training yet another student. Despite the many demands on his time, he always found some to discuss problems, regardless of the topic. I am indebted to his insight, ability to spot errors, and willingness to share his expertise. Without the first, this whole work may not have been possible, as it was his idea to formalize the time domain approach in the first place. Without the second, it would have taken much longer to troubleshoot my analyses. And without the third, I would not have grown as an individual and learned how to think and confidently approach problems like a physicist.

I thank my committee members Reeta Vyas and Surendra Singh and my advisory committee members Min Xiao, Salvador Barraza-Lopez, and Fisher Yu for their comments, feedback, and support through the years. This project is much better because of the questions they asked and the perspective they provided. I also am grateful to the physics department for providing space to work, study, and learn, and for all the help in navigating the bureaucracy of higher education. I thank my friends and fellow students for their support and camaraderie, and especially appreciate my friend Luke, who lent me his computer so that I could graduate on time.

I am grateful for everyone who encouraged me to pursue physics; my mom, who raised me to value education, hard work, and to follow my passions; my dad, who encouraged me to pursue a STEM field and provided support through school; John Gill, for creating a strong foundation of physics in high school; and Perry Rice, for getting me hooked on quantum optics and inspiring me to pursue this degree.

Finally, I am beholden to my wife; she supported me while I worked odd hours, was at school late to grade exams, and patiently listened when I described my research, regardless of whether I made sense. Without her support, encouragement, and understanding this would have been a much more difficult, and less rewarding, undertaking.

Forward

Before tackling the topic at hand, there are a few notes I would like to make. Throughout this document I will write in first person plural. That is, I will use the pronouns of 'we' and 'our'. This choice was made for several reasons. In science, one never works alone. The entire body of my work is predicated on basic quantum theory, electromagnetic theory, and information theory, not to mention the works actually cited in this tome; as such, in physics we often use first person plural even when publishing works with a single author. Additionally, this is written to bring you, the reader, along a logical journey through a complex topic. Finally, and perhaps most importantly, the work presented here is not mine alone; the impetus, and many ideas and solutions come from the mind of Julio Gea-Banacloche. To claim that this was all my own idea, or that I could have accomplished any of this without his help, support, and counsel would be disingenuous.

In all the analysis presented here I used python and mathematica to solve systems of equations, simplify expressions, and create plots. Specifically, in solving large systems of equations with non-commuting operators I used the NCAlgebra package for Mathematica found at https://github.com/NCAlgebra/NC. On the python front, I used the typical combination of numpy and Matplotlib for numerical computations and plotting, but also took advantage of the mpmath package to add arbitrary precision floating point operations and the pp package for parallelizing code. This document was written in LaTeX using ShareLaTeX, and was organized using the subfile package.

Contents

Chapter 1

Background and Motivation

1.1 Motivation and experimental progress

Light-matter interactions are of fundamental interest, as this sub-field of physics contains many interesting phenomena and underlies much of the technology that enables rapid, long-distance communication. At one time, strong light-matter coupling was primarily achieved through cavity quantum electrodynamics. In recent years, however, there has been an extraordinary amount of experimental progress made in controlling and confining single photons within waveguides and other one-dimensional structures. Various media have been used to accomplish this task, including nanowires [1], photonic crystals [2], and microwave waveguides. Additionally, aside from strongly coupling two level systems to guided modes (with some strengths reaching the regime where a Jaynes-Cummings Hamiltonian no longer applies [3]), high coupling efficiencies between the quantum systems and the guided modes have been achieved in excess of 90% [4].

The highly confining geometry of the waveguide combined with strong, controllable interactions between light and matter immediately suggests that such systems present a rich opportunity to explore new nonclassical effects and build useful devices for quantum information processing tasks. Both of these factors motivate the work presented here. We will develop novel methods of approaching both the single and multi-photon scattering problems to better understand and describe how photons interact with matter at the fundamental level. Additionally, we will analyze how to use this interaction to construct a quantum logical conditional phase (CPHASE) gate between two photons, where the presence of a control photon imparts a phase of π on a target photon.

This is by no means the first work to study the scattering of photons from emitters in one-dimensional geometries. Much of the earliest work was done by Shen and Fan using a scattering matrix formalism [5]. Their approach involves calculating the scattering

eigenstates of the Hamiltonian and has been successful in describing the scattering of single photons from a number of scatterers [6] and two photons from two scatterers [7]. Other authors have used a Lippmann-Schwinger formalism that amounts to finding the poles of a Green's function, each of which constitutes a particular path a photon can take [8]. Still others have approached the few-photon scattering problem from the perspective of counting all possible events and have developed diagrammatic approaches [9, 10]. Finally, the authors of [11] derived (concurrently to our work in [12]) the scattering of N photons from a single two level emitter (TLE) using a physical, time-domain approach. This last solution appears to provide identical results and scalability to our technique presented later in Chapter 3.

In this text we will primarily be concerned with describing the final, scattered state of the photons after they interact with an array of effective two level systems. In considering this, we are ignoring the rich entanglement that can arise between multiple atoms as a result of the absorption and re-emission of photons. Such entanglement has been considered in [13, 14], and much of the work by Baranger's group (see [15]) explores photon statistics as a function of time. The reason for ignoring such behavior is that we are, ultimately, looking to analyze the system's potential for functioning as a quantum logic gate. In such a context, two photons will interact with some sort of quantized system and leave to interfere with other photons at a later time in the computation. Thus, the behavior of the system itself only matters insofar as it modifies the properties of the two photons in the long time (scattering) limit.

We note that we will often use the term "atomic" to describe the system that the photons interact with. We use this term out of convenience rather than necessity, as our results are valid for any two level system that can be accurately described by a Jaynes-Cummings Hamiltonian [16, 17]. Such a system could certainly consist of trapped ions or cold atoms near a waveguide. It could also be accomplished by using superconducting circuits, quantum dots, ring resonators, nitrogen vacancy centers in

diamond, or anything else that has an effective two level structure. We will similarly treat the term 'waveguide' loosely. As mentioned above, there are many techniques used for confining light propagation to one dimension. When we refer to a waveguide, we are considering any system in which photons are constrained such that they can only propagate in one dimension.

Finally, one of the most important aspects of this work is its treatment of photons as wavepackets. Much of the research in quantum optics deals with single-mode photons, i.e. photons defined by only one frequency. This idealized version of a photon can be very useful and provide insight into many physical systems. It does not, however, describe realistic photon sources, as a single photon will have a finite duration and uncertainty in its frequency. These characteristics become especially important when considering photons as carriers of quantum information. When a photon interacts with an atomic system the frequency distribution comprising what we call the photon changes. If this change is significant enough, when it moves on to another step in the computation and interferes with a second photon they may not accurately perform the desired quantum information task. Additionally, when multiple photons interact simultaneously with an atomic system their wavefunctions can become highly entangled. Adding in this consideration has led to the failure of certain proposals to build quantum logic gates (see [18] and [19]). Ultimately this fact motivates the work here, as in Chapter 6 we will consider a system that passively and deterministically acts as a CPHASE gate between two photons after accounting for the effect of spectral entanglement.

1.2 Theoretical assumptions and general formalism

1.2.1 Field modes

All calculations that follow will make some basic assumptions about the systems in question and the quantization of the electromagnetic fields. We will not present a rigorous derivation of quantizing the electromagnetic field in general, leaving it to books, such as

[17] to describe the process. We will, however, provide some background on how to formally quantize the field in Appendix B, and we note a recent, interesting approach to quantization in [20] that essentially posits the existence of traveling photon modes from experimental results. Regardless of how the field is quantized, we will assume all photons are confined to move in one dimension within a waveguide and that this field can be accurately described by left and right traveling field modes.

The positive component of the electric field in the waveguide will have the form

$$E_a^{(+)}(t,z) = \sqrt{\frac{\hbar\omega_F}{2\epsilon_0}} \int d\omega e^{-i(\omega_F+\omega)t+i(k_F+\omega/c)z}\hat{a}_\omega$$
$$E_b^{(+)}(t,z) = \sqrt{\frac{\hbar\omega_F}{2\epsilon_0}} \int d\omega e^{-i(\omega_F+\omega)t-i(k_F+\omega/c)z}\hat{b}_\omega \tag{1.1}$$

where $\hat{a}_\omega$ and $\hat{b}_\omega$ are the annihilation operators for to photons travelling to the right (corresponding to spatial dependence $e^{i\omega z/c}$) or to the left (corresponding to spatial dependence $e^{-i\omega z/c}$) respectively. Frequencies are measured relative to ω_F, the central frequency of the incoming photon wavepacket. ω is the deviation from this frequency so that at $\omega = 0$ the field has the frequency of ω_F. Following the lead of other authors, we are also assuming that the bandwidth of the wavepacket is sufficiently narrow so that there is no dispersion in the waveguide, that is $\omega_F = ck_f$ for all frequencies. As usual, c represents the phase velocity of the photons in the waveguide and, with the aforementioned assumption, will be equal to the group velocity. We will also assume that all systems are lossless, that is all photons remain in the waveguide and all atoms emit only into the guided photon modes. The photon annihilation operators $\hat{a}_\omega$ and $\hat{b}_\omega$ have commutation relationships

$$[\hat{a}_\omega, \hat{a}^\dagger_{\omega'}] = [\hat{b}_\omega, \hat{b}^\dagger_{\omega'}] = \delta(\omega-\omega') \qquad [\hat{a}_\omega, \hat{b}^\dagger_{\omega'}] = [\hat{b}_\omega, \hat{a}^\dagger_{\omega'}] = [\hat{a}_\omega, \hat{b}_{\omega'}] = 0 \tag{1.2}$$

As mentioned in the preceding section, we will be treating the photons as wavepackets.

In the frequency basis a single photon is described by

$$|\psi\rangle = \int_{-\infty}^{\infty} d\omega \tilde{f}(\omega)\hat{a}_{\omega}^{\dagger}|0\rangle \tag{1.3}$$

Here the function $\tilde{f}(\omega)$ represents the frequency distribution of the photon pulse. Note that the limits of integration run from $-\infty$ to ∞: we are extending the lower limit from $-\omega_F$ to $-\infty$ for mathematical convenience. Such an approximation is well justified because we have assumed that the photons have a fairly narrow frequency spectrum. Combined with the fact that they must exist somewhere, that is $\int d\omega|\tilde{f}(\omega)|^2 = 1$, the probability of finding the frequency far from ω_F (corresponding to a large $\pm|\omega|$) is vanishingly small, allowing the extension of the limit of integration from $-\omega_F$ to $-\infty$. Additionally, while this state is fundamentally a linear superposition of an infinite number of possible frequencies, we will still describe it as a single photon due to the fact that one can construct a detector to register a single click for this wavefunction.

With this description of a photon wavepacket, a two-photon state is given by

$$|\psi\rangle = \frac{1}{\sqrt{2}} \int d\omega_1 d\omega_2 \tilde{f}(\omega_1, \omega_2)\hat{a}_{\omega_1}^{\dagger}\hat{a}_{\omega_2}^{\dagger}|0\rangle \qquad |\psi\rangle = \int d\omega_1 d\omega_2 \tilde{f}(\omega_1, \omega_2)\hat{a}_{\omega_1}^{\dagger}\hat{b}_{\omega_2}^{\dagger}|0\rangle \tag{1.4}$$

Note that there is a coefficient of $\frac{1}{\sqrt{2}}$ in front of the state containing two photons in the same mode. This is a normalization factor that arises from the action of the photon operators. Here the function $\tilde{f}(\omega_1, \omega_2)$ describes the frequency spectrum of the wave packet just as in the single photon case.

Throughout this paper we will also refer to a second set of photon modes, the standing wave modes. These are superpositions of the travelling photon operators and are given by

$$\hat{c}_{\omega} = \frac{\hat{a}_{\omega} + \hat{b}_{\omega}}{\sqrt{2}} \qquad\qquad \hat{d}_{\omega} = \frac{\hat{a}_{\omega} - \hat{b}_{\omega}}{\sqrt{2}} \tag{1.5}$$

Aside from being a second mathematically convenient, orthogonal basis of photon modes, these can also be directly excited by using a beamsplitter to transform traveling wave modes into standing wave modes. An arrangement of such a setup is shown in Fig. 1.1. Here an incoming travelling wave mode given by $\hat{c}_{in}$ is transformed by the beamsplitter

into the superposition of $(\hat{a}+\hat{b})/\sqrt{2}$. When the travelling wave modes $\hat{a}$ and $\hat{b}$ arrive back at the beamsplitter, they are transformed into $\hat{c}_{out} = (a+b)/\sqrt{2}$. This is in the same mode as $\hat{c}_{in}$ but is travelling in the opposite direction. A similar transformation occurs for a photon in the $\hat{d}_{in}$ mode, but, due to a phase difference imparted by the beamsplitter, photons in this mode will acquire a phase of π. Thus we have that $\hat{d}_{in} = -\hat{d}_{out}$.

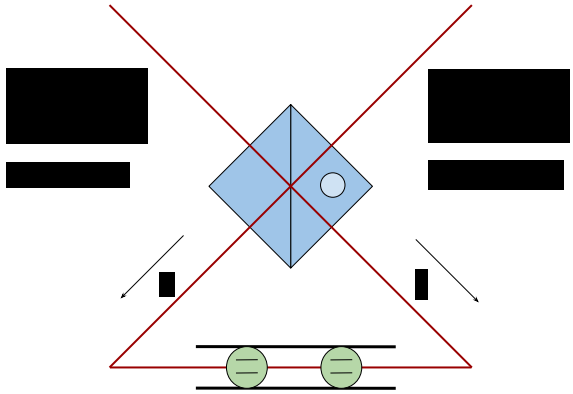

Figure 1.1: A diagram showing how to excite the standing-wave modes in a waveguide. Incoming travelling waves in the $\hat{c}$ and $\hat{d}$ modes are converted by the beamsplitter into standing waves given by the operators $(\hat{a}+\hat{b})/\sqrt{2}$ and $(\hat{a}-\hat{b})/\sqrt{2}$, respectively. In the absence of any scatterers in the waveguide, each incoming mode will leave in the same port of the beamsplitter it entered, with an overall phase difference of π between them.

Finally, we will often refer to waveguides that are 'unidirectional.' This means that the atom only interacts with one set of travelling modes and, as a result, photons will only propagate in one direction. Such a feat can be accomplished in several ways. One is to add a mirror at one end of a waveguide, place the atom very close to the mirror, and use nonreciprocal elements to separate the incoming and outgoing photons. The mirror ensures that all light leaves in the same way it entered, and if the atom is placed close to the mirror, and at an integer number of wavelengths away, it will couple strongly to the field. We have explored the field modes of this realization of a unidirectional waveguide in the appendix of [12]. Another way is to create a system in which scatterers couple asymmetrically to waveguide modes so that photons are only able to travel in one direction. An example of this has been studied in [21], where atoms will emit photons of different polarizations in

different directions. Finally, using the standing wave modes and beamsplitter arrangement in Fig. 1.1 along with a nonreciprocal element to separate incoming and outgoing photons also allows one to create an effective unidirectional waveguide. This is because an atom placed correctly in the waveguide will only interact with the $\hat{c}$ or $\hat{d}$ modes and the photon will always leave the beamsplitter in the same port it entered.

The opposite of this is a bidirectional waveguide, which is a structure that does not preferentially favor propagation in one direction or another and in which the scatterers couple equally to both left- and right-travelling photon modes. Most of the work presented here will focus on bidirectional waveguides, as they are far easier to construct.

1.2.2 Two level systems

The Hamiltonian for a single two level system interacting with the quantized waveguide modes (in a suitable interaction picture) can be given by Eq. 1.6. This is a typical Jaynes-Cummings interaction modified to account for the multimode nature of the incoming photons.

$$H_I = \hbar g\left[e^{ik_F z_j}\hat{A}(t - z_j/c) + e^{-ik_F z_j}\hat{B}(t + z_j/c)\right]e^{-i\delta t}\sigma_j^\dagger + H.c. \tag{1.6}$$

Here $\delta = \omega_F - \omega_A$ is the difference between the central frequency of the incoming pulse and the atom's transition frequency, z_j is the location of the atom along the waveguide, $\sigma_j^\dagger = |e\rangle_j\langle g|$ represent the raising operator for the j^{th} atom, and g is the coupling strength between the atoms and the field. We are making the Wigner-Weisskopf approximation by assuming that the photons are spectrally narrow enough that the coupling is proportional to $\sqrt{\omega_A}$ rather than $\sqrt{\omega_A + \omega}$ and thus is constant.

For compactness, we have introduced the field operators

$$\hat{A}(t) = \frac{1}{\sqrt{2\pi}}\int d\omega e^{-i\omega t}\hat{a}_\omega \qquad\qquad \hat{B}(t) = \frac{1}{\sqrt{2\pi}}\int d\omega e^{-i\omega t}\hat{b}_\omega \tag{1.7}$$

which satisfy commutation relations $[\hat{A}(t), \hat{A}^\dagger(t')] = \delta(t - t')$ and $[\hat{B}(t), \hat{B}^\dagger(t')] = \delta(t - t')$.

Additionally, as $\hat{A}$ and $\hat{B}$ represent different right-travelling and left-travelling photons respectively they commute with one another.

One point to note is that, technically, this Hamiltonian represents an atom with an infinite bandwidth. It has the same coupling for all input photons fields regardless of whether they are on resonance or not. In our treatment, the bandwidth is enforced by the finite width of the photon wavepackets seen in Eq. 1.3 and 1.4, as we will use functions that are normalized to one and that decay sufficiently fast so that only frequencies close to resonance will contribute to the overall solution.

Finally, while we will ultimately be concerned with describing only the state of the photons in the long time limit, while obtaining solutions we will be working with the atomic basis as well. As a result, we will be writing the total state of the atom-photon system in terms of products of the form of Eq. 1.8, presented for a single photon and multiple atoms.

$$|\psi(t)\rangle = |\psi_g(t)\rangle \otimes |G\rangle + \sum_{j=1}^{N} |\psi_j(t)\rangle \otimes |j\rangle \tag{1.8}$$

The state $|G\rangle = |g\rangle \otimes |g\rangle \ldots \otimes |g\rangle$, is a tensor product of each atom being in the ground state. Similarly, the state $|j\rangle = |g\rangle \otimes \ldots |e\rangle \ldots \otimes |g\rangle$ is a tensor product of the states of all atoms being in the ground state and the jth atom being in the excited state. Each of these states is associated with a corresponding photon wavefunction $|\psi_j(t)\rangle$ which, for a system containing only one quantum of energy, can be written as

$$|\psi_g(t)\rangle = \int d\omega \Big(f_a(t,\omega)\hat{a}_\omega + f_b(t,\omega)\hat{b}_\omega \Big)|0\rangle \qquad\qquad |\psi_j(t)\rangle = f_j(t)|0\rangle \tag{1.9}$$

where the state may have photons in both the $\hat{a}$ and $\hat{b}$ modes. Ultimately it is these functions, and particularly the function corresponding to the ground state of the atomic system, that will describe the scattered state of an incoming photon wavepacket.

1.3 Conditional quantum logic

In Chapters 2-5 we will develop and analyze photon scattering from two level systems coupled losslessly to a 1-D waveguide. In Chapter 6 we will use the results to analyze how one may use an array of atoms coupled to a waveguide to construct a quantum logic gate. Quantum logic opens up new possibilities; the ability to perform logical operations on superpositions of states, in principle, enables massive parallelization of computational tasks. Additionally, the logic present in quantum mechanics allows for certain algorithms to scale more efficiently than on a classical computer. These benefits have been practically challenging to achieve, however, as measurement of the output provides only probabilistic information about the final state of the computation. Quantum systems are incredibly sensitive to noise, and quantum computation typically requires pure quantum systems in which the experimenter has the maximum information allowed about the system. (See [22] and [23] for more on quantum computation and quantum information). In order to address the sensitivity issue, photons have been considered as carriers of quantum information. They can preserve their quantum state over large distances as they can be confined to materials where they interact weakly with their environment. Moreover, systems with strong light-matter coupling at the single photon level have been experimentally realized. This controllable interaction, along with the small timescale of photon processes, provides an ideal medium for quantum information processing (QIP).

The challenge associated with using photons for QIP lies in engineering a robust way for them to interact with one another. This is necessary for universal quantum computation, which requires a set of single photon operations and at least one conditional logic gate. The transformation we will be interested in is a conditional phase (or CPHASE)

gate. In terms of logical quantum states, this transformation is given by

$$\begin{aligned}
|0\rangle \otimes |0\rangle &\rightarrow |0\rangle \otimes |0\rangle \\
|1\rangle \otimes |0\rangle &\rightarrow e^{i\phi_1}|1\rangle \otimes |0\rangle \\
|0\rangle \otimes |1\rangle &\rightarrow e^{i\phi_1}|0\rangle \otimes |1\rangle \\
|1\rangle \otimes |1\rangle &\rightarrow e^{i\phi_2}|1\rangle \otimes |1\rangle
\end{aligned} \tag{1.10}$$

where the state $|1\rangle \otimes |0\rangle$ represents a two qubit state with one qubit (carrier of quantum information) in the $|1\rangle$ and the other in the $|0\rangle$ state. An ideal CPHASE gate will impart a conditional phase of π only when there are two photons present, given by $\phi_2 - 2\phi_1 = \pi$, though in principle any phase difference between ϕ_1 and ϕ_2 would enable universal quantum computation with photonic qubits. Such an operation requires nonlinear photon-photon interactions; a linear process will simply give $\phi_2 = 2\phi_1$, leading to no useful phase shift for computation.

Many methods have been proposed to achieve this operation between photons. Some, such as [24–26], use active elements or atomic systems controlled by classical fields to construct a CPHASE gate. This has the downside of being difficult to scale to large numbers of gates, as each gate requires a significant amount of resources to construct. Others, like that presented in [27], use only linear optics combined with destructive measurements and post-selection of certain events. The issue with this approach is that it successfully performs the desired operation in a probabilistic manner, requiring a computation to be redone multiple times to arrive at a correct result.

Many other designs to construct a CPHASE gate rely on nonlinear crystals. In these crystals, two photons can be absorbed simultaneously and re-emitted. Unfortunately, as shown by J. Shapiro [18] and J. Gea-Banacloche [19], if the photons are considered to be wavepackets rather than single-mode fields, the shape of the photons are significantly distorted by the entanglement introduced in the interaction. This distortion poses a problem for QIP tasks as, in later steps of the computation, photons which have interacted

will interfere differently than photons that have not interacted. Both [18] and [19] demonstrated that there is a fundamental trade-off between having a gate succeed at performing the CPHASE operation and the amount of phase shift.

Some have considered using two level or three level systems as phase gates. In [28] the authors pointed out that the nonlinearity present in the scattering of two photons from a V system could be leveraged to construct a quantum conditional-phase (CPHASE) gate. The difficulty that arises with this gate is that the entanglement created between the photons again tends to destroy the gate operation. Removing it would require reflecting the photons many, many times through the system to arrive at a phase shift of π. Additionally, Nysteen et. al. [29] studied the ability of a single two level emitter to act as a conditional phase gate. The highest operating fidelity they could accomplish was around 84%, again in part due to the spectral entanglement created between the photons by their interaction with the atom.

Recently, Brod and Combes [30] demonstrated that an array of approximately 20 atoms in a particular 1-D unidirectional setup could perform the CPHASE operation passively and deterministically, while preserving the spectral shape of the photons. Their work shows that it should be possible, in principle, to passively remove the effects of entanglement between the photons while still allowing them to interact. The challenge posed by their system is again one of scaling: the system they propose, which we will describe in more detail in Chapter 6, requires many non-reciprocal optical elements to ensure that photons continue to travel in the same direction. This would be incredibly difficult to construct experimentally without adding significant losses. We will show, however, that it is possible to use a transparency window between pairs of atoms to construct a CPHASE gate that works identically to the gate proposed in [30], but in a more experimentally achievable setting.

1.4 Entanglement

The final topic to address in this chapter is our working definition of entanglement. The study of entanglement is a very illuminating and complicated field, but the majority of entanglement measures (such as concurrence, three tangle, logarithmic negativity, etc.) do not easily extend to describe multimode photon states. They are generally defined for discrete quantum systems, such as the atomic basis introduced above.

The scattered states of photons will be entangled in two different senses; their spectral distributions will have components that are non-separable, and the final state will be a linear superposition of different terms. To see what we mean, consider the following wavefunction and its spectral distribution $\tilde{f}(\omega_1, \omega_2)$, which, in Section 3.4, will be shown to be the scattered state of two counter-propagating photons from a single two level emitter positioned at the origin.

$$|\psi\rangle = \int d\omega_1 d\omega_2 \tilde{f}(\omega_1, \omega_2) \hat{a}^\dagger_{\omega_1} \hat{a}^\dagger_{\omega_2} |0\rangle \tag{1.11}$$

$$\tilde{f}(\omega_1, \omega_2) = \frac{1}{\sqrt{2}} \Big[t(\omega_1)\tilde{f}(\omega_1) t(\omega_2)\tilde{f}(\omega_2) + r(\omega_1)\tilde{f}(\omega_1) r(\omega_2)\tilde{f}(\omega_2) + \frac{1}{2}\tilde{f}_{\text{ent}}(\omega_1, \omega_2) \Big] \tag{1.12}$$

This state is obviously entangled because it is a linear superposition of three different components, $t(\omega_1)\tilde{f}(\omega_1)t(\omega_2)\tilde{f}(\omega_2)$, $r(\omega_1)\tilde{f}(\omega_1)r(\omega_2)\tilde{f}(\omega_2)$ and $\frac{1}{2}\tilde{f}_{\text{ent}}(\omega_1, \omega_2)$. The state is also entangled as the final term $\frac{1}{2}\tilde{f}_{\text{ent}}(\omega_1, \omega_2)$ represents a non-separable, spectrally entangled component of the wavefunction, whereas the first two can be separated into a product of functions of ω_1 and ω_2. For multimode photons, separable states have a form similar to Eq. 1.13a, where the two photon state can be expressed as a product of single photon states. On the other hand, Eq. 1.13b represents a non-separable, and thus entangled, state, provided that it is not possible to write the function $\tilde{f}(\omega_1, \omega_2)$ in terms of

functions of ω_1 and ω_2 separately.

$$|\psi\rangle = \left(\int d\omega_1 \tilde{f}_a(\omega_1) \hat{a}^\dagger_{\omega_1} |0\rangle \right) \otimes \left(\int d\omega_2 \tilde{f}_b(\omega_2) \hat{b}^\dagger_{\omega_2} |0\rangle \right) \tag{1.13a}$$

$$|\psi\rangle = \int d\omega_1 d\omega_2 \tilde{f}(\omega_1, \omega_2) \hat{a}^\dagger_{\omega_1} \hat{b}^\dagger_{\omega_2} |0\rangle \tag{1.13b}$$

In what follows it is this non-separable part of the wavefunction that we will refer to as the entangled component of the wavefunction. We make this choice because the term arises from an entangling process between two photons that correlates either their arrival times or their frequencies. Additionally, it is this spectral, non-separable entangling term that leads to the failure of many of the proposals to perform quantum logic operations between photons and that is removed by the gate described in [30].

Chapter 2

Scattering of Single Photons From Many Atoms

2.1 Introduction

Single photon transport through materials has been extensively studied and, as of this writing, is an ongoing area of research [5, 31–36]. As a result, this chapter will focus on describing a new way to calculate single photon transmission coefficients, to explore the effect of dipole-dipole interactions on photon transport properties, and to study one particular transmission window that appears for a large number of unequally spaced atoms. Note that many of these results have already been presented in [37], specifically Sections 2.3.1, 2.4.1, and 2.5. This chapter begins by following a derivation of the single photon scattered state presented in [32]. After some analysis of this solution, we then connect it to a solution derived by considering the scatterers as mirrors with frequency-dependent transmission and reflection coefficients. Finally, we will use these approaches to analyze photon transport properties through multiple atoms.

2.2 Exact N-atom solution

2.2.1 Calculation of the scattered state

We begin with solving the scattered state of a photon from a system consisting of N identical atoms, at arbitrary positions, coupled to a 1-D waveguide supporting transport in both directions, as illustrated in Fig. 2.1.

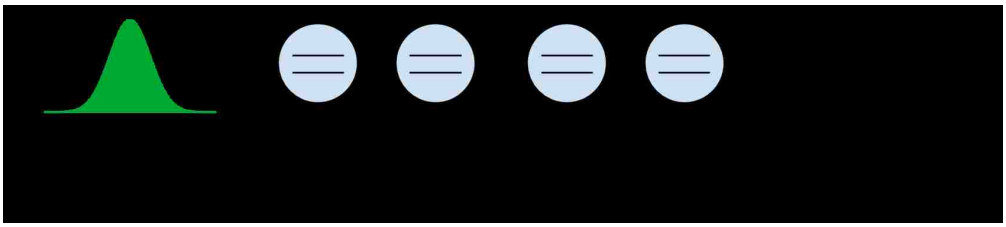

Figure 2.1: A diagram of the system being considered. All photons are constrained to move in one dimension in a waveguide coupled to an array of n atoms at arbitrary positions. In what follows, z will denote the distance along a waveguide with z=0 being the location of the center of the atomic array.

The interaction picture Hamiltonian for such a system is given by

$$H = \hbar g \sum_{j=1}^{N} \left(\hat{\phi}_j(t) e^{-i\delta t} \sigma_j^\dagger + \hat{\phi}_j^\dagger e^{i\delta t} \sigma_j \right) \tag{2.1}$$

where the operators $\sigma_j^\dagger$ and σ_j raise and lower the j^{th} atom and $\hat{\phi}_j$ is a superposition of the left and right traveling modes at position z_j.

$$\hat{\phi}_j(t) = e^{ik_F z_j} \hat{A}(t - z_j/c) + e^{-ik_F z_j} \hat{B}(t + z_j/c) \tag{2.2}$$

$\hat{A}(t)$ is the same as Eq. 1.7. These combined operators have the commutator $[\hat{\phi}_j(t), \hat{\phi}_k^\dagger(t_1)] = e^{ik_F(z_j - z_k)} \delta\big(t - t_1 - \frac{z_j - z_k}{c}\big) + e^{-ik_F(z_j - z_k)} \delta\big(t - t_1 + \frac{z_j - z_k}{c}\big)$. For a single photon, the state of the system at any time in the interaction picture can be expressed by Eq. 1.8, reproduced below.

$$|\psi(t)\rangle = |\psi_g(t)\rangle \otimes |G\rangle + \sum_{j=1}^{N} |\psi_j(t)\rangle \otimes |j\rangle \tag{2.3}$$

Substituting this into the Schrödinger equation and exploiting the orthogonality of the atomic basis yields differential equations for the photon states $|\psi_g(t)\rangle$ and $|\psi_j(t)\rangle$ of

$$|\dot{\psi_g}(t)\rangle = -ig \sum_{j=1}^{N} \hat{\phi}_j^\dagger e^{i\delta t} |\psi_j(t)\rangle \qquad\qquad |\dot{\psi_j}(t)\rangle = -ig \hat{\phi}_j(t) e^{-i\delta t} |\psi_g(t)\rangle \tag{2.4}$$

At this step we can formally integrate the ground state as

$$|\psi_g(t)\rangle = |\psi_I\rangle - g^2 \int_{-\infty}^{t} dt_1 \sum_{k=1}^{N} \hat{\phi}_k^\dagger(t_1) e^{i\delta t_1} |\psi_k(t_1)\rangle \tag{2.5}$$

and substitute it into the excited state. Note that $|\psi_I\rangle$ represents the initial state of the photon field, and in this case is given by $|\psi_I\rangle = \int d\omega \tilde{f}(\omega)\big(\alpha\hat{a}^\dagger_\omega + \beta\hat{b}^\dagger_\omega\big)|0\rangle$ where $\tilde{f}(\omega)$ is a normalized function describing the spectrum of the wavepacket and $|\alpha|^2 + |\beta|^2 = 1$. This describes a single photon that has (possibly) been sent down two different spatial modes by a linear element such as a beamsplitter. We have chosen to write the initial state in this form so that it will be easy to modify the final state to describe a photon incident from the left or the right. We are also assuming that the atoms are all initially in their ground state. The differential equation for the j^{th} excited state then becomes

$$\dot{|\psi_j(t)\rangle} = -ig\hat{\phi}_j(t)e^{-i\delta t}|\psi_I\rangle - g^2\sum_{k=1}^{N}\int_{-\infty}^{t} dt_1 \hat{\phi}_j(t)\hat{\phi}^\dagger_k(t_1)e^{-i\delta(t-t_1)}|\psi_j(t_1)\rangle \tag{2.6}$$

Normal ordering the photon operators $\hat{\phi}_j$ and applying their commutator gives the equation

$$\begin{aligned}\dot{|\psi_j(t)\rangle} = -ig\hat{\phi}_j(t)e^{-i\delta t}|\psi_I\rangle - g^2\sum_{k=1}^{N}\int_{-\infty}^{t} dt_1 \hat{\phi}^\dagger_k(t_1)\hat{\phi}_j(t)e^{-i\delta(t-t_1)}|\psi_j(t_1)\rangle \\ -g^2\sum_{k=1}^{N}\int_{-\infty}^{t} dt_1\Big[e^{ik_F(z_j-z_k)}\delta\big(t-t_1-\frac{z_j-z_k}{c}\big) + e^{-ik_F(z_j-z_k)}\delta\big(t-t_1+\frac{z_j-z_k}{c}\big)\Big]e^{-i\delta(t-t_1)}|\psi_j(t_1)\rangle\end{aligned} \tag{2.7}$$

With this, several terms in the expression will vanish. $\hat{\phi}_j(t)|\psi_k(t_1)\rangle = 0$ as the field is in the vacuum mode for this term. Additionally, as $t \geq t_1$, only delta functions where the position term is negative will contribute. Note also that if $j = k$ the delta function is only satisfied at the upper limit of integration, adding an extra factor of $1/2$ to this term. All this leads to the differential equation

$$\dot{|\psi_j(t)\rangle} = -ig\hat{\phi}_j(t)e^{-i\delta t}|\psi_I\rangle - g^2\sum_{k=1}^{N} e^{i(k_F-\delta)|z_j-z_k|}|\psi_k(t-|z_j-z_k|/c)\rangle \tag{2.8}$$

Here, following the work of [32], we transform to the Fourier domain. Doing so, $|\dot{\psi}_j(t)\rangle$ becomes

$$\dot{|\psi_j(t)\rangle} = \frac{1}{\sqrt{2\pi}}\int d\omega e^{-i\omega t}(-i\omega)|\tilde{\psi}_j(\omega)\rangle \tag{2.9}$$

Similarly, the initial state can be written as

$$-ig\hat{\phi}_j(t)e^{-i\delta t}|\psi_I\rangle = \frac{1}{\sqrt{2\pi}}\int d\omega' e^{-i(\omega'+\delta)t}\Big[\alpha e^{i(k_F+\omega'/c)z_j} + \beta e^{-i(k_F+\omega'/c)z_j}\Big]\tilde{f}(\omega)$$
$$= \frac{1}{\sqrt{2\pi}}\int d\omega e^{-i\omega t}\Big[\alpha e^{i(k_F+(\omega-\delta)/c)z_j} + \beta e^{-i(k_F+(\omega-\delta)/c)z_j}\Big]\tilde{f}(\omega-\delta) \qquad (2.10)$$

where we have defined $\omega = \omega' + \delta$ in this case. Transforming the last term of Eq. 2.8 to the Fourier domain and removing all the integrals and factors of $e^{-i\omega t}$ from the equation, we are left with

$$-i\omega|\tilde{\psi}_j(\omega)\rangle = -ig\Big[\alpha e^{i(k_F+(\omega-\delta)/c)z_j} + \beta e^{-i(k_F+(\omega-\delta)/c)z_j}\Big]\tilde{f}(\omega-\delta)$$
$$- g^2\sum_{k=1}^{N} e^{i(k_F+(\omega-\delta)/c)|z_i-z_j|}|\tilde{\psi}_j(\omega)\rangle \qquad (2.11)$$

We now define a matrix $|\tilde{\psi}_e(\omega)\rangle$ of atomic states, a matrix $\tilde{\theta}(\omega)$ containing the phase terms (both given below), and a $j \times j$ matrix $\tilde{M}(\omega)$ that has elements $\tilde{M}_{j,k}(\omega-\delta) = e^{i(k_F+(\omega-\delta)/c)|z_i-z_j|}$.

$$|\tilde{\psi}_e(\omega)\rangle = \begin{bmatrix} |\tilde{\psi}_1(\omega)\rangle \\ \vdots \\ |\tilde{\psi}_N(\omega)\rangle \end{bmatrix} \qquad \tilde{\theta}(\omega) = \begin{bmatrix} e^{i(k_F+\omega/c)z_1} \\ \vdots \\ e^{i(k_F+\omega/c)z_N} \end{bmatrix} \qquad (2.12)$$

With these definitions Eq. 2.11 becomes

$$-i\omega|\tilde{\psi}_e(\omega)\rangle = -ig\big[\alpha\tilde{\theta}(\omega-\delta) + \beta\tilde{\theta}^*(\omega-\delta)\big]\tilde{f}(\omega-\delta) - g^2\tilde{M}(\omega-\delta)|\tilde{\psi}_e(\omega)\rangle \qquad (2.13)$$

In terms of the matrix state, the solution to this equation is

$$|\tilde{\psi}_e(\omega)\rangle = -ig\big[g^2\tilde{M}(\omega-\delta) - i\omega\tilde{I}\big]^{-1}\big[\alpha\tilde{\theta}(\omega-\delta) + \beta\tilde{\theta}^*(\omega-\delta)\big]\tilde{f}(\omega-\delta) \qquad (2.14)$$

Eq. 2.14 can be substituted into Eq. 2.5 after similarly translating the ground state to the frequency domain. We are primarily concerned with the long time limit ($t \to \infty$) when the photon has left the system and all atoms are in their ground state. This scattered state is given by

$$|\psi_g(\infty)\rangle = \int d\omega\big(f_a(\omega)\hat{a}^\dagger_\omega + f_b(\omega)\hat{b}^\dagger_\omega\big)|0\rangle \qquad (2.15)$$

and the spectrum functions f_a and f_b describe the final state of the photon after interacting with the system. This leads to scattered spectrum functions

$$\begin{aligned} f_a(\omega) &= \alpha\tilde{f}(\omega) - g^2\tilde{\theta}^{*T}(\omega)\big[g^2\tilde{M}(\omega) - i(\omega+\delta)\tilde{I}\big]^{-1}\big[\alpha\tilde{\theta}(\omega) + \beta\tilde{\theta}^*(\omega)\big]\tilde{f}(\omega) \\ f_b(\omega) &= \beta\tilde{f}(\omega) - g^2\tilde{\theta}^{T}(\omega)\big[g^2\tilde{M}(\omega) - i(\omega+\delta)\tilde{I}\big]^{-1}\big[\alpha\tilde{\theta}(\omega) + \beta\tilde{\theta}^*(\omega)\big]\tilde{f}(\omega) \end{aligned} \tag{2.16}$$

where $\tilde{\theta}^T(\omega)$ is the transpose of $\tilde{\theta}(\omega)$.

From a computational perspective, it is useful to write this as a sum over the eigenvalues of $\big[g^2\tilde{M}(\omega) - i(\omega+\delta)\tilde{I}\big]^{-1}$. As the term containing $(\omega+\delta)$ is already diagonal, we diagonalize $\tilde{M}$ as $\tilde{M}(\omega) = \tilde{P}(\omega)\tilde{D}(\omega)\tilde{P}^{-1}(\omega)$. Using the fact that $\tilde{P}(\omega)\tilde{P}^{-1}(\omega) = \tilde{P}^{-1}(\omega)\tilde{P}(\omega) = \tilde{I}$, as it is made of normalized eigenvectors of $\tilde{M}(\omega)$, the whole matrix inverse becomes

$$\big[g^2\tilde{M}(\omega) - i(\omega+\delta)\tilde{I}\big]^{-1} = \tilde{P}(\omega)\big[g^2\tilde{D}(\omega) - i(\omega+\delta)\tilde{I}\big]^{-1}\tilde{P}^{-1}(\omega) \tag{2.17}$$

As written, the inverse $\big[g^2\tilde{D}(\omega) - i(\omega+\delta)\tilde{I}\big]^{-1}$ is diagonal and will have nonzero elements

$$\frac{1}{g^2\lambda_j(\omega) - i(\omega+\delta)} \tag{2.18}$$

where each $\lambda_j(\omega)$ is an eigenvalue of $\tilde{M}(\omega)$. Now the matrices can be converted to sums over the different eigenvalues so that the final spectrum becomes

$$\begin{aligned} f_a(\omega) &= \left(\alpha - g^2\sum_{i=1}^{N}\frac{\sum_{j,k=1}^{N} e^{-i(k_F+\omega/c)z_j}\big[\alpha e^{i(k_F+\omega/c)z_k} + \beta e^{-i(k_F+\omega/c)z_k}\big]\tilde{P}[j,i](\omega)\tilde{P}^{-1}[i,k](\omega)}{g^2\lambda_i(\omega) - i(\omega+\delta)}\right)\tilde{f}(\omega) \\ f_b(\omega) &= \left(\beta - g^2\sum_{i=1}^{N}\frac{\sum_{j,k=1}^{N} e^{i(k_F+\omega/c)z_j}\big[\alpha e^{i(k_F+\omega/c)z_k} + \beta e^{-i(k_F+\omega/c)z_k}\big]\tilde{P}[j,i](\omega)\tilde{P}^{-1}[i,k](\omega)}{g^2\lambda_i(\omega) - i(\omega+\delta)}\right)\tilde{f}(\omega) \end{aligned} \tag{2.19}$$

where $\tilde{P}[j,i]$ refers to the j,i^{th} element of $\tilde{P}$.

Assuming that the photon begins in the $\hat{A}$ mode (input in the waveguide from the left)

$\alpha = 1$, $\beta = 0$, and the output spectrum has the form

$$f_a(\omega) = \left(1 - g^2 \sum_{i=1}^{N} \frac{\sum_{j,k=1}^{N} e^{-i(k_F+\omega/c)(z_j - z_k)} \tilde{P}[j,i](\omega)\tilde{P}^{-1}[i,k](\omega)}{g^2\lambda_i(\omega) - i(\omega+\delta)}\right)\tilde{f}(\omega) = t(\omega)\tilde{f}(\omega)$$
$$f_b(\omega) = \left(-g^2 \sum_{i=1}^{N} \frac{\sum_{j,k=1}^{N} e^{i(k_F+\omega/c)(z_j + z_k)} \tilde{P}[j,i](\omega)\tilde{P}^{-1}[i,k](\omega)}{g^2\lambda_i(\omega) - i(\omega+\delta)}\right)\tilde{f}(\omega) = r(\omega)\tilde{f}(\omega) \tag{2.20}$$

where $t(\omega)$ and $r(\omega)$ are frequency-dependent transmission coefficients with the property that $|t(\omega)|^2 + |r(\omega)|^2 = 1$.

That the interaction can be described by two coefficients is a significant result that we will use to develop alternative means of deriving the transmission and reflection coefficients of the scattered photon. This occurs primarily because of the fact that the Jaynes-Cummings Hamiltonian only contains energy-conserving terms and, while the photon's overall wavefunction can be modified by its interaction with the atom, each individual frequency (i.e. $\hat{a}_\omega$) must be mapped to either the transmitted or reflected field.

2.3 Cavity solution

The fact that photon scattering from arrays of atoms can be described by frequency-dependent transmission and reflection coefficients suggests that one could treat the atom as a frequency-dependent beamsplitter and then apply techniques from classical optics to deal with the scattering of the photons. Here we present two different ways of conceptualizing what happens, the first by summing up all the possible events and the second by treating the system as an array of cavities. We note that the idea behind these methods underlies the transfer-matrix approach to photon scattering, which has been presented for N scatterers in [6, 33].

2.3.1 Summing events

The first technique presented is to sum a series of all possible reflection and transmission events for a photon initially in the $\hat{a}_\omega$ or $\hat{b}_\omega$ mode. By solving Eq. 2.19 for a single atom with the photon in either the $\hat{A}$ mode or the $\hat{B}$ mode it can be shown that only the reflection coefficient depends on the position of the scatterer. The coefficients are given below

$$r_R(z_0) = -\frac{g^2 e^{2i(k_F+\omega/c)z_0}}{g^2 - i(\omega+\delta)} \qquad r_L(z_0) = -\frac{g^2 e^{-2i(k_F+\omega/c)z_0}}{g^2 - i(\omega+\delta)} \qquad t = -\frac{i(\omega+\delta)}{g^2 - i(\omega+\delta)} \tag{2.21}$$

where r_R and r_L correspond to reflections from right-traveling left-traveling photons respectively and t is the frequency-dependent transmission coefficient. These are related to the final spectrum of the photons by

$$f_{\text{reflected}}(\omega) = r_{R,L}(z_0)\tilde{f}(\omega) \qquad\qquad f_{\text{transmitted}}(\omega) = t\tilde{f}(\omega) \tag{2.22}$$

For the case of a pair of atoms centered at $z = 0$ and with separation d we will define $r = r_R(-d/2) = r_L(d/2)$ and $r' = r_L(-d/2) = r_R(d/2)$, as the symmetry in the position of the two atoms makes the reflection and transmission coefficients symmetric as well. Assuming that the photon is incident from the left, by summing up all reflection and transmission coefficients we get that the total reflection coefficient is

$$r + t^2 r' + t^2 r'^3 + \ldots = r + \frac{t^2 r'}{1 - r'^2} \tag{2.23}$$

It is a simple matter from here to plug in the defined expressions in Eq. 2.21 to demonstrate that the reflection coefficient is identical to f_b from Eq. 2.20 for the same atomic positions. Similarly, the overall transmission coefficient is

$$t^2 + t^2 r'^2 + \ldots = \frac{t^2}{1 - r'^2} \tag{2.24}$$

and this yields precisely f_a when Eq. 2.20 is again evaluated with two atoms.

The possibility to view the two atoms as a "cavity" helps to explain why the atomic

separation affects both the amplitude and phase of the reflected and transmitted fields (or why it effectively changes the coupling and detuning of the system). Changing the separation between atoms modifies which frequencies are in resonance with the cavity, thus changing the transmitted and reflected spectra. "Atomic cavities," that is, cavities where the "mirrors" are atomic systems (generally consisting of more than two atoms), have been studied for various uses by a number of authors [38–40]. Additionally, a "cavity" formed by only two atoms has been studied by Gonzalez-Ballestero, Garcia-Vidal and Moreno in [41].

2.3.2 Coupled atomic cavities

Figure 2.2: The fields used to consider the system as a series of interactions.

The second technique presented is to envision an array of atoms as a series of coupled cavities and to apply methods from classical optics to find the total reflected and transmitted fields. To begin, we define left and right traveling fields inside each atomic 'cavity', as shown in Fig. 2.2. The fields in the j^{th} cavity can then be connected to the fields in the other cavities by the reflection and transmission coefficients defined in Eq. 2.21 via the recurrence relationships

$$\begin{aligned} E_j^R &= tE_{j-1}^R + r_R(z_j)E_j^L \\ E_j^L &= tE_{j+1}^L + r_L(z_{j+1})E_j^R \end{aligned} \tag{2.25}$$

A photon initially in the $\hat{A}$ mode (coming from the left) will have boundary conditions $E_0^R = 1$ and $E_N^L = 0$ and the reflected and transmitted fields are, respectively, given by E_0^L and E_N^R. It is possible to write the solution to these two fields in terms of several matrices,

though it is not presented here as the general form provides little insight. This method also does give precisely the expected form for Eq. 2.20 for two atoms.

The real advantage of this method in finding the scattered state of a photon is that it can much more easily deal with multiple, nonidentical atomic systems. The first method presented in this chapter, solving the Schrödinger equation directly, becomes significantly more complicated when the resonant energies of each of the scatterer is different. The second method of summing transmission and reflection events becomes challenging when dealing with more than two systems, as it requires dealing with multiple sums. This last method provides the most generality, as one can network any number or type of systems, provided the spectrum is only multiplied by a frequency-dependent reflection or transmission coefficient.

2.4 The Markovian approximation

Before analyzing the transmitted and reflected spectra of a single photon from an array of scatterers, we first explore a simplifying approximation. By using a coupling that is constant in frequency in our Hamiltonian we are assuming that the pulse is spectrally narrow enough that $\sqrt{\omega + ck_F} \approx \sqrt{ck_F}(1 + \frac{\omega}{2ck_F}) \approx \sqrt{ck_F}$. This suggests that the frequency component in exponential terms such as $e^{i(k_F+\omega/c)z_j}$ may be too small to make a meaningful contribution to the solution. While it is tempting to approximate the exponentials as $e^{i(k_F+\omega/c)z_j} \approx e^{ik_F z_j}$, the fact that the complex exponential is periodic means that for certain values of z_j, $\frac{\omega}{c}z_j$ may be on the order of 2π or greater. When this is the case, a small change in ω can lead to a significant change in the overall phase of the term. The characteristic length for this depends on the spectral width of the pulse, which we will represent as σ_ω. If the pulse bandwidth is on the order of a GHz, for $\mathcal{O}(\sigma_\omega z_j/c) \approx 2\pi$ the separation between atoms must be on the order of a meter. If the bandwidth is on the order of a MHz, for this term to be of order 2π, $z_j \approx 10^3 m = 1km$. For optical experiments with closely spaced atoms (often on the order of μm) these terms will certainly vanish.

Even for microwave experiments with a central frequency on the order of a GHz, sufficiently narrow band photons can still require separation on the order of 100-1000m, well beyond the length scale of most experiments.

Despite the rather large separations required to achieve a regime where terms like $\omega z_j/c$ will significantly modify the spectral distribution of the photon, there has been much interest in studying non-Markovian behavior. The validity of this approximation has been considered in several papers, notably in [41] where the authors explore this question in depth, and in [39, 40] where the non-Markovian properties are explored for particular systems. As mentioned in [41], there is a further consideration; if the coupling is on the order of the central frequency of the waveguide ($g^2 \approx ck_F$ in our formalism) then the Markovian approximation is no longer valid. This is not typically a problem, as the majority of atomic systems coupled to guided photon modes will have couplings on the order of a MHz or GHz, whereas optical photons will have frequencies on the order of 500THz.

In what follows, we show the numerical agreement between the Markovian and non-Markovian solutions, and visualize the difference between the two. To see how the system responds to a single photon it is useful to define an intensity transmission coefficient $\mathcal{T}(\omega) = |t(\omega)|^2$, where $t(\omega)$ is defined in Eq. 2.20. The utility of such a definition is that it is independent of the choice of input pulse shape and describes the atomic response to a monochromatic input. Note that in all figures we are choosing parameters that optimize transmission. The choice of parameters will be justified in section 2.4.2, but we present results here to show how well the Markovian approximation works for the transmission window we will be studying.

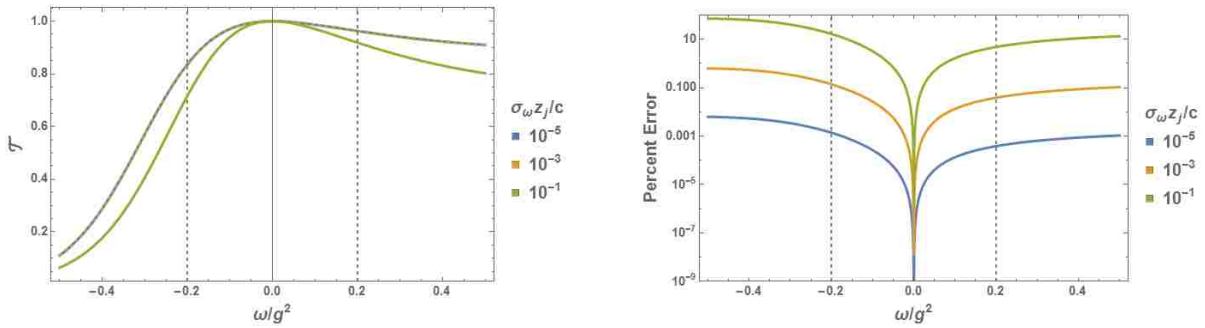

Figure 2.3: A comparison of the full intensity transmission coefficient $\mathcal{T} = |t(\omega)|^2$ for $N = 2$ atoms as a function of dimensionless parameter ω/g^2. The parameter $\sigma_\omega z_j/c$ represents the scaling of the position between the atoms. In this plot $\delta = g^2$ and the atoms are spaced at a distance $d = \frac{3\pi}{4k_F}$. Percent error is between the Markovian and full solutions.

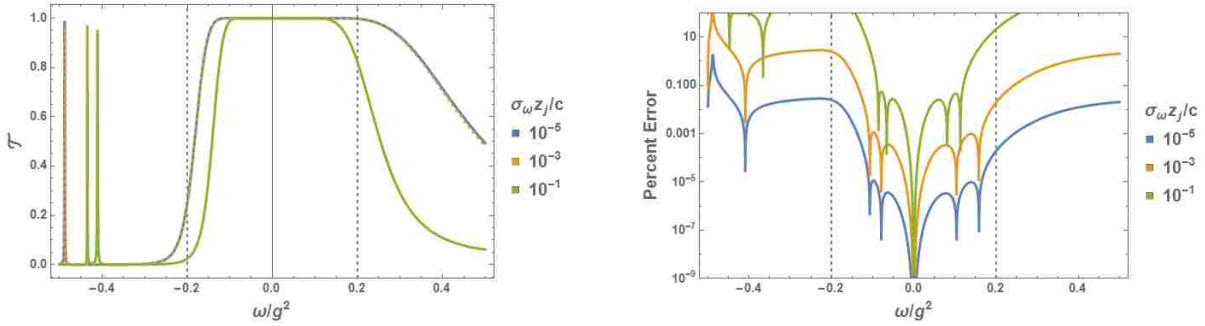

Figure 2.4: The same plots as Fig. 2.3 but with $N = 12$ atoms. The atoms have been spaced to optimize transmission, as will be described in Fig. 2.12

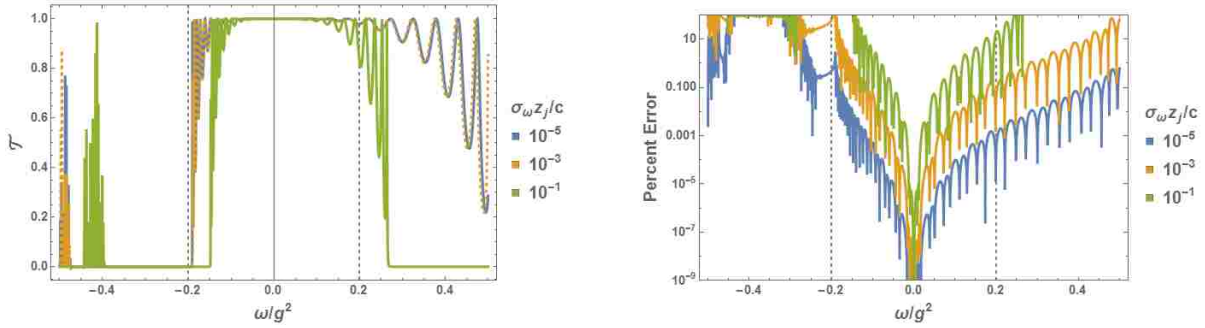

Figure 2.5: The same plots as Fig. 2.3 but with $N = 100$ atoms. The atoms have been spaced to optimize transmission, as will be described in Fig. 2.12

For a pulse of frequency bandwidth on the order of a GHz, a scaling factor of $\sigma_\omega z_j/c$ of order 10^{-5} would translate to a separation of 3 micrometers between each atom. If the

pulse is on the order of a MHz it would correspond to 3 mm between atoms, which is significantly larger than many experimental setups for quantum objects. As can be seen in these figures, the Markovian approximation and the full solution agree very well even as the number of atoms becomes very large. When $\sigma_\omega z_j/c$ is of order 10^{-5} the percent error between the exact and approximate terms is of order 1% or less in the region of high transmission. For $N = 100$ atoms, it is clear that the Markov approximation does not describe some of the periodic structure, but the magnitude of this difference becomes very small when transmission is high. As such, overall transport properties of a photon will not be significantly modified by ignoring Markovian effects.

This suggests that for spectrally narrow pulses interacting with quantum systems there is no need to consider the full, non-Markovian solution even when dealing with many atoms. Thus, in the following analysis we will make the Markovian approximation and neglect terms on the order of $\sigma_\omega z_j/c$. In practice, this means neglecting anything multiplied by z_j/c, as it will be too small to contribute meaningfully to the final solution.

2.4.1 Transport properties of one and two atoms

For a general arrangement of atoms it is impossible to derive an analytic solution for the transmission and reflection coefficients in Eq. 2.19 due to the need to invert a matrix. As such, we will present analytic results for the transmission properties of a single photon through one and two atoms, describe general properties of the solution for N atoms, and present some results for higher numbers of atomic systems. Note that in this section, unless otherwise specified, we will assume that the photon is initially input from the left (the $\hat{a}_\omega$ mode).

From Eq. 2.21, in the Markovian approximation a single photon scattering off a single atom from the left will have its spectra modified by

$$f_a(\omega) = t\tilde{f}(\omega) = -\frac{i(\omega+\delta)}{g^2 - i(\omega+\delta)}\tilde{f}(\omega) \quad f_b(\omega) = r_L(z_0)\tilde{f}(\omega) = -\frac{g^2 e^{2ik_F z_0}}{g^2 - i(\omega+\delta)}\tilde{f}(\omega) \quad (2.26)$$

This formula has been extensively studied [5, 12, 42], but for the purposes of this work it has two important properties. First, as mentioned before, the scattered state can be described by frequency-dependent reflection and transmission coefficients. Within these coefficients, the parameter g^2 gives the strength of the coupling between the atom and the waveguide photon modes and the parameter δ represents the detuning between the central field of the photon and the atom's transition frequency. Second, a reflected photon will pick up a phase dependent on its position (and frequency when the Markovian approximation cannot be applied).

We will analyze the behavior of this system using the intensity transmission coefficient $\mathcal{T}(\omega) = |t(\omega)|^2$. Fig. 2.6 shows how this parameter changes with respect to dimensionless variables ω/g^2 and δ/g^2. As expected, on resonance ($\delta = 0$) transmission is zero and by changing the detuning of the photon, the location of this zero point can be shifted.

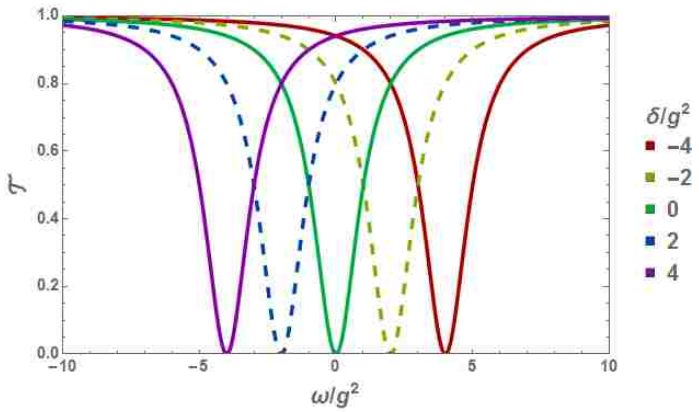

Figure 2.6: A plot of single photon transmission through a single atom in terms of dimensionless parameters ω/g^2 and δ/g^2. Note that detuning the photon from the atom merely shifts the location of the transmission minima.

For two atoms centered at position z_0 and separated by a distance d, the scattered

spectrum becomes

$$f_a(\omega) = t(\omega)\tilde{f}(\omega) = -\frac{1}{2}\Big[\frac{g^2\big(1+e^{-ik_Fd}\big)+i(\omega+\delta)}{g^2\big(1+e^{ik_Fd}\big)-i(\omega+\delta)} + \frac{g^2\big(1-e^{-ik_Fd}\big)+i(\omega+\delta)}{g^2\big(1-e^{ik_Fd}\big)-i(\omega+\delta)}\Big]\tilde{f}(\omega)$$
$$f_b(\omega) = r(\omega)\tilde{f}(\omega) = -\frac{1}{2}\Big[\frac{g^2\big(1+e^{-ik_Fd}\big)+i(\omega+\delta)}{g^2\big(1+e^{ik_Fd}\big)-i(\omega+\delta)} - \frac{g^2\big(1-e^{-ik_Fd}\big)+i(\omega+\delta)}{g^2\big(1-e^{ik_Fd}\big)-i(\omega+\delta)}\Big]e^{2ik_Fz_0}\tilde{f}(\omega) \tag{2.27}$$

This is slightly different than the form we presented in [37] and that was presented by others in [15, 32, 36, 41]. We have chosen to represent the scattered spectrum from two atoms as above to connect it to the eigenvalues of $\tilde{M}$, the $\lambda_j(\omega)$ terms in Eq. 2.20. As pointed out in [33], a chain of N atoms will have collective coupling and detuning rates given by the poles of Eq. 2.18. In the notation presented here, then, the effective coupling rates of a system are given by $Re[g^2\lambda_j(\omega)]$ and the effective detuning are $\delta - Im[g^2\lambda_j(\omega)]$. Without the Markovian approximation this leads to an infinite number of poles, as $\lambda_j(\omega)$ contains the periodic term $e^{i\omega z_j/c}$. When the Markovian approximation is applied the periodic functions vanish, however, and the number of poles reduces to just N.

These poles can be clearly seen in the denominator of Eq. 2.27; the terms $g^2Re[1 \pm e^{ik_Fd}]$ and $\delta \pm g^2Im[e^{ik_Fd}]$ correspond to the two effective couplings and detunings respectively. For two atoms, these factors represent the coupling of the system to the different standing wave modes given by Eq. 1.5, provided the pair is centered at the origin. As the traveling wave modes can be written as superpositions of the standing wave modes, it comes as no surprise that the final spectrum can be written as above. Finally, for comparison, we also give the same form presented in other works for the transmitted and reflected spectra, where we define $\phi = k_Fd$, as in the Markovian approximation all positions act effectively as phases.

$$f_a(\omega) = -\frac{(\omega+\delta)^2}{(g^2-i(\omega+\delta))^2 - g^4e^{2i\phi}}\tilde{f}(\omega)$$
$$\tilde{f}_b(\omega) = -g^2e^{-i\phi} \times \frac{(1+e^{2i\phi})(g^2-i(\omega+\delta)) - 2g^2e^{2i\phi}}{(g^2-i(\omega+\delta))^2 - g^4e^{2i\phi}}\tilde{f}(\omega) \tag{2.28}$$

The addition of a second atom opens up new transmission possibilities as compared to a

single atom. In agreement with other authors [15, 33, 43], we find that the intensity transmission coefficient $\mathcal{T}(\omega)$ for the two-atom system has the form of

$$\mathcal{T}(\omega) = \frac{(\omega+\delta)^4}{(\omega+\delta)^4 + 4g^4\left((\omega+\delta)\cos(k_F d) + g^2\sin(k_F d)\right)^2} \tag{2.29}$$

As noted by other authors [15, 33, 40], the presence of a second atom opens up a new transmission window so that on resonance ($\omega = 0$), unlike for a single atom, $\mathcal{T}(0) = 1$. This condition occurs when $\tan(k_F d) = -\delta/g^2$. At this point, the transmission coefficient becomes

$$\mathcal{T}(\omega, -\tan^{-1}(\delta/g^2)) = \frac{1}{1 + 4g^4\omega^2/(\omega+\delta)^4} \tag{2.30}$$

As can be seen in Fig. 2.7, when δ/g^2 is small, the transmission window is narrow and moderately asymmetric. As δ/g^2 approaches 1 the window broadens and becomes significantly less symmetric.

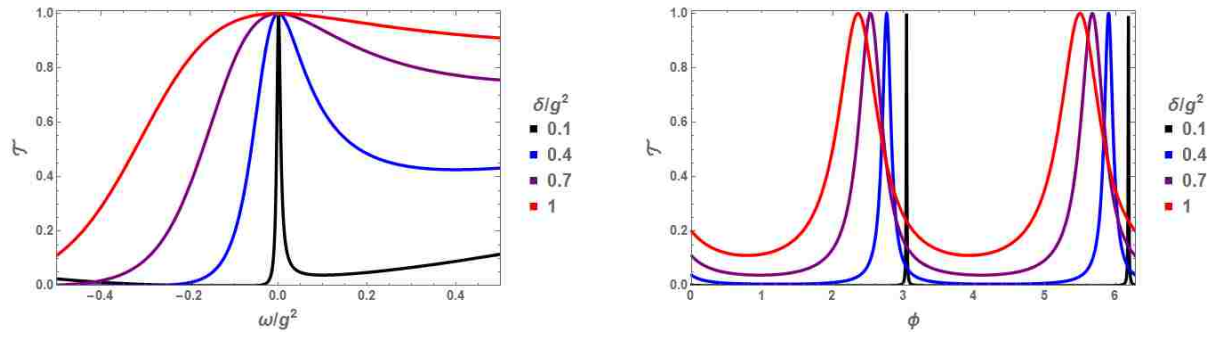

Figure 2.7: The transmission coefficient $\mathcal{T}(\omega)$ for various δ/g^2 as a function of dimensionless variable ω/g^2 with $\phi = k_F d = \pi - \arctan(\delta/g^2)$ (right) and $\phi = k_F d =$ with $\omega = 0$ (left).

In the limit when $g^2/\sigma_\omega \gg 1$, provided the system is tuned to this transmission window, the probability of reflection becomes virtually zero and the transmission coefficient becomes approximately

$$t(\omega) = \mathrm{Exp}\left\{ i\mathrm{Arg}\left[-\frac{(\omega+\delta)^2}{(g^2 - i(\omega+\delta))^2 - g^4 e^{-2i\arctan(\delta/g^2)}} \right] \right\} \tag{2.31}$$

If $g^2/\sigma_\omega \approx 1000$ or greater this can be written simply as a phase.

$$t(\omega) \approx -e^{2i\arctan(\delta/g^2)+2i\omega g^2/\delta} \tag{2.32}$$

This result is interesting, as it implies that two atoms can effectively provide a frequency-dependent phase shift to a photon while not modifying its direction of propagation. This behavior suggests that it may be useful for quantum information processing, a question that we will explore in Chapter 6. We also note that this limit, $g^2/\sigma_\omega \gg 1$, corresponding to either strong coupling ($g^2 \gg 1$) or a very narrow pulse bandwidth ($\sigma_\omega \ll 1$) is commonly referred to as the adiabatic limit.

2.4.2 Transport properties of N atoms

In general, evaluating the transmission properties for N atoms at arbitrary positions is an incredibly complicated task. There is one instance where the task becomes simple, however; if all atoms are separated by a distance that is a multiple of one half of a wavelength. This translates into a phase difference between atoms of $k_F|z_i - z_j| = n\pi$ for all pairs. When this condition is satisfied, all but one the eigenvalues of $\tilde{M}$ vanish. The remaining eigenvalue leads to the reflection and transmission coefficients (in the Markovian limit) of

$$t(\omega) = -\frac{i(\omega+\delta)}{Ng^2 - i(\omega+\delta)} \qquad r(\omega) = -\frac{Ng^2}{Ng^2 - i(\omega+\delta)} \tag{2.33}$$

This has the same form as 2.26, but with the coupling increased by a factor of N. Since the atoms are spaced at a multiple of half a wavelength, they will all experience the same magnitude of the electric field and thus act collectively. This result was also discovered in [33].

We now focus on maximizing the transmission of a single photon through an array of N atoms. The rationale behind this is that, as will be shown in Chapter 6, if a single photon can transmit with unit probability, the inherent nonlinear nature of a two level emitter

should enable the system to act as a passive, deterministic, phase gate for two counter-propagating photons. Looking for high transmission, we first consider the case where all atoms are identical and separated by the same distance d. With these conditions, Tsoi and Law in [33] found that transmission maxima can be found by

$$\cos(q\pi/N) = \frac{g^2}{\delta}\sin(k_F d) + \cos(k_F d) \tag{2.34}$$

as a function of N, where q is an integer that runs from 1 to $N-1$. We will also consider pairs of atoms, with each atom in the pair separated by a distance $d = \frac{\pi - \arctan(\delta/g^2) + 2m\pi}{k_F}$ and the centers of the pairs separated by a different distance, $a = \frac{\phi_a + 2m'\pi}{k_F}$. This is inspired by the transmission window for a single pair; if a photon will transmit through a single pair with high transmission, it is reasonable to suppose that it might transmit through multiple pairs of atoms. We also note that in the Markovian approximation the factors of $2m\pi$ in the definitions of d and a will not contribute. As such, from this point forward we will refer to $\phi_d = k_F d$ as the phase difference between two atoms in a pair and $\phi_a = k_F a$ as the phase difference between any two other pairs. A visual representation of these distances is given in Fig. 2.8.

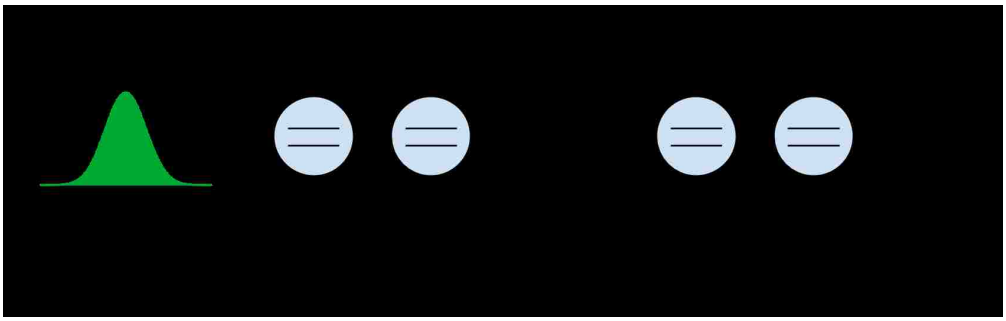

Figure 2.8: A diagram of the system of pairs of atoms with the pair distances labeled with ϕ_d corresponding to the distance between two atoms in a pair and ϕ_a between successive pairs.

The first question we are concerned with answering is how the transmission window for two atoms depends on the spacing between successive pairs. In order to answer this, we first perform an analytic analysis of the transmission coefficient. As has been shown, a

single pair exhibits high transmission when $\tan(\phi_d) = -\delta/g^2$. By treating a single pair as an individual scatterer with reflection and transmission coefficient defined in Eq. 2.27 and using the approach of Section 2.3.2, we derived an analytic form for two pairs (four atoms) separated by a distance $a = \phi_a/k_F$. A plot of the reflection coefficient ($\mathcal{R}(\omega) = |r(\omega)|^2$) for this system is given below.

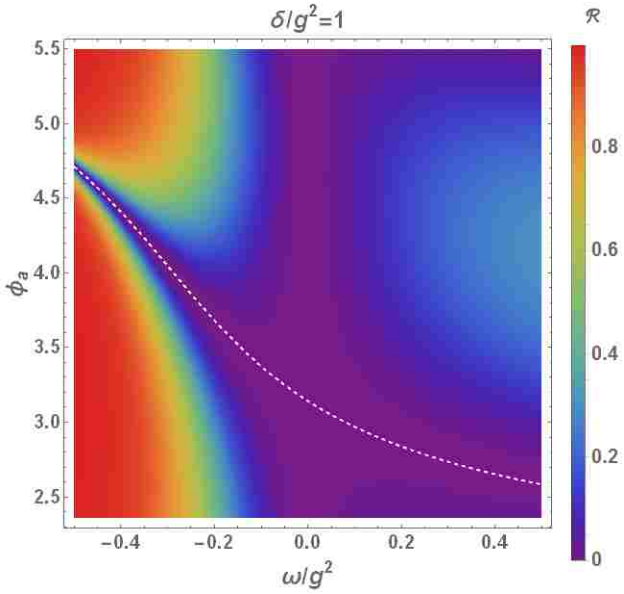

Figure 2.9: A plot of the reflection coefficient of two pairs of atoms as a function of dimensionless parameter ω/g^2 and ϕ_a for $\delta/g^2 = 1$. The dotted line is given by Eq. 2.35

As can be seen, on resonance the photon is never reflected. The reflection coefficient will also be zero when

$$\phi_a = \pi - \arctan\left(\frac{\delta^2(\delta+\omega)^2 + g^4(\omega^2 + 2\delta\omega - \omega^2)}{2g^2\left(\delta^3 + (g^4+\delta^2)\omega\right)}\right) \tag{2.35}$$

In the adiabatic limit, the pulse will be spectrally narrow; to achieve a high transmission probability, the reflection coefficient must be minimized near resonance. At this point (when $\omega = 0$), the ϕ_a that satisfies the above condition reduces to $\phi_a = \pi - \arctan\left(\frac{g^4-\delta^2}{2g^2\delta}\right)$. For the choice of $\delta/g^2 = 1$ this gives an optimal spacing of $\phi_a = \pi$. That this choice minimizes transmission in the adiabatic limit can be seen clearly in Fig. 2.10 where we have calculated the reflection probability for a Gaussian pulse of $\tilde{f}(\omega) = \frac{e^{-\omega^2/(4\sigma_\omega^2)}}{\sqrt{\sigma_\omega\sqrt{2\pi}}}$. From

this figure, where reflection probability is calculated with $g^2/\sigma_\omega = 100$ (so the system is in the adiabatic regime), $\phi_a = \pi$ leads to a minimum reflection probability for four atoms. Interestingly, at $\phi_a = 2\phi_d$ the reflection probability becomes quite high. This is likely due to the fact that the phase difference between all atoms becomes the same and the system becomes more like a Bragg mirror. This same choice of $\phi_a = \pi$ also minimizes the reflection probability of larger numbers of atoms, provided that they have all been arranged into pairs with phase ϕ_d between atoms in the pair and phase ϕ_a between centers of successive pairs.

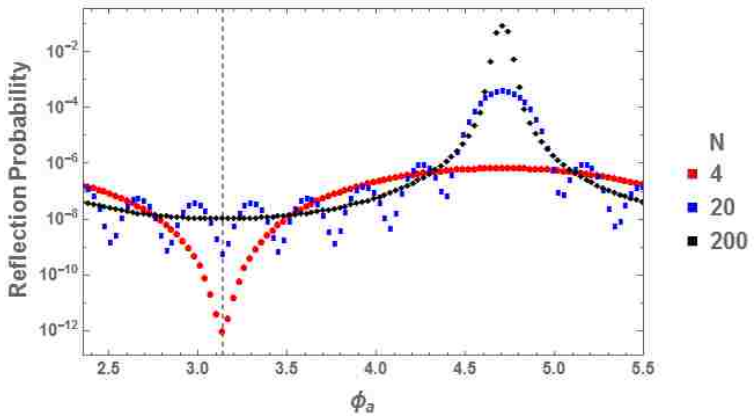

Figure 2.10: A plot of the reflection probability as a function of ϕ_a for various numbers of N atoms, assuming that the atoms are arranged into pairs with separation ϕ_d and that each pair is separated by ϕ_a from its nearest neighbors. All calculations were done with $g^2/\sigma_\omega = 100$ and $\delta/g^2 = 1$ using a Gaussian input pulse.

Next, we consider how the reflection probability depends on the value of g^2. In Fig. 2.11 we plot this quantity as a function of g^2. Reflection probability peaks around $g^2 \approx 1$. When the coupling is low the reflection probability is correspondingly low, as the photon does not significantly interact with the atom. As g^2 becomes very large the probability of reflection becomes smaller and smaller and appears to be even lower for multiples of four atoms. This is consistent with Fig. 2.9, as the feature corresponding to zero reflection is centered around $\omega/g^2 = 0$. If $\sigma_\omega \ll g^2$, it will be well within the window of low reflection seen in Fig. 2.9 for four atoms.

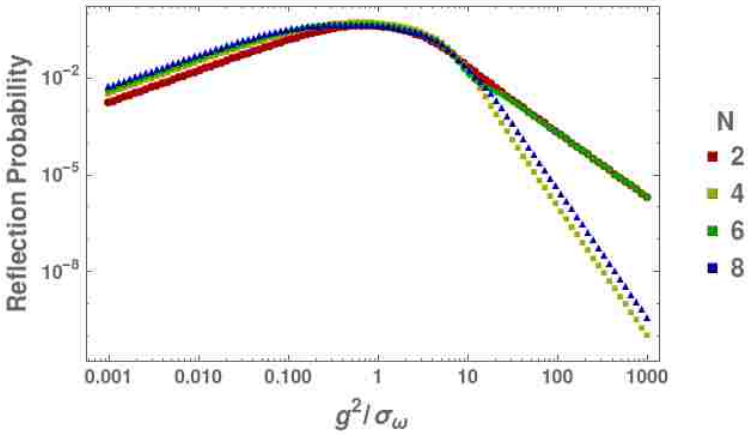

Figure 2.11: A plot of the reflection probability for a Gaussian initial state as a function of g^2/σ_ω for various numbers of N atoms. For all curves $\delta/g^2 = 1$.

We can actually decrease the reflection probability further. As described above, for two pairs the optimal difference in phase in the adiabatic limit is given by $\phi_a = \pi$ for $\delta/g^2 = 1$. Using these parameters, we defined reflection and transmission coefficients for the optimized four atom system. Using the methods of Section 2.3 we used these coefficients to arrive at an analytic form for an array of eight atoms where the phase difference between the two arrays of four atoms was undefined. We then optimized this spacing and defined new reflection and transmission coefficients for the array of eight atoms. This process was used twice more to analytically optimize the separation for up to thirty two atoms for $\delta/g^2 = 1$. It turns out that with this process, the optimal spacing to reduce reflections consists of a unit cell of four atoms. As depicted in Fig. 2.12, the cell consists of atoms separated by ϕ_d, $\phi_d/3$, and ϕ_d in that order. The closest atoms between each successive cell are then also separated by ϕ_d.

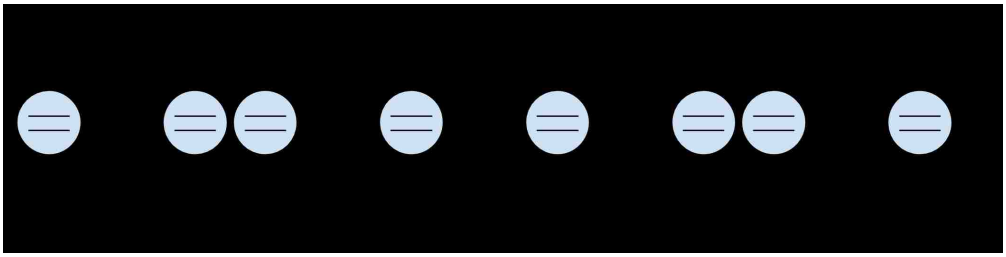

Figure 2.12: A diagram of the optimized position spacing for $\delta/g^2 = 1$ and $N = 12$ atoms. The values given are for the phase differences between successive atoms. Note that all phases can have a factor of $2m\pi$ added to them and that for the parameters chosen $\phi_d = 3\pi/4$.

In Fig. 2.13 we plot the reflection probability as a function of N. Here one can see that the reflection probability remains small even though the number of atoms becomes large whether one uses the optimized positions shown in Fig. 2.12 or uses an equal spacing of $\phi_a = \pi$ between pairs. The optimal spacing spacing leads to a significantly lower reflection probability than simply separating each pair by a phase of $\phi_a = \pi$, however.

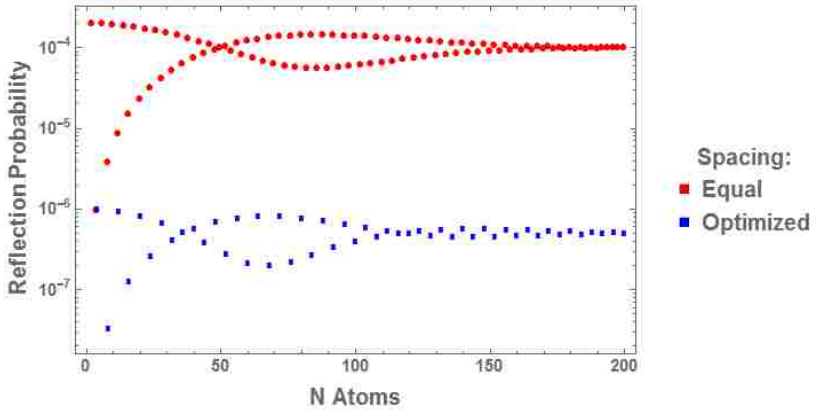

Figure 2.13: A plot of the reflection probability as a function of N atoms with $\phi_d = \pi - \arctan(\delta/g^2)$, $\delta/g^2 = 1$, and $g^2/\sigma_\omega = 100$. The points labeled "Equal" correspond to pairs that are evenly spaced at a distance of $\phi_a = \pi$ and the ones labeled "Optimized" correspond to the optimal spacing described in the text.

Finally, in Fig. 2.14, we compare the reflection probability of the transmission maxima given by Eq. 2.34 when all the atoms are separated by the same distance, the optimal spacing of Fig. 2.12, and the equal pair spacing where all pairs are separated by $\phi_a = \pi$. When g^2/σ_ω becomes large, the reflection probability dramatically decreases for the

optimized and π-pair cases as compared to the situation where all the atoms are periodically spaced. As expected, the optimized spacing has a lower reflection probability.

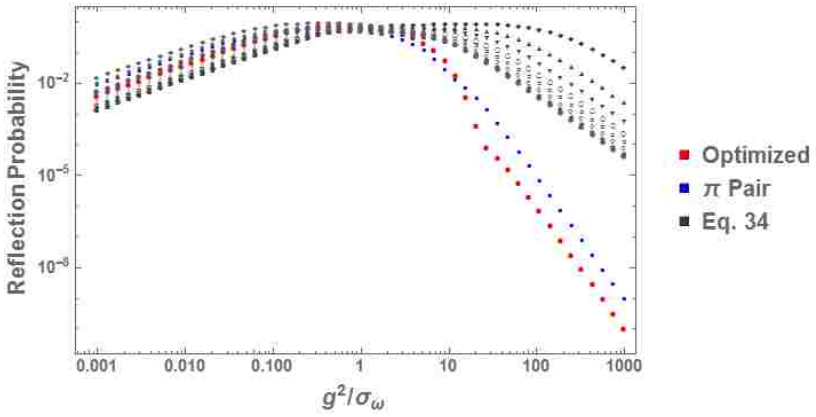

Figure 2.14: A plot of the reflection probability as a function of g^2/σ_ω for different inter-atomic distances. The points labeled "Equal" correspond to pairs that are evenly spaced at a distance of $\phi_a = \pi$, the ones labeled "Optimized" correspond to the optimal spacing shown in Fig. 2.12, and the grey curves represent the different maxima given by Eq. 2.34 for an array of equally spaced atoms.

From all of this it would appear that, at least for a photon that initially has a Gaussian frequency distribution, if the positions between atoms are chosen carefully an array of atoms may be able to function as a frequency-dependent phase shifter. To explore this, we posit that, if the atoms have been placed using the optimal spacing or as pairs separated by a phase of π, in the adiabatic limit of $g^2/\sigma_\omega \gg 1$, the transmission coefficient for N atoms should have an effective form of

$$t(\omega) = \mathrm{Exp}\left\{\frac{N}{2} i\mathrm{Arg}\left[-\frac{(\omega+\delta)^2}{(g^2 - i(\omega+\delta))^2 - g^4 e^{-2i\arctan(\delta/g^2)}}\right]\right\} \tag{2.36}$$

This is simply the transmission coefficient that would result from a photon transmitting through $N/2$ pairs of atoms, picking up a phase given by Eq. 2.31 at each site. To explore the validity of this approximation, we plot the magnitude and phase the transmission coefficient from the full solution in Eq. 2.20 for the optimized position spacing and a pairwise spacing with a phase of π between each pair, along with the approximate form of Eq. 2.36.

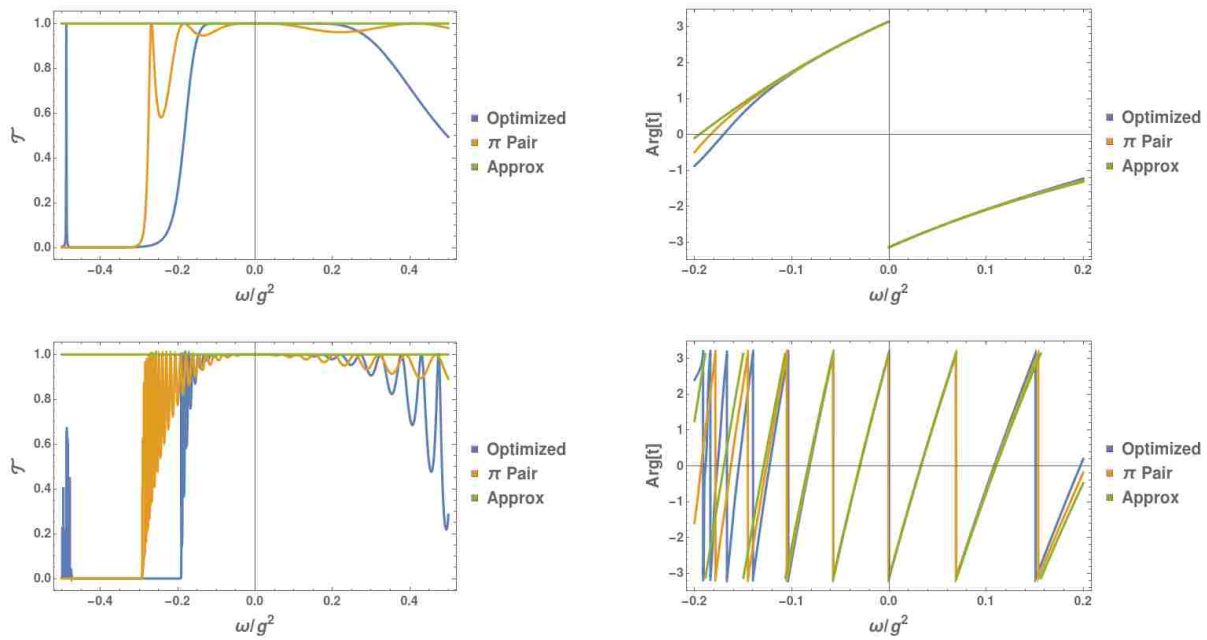

Figure 2.15: The absolute value of the intensity transmission coefficient $\mathcal{T} = |t(\omega)|^2$ (left column) and phase of $t(\omega)$ (right column) for $N = 12$ atoms (top row) and $N = 100$ atoms (bottom row). The curve labeled "Optimized" corresponds to the full solution to $t(\omega)$ when the atoms have been spaced as given in Fig. 2.12, "π Pair" corresponds to the case where each pair of atoms is separated by a phase of π, and "Approx" is the transmission coefficient given in Eq. 2.36. For all plots $\delta/g^2 = 1$. Note that the limits of ω/g^2 differ between the left and right columns.

As can be seen from Fig. 2.15, the approximation presented in Eq. 2.36 is certainly valid provided that the pulse is narrow enough in frequency. In terms of the bandwidth of the incoming photon this translates into $g^2/\sigma_\omega > 10$, as transmission is effectively 1 and the phase is nearly identical for $|\omega/g^2| < .1$. This window is very narrow, however; if $\omega/g^2 < -.2$ transmission becomes negligible. Additionally, it would appear that the transmission profile from the optimal position described in this text is more square around $\omega/g^2 \in [-.1, .1]$ than the π pair case. The phase of all three calculations similarly matches well in this region. Comparing the case where there are 12 atoms to the case where there are 100 atoms it is clear that as the number of atoms increases the phase of the photon is modified more.

It is worth noting that this high transmission window is also dependent on the value of

δ/g^2. If this ratio becomes small (say .1), the transmission window becomes incredibly narrow. Increasing δ/g^2 will broaden the transmission window, though as the photons become more and more detuned from the atomic resonance their interaction with the atom also becomes weaker. The most physically interesting regime is around $\delta/g^2 \approx 1$, as such a choice still allows for a nonzero interaction between the atoms and photon (seen most clearly in the fact that transmission can vary significantly in Fig. 2.15) but still maintains high transmission.

The behavior of an array of N atoms coupled to a one dimensional waveguide studied in this section implies that, in the adiabatic regime, the system can be made to be effectively unidirectional, in the sense that a single photon will transmit with near-unit probability, with a nontrivial phase added based on the number of pairs of atoms. This will become more important when we begin analyzing this system's ability to function as a passive, deterministic CPHASE gate in Chapter 6.

2.5 Dipole-dipole interactions

We now consider how the transmission spectra of a single photon can be modified by the presence of exchange- (or Förster-) type interactions [44] between the atoms. In order to deal with such a process, we introduce the interaction Hamiltonian

$$H_A = \hbar\Delta\big(|eg\rangle\langle ge| + |ge\rangle\langle eg|\big) \tag{2.37}$$

where the term Δ describes the strength of the interaction and the terms $|eg\rangle$ and $|ge\rangle$ correspond to the leftmost atom being in the excited state and the rightmost in the ground state or vice versa. Such a Hamiltonian has been used to model the interaction between neutral atoms [45–47] but can also describe other systems such as closely-spaced quantum dots or superconducing circuits. We note that there was a recent paper by Cheng, Xu and Agarwal [36] in which the authors study a model of the same form as Eq.2.37. Additionally, Liao, Nha and Zubairy [34] recently have considered a model for the

dipole-dipole interaction mediated by both the waveguide and non-waveguide modes. Their model does not appear to be equivalent to the form of Eq. 2.37 but qualitatively shares some features with our solution.

To derive the reflected and transmitted spectra of a single pair of atoms, it is most convenient to solve the Schrödinger equation directly using the standing wave photon modes and the atomic basis $|\pm\rangle = \frac{1}{\sqrt{2}}\big(|eg\rangle \pm |ge\rangle\big)$, as H_A is diagonal in this basis. By moving to a new interaction picture, the final scattered state can be found in the same manner as Eq. 2.20. This gives transmitted spectra of

$$\begin{aligned} f_a(\omega) &= -\frac{1}{2}\Big[\frac{g^2\big(1+e^{-i\phi_d}\big)+i(\omega+\delta-\Delta)}{g^2\big(1+e^{i\phi_d}\big)-i(\omega+\delta-\Delta)} + \frac{g^2\big(1-e^{-i\phi_d}\big)+i(\omega+\delta+\Delta)}{g^2\big(1-e^{i\phi_d}\big)-i(\omega+\delta+\Delta)}\Big]\tilde{f}(\omega) \\ f_b(\omega) &= -\frac{1}{2}\Big[\frac{g^2\big(1+e^{-i\phi_d}\big)+i(\omega+\delta-\Delta)}{g^2\big(1+e^{i\phi_d}\big)-i(\omega+\delta-\Delta)} - \frac{g^2\big(1-e^{-i\phi_d}\big)+i(\omega+\delta+\Delta)}{g^2\big(1-e^{i\phi_d}\big)-i(\omega+\delta+\Delta)}\Big]e^{2ik_F z_0}\tilde{f}(\omega) \end{aligned} \tag{2.38}$$

and thus a transmission coefficient of

$$\mathcal{T}(\omega,\phi) = \left(1 + \frac{4g^4(\Delta + (\omega+\delta)\cos(\phi_d) + g^2\sin(\phi_d))^2}{\big(-\Delta^2 - 2\Delta g^2\sin(\phi_d) + (\omega+\delta)^2\big)^2}\right)^{-1} \tag{2.39}$$

where ϕ_d again refers to $k_F d$, the phase acquired by a photon moving from one atom to the next.

The presence of Δ here opens up a new transmission window; for any non-zero value of Δ it is possible to achieve unit transmission on resonance, provided that ϕ_d is chosen appropriately. The condition on ϕ_d is

$$\Delta + \delta\cos\phi_d + g^2\sin\phi_d = 0 \tag{2.40}$$

We note that this condition has also been derived in [36], where the transmission peak is presented as an instance of Fano interference.

Fig. 2.16 plots $\mathcal{T}(\omega)$ for $\delta = 0$ and various values of Δ/g^2 where $\phi_d = -\arcsin(\Delta/g^2)$ has been chosen to satisfy the above condition to maximize transmission. We also plot how $\mathcal{T}$ depends on ϕ at resonance ($\omega = 0$).

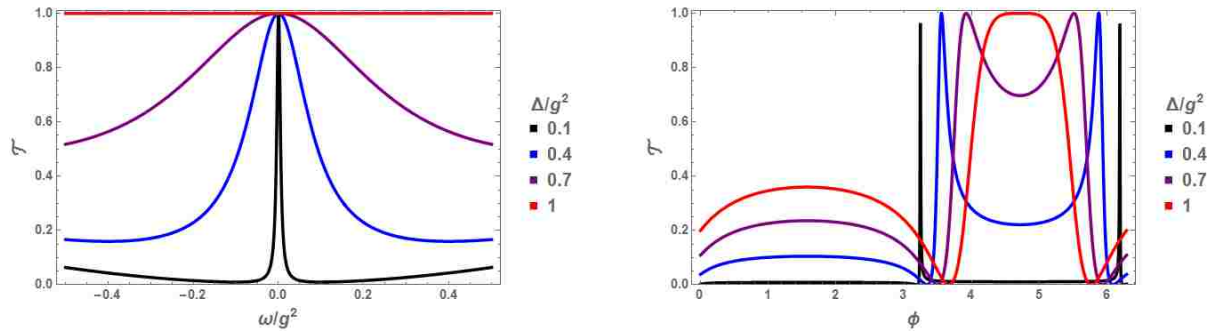

Figure 2.16: The transmission coefficient $\mathcal{T}(\omega)$ for various Δ/g^2 as a function of ω/g^2 with $\phi - \arcsin(\delta/g^2)$ (right) and ϕ with $\omega = 0$ (left). For both plots $\delta = 0$.

The most striking aspect of 2.16 is that when $\Delta = g^2$ and $\phi_d = 3\pi/2$ (or $\Delta = -g^2$ and $\phi = \pi/2$, if negative values of Δ are possible) the transmission curve becomes spectrally flat. This means that a single photon pulse will be entirely transmitted no matter what shape. This is, of course, only true as long as the Markovian approximation holds. Additionally, Fig. 2.16 shows that the dependence on ϕ_d is fairly broad, meaning that near-unit transmission will occur with high probability even if the spacing between atoms does not exactly match the condition given in Eq. 2.40.

The origin of this high transmission can be thought of as an example of quantum interference. When $\phi_d = 3\pi/2$ the incoming travelling-wave photon can be written as a superposition of the standing wave photon modes, and will equally couple to both $|+\rangle$ and $|-\rangle$. By also controlling Δ so that it cancels out the $g^2 e^{i\phi}$ terms in Eq. 2.16 the coupling and detuning to each of the standing wave modes will be identical. This leads to perfect transmission, as the $\hat{A}$ mode is the sum of the standing wave modes, and no reflection as the $\hat{B}$ mode is the difference of these two identical processes. The final transmitted photon pulse has the form

$$\tilde{f}_a(\omega) = -\frac{g^2 + i(\omega + \delta)}{g^2 - i(\omega + \delta)} \tilde{f}(\omega) \tag{2.41}$$

This spectrum is identical to that for a single photon scattering from an atom in a unidirectional waveguide (where the photons are constrained so that they must propagate

in one direction) or a standing-wave photon interacting with an atom (such as the setup shown in Fig. 1.1), but in this context it appears in the bidirectional geometry. This result is highly nontrivial, as it requires a second atom to work.

Furthermore, this behavior remains as the number of pairs of atoms increases. If N atoms are arranged so that every pair of atoms is separated from each other pair by a distance of at least several wavelengths, the exchange interaction will only occur between the atoms in each pair. Then, using the same arguments as in Section 2.3.2, the transmission coefficient for a photon passing through the entire system will be $t = \left(- \frac{g^2+i(\omega+\delta)}{g^2-i(\omega+\delta)} \right)^{N/2}$ and the reflection coefficient will be $r_R = r_L = 0$ for every pair. This leads to a transmitted spectrum of

$$\tilde{f}_a(\omega) = \left(- \frac{g^2 + i(\omega+\delta)}{g^2 - i(\omega+\delta)} \right)^{N/2} \tilde{f}(\omega) \tag{2.42}$$

Note that the exponent is $N/2$, as each transmission coefficient arises from the photon interacting with two atoms. This result suggests that by building a system with a strong interaction, one can create unidirectional (or chiral) behavior in what would typically be a bidirectional geometry.

2.6 Conclusions

In this chapter we explored different ways of looking at the scattering of a single photon from an array of two level systems coupled to a one-dimensional waveguide. Following the solution in [32], in Eq. 2.19 we presented the general transmission and reflection coefficients for a single photon scattering from an array of N two level systems at arbitrary positions. The most important feature of this solution is that the effect of the entire scattering process can be accurately described by a frequency-dependent transmission and reflection coefficient. Using this, we explored different approaches to the solution that treat the system as an effective cavity created by atomic 'mirrors' and argued that these lead to the same solution found using the method of [32].

We also explored the transport properties of a system of one, two and N atoms. Here we found that the presence of a second atom opened a transmission window when $\tan(k_F d) = -\delta/g^2$. We explored the behavior of this transmission window as the number of pairs of atoms increased and demonstrated that a single photon will transmit with very high probability, provided that the atoms have been arranged appropriately. We will explore this further in Chapters 4 and 5 as we will consider whether this window enables high transmission for two photons. Finally, we found that if one includes the effect of dipole-dipole interactions a pair, or array, of atoms is able to transmit a photon with unit probability while the photon acquires a nontrivial, frequency-dependent phase. Again, we will explore this window further with two photons in Chapter 4 and in Chapter 6 will show how it can be leveraged to construct a conditional logic gate.

Chapter 3

Scattering of Many Photons From One Atom: Space-time Description

3.1 Introduction

In this chapter we will pursue a different approach to the problem of photon scattering by using a spacetime description of photons. For the most part, studies of scattered photons describe the photons in terms of a wavepacket in either a frequency or position basis. Authors publishing works in this vein use techniques such as the S-matrix approach [5], finding scattering eigenstates [8, 48], input-output methods [49], Langevin equations of motion [42], or direct integration of the Schrödinger equation [50, 51]. Here we will follow the same procedure as the last two authors and solve the Schrödinger equation directly for an N photon wavepacket interacting with a single two-level-emitter (TLE) at the origin. The results and method presented in this chapter have been published in [12] and goes beyond most other analytic treatments of multiphoton scattering, as we can accurately describe the interaction of any number of photons with a single TLE. We also note that our solutions appear to be identical to that derived concurrently to our work by Roulet et al. in [11].

This chapter is organized as follows. We first demonstrate how to describe our system in the time domain. We next present an analytic result for the scattering of an N-photon wavepacket from a single TLE in a unidirectional waveguide. We convert the solution to a bidirectional geometry and explore how the shape of the photon wavepacket is modified by its interaction with a single TLE. Finally, we connect this to the work of other authors by presenting our results in the frequency domain.

3.1.1 Introducing the time domain

The Hamiltonian presented in Eq. 2.1 is written in terms of time-dependant operators. As such, we choose to quantize the field in terms of the $\hat{A}(t)$ and $\hat{B}(t)$ operators, which

correspond to creating a photon at time t in either the left-going or right-going modes of the waveguide. Formally, these connect to the frequency basis by a Fourier transform, given in Eq. 1.7 and reproduced below for $\hat{A}(t)$.

$$\hat{A}(t) = \frac{1}{\sqrt{2\pi}} \int_{-\infty}^{\infty} d\omega e^{-i\omega t} \hat{a}_\omega \tag{3.1}$$

$\hat{a}_\omega$ is the single-mode right-traveling field operator. As before, these operators satisfy $[\hat{a}_\omega, \hat{a}^\dagger_{\omega'}] = \delta(\omega - \omega')$, which leads to the commutator of $[\hat{A}(t), \hat{A}^\dagger(t')] = \delta(t - t')$.

We now show that this choice of basis fully describes a multimode, multiphoton wavefunction. The positive-frequency component of the electric field operator of a traveling-wave, multimode, one-dimensional field (defined by Eq. 1.1) can be written as

$$E^{(+)}(\tau) = \mathcal{E} e^{-i\omega_F \tau} \int e^{-i\omega\tau} \hat{a}_\omega = \mathcal{E} e^{-i\omega_F \tau} \sqrt{2\pi}\, \hat{A}(\tau) \tag{3.2}$$

where $\tau = t \pm z/c$, depending on the wave's direction of travel, and $\mathcal{E} = \sqrt{\hbar\omega_F / 2\epsilon_0}$. We define ω_F to be the central frequency of the field, and again assume that the bandwidth of the photons is narrow enough that any dependence of $\mathcal{E}$ on ω is negligible.

For such a field it is well-known [52] that the probability to detect two photons at different space-time points τ_1 and τ_2 is given by

$$P(\tau_1, \tau_2) \propto \left\| E^{(+)}(\tau_1) E^{(+)}(\tau_2) |\psi\rangle \right\|^2 \propto \left\| \hat{A}(\tau_1) \hat{A}(\tau_2) |\psi\rangle \right\|^2 \tag{3.3}$$

Recall from Chapter 1 that in general a two-photon wavepacket is given by

$$|\psi\rangle = \frac{1}{\sqrt{2}} \int \int d\omega_1 d\omega_2 \tilde{f}(\omega_1, \omega_2) \hat{a}^\dagger_{\omega_1} \hat{a}^\dagger_{\omega_2} |0\rangle \tag{3.4}$$

Provided that the two photons are in the same mode we can, without loss of generality, assume that $\tilde{f}(\omega_1, \omega_2)$ is symmetric in ω_1, ω_2, as photons are indistinguishable. When the photons are in different modes $\tilde{f}(\omega_1, \omega_2)$ may not be symmetric in ω_1 and ω_2. As long as both photons are guaranteed to be travelling in the same direction we can also assume that the integral of $|\tilde{f}|^2$ is equal to 1.

With all this, the action of $\hat{A}(\tau_a)\hat{A}(\tau_b)$ on $|\psi\rangle$ can be shown to be

$$\hat{A}(\tau_a)\hat{A}(\tau_b)|\psi\rangle = \sqrt{2}f(\tau_a, \tau_b)|0\rangle \tag{3.5}$$

where

$$f(t_1, t_2) = \frac{1}{2\pi}\int\int e^{-i(\omega_1 t_1 + \omega_2 t_2)}\tilde{f}(\omega_1, \omega_2)\, d\omega_1 d\omega_2 \tag{3.6}$$

is the two-dimensional Fourier transform of $\tilde{f}(\omega_1, \omega_2)$, the frequency distribution of the photon wavepacket. As a result, $P(\tau_a, \tau_b)$ of Eq. (3.3) is directly proportional to $|f(\tau_a, \tau_b)|^2$. This allows us to interpret $f(\tau_a, \tau_b)$ as an effective "two-photon wavefunction" in the time domain.

While it is certainly true that photons do not, strictly speaking, have wavefunctions in the Schrödinger sense (as one cannot construct a position operator for them), thinking of Eq. 3.3 as a wavefunction is a good approximation. In all of this work we, like most treatments of quantum optics, are tacitly working in the coulomb gauge and assuming that the electric field is purely transverse. This allows for an effective decoupling of the field that is produced (the photon) from its source. Additionally, this sort of description of a photon as having a wavefunction is consistent with experimental devices, as many kinds of photo-detectors will measure the arrival time of a photon rather than its frequency [53]. Finally, $f(t_1, t_2)$ clearly contains all the information on the state of the field, as it is proportional to $\tilde{f}(\omega_1, \omega_2)$ and its square is always normalized to 1, as is required by a probability distribution.

3.2 General scattered state for a multi-photon pulse

Here we will derive the scattered wavefunction of an N-photon Fock state interacting with a single two-level atom in a unidirectional, or "one-sided," waveguide, meaning that photons will only travel in one direction. While such a system is nontrivial to create (an example of such a atom-waveguide system is given in [21]) the mathematics describing the

interaction are much simpler and, as will be shown, the solution is identical for the standing-wave modes of a bidirectional, or "two-sided" waveguide.

In the interaction picture, the Hamiltonian takes the form

$$H = -i\hbar g\big(\sigma^\dagger \hat{A}(t) - \sigma \hat{A}^\dagger(t)\big) \tag{3.7}$$

where we have defined $\sigma^\dagger$ and σ to be the raising and lowering operators of the atom and $\hat{A}(t)$ to be the traveling-wave modes of the unidirectional waveguide. Note that here we have dropped the subscript for the atom used in Eq. 2.1 (as there is only one). Additionally, g is the frequency-independent coupling constant. In writing Eq. 3.7 we are assuming that the central frequency of the field is equal to the atomic transition frequency (i.e. $\delta = \omega_F - \omega_a = 0$) and that the atom is located at the origin (z=0). In Chapter 4 we will show how to account for significant detuning between the photon and the atom in the time domain (this has already been taken into account in Chapter 2) and in Chapter 5 we will generalize the approach to deal with systems that are not centered at the origin.

As the atom only has two levels, the total state of the system can be given, for any time, by $|\psi\rangle = |\psi_e\rangle \otimes |e\rangle + |\psi_g\rangle \otimes |g\rangle$, where $|e\rangle$ and $|g\rangle$ represent the excited and ground states of the atom and $|\psi_e(t)\rangle$ and $|\psi_g(t)\rangle$ correspond to the field states. We also define the coupling constant $\Gamma = g^2/2$ (which has dimensions of frequency) that is proportional to the inverse of the interaction time. With this, the equations of motion from the Schrödinger equation are

$$|\dot{\psi}_g(t)\rangle = \sqrt{2\Gamma}\hat{A}^\dagger(t)|\psi_e(t)\rangle \tag{3.8}$$

$$|\dot{\psi}_e(t)\rangle = -\sqrt{2\Gamma}\hat{A}(t)|\psi_g(t)\rangle \tag{3.9}$$

In the following derivation we will assume that the atom is initially in the ground state and $|\psi_I\rangle$ is the initial photon wavefunction. We then integrate Eq. 3.8 to obtain

$$|\psi_g(t)\rangle = |\psi_I\rangle + \sqrt{2\Gamma}\int_{-\infty}^{t} dt_1 \hat{A}^\dagger(t_1)\hat{A}^\dagger(t)|\psi_e(t_1)\rangle \tag{3.10}$$

where Eq. 3.10 is then substituted into Eq. 3.9 to obtain

$$|\dot{\psi}_e(t)\rangle = -2\Gamma \int_{-\infty}^{t} dt_1 \hat{A}^\dagger(t_1)\hat{A}(t)|\psi_e(t)\rangle - \sqrt{2\Gamma}\hat{A}(t)|\psi_I\rangle \tag{3.11}$$

From here we normal order the operators $\hat{A}^\dagger(t_1)\hat{A}(t)$ and evaluate the resulting delta function (noting that a factor of 1/2 appears as $\delta(t-t_1) \neq 0$ only at the upper limit of integration). Doing so yields

$$|\dot{\psi}_e(t)\rangle = -\Gamma|\psi_e(t)\rangle - 2\Gamma \int_{-\infty}^{t} dt_1 \hat{A}^\dagger(t_1)\hat{A}(t)|\psi_e(t)\rangle - \sqrt{2\Gamma}\hat{A}(t)|\psi_I\rangle \tag{3.12}$$

Eq. 3.12 can be solved using an integrating factor of $e^{\Gamma t}$ and substituted into itself, becoming

$$|\psi_e(t)\rangle = -\sqrt{2\Gamma}\int_{-\infty}^{t} dt_1 e^{-\Gamma(t-t_1)}\hat{A}(t_1)|\psi_I\rangle - 2\Gamma\int_{-\infty}^{t} dt_1 \int_{-\infty}^{t_1} dt_2 e^{-\Gamma(t-t_1)}\hat{A}^\dagger(t_2)\hat{A}(t_1)|\psi_e(t_2)\rangle \tag{3.13}$$

This represents the beginning of a recursive solution that will eventually truncate after $N-1$ iterations, where N is the number of photons in $|\psi_I\rangle$. The process leading to such a solution is as follows; first, one must substitute Eq. 3.13 into itself. Next, one places all photon operators in normal order using the commutator $[A(t), A^\dagger(t')] = \delta(t-t')$. If the difference in the time indices is more than one, the term containing the delta function will vanish due to the limits of integration.

As an example, consider substituting Eq. 3.13 into itself once. This will yield the following expression;

$$+ 4\Gamma^2 \int_{-\infty}^{t} dt_1 \int_{-\infty}^{t_1} dt_2 \int_{-\infty}^{t_2} dt_3 \int_{-\infty}^{t_3} dt_4 e^{-\Gamma(t_1-t_2)-\Gamma(t_3-t_4)}\hat{A}^\dagger(t_2)\hat{A}(t_1)\hat{A}^\dagger(t_3)\hat{A}(t_4)|\psi_e(t_4)\rangle \tag{3.14}$$

Normal ordering the operators $\hat{A}(t_1)\hat{A}^\dagger(t_3)$ will lead to an integral of the form

$$\int_{-\infty}^{t} dt_1 \int_{-\infty}^{t_1} dt_2 \int_{-\infty}^{t_2} dt_3 \int_{-\infty}^{t_3} dt_4 \delta(t_1-t_3) f(t_1,t_2,t_3,t_4) \tag{3.15}$$

This can be re-written in terms of step functions as

$$\int_{-\infty}^{\infty} dt_1 dt_2 dt_3 dt_4 \Theta(t-t_1)\Theta(t_1-t_2)\Theta(t_2-t_3)\Theta(t_3-t_4)\delta(t_1-t_3)f(t_1,t_2,t_3,t_4) \tag{3.16}$$

Integrating with respect to t_3 yields the step functions $\Theta(t-t_1)\Theta(t_1-t_2)\Theta(t_2-t_1)\Theta(t_1-t_4)$. This restricts integration to the region where the inequality $t \geq t_1 \geq t_2 \geq t_1$ is satisfied. This inequality will only be true at one point, where $t_2 = t_1$. As such, when the t_1 integral is evaluated it will yield zero and the entire term will vanish. This cancellation will always occur provided that the time indices are separated by more than one.

The vanishing of all delta function terms means that under the integrals the photon operators will effectively commute. Therefore, at the k^{th} iteration there will be k lowering operators acting on the initial state and $|\psi_e\rangle$. Once $k = N$ all further iterations will yield zero as there will be more lowering operators than excitations to remove. We present the first few terms of the iteration below.

$$\begin{aligned}
|\psi_e(t)\rangle = &-\sqrt{2\Gamma}\int_{-\infty}^{t} dt_1 e^{-\Gamma(t-t_1)}\hat{A}(t_1)|\psi_I\rangle \\
&+(2\Gamma)^{3/2}\int_{-\infty}^{t} dt_1 \int_{-\infty}^{t_1} dt_2 \int_{-\infty}^{t_2} dt_3 e^{-\Gamma(t-t_1)}e^{-\Gamma(t_2-t_3)}\hat{A}^\dagger(t_2)\hat{A}(t_1)A(t_3)|\psi_I\rangle \\
&-(2\Gamma)^{5/2}\int_{-\infty}^{t} dt_1 \int_{-\infty}^{t_1} dt_2 \int_{-\infty}^{t_2} dt_3 \int_{-\infty}^{t_3} dt_4 \int_{-\infty}^{t_4} dt_5 \\
&e^{-\Gamma(t-t_1)}e^{-\Gamma(t_2-t_3)}e^{-\Gamma(t_4-t_5)}\hat{A}^\dagger(t_2)\hat{A}^\dagger(t_4)\hat{A}(t_1)\hat{A}(t_3)\hat{A}(t_5)|\psi_I\rangle + \ldots
\end{aligned} \tag{3.17}$$

The coefficient in front of the k^{th} term is given by $(2\Gamma)^{k+\frac{1}{2}}(-1)^{k+1}$ and each successive term will add an extra $\hat{A}^\dagger(t_k)e^{-\Gamma(t_k-t_{k+1})}\hat{A}(t_{k+1})$. This can in turn be used to write down $|\psi_e(t)\rangle$ for an arbitrary $|\psi_I\rangle$.

We now substitute Eq. 3.17 into Eq. 3.10 and let $t \to \infty$ to find the scattered state of

the photons after all interaction with the atom has ceased. This is given as

$$|\psi_g(\infty)\rangle = |\psi_I\rangle - 2\Gamma \int_{-\infty}^{\infty} dt_1 \int_{-\infty}^{t_1} dt_2 e^{-\Gamma(t_1-t_2)} \hat{A}^\dagger(t_1)\hat{A}(t_2)|\psi_I\rangle$$
$$+(2\Gamma)^2 \int_{-\infty}^{\infty} dt_1 \int_{-\infty}^{t_1} dt_2 \int_{-\infty}^{t_2} dt_3 \int_{-\infty}^{t_3} dt_4 e^{-\Gamma(t_1-t_2)} e^{-\Gamma(t_3-t_4)} \hat{A}^\dagger(t_1)\hat{A}^\dagger(t_3)\hat{A}(t_2)\hat{A}(t_4)|\psi_I\rangle$$
$$-(2\Gamma)^3 \int_{-\infty}^{\infty} dt_1 \int_{-\infty}^{t_1} dt_2 \int_{-\infty}^{t_2} dt_3 \int_{-\infty}^{t_3} dt_4 \int_{-\infty}^{t_4} dt_5 \int_{-\infty}^{t_5} dt_6$$
$$e^{-\Gamma(t_1-t_2)} e^{-\Gamma(t_3-t_4)} e^{-\Gamma(t_5-t_6)} \hat{A}^\dagger(t_1)\hat{A}^\dagger(t_3)\hat{A}^\dagger(t_5)\hat{A}(t_2)\hat{A}(t_3)\hat{A}(t_6)|\psi_I\rangle + \ldots \tag{3.18}$$

As we will show in the next section, this equation allows one to easily obtain the scattered state of the photons. We also note that Eq. 3.17 and Eq. 3.18 can be used to obtain the evolution of the excited state of the atom and the field as a function of time by not letting $t \to \infty$ in Eq. 3.18, though generally obtaining such results will require numerical integration.

Additionally, while we are not considering the case of far-detuned photons here, as we will show in Chapters 4 and 5, if the photon is significantly detuned from resonance the solution will have exactly the same form as presented in Eq. 3.17 but with $\Gamma \equiv g^2/2 - i\delta$, where δ is the frequency difference between the atom and the incoming photon. This is also the same form as the the effective coupling and detuning of a pair of atoms described in Section 2.4.1.

3.2.1 The single photon case

Starting with Eq. 3.18 we first consider the scattering of a single photon from a single emitter. In this case, the initial photon state has the form

$$|\psi_I\rangle = \int dt f(t)\hat{A}^\dagger(t)|0\rangle \tag{3.19}$$

with $f(t)$ describing the space-time profile of the photon as would be measured by a photo-detector. Substituting this into Eq. 3.18, only the first two terms survive, as all

other terms contain two or more lowering operators. This leads to

$$|\psi_g(\infty)\rangle = |\psi_I\rangle - 2\Gamma \int_{-\infty}^{\infty} dt_1 \int_{-\infty}^{t_1} dt_2 e^{-\Gamma(t_1-t_2)} \hat{A}^\dagger(t_1)\hat{A}(t_2)|\psi_I\rangle \tag{3.20}$$

Evaluating this expression gives a final, scattered state of

$$|\psi_g(\infty)\rangle = \int dt f(t)\hat{A}^\dagger(t)|0\rangle - 2\Gamma \int_{-\infty}^{\infty} dt \int_{-\infty}^{t} dt_1 e^{-\Gamma(t-t_1)} f(t_1)\hat{A}^\dagger(t_1)|\psi_0\rangle \tag{3.21}$$

The spacetime profile $f_g(t)$ of the scattered state of the photon, related to the overall state by $|\psi_g(\infty)\rangle = \int dt f_g(t)\hat{A}^\dagger(t)|0\rangle$, is then

$$f_g(t) = f(t) - 2\Gamma G_\Gamma(t) \tag{3.22}$$

where we have defined the function G_Γ as

$$G_\Gamma(t) = e^{-\Gamma t} \int_{-\infty}^{t} e^{\Gamma t'} f(t') dt' \tag{3.23}$$

which, by the first term in Eq. 3.17 is (up to a factor of $\sqrt{2\Gamma}$) the single-photon excitation probability amplitude. The expression in Eq. 3.22 then is simply the sum of the probability amplitude that the photon does not interact with the atom ($f(t)$) with the probability that the atom was excited. As we are working with a unidirectional waveguide the photon is guaranteed to scatter into the same spatial mode, and this function represents the distortion to the space-time profile caused by the interaction with the atom.

It is also worth noting that the frequency representation of this interaction is exactly equal to Eq. 2.41, that is

$$\mathcal{F}[f_g(t)] = \frac{1}{\sqrt{2\pi}} \int_{-\infty}^{\infty} dt e^{i\omega t} f_g(t) = -\frac{\Gamma + i\omega}{\Gamma - i\omega} \tilde{f}(\omega) \tag{3.24}$$

In terms of frequency, a single atom in a unidirectional geometry will add a frequency-dependent phase but not modify the overall distribution of the photon.

3.2.2 The two photon case

We now turn our attention to the particular case where the initial state consists of only two photons. In terms of the space-time description previously described, $|\psi_I\rangle$ can be written as

$$|\psi_I\rangle = \frac{1}{\sqrt{2}} \int \int dt_1 dt_2 f(t_1, t_2) \hat{A}^\dagger(t_1) \hat{A}^\dagger(t_2) |0\rangle \tag{3.25}$$

where $f(t_1, t_2)$ represents the space-time profile of the pulse as would be measured by a photo-detector. Using this initial state in Eq. 3.18 yields

$$\begin{aligned} |\psi_g(\infty)\rangle = \frac{1}{\sqrt{2}} \int_{-\infty}^{\infty} dt_1 \int_{-\infty}^{\infty} dt_2 f(t_1, t_2) \hat{A}^\dagger(t_1) \hat{A}^\dagger(t_2) |0\rangle \\ -2\sqrt{2}\,\Gamma \int_{-\infty}^{\infty} dt_1 \int_{-\infty}^{\infty} dt_2 \int_{-\infty}^{t_2} dt_3 e^{-\Gamma(t_2 - t_3)} f(t_1, t_3) \hat{A}^\dagger(t_1) \hat{A}^\dagger(t_2) |0\rangle \\ +4\sqrt{2}\,\Gamma^2 \int_{-\infty}^{\infty} dt_1 \int_{-\infty}^{t_1} dt_2 \int_{-\infty}^{t_2} dt_3 \int_{-\infty}^{t_3} dt_4 e^{-\Gamma(t_1 - t_2)} e^{-\Gamma(t_3 - t_4)} f(t_2, t_4) \hat{A}^\dagger(t_1) \hat{A}^\dagger(t_3) |0\rangle \end{aligned} \tag{3.26}$$

Here, the first term corresponds to the photons not interacting with the atom at all, the second to only one photon interacting with the atom, and the third to the case where both photons interact with the atom. Because of these three separate processes, we express the final scattered space-time profile in terms of $f_g(t_1, t_2) = f(t_1, t_2) + f_1(t_1, t_2) + f_2(t_1, t_2)$. For a particular form of f, the component $f_1(t_1, t_2)$ is easy to evaluate, as it corresponds to a single integral. It is given by

$$f_1(t_1, t_2) = -2\Gamma \int_{-\infty}^{t_1} dt' e^{-\Gamma(t_1 - t')} f(t', t_2) - 2\Gamma \int_{-\infty}^{t_2} dt' e^{-\Gamma(t_2 - t')} f(t_1, t') \tag{3.27}$$

This result has a physically intuitive interpretation. It represents the process in which one of the photons does not interact with the atom while the other photon is absorbed at t' and emitted at a later time, with the separation in time being governed by the exponential decay rate of Γ.

Note that this expression is explicitly symmetric in t_1 and t_2 while the integral in Eq. 3.26 is not. We have chosen to present it this way in order to highlight the fact that the

final wavefunction must be symmetric. Physically, this arises because the two photons are indistinguishable, as they are travelling in the same direction and have the same polarization. Mathematically, it arises from the ambiguity in assigning variables under integration. As an example of what we mean, consider that the total scattered state is given by

$$\begin{aligned}|\psi_g\rangle &= \frac{1}{\sqrt{2}}\int dt_a dt_b f_g(t_a,t_b)\hat{A}^\dagger(t_a)\hat{A}^\dagger(t_b)|0\rangle \\ &= \frac{1}{\sqrt{2}}\int dt_1 dt_1 \big[f(t_1,t_2)+f_1(t_1,t_2)+f_2(t_1,t_2)\big]\hat{A}^\dagger(t_1)\hat{A}^\dagger(t_2)|0\rangle \end{aligned} \tag{3.28}$$

As the integration is over both variables, and all variables are matched with the same $\hat{A}$ photon mode, it is valid to assign $t_1 = t_a$ or $t_2 = t_a$ when comparing the profile functions. As both choices are valid, the final state must exhibit this ambiguity, and therefore is symmetric in its component variables. We note also that we can force the function to be symmetric by simply using the fact that, if f_1 is symmetric, then $f_1(t_1,t_2) = 1/2\Big(f_1(t_1,t_2)+f_1(t_2,t_1)\Big)$.

With this in mind, we consider the third and final term in the scattered state. To write this in a meaningful way, we first convert the integral over t_3 from $\int_{-\infty}^{t_2} dt_3$ to $\int_{-\infty}^{\infty} dt_3\Theta(t_2-t_3)$. This allows us to extract only the functional form of f_2, which can be written (after symmetrizing the function) in terms of f_1 as

$$f_2(t_1,t_2) = -\Gamma\Theta(t_1-t_2)\int_{t_2}^{t_1} e^{-\Gamma(t_1-t')}f_1(t_2,t')\,dt' - \Gamma\Theta(t_2-t_1)\int_{t_1}^{t_2} e^{-\Gamma(t_2-t')}f_1(t_1,t')\,dt' \tag{3.29}$$

As also described in [11], the form of f_2 arises from the fact that two photons cannot be absorbed at the same time by a system with only one excited state. To see how, consider the first term multiplied by $\Theta(t_1-t_2)$: this step function ensures that $t_1 \geq t_2$. f_2 then represents the process where one photon is absorbed and emitted at t_2, shown by the function $f_1(t_2,t')$. At a time $t' \geq t_2$ (enforced by the limits on the integral) a second photon is absorbed and is re-emitted at time t_1.

We now consider a particular class of initial states; when the photons are identical and

initially uncorrelated so that $f(t_1, t_2) = f(t_1)f(t_2)$. With this, the above result for $f_g(t_1, t_2)$ reduces to the relatively compact form of

$$f(t_1, t_2) = \Big(f(t_1) - 2\Gamma G_\Gamma(t_1)\Big)\Big(f(t_2) - 2\Gamma G_\Gamma(t_2)\Big) - 4\Gamma^2 e^{-\Gamma|t_1 - t_2|} G_\Gamma^2(t_<) \tag{3.30}$$

where $t_<$ is the smallest of t_1, t_2. To derive this we performed an integration by parts in Eq. 3.29 using $u = \Theta(t_2 - t_3)$ and $v = \int_{-\infty}^{t_2} dt' \Theta(t_1 - t') e^{-\Gamma(t_1 - t_2)} f(t_2, t_4)$. Simplifying the result and symmetrizing the final solution yields the above form of Eq. 3.30.

The first term in Eq. 3.30 is explicitly factorizable, meaning here that the wavepackets of the two photons can be written as a product of the form $|\psi\rangle \otimes |\psi\rangle$. Practically, in this formalism it means that the wavefunction can be written as a product of functions of the form $f(t_1)f(t_2)$. It is important to note here that the function $f(t) - 2\Gamma G_\Gamma(t)$ is exactly the scattered state of a single photon, and the whole product state represents the two photons interacting with the atom independently of one another.

The second term is a time- (or frequency-) entangled state. This has been described in other literature as well, being called a "bound" state in [5] and a "nonlinear" term in [50]. The origin of the terminology of bound state is that, while the photons are travelling in the same direction, the probability to detect both photons is limited by $e^{-\Gamma|t_1 - t_2|}$. This would lead to an exponential decay in the probability to detect two photons separated by a spacetime distance $\tau = t - z/c$, just as what would be expected in the bound state found in materials.

There has been a decent amount of research on two-photon bound states in different systems [45, 54, 55] along with a recent experimental demonstration [56]. We will not use the terminology of a bound state, however, as we will show that photons traveling in opposite directions can also have their detection times correlated by the same function. This is an entanglement effect and we will refer to it as such in the rest of our work, defining the function

$$f_{\text{ent}}(t_1, t_2) \equiv -4\Gamma^2 \, e^{-\Gamma|t_1 - t_2|} G_\Gamma^2(t_<) \tag{3.31}$$

to represent the entangled component of the photons.

This entanglement ultimately arises from the inherent nonlinearity of the two level emitter, that only one photon can be absorbed at a time. The particular form of f_{ent} suggests, however, that it also can be explained as an example of stimulated emission or stimulated absorption. As $G_\Gamma(t)$ is evaluated twice at the same time argument, it suggests that the photons are only entangled when they excite the atom essentially simultaneously at the earlier of the two times t_1 and t_2. They can be detected at different times due to the finite lifetime of $1/\Gamma$ of the excited state providing some uncertainty as to when they are emitted.

Additionally, we point out that one can view the two-photon state described by 3.31 as an example of the time-entangled states considered by Franson [57]. Such states are in turn similar to the Einstein-Podolsky-Rosen entangled states [58], where the properties that become well-defined here (provided that $\Gamma \to \infty$) are the energy given by $\omega_1 + \omega_2$ (see Eq. 3.56 for details) and the separation in emission times $t_1 - t_2$.

3.2.3 Higher photon numbers and extensions

The solution in Eq. 3.18 is not limited to two photons; the recursive formalism can clearly be continued N times to deal with a different $|\psi_I\rangle$. As this continues, the expression quickly becomes cumbersome. As such, for clarity we will focus on states of N photons that are factorizable. These are essentially multimode Fock states and are defined by

$$|N\rangle = \frac{1}{\sqrt{N!}} \left(\int dt f(t) \hat{A}^\dagger(t) \right)^N |0\rangle \tag{3.32}$$

$|N\rangle$ has the property that $\hat{A}(t)|N\rangle = \sqrt{N}\, f(t)|N-1\rangle$, just as one would expect for a Fock state. Unfortunately, it is *not* true that $\hat{A}^\dagger|N\rangle = \sqrt{N+1} f(t)|N+1\rangle$. Using this

particular state, we re-write Eq. 3.18 below.

$$|\psi_g(\infty)\rangle = |N\rangle - 2\Gamma\sqrt{N}\int_{-\infty}^{\infty} dt_1 G_\Gamma(t_1)\hat{A}^\dagger(t_1)|N-1\rangle$$
$$+(2\Gamma)^2\sqrt{N(N-1)}\int_{-\infty}^{\infty} dt_1\int_{-\infty}^{t_1} dt_2\Big(G_\Gamma(t_1) - e^{\Gamma(t_1-t_2)}G_\Gamma(t_2)\Big)G_\Gamma(t_2)\hat{A}^\dagger(t_1)\hat{A}^\dagger(t_2)|N-2\rangle$$
$$-(2\Gamma)^3\sqrt{N(N-1)(N-2)}\int_{-\infty}^{\infty} dt_1\int_{-\infty}^{t_1} dt_2\int_{-\infty}^{t_2} dt_3\Big(G_\Gamma(t_1)$$
$$-e^{-\Gamma(t_1-t_2)}G_\Gamma(t_2)\Big)\Big(G_\Gamma(t_2) - e^{-\Gamma(t_2-t_3)}G_\Gamma(t_3)\Big)G_\Gamma(t_3)\hat{A}^\dagger(t_1)\hat{A}^\dagger(t_2)\hat{A}^\dagger(t_3)|N-3\rangle + \ldots \quad (3.33)$$

With this, one can directly write the final state for any initial $|N\rangle$. We present an explicit form for $N = 3$ in Eq. 3.34. Care must be taken to symmetrize the state properly and, for brevity, we choose to leave our expression in the raw, asymmetric form.

$$f(t_1,t_2,t_3) = \prod_{i=1}^{3}(f(t_i) - 2\Gamma G_\Gamma(t_i)) - (2\Gamma)^2\sum_{i=1}^{3} f(t_i)e^{-\Gamma|t_j-t_k|}G_\Gamma^2(\min(t_j,t_k))$$
$$+(2\Gamma)^3\sqrt{6}\Big[e^{-\Gamma(t_2-t_3)}G_\Gamma(t_1)G_\Gamma^2(t_3) - e^{-\Gamma(t_1-t_3)}G_\Gamma(t_2)G_\Gamma^2(t_3)$$
$$+ e^{-\Gamma(t_1-t_2)}G_\Gamma^2(t_2)G_\Gamma(t_3)\Big]\Theta(t_1-t_2)\Theta(t_2-t_3) \quad (3.34)$$

In this expression, the first two terms clearly relate to the $N = 2$ case. The first arises from three independent single-photon interactions, similar to the first term of Eq. 3.30. The second gives the case where two photons interact with the atom and become entangled as described by Eq. 3.31, while the third photon is a "spectator" and does not become entangled. The final term describes the entanglement between all three photons produced by the nonlinear nature of the emitter constraining the absorption times of each individual photon.

3.3 Extending the two-photon solution to a bidirectional geometry

3.3.1 General formalism

We now return to studying the case of an incident two-photon, symmetric pulse, but now consider a two-level-emitter coupled to both left- and right-traveling wave modes in a waveguide. As such, we again map the operators $\hat{A}(t)$ and $\hat{B}(t)$ to the different directions

of propagation. As in Eq. 3.7, we will assume that the atom is at the origin. With these two modes, the Hamiltonian becomes

$$H = -i\hbar g\sigma_+\Big(A(t) + B(t)\Big) + i\hbar g\sigma_-\Big(\hat{A}^\dagger(t) + \hat{B}^\dagger(t)\Big) \tag{3.35}$$

By defining the time-domain standing wave operators $\hat{C}(t) = \frac{1}{\sqrt{2}}\big(\hat{A}(t) + \hat{B}(t)\big)$ and $\hat{D}(t) = \frac{1}{\sqrt{2}}\big(\hat{A}(t) - \hat{B}(t)\big)$ (see Section 1.2.1 for more details on how to access the standing wave modes) the Hamiltonian becomes

$$H = -i\hbar g\sqrt{2}\Big(\sigma_+\hat{C}(t) - \sigma_-\hat{C}^\dagger(t)\Big) \tag{3.36}$$

which is exactly the same in form as Eq. 3.7, excepting the factor of $\sqrt{2}$. As a result, by defining $\Gamma = g^2$ in the bidirectional geometry and writing a traveling field in terms of standing wave modes, we can use the same general solution derived in Eq. 3.18, except with $\hat{A}$ being replaced by $\hat{C}$.

With both directions of propagation being considered, a general wavepacket describing an identical set of M left-traveling photons and N right-traveling photons is given by

$$|\psi_I\rangle = |M, N\rangle \equiv \frac{1}{\sqrt{M!N!}}\left(\int dt f(t)\hat{A}^\dagger(t)\right)^M\left(\int dt f(t)\hat{B}^\dagger(t)\right)^N|0,0\rangle \tag{3.37}$$

where again $f(t)$ describes the spacetime profile of the pulse, connected to the pulse's spectrum by $\tilde{f}(\omega) = \frac{1}{\sqrt{2\pi}}\int dt f(t)e^{i\omega t}$. For future reference, we also note that the action of $\hat{C}(t)$ on such a state is given by

$$\hat{C}(t)|M, N\rangle = \frac{f(t)}{\sqrt{2}}\Big(\sqrt{M}|M-1, N\rangle + \sqrt{N}|M, N-1\rangle\Big) \tag{3.38}$$

3.3.2 Two photons arriving from the same direction ($M = 2, N = 0$)

We first consider the case where the two photons are initially travelling to the right, which in terms of Eq. 3.37 is given by $|\psi_I\rangle = |2, 0\rangle$. By replacing the $\hat{A}(t)$ operators in Eq.

3.18 with $\hat{C}(t)$ operators and substituting this state into the equation we arrive at

$$|\psi_g(\infty)\rangle = |2,0\rangle - 2\Gamma \int_{-\infty}^{\infty} dt G_\Gamma(t)\hat{C}^\dagger(t)|1,0\rangle \\ + 2\sqrt{2}\Gamma^2 \int_{-\infty}^{\infty} dt \int_{-\infty}^{t} dt' G_\Gamma(t')[G_\Gamma(t) - e^{\Gamma(t'-t)}G_\Gamma(t')]\hat{C}^\dagger(t)\hat{C}^\dagger(t')|0,0\rangle \tag{3.39}$$

for the final scattered state in terms of G_Γ defined in Eq. 3.23.

From here, we convert the standing wave $\hat{C}$ operators back into traveling wave modes $\hat{A}$ and $\hat{B}$ and collect the terms into the component where both photons are transmitted ($f_{a_{2,0}}$), where both photons are reflected ($f_{b_{2,0}}$), and the "split" part where the photons end up in different modes ($f_{\mathrm{split}_{2,0}}$). The corresponding spacetime probability amplitudes are

$$\begin{aligned} f_{a_{2,0}}(t_1,t_2) &= \big(f(t_1) - \Gamma G_\Gamma(t_1)\big)\big(f(t_2) - \Gamma G_\Gamma(t_2)\big) + \frac{1}{4} f_{\mathrm{ent}}(t_1,t_2) \\ f_{b_{2,0}}(t_1,t_2) &= \Gamma^2 G_\Gamma(t_1) G_\Gamma(t_2) + \frac{1}{4} f_{\mathrm{ent}}(t_1,t_2) \\ f_{\mathrm{split}_{2,0}}(t_1,t_2) &= -\sqrt{2}\,\Gamma\big(f(t_1) - \Gamma G_\Gamma(t_1)\big) G_\Gamma(t_2) + \frac{\sqrt{2}}{4} f_{\mathrm{ent}}(t_1,t_2) \end{aligned} \tag{3.40}$$

Here we note that $f_{a_{2,0}}$ and $f_{b_{2,0}}$ are explicitly symmetric but $f_{\mathrm{split}_{2,0}}$ is asymmetric, as the operator product $A^\dagger(t_1)B^\dagger(t_2)$ represents distinguishable modes and the reflected photon (indexed by t_2) may have a different shape than the transmitted one. This component also has an extra factor of $\sqrt{2}$ due to the fact that it contains one photon in each mode, and thus has a different normalization than the states with both photons co-propagating (see Eq. 3.37 for the factors).

It turns out that the Fourier transform of $f(t_1) - \Gamma G_\Gamma(t_1)$ is $t(\omega)\tilde{f}(\omega) = -i\frac{\omega}{\Gamma - i\omega}\tilde{f}(\omega)$ and the Fourier transform of $-\Gamma^2 G_\Gamma(t_1)$ is $r(\omega)\tilde{f}(\omega) = -\frac{\Gamma}{\Gamma - i\omega}\tilde{f}(\omega)$. These are identical to the reflection and transmission coefficients defined in Eq. 2.21 for a single photon and single atom, provided that the atom is at the origin ($z = 0$) and the photons are on resonance ($\delta = 0$). With this, the form of the wavefunction in Eq. 3.40 make intuitive sense; the function $f_{a_{2,0}}$ consists of a term that gives the probability amplitude of both photons being transmitted and the entanglement generated by their interaction with the atom. Similarly, $f_{b_{2,0}}$ gives the result for both photons being reflected and being entangled

by the atom. Finally $f_{\mathrm{split}_{2,0}}$ describes one photon being transmitted and one being reflected. We also point out that the entangled term f_{ent} appears in all three possible outcomes. This is most interesting in the "split" case, as the two photons can be measured at far separated points in space yet still have their detection times correlated.

Next, we present results for the properties of the scattered state. We will use two different wavepackets. One is a Gaussian defined by

$$f(t) = \frac{1}{\sqrt{T\sqrt{2\pi}}} e^{-t^2/4T^2} \tag{3.41}$$

For this pulse the function $G_\Gamma(t)$ is

$$G_\Gamma(t) = \sqrt[4]{\frac{\pi}{2}}\sqrt{T}\, e^{\Gamma^2 T^2}\, e^{-\Gamma t}\left(\mathrm{erf}\left(\frac{t}{2T} - \Gamma T\right) + 1\right) \tag{3.42}$$

The other pulse shape we will consider is a smooth "square" (or "flat-top") pulse defined by

$$f(t) = \frac{1}{2\sqrt{\mathcal{N}}}\Big(\mathrm{erf}\big[a(t-t_0)\big] - \mathrm{erf}\big[a(t-\mathcal{T}-t_0)\big]\Big) \tag{3.43}$$

where the normalization factor $\mathcal{N}$ is

$$\mathcal{N} = \frac{1}{a}\sqrt{\frac{2}{\pi}}\left(e^{-a^2\mathcal{T}^2/2} - 1\right) + \mathcal{T}\,\mathrm{erf}\left(\frac{a\mathcal{T}}{\sqrt{2}}\right) \tag{3.44}$$

For this pulse, a (which will be 1 in what follows) describes the rate at which the pulse rises and $\mathcal{T}$ describes the pulse's approximate width. To more fairly compare the two pulses we use the standard deviation as our measure of pulse width. For the Gaussian pulse, the standard deviation is simply $\sigma_t = T$ whereas for the "flat-top" pulse it is given by $\sigma_t \equiv \left[\int dt f^2(t) t^2\right]^{1/2}$. For $\mathcal{T}$ greater than about .5 this has the approximate form of $\sigma_t \simeq 0.283\mathcal{T} - 0.098$. As will be shown, using this to define a dimensionless coupling parameter $\Gamma\sigma_t$ and dimensionless time variable t_i/σ_t yields comparable results when comparing the two pulses.

The function G_Γ for the flat top pulse has the analytic form

$$G_\Gamma(t) = \frac{f(t)}{\Gamma} + \frac{e^{-\Gamma t}}{2\Gamma\sqrt{\mathcal{N}}}\left(e^{\Gamma(4a(t_0+\mathcal{T})+\Gamma)/4a^2}\text{erfc}\left(\frac{\Gamma}{2a} - at + t_0 + \mathcal{T}\right) \right.$$
$$\left. - e^{\Gamma(4at_0+\Gamma)/4a^2}\text{erfc}\left(\frac{\Gamma}{2a} - at + t_0\right)\right) \tag{3.45}$$

Regardless of the shape of the pulse, each of the functions in Eq. 3.40 gives the overall probability of the respective scattering process. Fig. 3.1 describes the probabilities of each process, plotted as a function of the dimensionless coupling $\Gamma\sigma_t$.

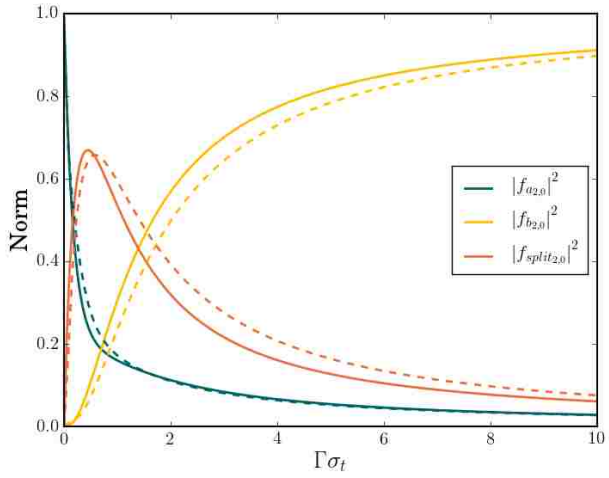

Figure 3.1: The probabilities to find the two photons in the right-traveling modes, left-traveling modes, or one left and one right mode, after interacting with the atom, as a function of $\Gamma\sigma_t$ for the Gaussian pulse (solid line) and the flat top pulse (dashed line).

As can be seen, for large enough coupling (or equivalently a long enough pulse duration) it becomes overwhelmingly likely that both photons will be reflected. In the intermediate regime there is a maximum probability of .669 for the two photons to be split equally among the two directions of the waveguide. If the coupling is small or the pulse is short, photons are transmitted with probability approaching one.

We will also consider the specific way the pulses change shape as a result of their interaction with the atom by looking at the photon detection probabilities given by $|f_{a_{2,0}}|^2$, $|f_{b_{2,0}}|^2$, and $|f_{\text{split}_{2,0}}|^2$. We first consider the modification of a Gaussian pulse as shown in

Fig. 3.2. As can be seen, for small enough ΓT the transmitted and split scattering events display a relatively large component delayed in time. For the split case, this delayed component is primarily in the reflected photon. As ΓT increases (corresponding to a longer pulse or stronger coupling) the delay becomes much less significant. In this limit, the detection probability of the two reflected photons increases and is symmetrically delayed relative to the initial pulse while the other two distributions become much narrower. When ΓT is very large the transmitted and split possibilities have very strongly bunched peaks corresponding primarily to the presence of f_{ent} in each of the states. The reflected component strongly resembles the original pulse, but is missing a "slice" in the middle, which indicates it is antibunched as $f_{b_{2,0}}(\tau, \tau) = 0$. This 'missing' component arises from destructive interference between the components of the state.

We also plot the detection probabilities for the flat-top pulse in Fig. 3.3. While the results for this initial pulse shape are similar to those seen in Fig. 3.2, the fact that it has sharp edges leads to some differences. Aspects of the functions, such as those appearing in Fig. 3.2d, are now at the trailing edge of the flat top pulse (see Fig. 3.3a or 3.3d). Additionally, Fig. 3.3g shows a tendency to find the reflected photons to be detected near the edges of the pulse, while Figs. 3.3h and 3.3k demonstrate that it is possible to find the transmitted photon inside and the reflected photon near the edge of the pulse. (These results are similar to the "edge effects" predicted for sharp square pulses in [50].)

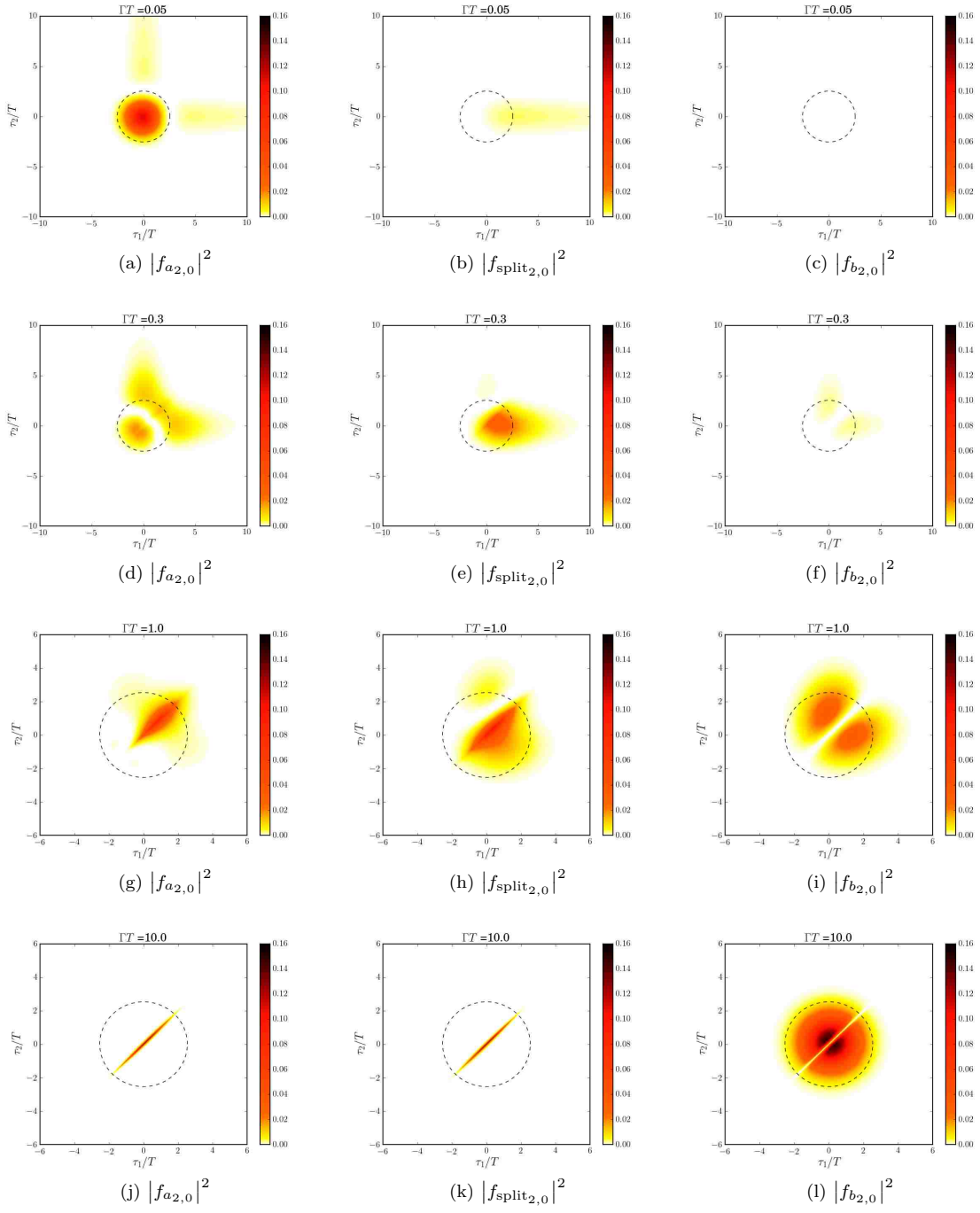

(a) $|f_{a_{2,0}}|^2$ (b) $|f_{\mathrm{split}_{2,0}}|^2$ (c) $|f_{b_{2,0}}|^2$

(d) $|f_{a_{2,0}}|^2$ (e) $|f_{\mathrm{split}_{2,0}}|^2$ (f) $|f_{b_{2,0}}|^2$

(g) $|f_{a_{2,0}}|^2$ (h) $|f_{\mathrm{split}_{2,0}}|^2$ (i) $|f_{b_{2,0}}|^2$

(j) $|f_{a_{2,0}}|^2$ (k) $|f_{\mathrm{split}_{2,0}}|^2$ (l) $|f_{b_{2,0}}|^2$

Figure 3.2: Detection probabilities for both photons being found in the $\hat{A}$ mode (both transmitted, leftmost column), $\hat{B}$ mode (both reflected, rightmost column), or one in each (middle column). ΓT is as labeled. The dotted circle gives the shape of the initial Gaussian pulse.

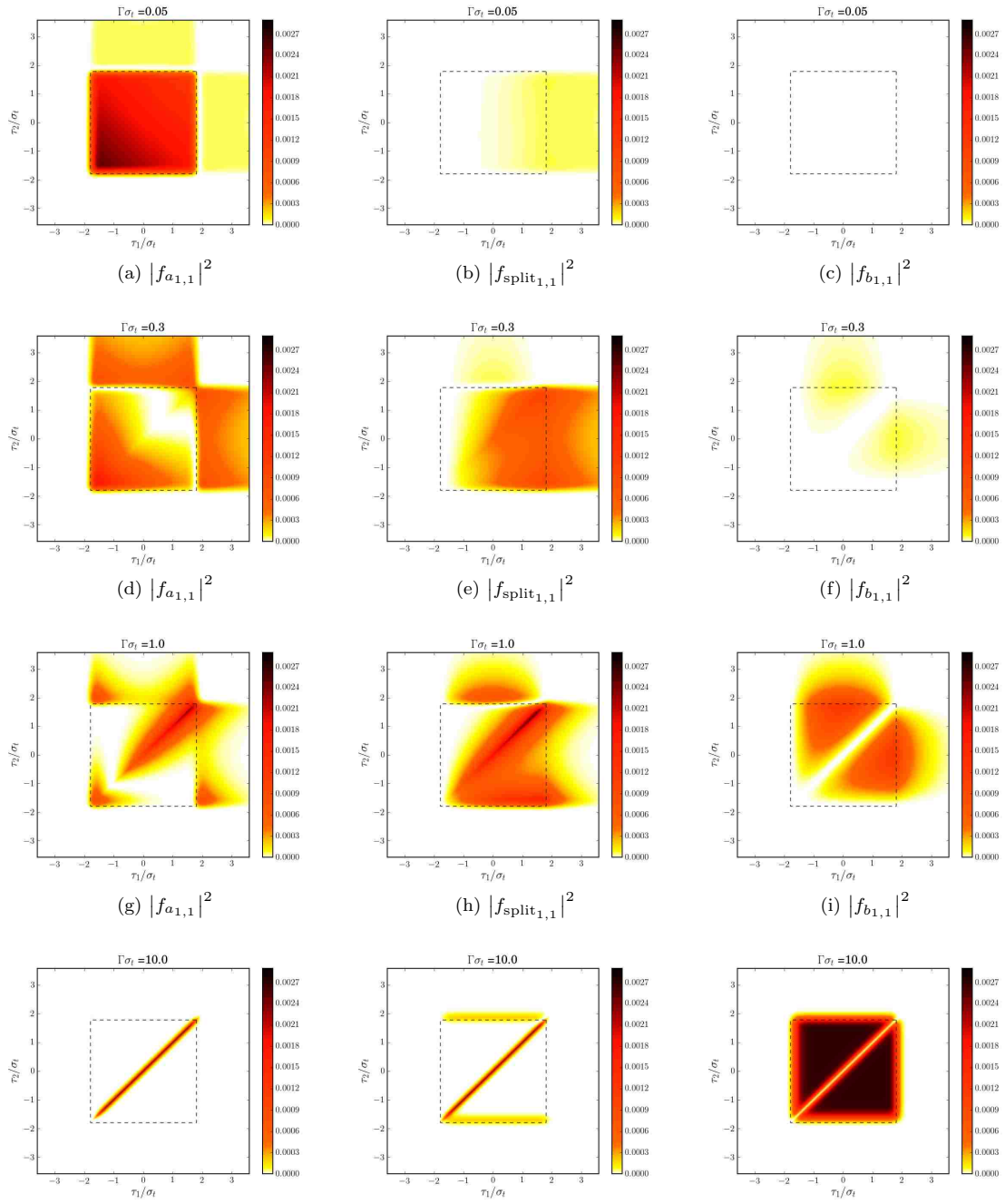

(a) $|f_{a_{1,1}}|^2$ (b) $|f_{\mathrm{split}_{1,1}}|^2$ (c) $|f_{b_{1,1}}|^2$

(d) $|f_{a_{1,1}}|^2$ (e) $|f_{\mathrm{split}_{1,1}}|^2$ (f) $|f_{b_{1,1}}|^2$

(g) $|f_{a_{1,1}}|^2$ (h) $|f_{\mathrm{split}_{1,1}}|^2$ (i) $|f_{b_{1,1}}|^2$

(j) $|f_{a_{1,1}}|^2$ (k) $|f_{\mathrm{split}_{1,1}}|^2$ (l) $|f_{b_{1,1}}|^2$

Figure 3.3: The same as for figure 6, but for a smooth square pulse. Note that the dotted square corresponds to the area of the initial pulse in all images.

3.3.3 Two photons arriving from opposite directions ($M = 1$, $N = 1$)

We also turn our attention to consider a pulse in which one photon comes from the right and another from the left. We can express this initial state as

$$\begin{aligned}|1,1\rangle &= \int_{-\infty}^{\infty} dt_1 \int_{-\infty}^{\infty} dt_2\, f(t_1) f(t_2) \hat{A}^\dagger(t_1) \hat{B}^\dagger(t_2) |0,0\rangle \\ &= \frac{1}{2} \int_{-\infty}^{\infty} dt_1 \int_{-\infty}^{\infty} dt_2\, f(t_1) f(t_2) \left(\hat{C}^\dagger(t_1) \hat{C}^\dagger(t_2) - \hat{D}^\dagger(t_1) \hat{D}^\dagger(t_2) \right) |0,0\rangle \end{aligned} \tag{3.46}$$

As there are no cross-terms, this is relatively straightforward to evaluate: the final result will involve the equivalent unidirectional result presented in Eq. 3.30 on the component with $\hat{C}$ modes and will leave the $\hat{D}$ mode component unchanged. In terms of traveling-wave modes, this leads to the solution of

$$\begin{aligned} f_{a_{1,1}}(t_1,t_2) = f_{b_{1,1}}(t_1,t_2) =& \frac{1}{\sqrt{2}} \Big(-\Gamma G_\Gamma(t_1) \big(f(t_2) - \Gamma G_\Gamma(t_2) \big) \\ & - \big(f(t_1) - \Gamma G_\Gamma(t_1) \big) \Gamma G_\Gamma(t_2) + \frac{1}{2} f_{\text{ent}}(t_1,t_2) \Big) \\ f_{\text{split}_{1,1}}(t_1,t_2) =& \big(f(t_1) - \Gamma G_\Gamma(t_1) \big) \big(f(t_2) - \Gamma G_\Gamma(t_2) \big) + \Gamma^2 G_\Gamma(t_1) G_\Gamma(t_2) + \frac{1}{2} f_{\text{ent}}(t_1,t_2) \end{aligned} \tag{3.47}$$

By comparing this with Eq. 3.40 one can see that the case when the two photons leave in the same direction can be expressed as a sum of the two "split" processes in Eq. 3.40. This makes physical sense, because for the two photons to be found in the same mode one must be transmitted, one must be reflected, and both processes are indistinguishable. In the same way the "split" case is the sum of the outcomes in Eq. 3.40 in which both photons are transmitted or both photons are reflected. These observations are perhaps easier to see by comparison with the frequency mode results, as shown in Eq. 3.59 the end of this chapter.

We note that the addition of these processes occurs at the level of the probability *amplitudes* so the actual probabilities of each event are not additive. This fact plays out in Fig. 3.4, which details the likelihood of each event calculated using Eq. 3.47, where the split mode probability is not simply equal to the sum of the other events.

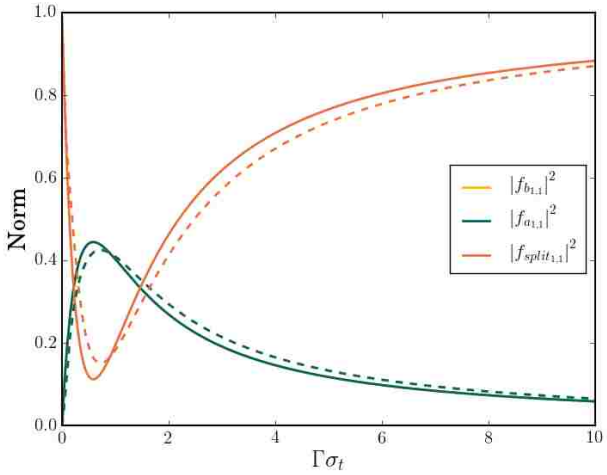

Figure 3.4: The probabilities of the various scattering possibilities for the initial state of Eq. 3.46 plotted as a function of $\Gamma\sigma_t$ for the Gaussian pulse (solid line) and the flat top pulse (dashed line). Note that the probabilities for the two photons to end in the left and right modes are equal and thus on top of one another in this plot.

Here we see that for both large and small $\Gamma\sigma_t$ the most probable event is that one photon remains travelling in each direction. The peak probability for two photons to leave in the same direction occurs at $\Gamma T = .586$ (for the Gaussian pulse) with a value of .444 for each of $f_{a_{1,1}}$ or $f_{b_{1,1}}$ or .888 in total. It is interesting that while a single TLE can act like a mirror on resonance (in the sense that it will reflect both photons) it does not act as a perfect $50-50$ beamsplitter when the photons are incident from different directions. Such a beamsplitter would scatter both photons in the same direction due to the Hong-Ou-Mandel effect [59]. We note that Roulet et al. have shown that this kind of ideal beamsplitter behavior is, in fact, exhibited for this system when the photon is detuned a particular amount from the atomic resonance [60]. Finally, as before, the probability of each event is similar regardless of the initial state of the pulses.

Just as for the co-propagating photons, we consider how the shape of the photon wavepacket is modified by its interaction with the atom. Fig. 3.5 shows the two-photon detection probabilities for a Gaussian pulse and Fig. 3.6 gives the same for a flat-top pulse.

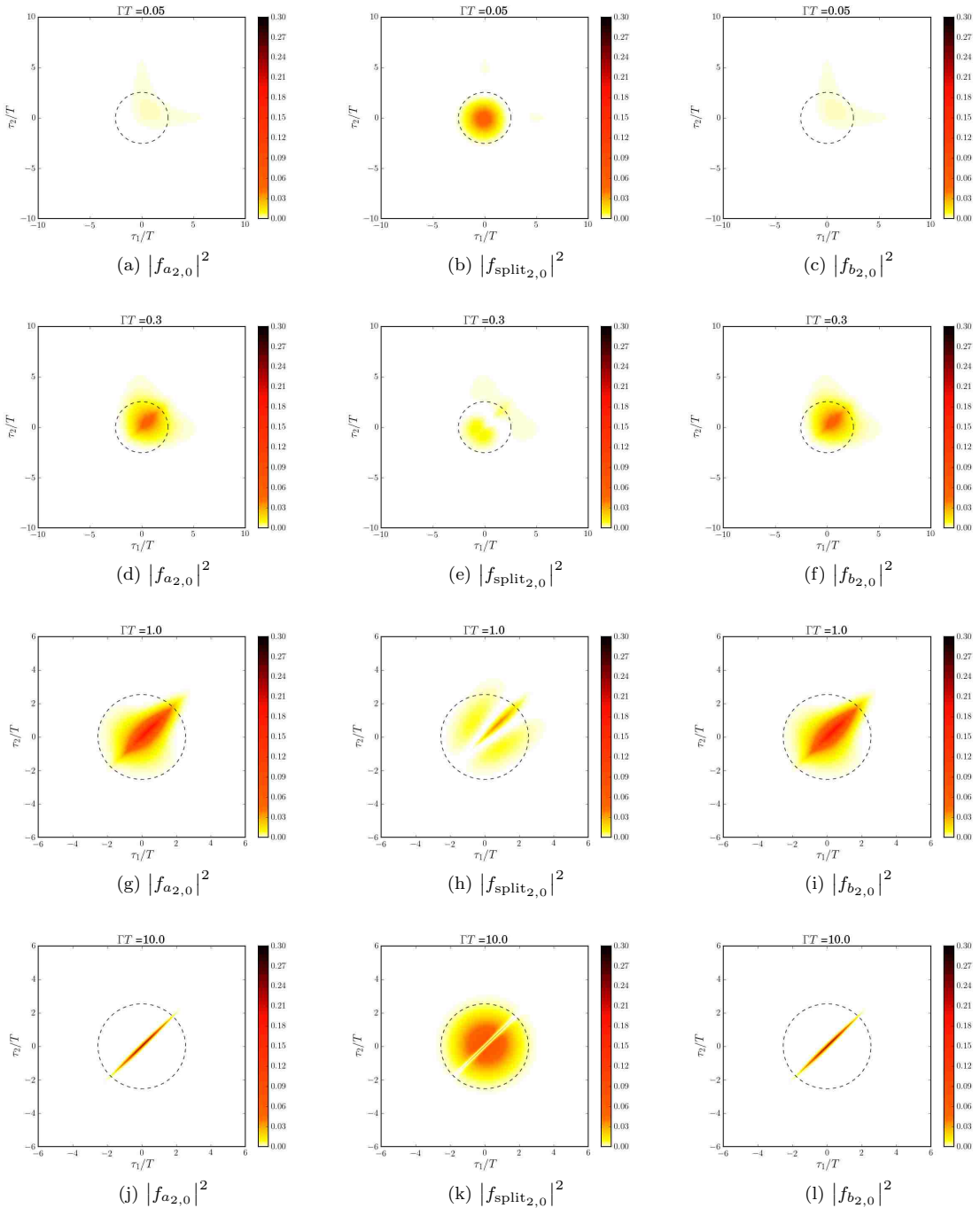

(a) $|f_{a_{2,0}}|^2$ (b) $|f_{\mathrm{split}_{2,0}}|^2$ (c) $|f_{b_{2,0}}|^2$

(d) $|f_{a_{2,0}}|^2$ (e) $|f_{\mathrm{split}_{2,0}}|^2$ (f) $|f_{b_{2,0}}|^2$

(g) $|f_{a_{2,0}}|^2$ (h) $|f_{\mathrm{split}_{2,0}}|^2$ (i) $|f_{b_{2,0}}|^2$

(j) $|f_{a_{2,0}}|^2$ (k) $|f_{\mathrm{split}_{2,0}}|^2$ (l) $|f_{b_{2,0}}|^2$

Figure 3.5: Detection probabilities for both photons being found in the $\hat{A}$ mode (both transmitted, leftmost column), $\hat{B}$ mode (both reflected, rightmost column), or one in each (middle column, where the index τ_a labels the reflected, and τ_b the transmitted, photon). ΓT is as labeled. The dotted circle indicates in each case the area of the initial Gaussian pulse.

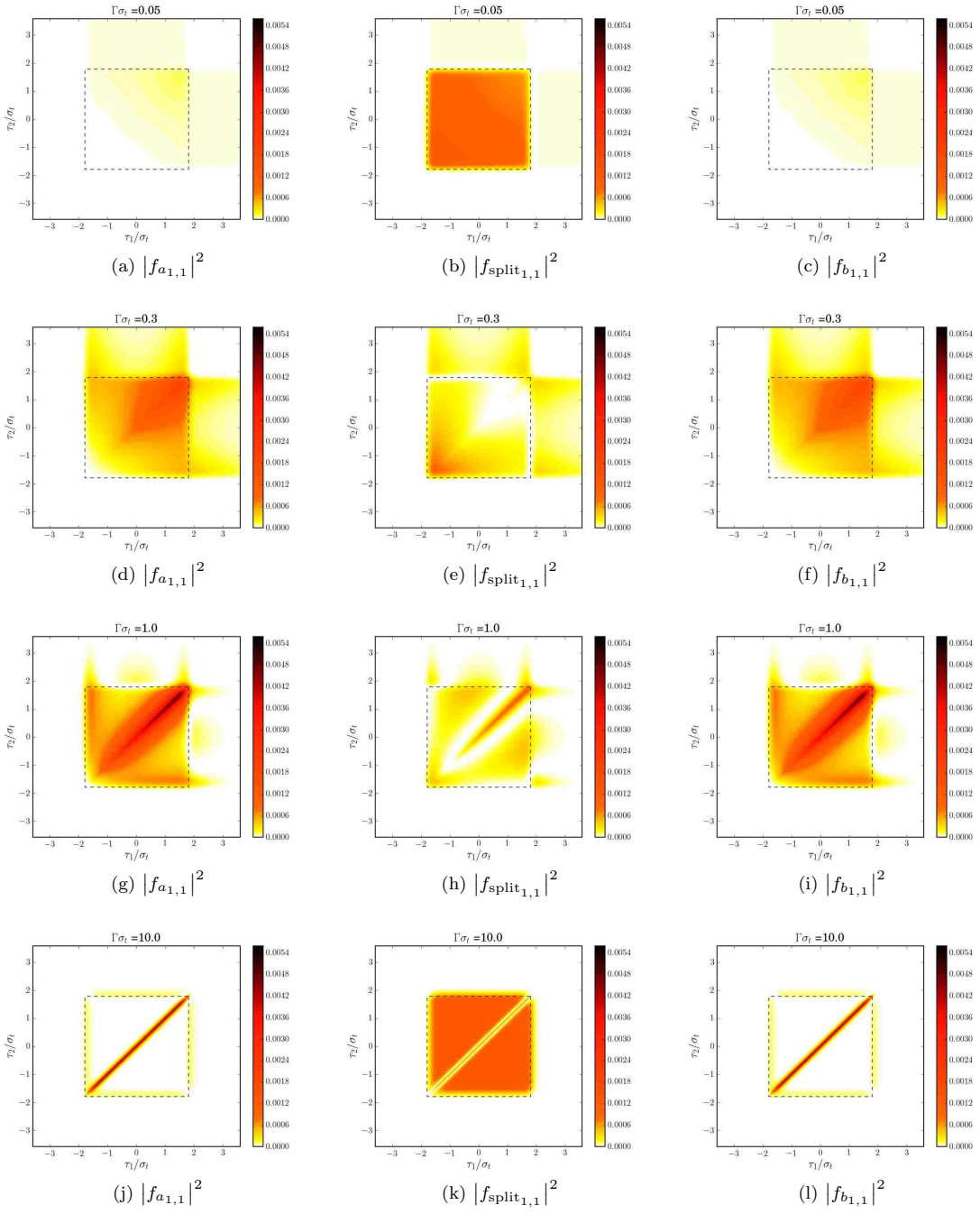

(a) $|f_{a_{1,1}}|^2$ (b) $|f_{\text{split}_{1,1}}|^2$ (c) $|f_{b_{1,1}}|^2$

(d) $|f_{a_{1,1}}|^2$ (e) $|f_{\text{split}_{1,1}}|^2$ (f) $|f_{b_{1,1}}|^2$

(g) $|f_{a_{1,1}}|^2$ (h) $|f_{\text{split}_{1,1}}|^2$ (i) $|f_{b_{1,1}}|^2$

(j) $|f_{a_{1,1}}|^2$ (k) $|f_{\text{split}_{1,1}}|^2$ (l) $|f_{b_{1,1}}|^2$

Figure 3.6: The same as for figure 11, but for the flat-top pulse described in the text. Note that the dotted square corresponds to the area of the initial pulse in all images.

Considering first the Gaussian pulse in Fig. 3.5, we can see that the pulse is modified in a way similar to the $M = 2$, $N = 0$ case. The primary difference is that the shapes have flipped between the split case and the other two. When the dimensionless coupling is small,

the split pulse is effectively just the input state. As $\Gamma\sigma_t$ increases the two-reflected or two-transmitted events become more likely while the shape of the split pulse is similar to that in Fig. 3.2d. When $\Gamma\sigma_t$ is large the co-propagating events are again highly bunched and the split case is antibunched, though in this case $f_{\mathrm{split}_{1,1}}(\tau,\tau) \neq 0$. The results for the flat-top pulse again have the same edge effects but exhibit essentially the same behavior as the Gaussian results.

3.3.4 Adiabatic approximation

By moving to the adiabatic limit, specifically when $\Gamma\sigma_t$ is large, we can greatly simplify the above expressions. Physically, this limit corresponds to strong coupling (fast atomic process) or a long pulse duration (large σ_t). In general, $G_\Gamma(t)$ can be written in terms of derivatives of $f(t)$ by integrating Eq. 3.23 by parts with $dv = e^{\Gamma t'}dt'$ and $u = f^{(k)}(t)$. This leads to the following series:

$$G_\Gamma(t) \approx \sum_{k=0}^{n} \frac{(-1)^k}{\Gamma^{k+1}} f^{(i)}(t) \tag{3.48}$$

For a simple pulse, like the Gaussian, we expect that each derivative with respect to t will pull out a factor of $1/\sigma_t$ so that the k^{th} term will effectively be multiplied by $1/(\Gamma\sigma_t)^k$. In the strong coupling regime, then, we can neglect the higher order terms. Choosing to keep only up to $k = 1$ we get

$$G_\Gamma(t) \approx \frac{f(t)}{\Gamma} - \frac{f'(t)}{\Gamma^2} \tag{3.49}$$

With this, the entangled term of Eq. 3.31 becomes

$$f_{\mathrm{ent}}(t_1,t_2) \approx 4f(t_<)e^{-\Gamma|t_1-t_2|}\left(\frac{2f'(t_<)}{\Gamma} - f(t_<)\right) \tag{3.50}$$

For the $M = 2, N = 0$ case we can express Eqs. (3.40) as

$$\begin{aligned}
f_{a_{2,0}}(t_1, t_2) &\approx \frac{f_{\text{ent}}(t_1, t_2)}{4} \\
f_{b_{2,0}}(t_1, t_2) &\approx f(t_1)f(t_2) - \frac{f(t_1)f'(t_2)}{\Gamma} - \frac{f(t_2)f'(t_1)}{\Gamma} + \frac{f_{\text{ent}}(t_1, t_2)}{4} \\
f_{\text{split}_{2,0}}(t_1, t_2) &\approx -\frac{f(t_1)f'(t_2)}{\Gamma} + \frac{f_{\text{ent}}(t_1, t_2)}{4}
\end{aligned} \tag{3.51}$$

From this expression it is clear that when Γ becomes large the entangled component of the wavefunction is responsible for the strong bunching effect in the transmitted and split modes, to the point where Figs. 3.2j,k and 3.3j,k effectively consist only of the two photon detection probability associated with this component of the wavefunction. In principle, then, it is possible to isolate this highly entangled photon state by post-selecting events in which both photons are detected in the transmitted modes.

Eq. 3.51 also shows how the reflected modes very closely replicate the initial pulse, as the first term is simply the input spectrum and the other factors coming from the entangled component will be small when Γ is large. This contribution from the entangled state is the slice "missing" from the pulse in Fig. 3.2l and 3.3l. Additionally, from looking at the form of $f_{b_{2,0}}$ in Eq. 3.51, it is clear that regardless of how large Γ becomes the pulse will always be maximally antibunched ($f_{b_{2,0}} = 0$) when $t_1 = t_2$, though the width of this slice becomes smaller as Γ becomes larger.

In the same way, for $M = 1, N = 1$ we have the following approximate form for Eq. 3.47:

$$\begin{aligned}
f_{a_{1,1}}(t_1, t_2) = f_{b_{1,1}}(t_1, t_2) &\approx \frac{1}{\sqrt{2}}\Big[-\frac{f(t_1)f'(t_2)}{\Gamma} - \frac{f(t_2)f'(t_1)}{\Gamma} + \frac{f_{\text{ent}}(t_1, t_2)}{2}\Big] \\
f_{\text{split}_{1,1}}(t_1, t_2) &\approx f(t_1)f(t_2) - \frac{f(t_1)f'(t_2)}{\Gamma} - \frac{f(t_2)f'(t_1)}{\Gamma} + \frac{f_{\text{ent}}(t_1, t_2)}{2}
\end{aligned} \tag{3.52}$$

Here the bound state dominates the co-propagating modes and the split mode reproduces the initial state with some of the state removed at $t_1 = t_2$. Note here that because there is a factor of $\frac{1}{2}$ instead of $\frac{1}{4}$ on the f_{ent} term, $f_{\text{split}_{1,1}}(t_1, t_2)$ is prevented from going to zero at $t_1 = t_2$.

3.4 Frequency-domain results

In this section we show how the result presented in Eq. 3.18 for the output spacetime pulse can be written in terms of a frequency wavepacket as presented by other authors. Starting with the unidirectional solution and taking the double Fourier transform over both time indices leads to the final spectrum of

$$\begin{aligned}\tilde{f}_{\text{uni}}(\omega_1,\omega_2) = \tilde{f}(\omega_1,\omega_2) - 2\Gamma\Big[\frac{\tilde{f}(\omega_1,\omega_2)}{\Gamma - i\omega_1} + \frac{\tilde{f}(\omega_1,\omega_2)}{\Gamma - i\omega_2}\Big] + \frac{4\Gamma^2\tilde{f}(\omega_1,\omega_2)}{(\Gamma - i\omega_1)(\Gamma - i\omega_2)} \\ -\frac{2\Gamma^2}{\pi}\Big[\frac{1}{\Gamma - i\omega_1} + \frac{1}{\Gamma - i\omega_2}\Big]\int \frac{d\omega_a d\omega_b \tilde{f}(\omega_a,\omega_b)\delta(\omega_1+\omega_2-\omega_a-\omega_b)}{(\Gamma - i\omega_a)(\Gamma - i\omega_b)}\end{aligned} \tag{3.53}$$

where $\tilde{f}(\omega_a,\omega_b) = \frac{1}{2\pi}\int dt_1 dt_2 e^{i\omega_a t_1 + i\omega_b t_2} f(t_1,t_2)$. In terms of the single photon transmission and reflection coefficients defined in Eq. 2.21

$$t_\omega = -\frac{i\omega}{\Gamma - i\omega} \qquad\qquad r_\omega = -\frac{\Gamma}{\Gamma - i\omega} \tag{3.54}$$

Eq. 3.53 becomes

$$\begin{aligned}\tilde{f}_{\text{uni}}(\omega_1,\omega_2) =& \tilde{f}(\omega_1,\omega_2)(r_{\omega_1}+t_{\omega_1})(r_{\omega_2}+t_{\omega_2}) \\ &- \frac{2\Gamma^2}{\pi}\Big[\frac{1}{\Gamma - i\omega_1} + \frac{1}{\Gamma - i\omega_2}\Big]\int \frac{d\omega_a d\omega_b \tilde{f}(\omega_a,\omega_b)\delta(\omega_1+\omega_2-\omega_a-\omega_b)}{(\Gamma - i\omega_a)(\Gamma - i\omega_b)}\end{aligned} \tag{3.55}$$

Studying the integral component of Eq. 3.55 it becomes clear that in terms of frequencies, the nonliterary of the two level system can be understood as a consequence of energy conservation. Due to the uncertainty in arrival times of the photons, is is possible for them to both be absorbed and re-emitted at virtually the same time. When this happens, the delta function $\delta(\omega_1+\omega_2-\omega_a-\omega_b)$ constrains the energy of the process such that the sum of the incoming frequencies $\omega_a+\omega_b$ must equal the sum of the outgoing frequencies $\omega_1+\omega_2$. In principle any mapping of $\omega_a,\omega_b \to \omega_1,\omega_2$ is valid, provided that the delta function is satisfied. This process is constrained by the bandwidth of $f(t)$, but will still introduce significant distortions to the pulse because, while it conserves energy, it does not preserve the energy of each individual photon and thus causes them to become

spectrally entangled.

Eq. 3.55 is general for any sort of two-photon input state. If, instead, the state is separable ($\tilde{f}(\omega_a, \omega_b) = \tilde{f}(\omega_a)\tilde{f}(\omega_b)$) the last term in (3.53) can be expressed as a convolution:

$$\begin{aligned}\tilde{f}_{\text{uni}}(\omega_1, \omega_2) &= \tilde{f}(\omega_1)\tilde{f}(\omega_2)(r_{\omega_1} + t_{\omega_1})(r_{\omega_2} + t_{\omega_2}) \\ &- \frac{2\Gamma^2}{\pi}\Big[\frac{1}{\Gamma - i\omega_1} + \frac{1}{\Gamma - i\omega_2}\Big]\left[\left(\frac{\tilde{f}(\omega_1 + \omega_2)}{(\Gamma - i(\omega_1 + \omega_2))}\right) * \left(\frac{\tilde{f}(\omega_1 + \omega_2)}{(\Gamma - i(\omega_1 + \omega_2))}\right)\right] \quad (3.56)\end{aligned}$$

where the * gives the convolution between the functions inside the parentheses. This notation is meant to suggest that the result of the convolution is a function of $\omega_1 + \omega_2$. Note also that this convolution term is the Fourier transform of the entangled component of the photon state.

In the bidirectional waveguide, Eq. 3.40 (an initial state of $|2, 0\rangle$) has a spectral representation of

$$\begin{aligned}\tilde{f}_{a_{2,0}}(\omega_1, \omega_2) &= t_{\omega_1} t_{\omega_2} \tilde{f}(\omega_1)\tilde{f}(\omega_2) + \frac{1}{4}\tilde{f}_{\text{ent}}(\omega_1, \omega_2) \\ \tilde{f}_{b_{2,0}}(\omega_1, \omega_2) &= r_{\omega_1} r_{\omega_2} \tilde{f}(\omega_1)\tilde{f}(\omega_2) + \frac{1}{4}\tilde{f}_{\text{ent}}(\omega_1, \omega_2) \\ \tilde{f}_{\text{split}_{2,0}}(\omega_1, \omega_2) &= t_{\omega_1} r_{\omega_2} \tilde{f}(\omega_1)\tilde{f}(\omega_2) + \frac{1}{4}\tilde{f}_{\text{ent}}(\omega_1, \omega_2) \quad (3.57)\end{aligned}$$

where

$$\tilde{f}_{\text{ent}}(\omega_1, \omega_2) = -\frac{2\Gamma^2}{\pi}\Big[\frac{1}{\Gamma - i\omega_1} + \frac{1}{\Gamma - i\omega_2}\Big]\left[\left(\frac{\tilde{f}(\omega_1 + \omega_2)}{(\Gamma - i(\omega_1 + \omega_2))}\right) * \left(\frac{\tilde{f}(\omega_1 + \omega_2)}{(\Gamma - i(\omega_1 + \omega_2))}\right)\right] \quad (3.58)$$

As can be seen, the ordering of the reflection and transmission coefficients exactly matches which process must occur for photons to arrive in each of the final scattered possibilities. We note that the equations as presented here have the same form as Eq. 22 in [8].

For two pulses coming from opposite directions, we have

$$\tilde{f}_{a_{1,1}}(\omega_1,\omega_2)=\tilde{f}_{b_{1,1}}(\omega_1,\omega_2)=\frac{1}{\sqrt{2}}\Big((r_{\omega_1}t_{\omega_2}+r_{\omega_2}t_{\omega_1})\tilde{f}(\omega_1)\tilde{f}(\omega_2)+\frac{1}{2}\tilde{f}_{\text{ent}}(\omega_1,\omega_2)\Big)$$
$$\tilde{f}_{\text{split}_{1,1}}(\omega_1,\omega_2)=(r_{\omega_1}r_{\omega_2}+t_{\omega_2}t_{\omega_1})\tilde{f}(\omega_1)\tilde{f}(\omega_2)+\frac{1}{2}\tilde{f}_{\text{ent}}(\omega_1,\omega_2) \tag{3.59}$$

which again has the appropriate reflection and transmission coefficients to match the scattering processes involved.

Finally, we present the explicit form of $\tilde{f}_{\text{ent}}$ for both the Gaussian and flat-top pulses used above. For the Gaussian pulse we have

$$\tilde{f}_{\text{ent}}=-\frac{4\Gamma^2T\sqrt{\frac{2}{\pi}}}{(\Gamma-i\omega_1)(\Gamma-i\omega_2)}e^{-((1+i)\Gamma+\omega_1+\omega_2)((-1+i)\Gamma+\omega_1+\omega_2)T^2}\text{erfc}\left[\frac{T}{\sqrt{2}}\left(2\Gamma-i(\omega_1+\omega_2)\right)\right] \tag{3.60}$$

And for the flat-top pulse the entangled component in the spectral domain is

$$\begin{aligned}\tilde{f}_{\text{ent}}(\omega_1,\omega_2)=\frac{2\Gamma e^{-(\omega_1+\omega_2)(2i\Gamma+\omega_1+\omega_2-4ia^2t_0)/4a^2}}{\pi\mathcal{N}(\Gamma-i\omega_1)(\Gamma-i\omega_2)(\Gamma-i(\omega_1+\omega_2))}\Bigg[e^{\Gamma^2/2a^2}\Bigg((1+e^{i\mathcal{T}(\omega_1+\omega_2)})\text{erfc}\big[\frac{2\Gamma-i(\omega_1+\omega_2)}{2\sqrt{2}a}\big]\\ -e^{\Gamma\mathcal{T}}\text{erfc}\big[\frac{2a^2\mathcal{T}+2\Gamma-i(\omega_1+\omega_2)}{2\sqrt{2}a}\big]+e^{-\Gamma\mathcal{T}+i\mathcal{T}(\omega_1+\omega_2)}\Bigg(\text{erfc}\big[\frac{2a^2\mathcal{T}-2\Gamma+i(\omega_1+\omega_2)}{2\sqrt{2}a}\big]-2\Bigg)\Bigg)\\ -\frac{(2i\Gamma+\omega_1+\omega_2)e^{i\Gamma(\omega_1+\omega_2)/2a^2}}{\omega_1+\omega_2}\Bigg(\text{erf}\left(\frac{2a^2\mathcal{T}-i(\omega_1+\omega_2)}{2\sqrt{2}a}\right)\\ -e^{i\mathcal{T}(\omega_1+\omega_2)}\text{erf}\left(\frac{2a^2\mathcal{T}+i(\omega_1+\omega_2)}{2\sqrt{2}a}\right)+i\left(1+e^{i\mathcal{T}(\omega_1+\omega_2)}\right)\text{erfi}\left(\frac{\omega_1+\omega_2}{2\sqrt{2}a}\right)\Bigg)\Bigg]\end{aligned} \tag{3.61}$$

3.5 Conclusions

In this chapter we presented a technique to solve for the evolution of a quantized, multimode field interacting with a two-level-emitter in a one-dimensional waveguide. We studied in detail the scattered state of a two photon pulse and showed how the single photon reflection and transmission coefficients appear in this state. Additionally, we have shown how the "unidirectional" and "bidirectional" waveguides can be related to one another for a single emitter. Finally we considered two specific input spectra and explored how interaction with the emitter changes the spacetime profile of the output photons.

Perhaps the most important conclusion from this chapter is that a two level system functions as a nonlinear element, but that this nonliterary introduces a significant distortion to the spacetime profile (and thus the spectrum) of the photons by bunching them in time or entangling their individual spectra. This is the effect described in [19] which poses a problem for using photons as carriers of quantum information, as after each interaction with a quantum gate the photons will become more and more distorted and it will become harder to predict exactly when they will arrive at a particular gate. Additionally, this distortion changes how they will interfere and, depending on the magnitude of the distortion, can destroy the gate operation.

Chapter 4

Scattering of Two Photons From Two Atoms

4.1 Introduction

In this chapter we will extend our results for a two photon pulse interacting with a single two level emitter (TLE) to deal with the scattering of a two photon pulse from two interacting emitters. We will show how to apply the Markovian approximation detailed in Chapter 2 to the time domain solution presented in Chapter 3. Finally, we will explore the transmission properties of the system and especially explore whether the conditions of high transmission for single photons derived in Chapter 2 persist for two photons. Finally, we note that the derivation of the final two-photon scattered state will rely heavily on the standing wave modes introduced in Section 1.2.1. Most of the material in this chapter was published in [37], though here we present a more detailed derivation of the solution.

4.2 Hamiltonian and setup

In terms of the variables given in Chapter 2 the atom-field interaction-picture Hamiltonian we will be using is given below as

$$H_A = \hbar g\Big[\hat{\phi}_1(t)e^{-i\delta t}\big(|eg\rangle\langle gg| + |ee\rangle\langle ge|\big) + \hat{\phi}_2^\dagger e^{i\delta t}\big(|ge\rangle\langle gg| + |ee\rangle\langle eg|\big)\Big] + H.C. \tag{4.1}$$

where the operators $\hat{\phi}_j$ are again a superposition of the left and right traveling modes

$$\hat{\phi}_j(t) = e^{ik_F z_j}\hat{A}(t - z_j/c) + e^{-ik_F z_j}\hat{B}(t + z_j/c) \tag{4.2}$$

Here $|eg\rangle$ represents the atomic state when the leftmost atom is excited and the rightmost is in the ground state, $|ge\rangle$ represents when the rightmost atom is excited and the leftmost is in the ground state, $|ee\rangle$ represents when both atoms are excited, and $|gg\rangle$ represents when both atoms are in their ground state. As there are only two atoms, we have chosen to label each possible state individually rather than writing the atomic operators as $\sigma_j^\dagger$ and σ_j as was done in Eq. 2.1 and Eq. 3.7. In this chapter we will be

assuming that $z_1 = -d/2$ and $z_2 = d/2$ so that d represents the separation between the atoms and that they are centered at the origin.

Additionally, we will also be using a Hamiltonian of the form

$$H_I = \hbar\Delta\Big(|eg\rangle\langle ge| + |ge\rangle\langle eg|\Big) + \hbar\beta|ee\rangle\langle ee| \tag{4.3}$$

to describe the interaction between the two atoms. Here the term containing Δ is the same exchange- (or Förster-) type interaction presented in Eq. 2.37. The term proportional to β gives a detuning of the doubly excited state (when both atoms are excited) due to a Van der Walls interaction such as would be seen in two close Rydberg atoms.

At this point it is convenient to introduce the atomic superposition states and photon operators

$$|\pm\rangle = \frac{|eg\rangle \pm |ge\rangle}{\sqrt{2}} \qquad\qquad \hat{\phi}_\pm = \frac{\phi_1(t) \pm \phi_2(t)}{\sqrt{2}} \tag{4.4}$$

We note that the atomic $|\pm\rangle$ states are orthogonal and $\big[\hat{\phi}_\pm(t_i), \hat{\phi}^\dagger_\mp(t_j)\big] = 0$. Using the commutator from Chapter 2 for $\hat{\phi}_j$ we can show that

$$\big[\hat{\phi}_\pm(t_i), \hat{\phi}^\dagger_\pm(t_j)\big] = 2\delta\big(t_i - t_j\big) \pm e^{ik_F d}\delta\big(t_i - t_j - d/c\big) \pm e^{-ik_F d}\delta\big(t_i - t_j + d/c\big) \tag{4.5}$$

With these definitions, the Hamiltonian can be written as

$$\begin{aligned} H = \hbar g e^{-i\delta t}\Big(\hat{\phi}_+(t)|+\rangle\langle gg| + \hat{\phi}_+(t)|ee\rangle\langle +| + \hat{\phi}_-(t)|-\rangle\langle gg| - \hat{\phi}_-(t)|ee\rangle\langle -|\Big) + H.C. \\ +\hbar\Delta\Big(|+\rangle\langle +| - |-\rangle\langle -|\Big) + \hbar\beta|ee\rangle\langle ee| \end{aligned} \tag{4.6}$$

As the interaction component from H_I is independent of time and diagonal in the atomic $|\pm\rangle$ basis, we move to a second interaction picture with
$H_0 = \hbar\Delta\Big(|+\rangle\langle +| - |-\rangle\langle -|\Big) + \hbar\beta|ee\rangle\langle ee|$. With this, we can write

$$e^{i\frac{t}{\hbar}H_0} = |gg\rangle\langle gg| + e^{i\Delta t}|+\rangle\langle +| + e^{-i\Delta t}|-\rangle\langle -| + e^{i\beta t}|ee\rangle\langle ee| \tag{4.7}$$

and, further defining $\delta_\pm = \delta \mp \Delta$ and $\delta'_\pm = \delta \pm \Delta - \beta$, the transformed Hamiltonian (given

by $e^{it/\hbar H_0} H e^{-it/\hbar H_0}$) becomes

$$H = \hbar g\Big(\hat{\phi}_+(t)e^{-i\delta'_+ t}|ee\rangle\langle +| + \hat{\phi}_+(t)e^{-i\delta_+ t}|+\rangle\langle gg| + \hat{\phi}_-(t)e^{-i\delta_- t}|-\rangle\langle gg| - \hat{\phi}_-(t)e^{-i\delta'_- t}|ee\rangle\langle -|\Big) + H.C. \tag{4.8}$$

4.2.1 Solution and Markovian approximation

We now solve the Schrödinger equation. We will write the total state by

$$|\psi(t)\rangle = |\psi_{gg}(t)\rangle \otimes |gg\rangle + |\psi_+(t)\rangle \otimes |+\rangle + |\psi_-(t)\rangle \otimes |-\rangle + |\psi_{ee}(t)\rangle \otimes |ee\rangle \tag{4.9}$$

where each component is separated by the number of photons in the state. Note that in this derivation we will be only considering initial states with two photons, though the process can be applied to deal with N photons in the same way as presented in Chapter 3.

Using this notation, we arrive at the following equations of motion for the field components of the system.

$$|\dot{\psi_{gg}}\rangle = -ig\Big(\hat{\phi}^\dagger_+(t)e^{-i\delta_+ t}|\psi_+\rangle + \hat{\phi}^\dagger_-(t)e^{i\delta_- t}|\psi_-\rangle\Big) \tag{4.10a}$$

$$|\dot{\psi_+}\rangle = -ig\Big(\hat{\phi}_+(t)e^{-i\delta_+ t}|\psi_{gg}\rangle + \hat{\phi}^\dagger_+(t)e^{-i\delta'_+ t}|\psi_{ee}\rangle\Big) \tag{4.10b}$$

$$|\dot{\psi_-}\rangle = -ig\Big(\hat{\phi}_-(t)e^{-i\delta_- t}|\psi_{gg}\rangle - \hat{\phi}^\dagger_-(t)e^{-i\delta'_- t}|\psi_{ee}\rangle\Big) \tag{4.10c}$$

$$|\dot{\psi_{ee}}\rangle = -ig\Big(\hat{\phi}_+(t)e^{i\delta'_+ t}|\psi_+\rangle - \hat{\phi}_-(t)e^{i\delta'_- t}|\psi_-\rangle\Big) \tag{4.10d}$$

For compactness, in what follows we will re-define the $\hat{\phi}_+$ and $\hat{\phi}_-$ operators to include the exponential detuning terms so that

$$\hat{\phi}_+(t_i)e^{-i\delta_+ t_i} \to \hat{\phi}_{+,i} \quad \hat{\phi}_+(t_i)e^{-i\delta'_+ t} \to \hat{\phi}'_{+,i} \quad \hat{\phi}_-(t_i)e^{-i\delta'_- t_i} \to \hat{\phi}_{-,i} \quad \hat{\phi}_-(t_i)e^{-i\delta'_+ t_i} \to \hat{\phi}'_{-,i} \tag{4.11}$$

Next we formally integrate $|\psi_{gg}\rangle$, yielding

$$|\psi_{gg}(t)\rangle = |\psi_I\rangle - ig\int_{-\infty}^{t}\Big(\hat{\phi}^\dagger_{+,1}|\psi_+(t_1)\rangle + \hat{\phi}^\dagger_{-,1}|\psi_-(t_1)\rangle\Big) \tag{4.12}$$

We substitute this equation into the equations for $|\dot{\psi_+}(t)\rangle$ and $|\dot{\psi_-}(t)\rangle$ and normal order

the operators. Doing so and evaluating all the delta functions produced by commuting $\hat{\phi}_{+,t}\hat{\phi}^{\dagger}_{+,1}$ and $\hat{\phi}_{-,t}\hat{\phi}^{\dagger}_{-,1}$ leads to the differential equations

$$\dot{|\psi_+(t)\rangle} + g^2|\psi_+(t)\rangle + g^2 e^{ik_F d - i\delta_+ d/c}|\psi_+(t-d/c)\rangle =$$
$$-ig\hat{\phi}_{+,t}|\psi_I\rangle - ig\hat{\phi}'^{\dagger}_{+,t}|\psi_{ee}(t)\rangle - g^2\int_{-\infty}^{t} dt_1\Big(\hat{\phi}^{\dagger}_{+,1}\hat{\phi}_{+,t}|\psi_+(t_1)\rangle + \hat{\phi}^{\dagger}_{-,1}\hat{\phi}_{+,t}|\psi_-(t_1)\rangle\Big) \quad (4.13a)$$

$$\dot{|\psi_-(t)\rangle} + g^2|\psi_-(t)\rangle - g^2 e^{ik_F d - i\delta_- d/c}|\psi_-(t-d/c)\rangle =$$
$$-ig\hat{\phi}_{-,t}|\psi_I\rangle + ig\hat{\phi}'^{\dagger}_{-,t}|\psi_{ee}(t)\rangle - g^2\int_{-\infty}^{t} dt_1\Big(\hat{\phi}^{\dagger}_{+,1}\hat{\phi}_{-,t}|\psi_+(t_1)\rangle + \hat{\phi}^{\dagger}_{-,1}\hat{\phi}_{-,t}|\psi_-(t_1)\rangle\Big) \quad (4.13b)$$

Note that there is no $|\psi_\pm(t+d/c)\rangle$ term, as the delta function is evaluated at a point beyond the limits of integration (the integral over dt_j is over $[-\infty, t]$ but the delta function is defined for the point $t_j = t + d/c$). Eqs. 4.13a and 4.13b represent delay differential equations that account for the time it takes for a photon to travel between atoms. These are incredibly difficult to solve exactly, however, and are similar to Eq. 2.8. Fortunately, if we make the Markovian approximation we can remove the time shift. This will be valid as long as the timescale of the pulse is much much larger than the shift in time.

In Section 2.4 we demonstrated that the Markovian approximation works well provided that $\sigma_\omega d/c$ is small. This translates to a temporal pulse width of the order of $\sigma_t \approx 1/\sigma_\omega$. Then a pulse with frequency bandwidth on the order of a GHz will have a temporal width on the order of a few nanoseconds. This is certainly an achievable result; this is typically the timescale of atomic processes. If the atoms are separated on the order of a few μm, d/c will be on the order of 10^{-14}s, which represents a negligible shift compared to the duration and thus can safely be ignored.

We will also simplify the phase term $e^{ik_F d - i\delta_\pm d/c}$ by assuming that terms on the order of d/c will be too small to contribute. This is justified by the same scaling argument used in the Markovian approximation. Realistically, both δ and Δ will not likely be larger than a few GHz or so. Values for the detunings caused by doubly excited atom-atom dipole energy shifts (β) will be on the order of 10π MHz ([61]) or 50 Mhz ([62]). As this term is often

larger than Δ, we can safely say that multiplying these terms by d/c will lead to a negligible contribution in realistic system. If $\delta_\pm$ is on the order of 1 GHz, we would have $\delta_\pm d/c \approx 10^{-5}$ and thus $e^{i\delta_\pm d/c} \approx 1$.

With this approximation Eqs. 4.13a and 4.13b become

$$\dot{|\psi_+(t)\rangle} + g^2\big(1 + e^{ik_F d/c}\big)|\psi_+(t)\rangle = -ig\hat{\phi}_{+,t}|\psi_I\rangle - ig\hat{\phi}'^{\dagger}_{+,t}|\psi_{ee}(t)\rangle - g^2\int_{-\infty}^{t} dt_1\Big(\hat{\phi}^{\dagger}_{+,1}\hat{\phi}_{+,t}|\psi_+(t_1)\rangle + \hat{\phi}^{\dagger}_{-,1}\hat{\phi}_{+,t}|\psi_-(t_1)\rangle\Big) \tag{4.14a}$$

$$\dot{|\psi_-(t)\rangle} + g^2\big(1 - e^{ik_F d/c}\big)|\psi_-(t)\rangle = -ig\hat{\phi}_{-,t}|\psi_I\rangle + ig\hat{\phi}'^{\dagger}_{-,t}|\psi_{ee}(t)\rangle - g^2\int_{-\infty}^{t} dt_1\Big(\hat{\phi}^{\dagger}_{+,1}\hat{\phi}_{-,t}|\psi_+(t_1)\rangle + \hat{\phi}^{\dagger}_{-,1}\hat{\phi}_{-,t}|\psi_-(t_1)\rangle\Big) \tag{4.14b}$$

We can formally integrate these first-order differential equations by using the integrating factor $g_\pm = g^2\big(1 \pm e^{ik_F d/c}\big)$ to obtain

$$|\psi_+(t)\rangle = -ig\int_{-\infty}^{t} dt_1 e^{-g_+(t-t_1)}\hat{\phi}_{+,1}|\psi_I\rangle - ig\int_{-\infty}^{t} dt_1 e^{-g_+(t-t_1)}\hat{\phi}'^{\dagger}_{+,1}|\psi_{ee}(t_1)\rangle - g^2\int_{-\infty}^{t} dt_1 e^{-g_+(t-t_1)}\int_{-\infty}^{t_1} dt_2\Big(\hat{\phi}^{\dagger}_{+,2}\hat{\phi}_{+,1}|\psi_+(t_2)\rangle + \hat{\phi}^{\dagger}_{-,2}\hat{\phi}_{+,1}|\psi_-(t_2)\rangle\Big) \tag{4.15a}$$

$$|\psi_-(t)\rangle = -ig\int_{-\infty}^{t} dt_1 e^{-g_-(t-t_1)}\hat{\phi}_{-,1}|\psi_I\rangle + ig\int_{-\infty}^{t} dt_1 e^{-g_-(t-t_1)}\hat{\phi}'^{\dagger}_{-,1}|\psi_{ee}(t_1)\rangle - g^2\int_{-\infty}^{t} dt_1 e^{-g_-(t-t_1)}\int_{-\infty}^{t_1} dt_2\Big(\hat{\phi}^{\dagger}_{+,2}\hat{\phi}_{-,1}|\psi_+(t_2)\rangle + \hat{\phi}^{\dagger}_{-,2}\hat{\phi}_{-,1}|\psi_-(t_2)\rangle\Big) \tag{4.15b}$$

Next, we substitute Eq. 4.15a and Eq. 4.15b into themselves. Ideally, only the first term containing the initial photon state would contribute leading to a truncating series. Provided that the system is Markovian and the pulse duration, σ_t, is much greater than d/c this is what happens. To demonstrate how, consider one of the terms after Eq. 4.15a is substituted into itself:

$$\int_{-\infty}^{t} dt_1\int_{-\infty}^{t_1} dt_2\int_{-\infty}^{t_2} dt_3\int_{-\infty}^{t_3} dt_4 e^{-g_+(t_1-t_2)-G_{\Gamma_+}(t_3-t_4)}\hat{\phi}^{\dagger}_{+,2}\hat{\phi}_{+,1}\hat{\phi}^{\dagger}_{+,4}\hat{\phi}_{+,3}|\psi_+(t_4)\rangle \tag{4.16}$$

This can be re-written as a four-dimensional integral with limits of $\pm\infty$ in terms of step

functions.

$$\int_{-\infty}^{\infty} dt_1 dt_2 dt_3 dt_4 \Theta(t-t_1)\Theta(t_1-t_2)\Theta(t_2-t_3)\Theta(t_3-t_4) e^{-g_+(t_1-t_2)-G_{\Gamma_+}(t_3-t_4)} \hat{\phi}^\dagger_{+,2}\hat{\phi}_{+,1}\hat{\phi}^\dagger_{+,4}\hat{\phi}_{+,3}|\psi_+(t_4)\rangle \tag{4.17}$$

Normal ordering the operators yields three delta function terms, $2\delta(t_1 - t_4)$, $e^{-ik_F d - i\delta_+(t_1-t_4)}\delta(t_1 - t_4 - d/c)$, and $e^{ik_F d - i\delta_+(t_1-t_4)}\delta(t_1 - t_4 - d/c)$.

The first of these, $2\delta(t_1 - t_4)$, is nested too deep and will only be nonzero at one point in the same manner as shown in Chapter 3. This arises from the fact that the integrals constrain the variables to be $t_1 \geq t_2 \geq t_3 \geq t_4$, but the delta function causes $t_4 = t_1$. Here the t_3 integral is then only nonzero at one point, when $t_3 = t_2 = t_1$ at the upper limit, and thus the integral is zero.

The last term, $e^{ik_F d - i\delta_+(t_1-t_4)}\delta(t_1 - t_4 - d/c)$ is also zero, as the delta function is only satisfied for $t_4 = t_1 + d/c$ but the integral ordering again constrains $t_4 \leq t_1$.

The middle term does provide a nonzero contribution. In the absence of the Markovian approximation this term would prevent a truncating series from being possible to obtain. Within the Markovian approximation, it will contribute very little to the overall solution and therefore can be ignored. This delta function constrains the time variables so that $t_1 \geq t_2 \geq t_3 \geq t_1 - d/c$. In terms of t_1, then, the maximum limits of integration of the t_3 integral are $[t_1 - d/c, t_1]$. This represents a vanishingly small component of the wavefunction as compared to the overall time scale of the pulse.

The net effect of this is that for any operators with time indices t_i and t_j, when $j - i > 1$ the operators effectively commute. This effect can be derived in a simpler way by noting that applying the Markovian approximation means approximating delay functions as $f(t \pm d/c) \approx f(t)$. We did not make this approximation to the commutator of $\hat{\phi}_+$ and $\hat{\phi}_-$ (Eq. 4.5) initially, however, because the time ordering of the integrals causes any delta function of the form $\delta(t_i - t_j + d/c)$ to evaluate to zero. Had we made a Markovian approximation to all terms of Eq. 4.5, the solution would include the unphysical scenario where the future state of the system could affect the present state.

In the context of the time ordered integrals, we now define effective commutators for $\hat{\phi}_+$ and $\hat{\phi}_-$ in the Markovian regime that only include the first two terms of Eq. 4.5.

$$[\hat{\phi}_\pm(t_i), \hat{\phi}^\dagger_\pm(t_j)] \approx 2\big(1 \pm e^{ik_F d}\big)\delta(t_i - t_j) \tag{4.18}$$

Now, when we substitute Eq. 4.15a and 4.15b into themselves only the first integral contributes. This follows from the fact that $|\psi_\pm\rangle$ have only one photon each, and $|\psi_{ee}\rangle$ has none. One then arrives at

$$|\psi_+(t)\rangle = -ig\int_{-\infty}^{t} dt_1 e^{-g_+(t-t_1)}\hat{\phi}_{+,1}|\psi_I\rangle - ig\int_{-\infty}^{t} dt_1 e^{-g_+(t-t_1)}\hat{\phi}'^\dagger_{+,1}|\psi_{ee}(t_1)\rangle$$
$$+ig^3\int_{-\infty}^{t} dt_1\int_{-\infty}^{t_1} dt_2\int_{-\infty}^{t_2} e^{-g_+(t-t_1)}\Big[e^{-g_+(t_2-t_3)}\hat{\phi}^\dagger_{+,2}\hat{\phi}_{+,1}\hat{\phi}_{+,3} + e^{-g_-(t_2-t_3)}\hat{\phi}^\dagger_{-,2}\hat{\phi}_{+,1}\hat{\phi}_{-,3}\Big]|\psi_I\rangle \tag{4.19a}$$

$$|\psi_-(t)\rangle = -ig\int_{-\infty}^{t} dt_1 e^{-g_-(t-t_1)}\hat{\phi}_{-,1}|\psi_I\rangle + ig\int_{-\infty}^{t} dt_1 e^{-g_-(t-t_1)}\hat{\phi}'^\dagger_{-,1}|\psi_{ee}(t)\rangle$$
$$+ig^3\int_{-\infty}^{t} dt_1\int_{-\infty}^{t_1} dt_2\int_{-\infty}^{t_2} e^{-g_-(t-t_1)}\Big[e^{-g_+(t_2-t_3)}\hat{\phi}^\dagger_{+,2}\hat{\phi}_{-,1}\hat{\phi}_{+,3} + e^{-g_-(t_2-t_3)}\hat{\phi}^\dagger_{-,2}\hat{\phi}_{-,1}\hat{\phi}_{-,3}\Big]|\psi_I\rangle \tag{4.19b}$$

The next step is to substitute Eq. 4.19a and Eq. 4.19b into Eq. 4.10d. Doing so, one finds that the contribution of the triple integral terms of Eq. 4.19a and Eq. 4.19b vanish. This is accomplished by moving the $\hat{\phi}'_+$ or $\hat{\phi}'_-$ operators on the far left past the first creation operator under the integral sign, which can be done because their indices differ by more than one and thus they effectively commute. By putting the $|\psi_{ee}(t)\rangle$ term in normal order and making the same approximations as above, one obtains the differential equation for the doubly excited state of

$$\dot{|\psi_{ee}}(t)\rangle + (g_+ + g_-)|\psi_{ee}(t)\rangle = -g^2\int_{-\infty}^{t} dt_1\Big[e^{-g_+(t-t_1)}\hat{\phi}'_{+,t}\hat{\phi}_{+,1} - e^{-g_-(t-t_1)}\hat{\phi}_{-,t}\hat{\phi}_{-,1}\Big]|\psi_I\rangle \tag{4.20}$$

Defining an integrating factor of $\gamma' = g_+ + g_- = 2g^2$ the excited state can be written exclusively in terms of the initial state $|\psi_I\rangle$.

$$|\psi_{ee}(t)\rangle = -g^2\int_{-\infty}^{t} dt_1\int_{-\infty}^{t_1} dt_2 e^{-\gamma' t+\gamma' t_1}\Big[e^{-g_+(t_1-t_2)}\hat{\phi}'_{+,1}\hat{\phi}_{+,2} - e^{-g_-(t_1-t_2)}\phi'_{-,1}\hat{\phi}_{-,2}\Big]|\psi_I\rangle \tag{4.21}$$

We now substitute this in to Eq. 4.19a and Eq. 4.19b to obtain explicit solutions for $|\psi_{\pm}(t)\rangle$. Note that these can be used to find the population of each of the $|\pm\rangle$ states (and thus the atoms) as a function of time.

$$|\psi_+(t)\rangle = -ig\int_{-\infty}^{t} dt_1 e^{-g_+(t-t_1)}\hat{\phi}_{+,1}|\psi_I\rangle$$
$$+ig^3\int_{-\infty}^{t}dt_1\int_{-\infty}^{t_1}dt_2\int_{-\infty}^{t_2}dt_3 e^{-g_+(t-t_1)}\Big[e^{-g_+(t_2-t_3)}\big(\hat{\phi}^{\dagger}_{+,2}\hat{\phi}_{+,1}\hat{\phi}_{+,3}+e^{-2g^2(t_1-t_2)}\hat{\phi}'^{\dagger}_{+,1}\hat{\phi}'_{+,2}\hat{\phi}_{+,3}\big)$$
$$+e^{-g_-(t_2-t_3)}\big(\hat{\phi}^{\dagger}_{-,2}\hat{\phi}_{+,1}\hat{\phi}_{-,3}-e^{-\gamma' t_1+\gamma' t_2}\hat{\phi}'^{\dagger}_{+,1}\hat{\phi}_{-,2}\hat{\phi}_{-,3}\big)\Big]|\psi_I\rangle \tag{4.22a}$$

$$|\psi_-(t)\rangle = -ig\int_{-\infty}^{t} dt_1 e^{-g_-(t-t_1)}\hat{\phi}_{-,1}|\psi_I\rangle$$
$$+ig^3\int_{-\infty}^{t}dt_1\int_{-\infty}^{t_1}dt_2\int_{-\infty}^{t_2}dt_3 e^{-g_-(t-t_1)}\Big[e^{-g_+(t_2-t_3)}\big(\hat{\phi}^{\dagger}_{+,2}\hat{\phi}_{-,1}\hat{\phi}_{+,3}+e^{-2g^2(t_1-t_2)}\hat{\phi}'^{\dagger}_{-,1}\hat{\phi}'_{+,2}\hat{\phi}_{+,3}\big)$$
$$+e^{-g_-(t_2-t_3)}\big(\hat{\phi}^{\dagger}_{-,2}\hat{\phi}_{-,1}\hat{\phi}_{-,3}-e^{-\gamma' t_1+\gamma' t_2}\hat{\phi}'^{\dagger}_{-,1}\hat{\phi}_{-,2}\hat{\phi}_{-,3}\big)\Big]|\psi_I\rangle \tag{4.22b}$$

Finally, we substitute this into Eq. 4.10a to obtain an expression for $|\psi_{gg}(t)\rangle$ given a two photon input pulse. We present the final solution after transforming back to $\hat{\phi}_+(t)$ and $\hat{\phi}_-(t)$ to more explicitly show the presence of detuning, and define parameters

$$\begin{aligned}\Gamma_+ &= g_+ - i\delta_+ = g^2\big(1+e^{ik_F d}\big) - i(\delta-\Delta)\\ \Gamma_- &= g_- - i\delta_- = g^2\big(1-e^{ik_F d}\big) - i(\delta+\Delta)\\ \gamma &= \gamma' - i(\delta'_+ + \delta'_-) = 2g^2 - i(2\delta-\beta)\end{aligned} \tag{4.23}$$

where the $\Gamma_{\pm}$ terms are identical to the effective coupling and detuning of Eq. 2.27 for two atoms. The real component of γ describes the coupling and the imaginary component of γ detuning between the $|\pm\rangle$ states and the $|ee\rangle$ state.

We now arrive at Eq. 31 in [37]

$$
\begin{aligned}
|\psi_g(t)\rangle = |\psi_I\rangle &- g^2 \int_{-\infty}^{t} dt_1 \int_{-\infty}^{t_1} dt_2 \Big(e^{-\Gamma_+(t_1-t_2)} \hat{\phi}_+^\dagger(t_1)\hat{\phi}_+(t_2) + e^{-\Gamma_-(t_1-t_2)} \hat{\phi}_-^\dagger(t_1)\hat{\phi}_-(t_2) \Big) |\psi_I\rangle \\
&+ g^4 \int_{-\infty}^{t} dt_1 \int_{-\infty}^{t_1} dt_2 \int_{-\infty}^{t_2} dt_3 \int_{-\infty}^{t_3} dt_4 \\
&\quad \Big[e^{-\Gamma_+(t_1-t_2)} \hat{\phi}_+^\dagger(t_1) \Big(e^{-\Gamma_+(t_3-t_4)} \hat{\phi}_+^\dagger(t_3)\hat{\phi}_+(t_4) + e^{-\Gamma_-(t_3-t_4)} \hat{\phi}_-^\dagger(t_3)\hat{\phi}_-(t_4) \Big) \hat{\phi}_+(t_2) \\
&\quad + e^{-\Gamma_-(t_1-t_2)} \hat{\phi}_-^\dagger(t_1) \Big(e^{-\Gamma_+(t_3-t_4)} \hat{\phi}_+^\dagger(t_3)\hat{\phi}_+(t_4) + e^{-\Gamma_-(t_3-t_4)} \hat{\phi}_-^\dagger(t_3)\hat{\phi}_-(t_4) \Big) \hat{\phi}_-(t_2) \Big] |\psi_I\rangle \\
&+ g^4 \int_{-\infty}^{t} dt_1 \int_{-\infty}^{t_1} dt_2 \int_{-\infty}^{t_2} dt_3 \int_{-\infty}^{t_3} dt_4 \Big(e^{-\Gamma_+(t_1-t_2)} \hat{\phi}_+^\dagger(t_1)\hat{\phi}_+^\dagger(t_2) - e^{-\Gamma_-(t_1-t_2)} \hat{\phi}_-^\dagger(t_1)\hat{\phi}_-^\dagger(t_2) \Big) \\
&\quad \times e^{-(2g^2 - i(2\delta-\beta))(t_2-t_3)} \Big(e^{-\Gamma_+(t_3-t_4)} \hat{\phi}_+(t_3)\hat{\phi}_+(t_4) - e^{-\Gamma_-(t_3-t_4)} \hat{\phi}_-(t_3)\hat{\phi}_-(t_4) \Big) |\psi_I\rangle
\end{aligned}
\tag{4.24}
$$

While Eq. 4.24 appears to be complex, it has a very physical structure; it contains all the possible scattering channels for two photons. The structure is similar to that presented in Eq. 3.18 for a single atom (and derived in [12]), as the first three terms represent the same scattering events. The term $|\psi_I\rangle$ corresponds to the event where neither photon is absorbed. The double-integral terms correspond to the case where only one photon interacts with one of the $|\pm\rangle$ modes. The first four-fold integral term represents the possibility that both photons have interacted with the system and may interact with any combination of the $|\pm\rangle$ atomic states. Finally, the second four-fold integral term in Eq. 4.24 represents a new scattering process that corresponds to both photons being absorbed simultaneously. Interestingly, as we will show, this contribution is entangled in the same way as the photons that interacted with a single atom despite the fact that it arises from the two photons being absorbed simultaneously.

We also note that, in the same way as the solution given in Chapter 3, this can be used to explore the time evolution of the atomic populations and field states. In what follows we will only consider the case where $t \to \infty$ corresponding to the scattered photons.

The final step of this derivation is to apply the Markovian approximation to the $\hat{\phi}$ operators, as they also contain time delays. Defining the standing wave mode operators

equivalent to $\hat{A}$ and $\hat{B}$ (as done in Section 3.3.1) as

$$\hat{C}(t) = \frac{\hat{A}(t) + \hat{B}(t)}{\sqrt{2}} \qquad\qquad \hat{D}(t) = \frac{\hat{A}(t) - \hat{B}(t)}{\sqrt{2}} \tag{4.25}$$

we find that the $\hat{\phi}_+$ and $\hat{\phi}_-$ operators can be written in terms of $\hat{C}$ and $\hat{D}$ by

$$\begin{aligned}\hat{\phi}_+(t) &= e^{ik_F d/2}\hat{C}(t - d/2c) + e^{-ik_F d/2}\hat{C}(t + d/2c) \\ \hat{\phi}_-(t) &= e^{ik_F d/2}\hat{D}(t - z/2c) - e^{-ik_F d/2}\hat{D}(t + z/2c)\end{aligned} \tag{4.26}$$

Within the Markovian approximation one can neglect the time delays in these functions so that

$$\hat{\phi}_+(t) \approx 2\cos\big(k_F d/2\big)\hat{C}(t) \qquad\qquad \hat{\phi}_-(t) \approx -i2\sin\big(k_F d/2\big)\hat{D}(t) \tag{4.27}$$

In order to consider why it is safe to make this approximation at this step, consider the following action of $\hat{\phi}_+$ on initial state of the form

$$|\psi_I\rangle = |M, N\rangle \equiv \frac{1}{\sqrt{M!N!}}\left(\int dt f_0(t)\hat{C}^\dagger(t)\right)^M \left(\int dt f_0(t)\hat{D}^\dagger(t)\right)^N |0, 0\rangle \tag{4.28}$$

When the lowering operator acts on this state we have

$$\hat{\phi}_+(t)|M, N\rangle = \frac{1}{\sqrt{M}}\Big(e^{ik_F d/2}f(t - d/2c) + e^{-ik_F d/2}f(t + d/2c)\Big)|M - 1, N\rangle \tag{4.29}$$

In the Markovian approximation this becomes
$\hat{\phi}_+(t)|M, N\rangle \approx 2\cos(k_F d/2)f(t)|M - 1, N\rangle$. The reason that we can safely approximate the operators as in Eq. 4.26 at this point in the solution is that the operators are in normal order and will not commute any more. As seen previously, when they commute the time ordering of the integrals ensures that only the past action of the system can affect the system at the present time t. Mathematically, this came about because one of the delta functions from the commutator (corresponding to $e^{-ik_F d/2}\hat{C}(t + d/2c)$ in Eq. 4.26 above) was always zero. When the $\hat{\phi}$ operators act on the initial state, however, there is no time ordering and both terms can contribute.

We now define auxiliary terms $\Gamma_c = \mathrm{Re}[\Gamma_+] = 2g^2\cos^2\big(k_F d/2\big)$ and

$\Gamma_s = \mathrm{Re}[\Gamma_-] = 2g^2 \sin^2\left(k_F d/2\right)$ so that we can write the entire expression in Eq. 4.24 in terms of the $\hat{C}$ and $\hat{D}$ operators. In deriving Γ_c and Γ_s we have used the trig identities $2\sin(\theta/2) = 1 - \cos(\theta)$ and $2\cos(\theta/2) = 1 + \cos(\theta)$. This becomes

$$
\begin{aligned}
|\psi_g(t)\rangle = |\psi_I\rangle &- 2\int_{-\infty}^{t} dt_1 \int_{-\infty}^{t_1} dt_2 \Big(\Gamma_c e^{-\Gamma_+(t_1-t_2)}\hat{C}^\dagger(t_1)\hat{C}(t_2) + \Gamma_s e^{-\Gamma_-(t_1-t_2)}\hat{D}^\dagger(t_1)\hat{D}(t_2)\Big)|\psi_I\rangle \\
&+ 4\int_{-\infty}^{t} dt_1 \int_{-\infty}^{t_1} dt_2 \int_{-\infty}^{t_2} dt_3 \int_{-\infty}^{t_3} dt_4 \\
&\quad \Big[\Gamma_c e^{-\Gamma_+(t_1-t_2)}\hat{C}^\dagger(t_1)\left(\Gamma_c e^{-\Gamma_+(t_3-t_4)}\hat{C}^\dagger(t_3)\hat{C}(t_4) + \Gamma_s e^{-\Gamma_-(t_3-t_4)}\hat{D}^\dagger(t_3)\hat{D}(t_4)\right)\hat{C}(t_2) \\
&\quad + \Gamma_s e^{-\Gamma_-(t_1-t_2)}\hat{D}^\dagger(t_1)\left(\Gamma_c e^{-\Gamma_+(t_3-t_4)}\hat{C}^\dagger(t_3)\hat{C}(t_4) + \Gamma_s e^{-\Gamma_-(t_3-t_4)}\hat{D}^\dagger(t_3)\hat{D}(t_4)\right)\hat{D}(t_2)\Big]|\psi_I\rangle \\
&+ 4\int_{-\infty}^{t} dt_1 \int_{-\infty}^{t_1} dt_2 \int_{-\infty}^{t_2} dt_3 \int_{-\infty}^{t_3} dt_4 \Big(\Gamma_c e^{-\Gamma_+(t_1-t_2)}\hat{C}^\dagger(t_1)\hat{C}^\dagger(t_2) - \Gamma_s e^{-\Gamma_-(t_1-t_2)}\hat{D}^\dagger(t_1)\hat{D}^\dagger(t_2)\Big) \\
&\quad \times e^{-(2g^2 - i(2\delta-\beta))(t_2-t_3)}\Big(\Gamma_c e^{-\Gamma_+(t_3-t_4)}\hat{C}(t_3)\hat{C}(t_4) - \Gamma_s e^{-\Gamma_-(t_3-t_4)}\hat{D}(t_3)\hat{D}(t_4)\Big)|\psi_I\rangle
\end{aligned}
\tag{4.30}
$$

By comparing the structure of this equation to the form of the solution for a single atom given in Eq. 3.18 it is immediately clear that the coupling to the $|\pm\rangle$ modes is given by $\mathrm{Re}[\Gamma_\pm]$ and the detuning is given by $\mathrm{Im}[\Gamma_\pm]$. The doubly excited state is also detuned, but by $2\delta - \beta$. We show the level structure with detunings and transitions labeled below in Fig. 4.1.

Figure 4.1: A level diagram of the two atoms in the $|\pm\rangle$ basis. Transitions with couplings and photon operators are presented along with the detunings of each of the states.

4.3 Particular solutions

We now move on to describing particular input states, and we will specifically study the case where the initial states are separable as in Chapter 3. We will start by considering the scattered state if the photons are initially in the standing wave modes, and then describe the solution for travelling waves. Note that at this point the quantity $k_F d$ appears exclusively in trig functions or complex exponentials. This is a consequence of the Markovian approximation; the phase acquired when a photon travels between the atoms contributes to the final solution, but the time delay is too small to modify the state. Because $k_F d$ has been reduced to a phase, in our analysis of the scattered state of the photons we will define the phase term $\phi \equiv k_F d$ just as in Section 2.4.

4.3.1 Scattering of a single photon

We present results for the single photon to show that the solution is the same as the frequency domain solution derived in Section 2.4.1. In the time domain, solving the single photon case is relatively trivial. As there is only one photon in the initial state, only the first integral term in Eq. 4.30 will contribute. Writing again Eq. 3.23

$$G_{\Gamma_i}(t) = e^{-\Gamma_i t} \int_{-\infty}^{t} dt' e^{\Gamma_i t'} f(t') \tag{4.31}$$

the space-time profile for a scattered photon initially in the $\hat{C}$ mode with initial wavepacket $f(t)$ is

$$f_c(t) = f(t) - 2\Gamma_c G_{\Gamma_+}(t) \tag{4.32}$$

If the photon is initially in the $\hat{D}$ mode we will have

$$f_d(t) = f(t) - 2\Gamma_s G_{\Gamma_-}(t) \tag{4.33}$$

Taking the Fourier transform of these functions gives the frequency spectra of the

scattered photon as

$$\tilde{f}_c(\omega) = -\frac{\Gamma_+^* + i\omega}{\Gamma_+ - i\omega}\tilde{f}(\omega) \qquad\qquad \tilde{f}_d(\omega) = -\frac{\Gamma_-^* + i\omega}{\Gamma_- - i\omega}\tilde{f}(\omega) \tag{4.34}$$

We point this out as these have the same form as the individual terms of Eq. 2.27, as we can write $\Gamma_\pm = g^2\big(1 \pm e^{i\phi}\big) - i\delta$.

If a photon is initially in the $\hat{A}$ mode its initial state can be written in terms of a superposition of the $\hat{C}$ and $\hat{D}$ modes by

$$|\psi_I\rangle = \int dt f(t)\hat{A}^\dagger(t)|0\rangle = \frac{1}{\sqrt{2}}\int dt f(t)\Big(\hat{C}^\dagger(t) + \hat{D}^\dagger(t)\Big)|0\rangle \tag{4.35}$$

Using Eqs. 4.32 and 4.33 to transform the state and then re-writing the expression in terms of traveling waves, we have that the transmitted (τ) and reflected (ρ) photons have space-time profiles given by

$$\tau(t) = f(t) - \Gamma_c G_{\Gamma_+}(t) - \Gamma_s G_{\Gamma_-}(t) \qquad\qquad \rho(t) = -\Gamma_c G_{\Gamma_+}(t) + \Gamma_s G_{\Gamma_-}(t) \tag{4.36}$$

The Fourier transform of these functions are again identical to the reflection and transmission spectra given in Eq. 2.27. Finally, we present the transmission probabilities of the photon for various values of Δ, δ, g, and ϕ in order to give some sense of what is possible. The transmission window given in Eq. 2.40 can be seen in the regions of high transmission found in Fig. 4.2 b-c when $\Delta \neq 0$ or $\delta \neq 0$. These transmission probabilities were calculated for a square pulse shape of

$$f(t) = \frac{1}{\sqrt{2T}}\big(\Theta(t+T) - \Theta(t-T)\big) \tag{4.37}$$

In all calculations we have set $T = \sqrt{3}$ so that the standard deviation of the pulse, $\sigma_t = \int dt f^2(t)t^2 = T^2/3$, equals one.

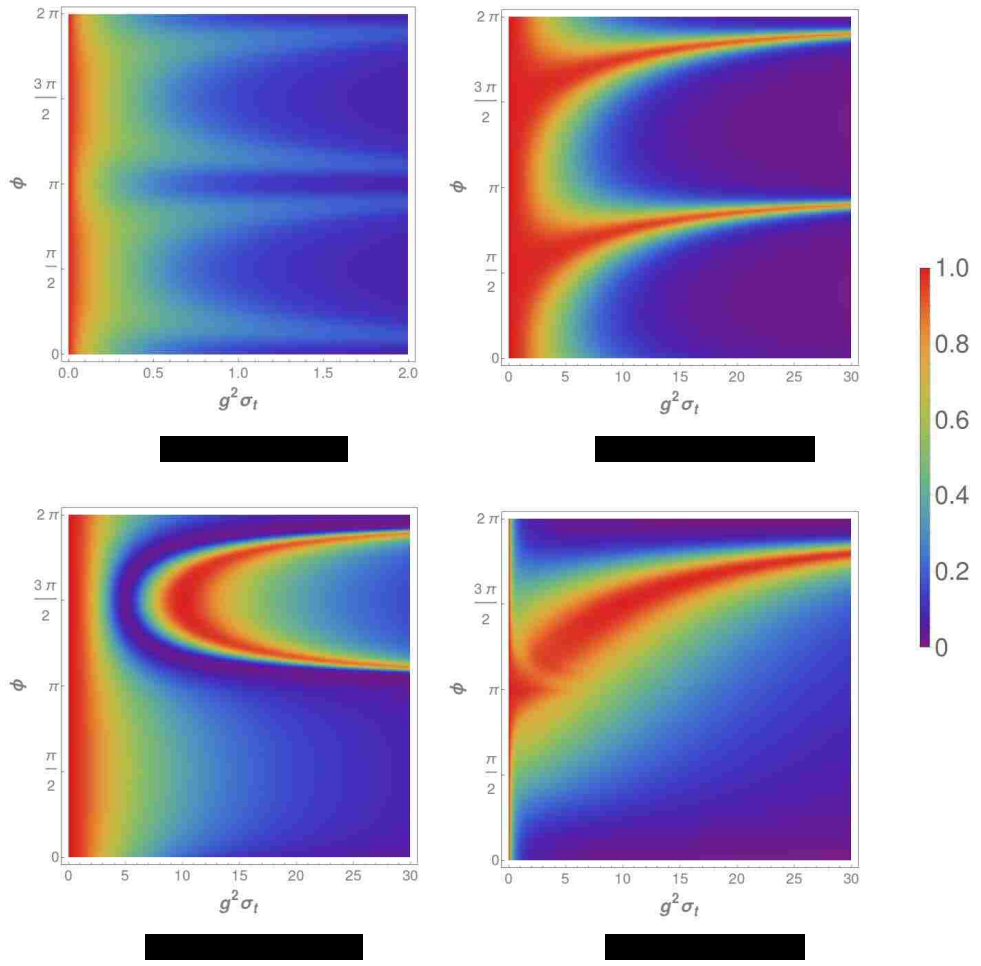

Figure 4.2: Transmission of a square pulse of duration σ_t through the two-atom "cavity" system, as a function of ϕ and $g^2\sigma_t$, for the values of $\delta\sigma_t$ and $\Delta\sigma_t$ shown.

4.3.2 Two-photon standing wave solutions

To analyze the standing wave solutions, we first consider the case where both photons begin in the $\hat{C}$ standing wave mode. The initial state will then have the form

$$|\psi_I\rangle = \frac{1}{\sqrt{2}} \int dt_1 dt_2 f(t_1) f(t_2) \hat{C}^\dagger(t_1) \hat{C}^\dagger(t_2) |0\rangle \tag{4.38}$$

In this case many of the terms in Eq. 4.30 vanish and the two photons will either both end up in the $\hat{C}$ modes or in the $\hat{D}$ modes. This last possibility is due to the fact that if both photons are absorbed at once, the atoms are able to decay into either the $\hat{C}$ or $\hat{D}$

modes. By comparison with the single atom solution in Eq. 3.18 (and Eq. 8 in [12]), we can write down the two-photon wavefunction for the final state in the time domain. We also define a function similar to $G_{\Gamma_\pm}$ to describe the contribution of the doubly excited state to the space-time profile. This is

$$\mathcal{E}_{\Gamma_\pm}(t) = \int_{-\infty}^{t} dt' e^{-(2g^2 - i(2\delta-\beta))(t-t')} f(t') G_{\Gamma_\pm}(t') \tag{4.39}$$

$\mathcal{E}_{\Gamma_\pm}$ is directly related to the double excitation probability in the same way that $G_{\Gamma_\pm}$ is related to the single-photon excitation probability. To see how, consider that for two photons we can write the doubly-excited component of the wavefunction as $|\psi_{ee}(t)\rangle = \psi_e(t)|0\rangle$ because there are no photons remaining in the field. Plugging this into Eq. 4.21 we arrive at

$$\psi_e(t) = -e^{-i(2\delta+\beta)t}\sqrt{2}\, g^2 \cos^2(\phi/2)\mathcal{E}_{\Gamma_+}(t) \tag{4.40}$$

We get a similar result if both photons are initially in the $\hat{D}$ modes (changing the cosine to a sine, and $\mathcal{E}_{\Gamma_+}$ to $\mathcal{E}_{\Gamma_-}$). From here, the probability of the atoms being in this state is given by

$$\langle\psi_{ee}(t)|\psi_{ee}(t)\rangle = |\psi_e(t)|^2 = 2g^4 \cos^4(\phi/2)|\mathcal{E}_{\Gamma_+}(t)|^2 \tag{4.41}$$

And thus one can see that Eq. 4.39 is effectively the probability amplitude for the atomic state $|ee\rangle$.

With all this, we can write the total scattered photon state for the initial state in Eq. 4.38 as

$$|\psi\rangle = \frac{1}{\sqrt{2}} \int dt_1 dt_2 \Big(f_{cc}(t_1,t_2)\hat{C}^\dagger(t_1)\hat{C}^\dagger(t_2) + f_{dd}(t_1,t_2)\hat{D}^\dagger(t_1)\hat{D}^\dagger(t_2) \Big)|0\rangle \tag{4.42}$$

and we will have the following for the component corresponding to both photons being

scattered in the $\hat{C}$ mode

$$f_{cc}(t_1,t_2) = \left(f(t_1) - 2\Gamma_c G_{\Gamma_+}(t_1)\right)\left(f(t_2) - 2\Gamma_c G_{\Gamma_+}(t_2)\right) - 4\Gamma_c^2 e^{-\Gamma_+|t_1-t_2|}\left(G_{\Gamma_+}^2(t_<) - \mathcal{E}_{\Gamma_+}(t_<)\right) \tag{4.43}$$

Here, $t_<$ is the smaller of t_1 and t_2. The first term in Eq. 4.43 represents the two photons interacting independently with the two-atom system. The second term is the entangled state where the first part is identical in form to that derived in Chapter 3 for a single atom and the second part (containing $\mathcal{E}$) is the contribution from the doubly excited state.

In the same way, the component of the two-photon wavefunction corresponding to the case where both photons exit in the $\hat{D}$ mode is constructed of just the two-photon, two-atom term and is

$$f_{dd}(t_1,t_2) = 4\Gamma_c\Gamma_s e^{-\Gamma_-|t_1-t_2|}\mathcal{E}_{\Gamma_+}(t_<) \tag{4.44}$$

Provided that the standing wave modes are being accessed as described in Section 1.2.1, where a beamsplitter is used to transform travelling wave photons to standing wave photons, we have a situation where two unentangled photons can enter one port of the beamsplitter (the $\hat{C}$ mode) and leave in the other port (the $\hat{D}$ mode) in an entangled (i.e. non-separable) state. It would be convenient if there was a combination of parameters that would ensure that this swapping occurred with unit probability, as the system could be used deterministically to generate entangled states or to discriminate between one and two photon pulses. Unfortunately, the best that we have found for the norm of Eq. 4.44 is approximately .593 for a square pulse. This occurs around $g^2\sigma_t = .91$, $\phi = 3\pi/2$, and $\Delta = g^2$ for $\delta = \beta = 0$. This system is similar to the two-photon discriminator proposed by Witthaut and co-workers [63], which we analyzed in [12]. In fact, when using the same square pulse shape, their device succeeds with a maximum success probability of 0.584 to separate a two photon and a single photon state in a single pass.

Generally speaking, evaluating the function $\mathcal{E}_{\Gamma_\pm}(t)$ is challenging, though an analytic expression can be obtained for a square pulse and a lowering exponential pulse. We instead consider the adiabatic limit, that is when the product $g^2\sigma_t \gg 1$, with σ_t being the standard deviation of the initial pulse shape $f(t)$. This is also the nearly monochromatic limit, as a long pulse in time (or space) corresponds to a very narrow frequency bandwidth. As shown in Eq. 3.49, $G_{\Gamma_\pm} \simeq f(t)/\Gamma_\pm$ to first order. Using this we can approximate $\mathcal{E}_{\Gamma_\pm}$ to first order by

$$\mathcal{E}_{\Gamma_\pm}(t) \simeq \frac{1}{\gamma\Gamma_\pm} f^2(t) \tag{4.45}$$

The factors in the denominator come from the conditions for 1- and 2- photon resonance. By choosing $\phi = 3\pi/2$, which maximizes the factor $\Gamma_c\Gamma_s$ and sets $|\Gamma_+| = |\Gamma_-|$, we find that further choosing $\beta = 2\delta$ and $g^2 = \delta + \Delta$ will maximize the norm of $\mathcal{E}_{\Gamma_+}$ and also maximize the norm of f_{dd}. It is, however, impossible to satisfy both conditions at the same time unless the atoms are able to interact (i.e. $\Delta \neq 0$ and $\beta \neq 0$). When these conditions are met, the entangled state Eq. 4.44 has the approximate form of $2e^{-g^2|t_1-t_2|}f^2(t_<)$ multiplied by a phase, and is about 1/2 of the magnitude of the $G^2_{\Gamma_+}$ term for the same choice of parameters.

The two terms can be made to be of the same order, however. For example, choosing $k_F a = 2n\pi$ makes $\Gamma_s = 0$, which causes Eq. 4.44 to vanish and makes it possible to set $\Gamma_+ = 2g^2$. When this happens the entangled component of Eq. 4.43 will approximately vanish. We note that this approximate cancellation requires both that the product of the coupling and the pulse duration $g^2\sigma_t$ must be large (so that the approximate forms for G_{Γ_+} and $\mathcal{E}_{\Gamma_+}$ can be used) and that $\beta = 2\delta$ and $\delta = \Delta$ (which if $\delta = 0$ can be satisfied in the absence of atom-atom interactions). This result is somewhat interesting because, even though in this regime the atoms are interacting only with the $\hat{C}$ standing wave mode, there are still two photons in the system and thus the vanishing of the nonlinear terms is nontrivial: it suggests that it is possible to use the nonlinearity introduced by the presence

of the second atom to negate the entanglement generated by the individual atoms.

4.3.3 Travelling wave solutions

Two photons arriving from the same direction

If we consider the initial, separable state where both photons are in the $\hat{A}$ mode (travelling to the right) $|\psi_I\rangle$ will be

$$|\psi_I\rangle = \frac{1}{\sqrt{2}} \int dt_1 dt_2 f(t_1) f(t_2) \hat{A}^\dagger(t_1) \hat{A}^\dagger(t_2) |0\rangle \tag{4.46}$$

From here, we use the fact that the defininton of the $\hat{C}$ and $\hat{D}$ operators can be inverted to give

$$\hat{A}(t) = \frac{1}{\sqrt{2}} \left(\hat{C}(t) + \hat{D}(t) \right) \qquad\qquad \hat{B}(t) = \frac{1}{\sqrt{2}} \left(\hat{C}(t) - \hat{D}(t) \right) \tag{4.47}$$

With this, we convert the initial state to a standing wave mode description and use Eq. 4.30 to determine how the state changes. Finally, we convert back to a travelling wave mode basis and collect terms corresponding to each of the three possible scattering outcomes; when both photons are transmitted, both photons are reflected, or they are "split" and one is transmitted while the other is reflected. We will use the single photon reflection and transmission functions defined in Eq. 4.36 to write the components of the total scattered wavefunction as

$$f_{aa}(t_1, t_2) = \tau(t_1)\tau(t_2) + f^+_{G^2,aa}(t_1, t_2) + f^+_{\mathcal{E},aa}(t_1, t_2) \tag{4.48a}$$

$$f_{bb}(t_1, t_2) = \rho(t_1)\rho(t_2) + f^-_{G^2,aa}(t_1, t_2) + f^+_{\mathcal{E},aa}(t_1, t_2) \tag{4.48b}$$

$$f_{ab}(t_1, t_2) = \tau(t_1)\rho(t_2) + f_{G^2,ab}(t_1, t_2) + f^-_{\mathcal{E},aa}(t_1, t_2) \tag{4.48c}$$

The nonlinear components, $f^{\pm}_{G^2,aa}$, $f_{G^2,ab}$, and $f^{+}_{\mathcal{E},aa}$ are given by

$$
\begin{aligned}
f^{\pm}_{\mathcal{E},aa}(t_1,t_2) &= \left(\Gamma_c e^{-\Gamma_+|t_1-t_2|} \pm \Gamma_s e^{-\Gamma_-|t_1-t_2|}\right)\left(\Gamma_c \mathcal{E}_{\Gamma_+}(t_<) + \Gamma_s \mathcal{E}_{\Gamma_-}(t_<)\right) \\
f^{\pm}_{G^2,aa}(t_1,t_2) &= -\left(\Gamma_c G_{\Gamma_+}(t_<) \pm \Gamma_s G_{\Gamma_-}(t_<)\right)\left(\Gamma_c e^{-\Gamma_+|t_1-t_2|} G_{\Gamma_+}(t_<) \pm \Gamma_s e^{-\Gamma_-|t_1-t_2|} G_{\Gamma_-}(t_<)\right) \\
f_{G^2,ab}(t_1,t_2) &= -\left(\Gamma_c G_{\Gamma_+}(t_<) - sgn(t_1-t_2)\Gamma_s G_{\Gamma_-}(t_<)\right) \\
&\quad \times \left(\Gamma_c e^{-\Gamma_+|t_1-t_2|} G_{\Gamma_+}(t_<) + sgn(t_1-t_2)\Gamma_s e^{-\Gamma_-|t_1-t_2|} G_{\Gamma_-}(t_<)\right)
\end{aligned}
\tag{4.49}
$$

Here, unlike the scattered state from the single atoms in Eq. 3.40, all three scattering possibilities have different entangled components. In general, the components related to the doubly excited state will interfere with the single-atom nonlinear effects, with the effect most pronounced around $\phi = n\pi$ when the atoms are coupled to only one of the standing wave modes (i.e. one of Γ_c or Γ_s is zero). This may be useful for applications where extra entanglement is to be avoided.

The nonlinear effects become large when the coupling to both the $|+\rangle$ and $|-\rangle$ states is of equal strength, requiring $\phi = (n + \frac{1}{2})\pi$. As discussed above, it is possible to have $G^2_{\Gamma_\pm}$ on the order of $2\mathcal{E}_{\Gamma_\pm}$, so no cancellation will generally occur between the single- and two-atom terms. In this new geometry some of the terms can cancel individually. For example, when $\Gamma_+ = \Gamma_-$, by choosing the appropriate Δ, it can be true that $f^{-}_{\mathcal{E},aa} = f^{-}_{G^2,aa} = f_{G^2,ab} = 0$. Regardless of the value of Δ, the terms will cancel approximately provided that $\Gamma_c = \Gamma_s$.

Perhaps the biggest effect of the nonlinear terms can be seen when they cause something to happen that would not otherwise occur if the atomic response was purely linear. These can be seen most prominently along the high transmission regions presented in Fig. 4.2. Here, the entangled term from the doubly excited state strongly reduces the transmission probability. This is perhaps to be expected, as these regions of high transmission occur near resonances of the system, which in turn increase the size of the nonlinear terms, as suggested by Eq. 4.45.

We present an example of this in Fig. 4.3, where we show the norm of f_{aa}, f_{bb}, and f_{ab} for a square pulse shape. We have chosen to work with a square pulse in this section

because it is possible to obtain an analytic form for $\mathcal{E}_{\Gamma_\pm}$ and because the transmission properties of a single atom appear to be largely independent of the pulse shape for $g^2 \approx \sigma_t$. The pulse shape we are considering is

$$f(t) = \frac{1}{\sqrt{2T}}\big(\Theta(t+T) - \Theta(t-T)\big) \tag{4.50}$$

and it has auxiliary functions

$$G_\Gamma(t) = \frac{1}{\sqrt{2T}\Gamma}\Big[\big(1-e^{-\Gamma(t+T)}\big)\Theta(t+T) - \big(1-e^{-\Gamma(t-T)}\big)\Theta(t-T)\Big] \tag{4.51}$$

$$\begin{aligned} E_\Gamma(t) = {} & \Theta(t+T)\Theta(T-t)\frac{e^{\gamma t}}{2T(\gamma-\Gamma)}\Big(\frac{1}{\Gamma}\big(1-e^{-\Gamma(t+T)}\big) - \frac{1}{\gamma}\big(1-e^{-\gamma(t+T)}\big)\Big) \\ & +\Theta(t-T)\frac{e^{\gamma T}}{2T(\gamma-\Gamma)}\Big(\frac{1}{\Gamma}\big(1-e^{-2\Gamma T}\big) - \frac{1}{\gamma}\big(1-e^{-2\gamma T}\big)\Big) \end{aligned} \tag{4.52}$$

Note that when β, δ, and Δ are zero, $\gamma - \Gamma$ will also be zero. At this point the function is equal to

$$E_\Gamma(t) = -\Theta(t+T)\Theta(T-t)\frac{e^{-\Gamma T}}{2T\Gamma^2}\big(\Gamma(t+T)+1-e^{\Gamma(t+T)}\big) - \Theta(t-T)\frac{e^{-\Gamma T}}{2T\Gamma^2}\big(2\Gamma T+1-e^{2\Gamma T}\big) \tag{4.53}$$

In Fig. 4.3 we have chosen the detunings to fit the transmission window that appears when $\Delta = -g^2 \sin\phi$ for $\delta = 0$ as given by Eq. 2.40. Additionally, we have chosen g to maximize the contribution of the nonlinear terms. Small values of $g^2\sigma_t$ lead to a small modification of the photon wavepacket by the atom, whereas for large values the timescale of the interaction is short and the modification of the pulse shape is constrained by $e^{-\Gamma|t_1-t_2|}$. From the single photon analysis in Section 2.5, we expect that at $\phi = 3\pi/2$ the system should transmit with near unit probability (that is both photons should be in the $\hat{A}$ mode). This effect can be seen in the solid black curve in Fig. 4.3, representing the linear solution, which itself is a product of two single-photon interactions (or alternatively Eq. 4.48 where the entangled components have been removed).

The full solution, however, has a relatively large reflection probability. To understand where it comes from, consider that when $\phi = 3\pi/2$ we have that $\Gamma_+ = \Gamma_-$ and $\Gamma_c = \Gamma_s$. As

a result, for any combination of t_1 and t_2, $f^{\pm}_{G^2,aa}(t_1,t_2) = f_{G^2,ab}(t_1,t_2) = 0$. This ensures that any deviation from the linear terms at this point is exclusively due to the double excitation entangled term $f^{+}_{\mathcal{E},aa}(t_1,t_2)$.

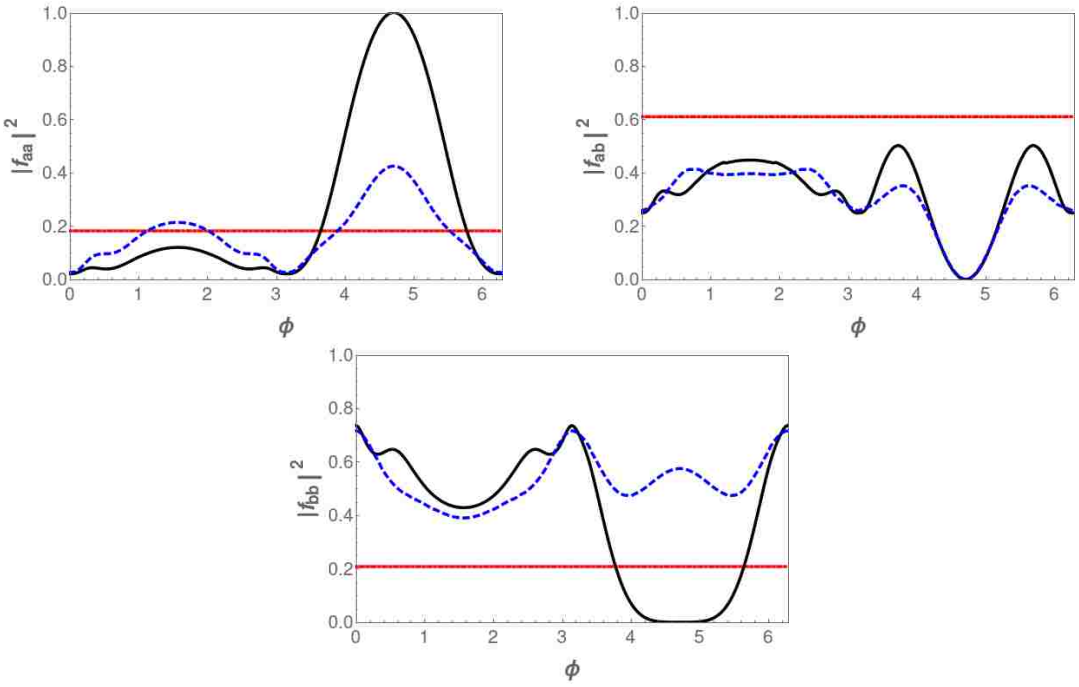

Figure 4.3: Probabilities of two-photon reflection, one reflection and one transmission, and two-photon transmission for an initial state with both photons in the $\hat{A}$ mode (travelling to the right) and with a square pulse shape of duration $T = \sqrt{3}$. Other parameters are $\Delta = g^2|\sin(k_F a)|$, $\delta = \beta = 0$, and $g^2\sigma_t = 1$. The red, constant line gives the probability of each event for a single atom. The blue, dashed line shows the full solution and the solid, black line shows the contribution of just the linear terms.

Finally, in Fig. 4.4 we present the probability that both photons are transmitted as a function of both the dimensionless coupling parameter $g^2\sigma_t$ and ϕ for the same parameters as in Fig. 4.2. As can be seen, in the absence of atomic interactions or detuning, the phase difference between the atoms due to their separation matters little; as $g^2\sigma_t$ increases the probability that both photons remain in the initial mode decreases. When detuning is present the shape of the plot is nearly identical in form to that seen for a single photon in Fig. 4.2, though the transmission probability of Fig. 4.4c is less than one at $\phi = 3\pi/2$ and $g^2\sigma_t = 10$ due to the contribution from the doubly excited state as described above.

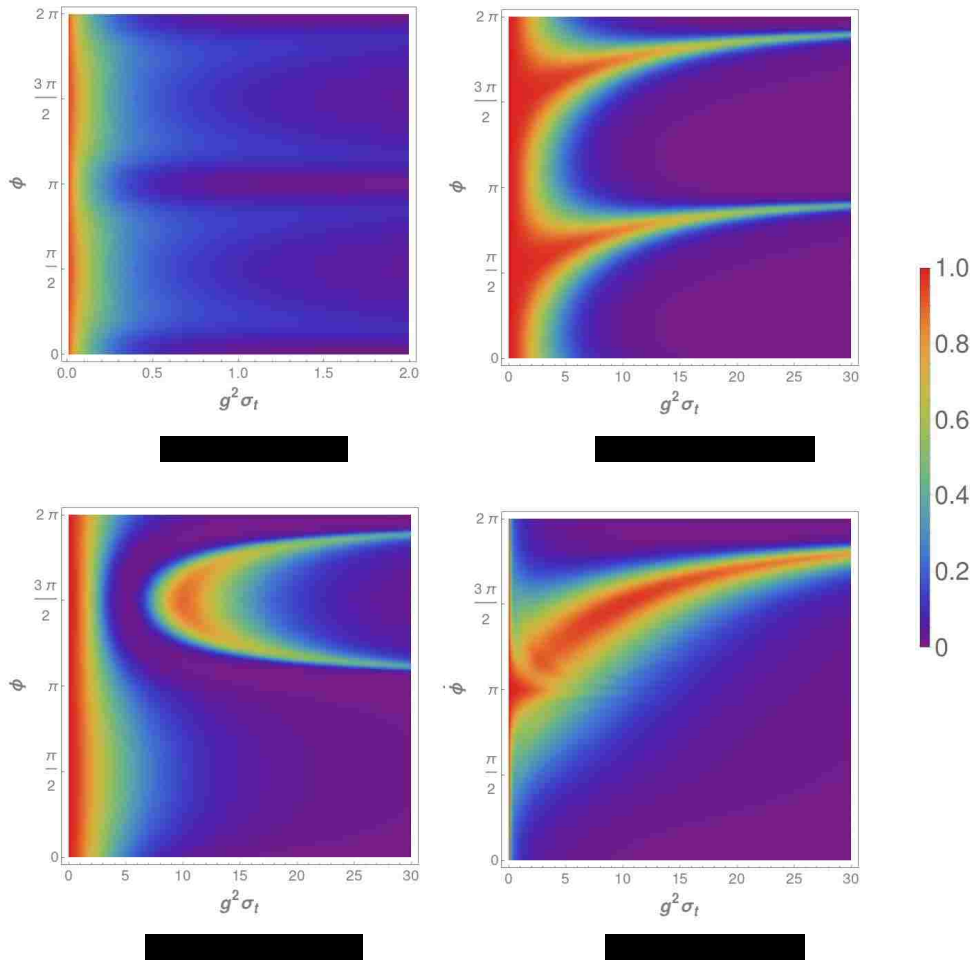

Figure 4.4: The probability that both photons are transmitted as a function of $g^2\sigma_t$ and ϕ. For all plots $\beta = 0$ and the other parameters are a) $\delta = \Delta = 0$, b) $\delta = 10\sigma_t$, $\Delta = 0$, c) $\Delta = 10\sigma_t$, $\delta = 0$.

Two photons arriving from opposite directions

When the photons are initially counter-propagating, that is they are moving in opposite directions, identical, and uncorrelated, the initial state will be of the form

$$|\psi_I\rangle = \int\int dt_1 dt_2 f(t_1) f(t_2) \hat{A}^\dagger(t_1) \hat{B}^\dagger(t_2) |0\rangle \tag{4.54}$$

The calculation to arrive at the final scattered wavefunction is somewhat more involved in this case, but the process is the same, where we convert the initial state to the $\hat{C}$ and $\hat{D}$

modes, evaluate Eq. 4.30, and then convert the final solution back to the travelling wave modes. In the end, the final result is

$$f_{aa}(t_1,t_2) = f_{bb}(t_1,t_2) = \frac{1}{\sqrt{2}}\Big[\tau(t_1)\rho(t_2) + \tau(t_2)\rho(t_1)\Big] + \sqrt{2}f^{+}_{ent,ab}(t_1,t_2)$$
$$f_{ab}(t_1,t_2) = \tau(t_1)\tau(t_2) + \rho(t_1)\rho(t_2) + 2f^{-}_{ent,ab}(t_1,t_2) \tag{4.55}$$

where we have written these in terms of the reflection and transmission functions defined in Eq. 4.36. We also have once again introduced another nonlinear term, given below.

$$\begin{aligned} f^{\pm}_{ent,ab} = &- \left(\Gamma_c^2 e^{-\Gamma_+|t_1-t_2|} G_{\Gamma_+}(t_<)^2 \mp \Gamma_s^2 e^{-\Gamma_-|t_1-t_2|} G_{\Gamma_-}(t_<)^2\right) \\ &+ \left(\Gamma_c e^{-\Gamma_+|t_1-t_2|} \pm \Gamma_s e^{-\Gamma_-|t_1-t_2|}\right)\left(\Gamma_c \mathcal{E}_{\Gamma_+}(t_<) - \Gamma_s \mathcal{E}_{\Gamma_-}(t_<)\right) \end{aligned} \tag{4.56}$$

As discussed in the "split" solution for the single atom in Chapter 3, there is a factor of $1/\sqrt{2}$ between the co- and counter-propagating components of the scattered photon state that arises from a difference in the normalization of the two states.

Looking at the linear components of Eq. 4.56 one can see that the split outcome f_{ab} will approach one when the single-photon case exhibits unit transmission or reflection. This is potentially useful for applications in quantum information processing, as it suggests that the photons may be able to interact with the atoms and remain in their respective modes. This allows for highly controllable interactions that, as we will see, can in principle be used to implement conditional quantum logic between photons.

Because of this application, the rest of our analysis will focus on the scattered wavefunction of the two photons when the system is tuned to the two windows of high transmission given in Chapter 2, $\tan(\phi) = -\delta/g^2$ and $\sin(\phi) = -\Delta/g^2$. These windows can be seen in Fig. 4.5, where we present the probability that both photons will remain in the split modes. Note that the transmission windows described can be clearly seen, just as in the single photon case. If the central frequency of the photon is on resonance and there are no direct atom-atom interactions, changing the spacing between the atoms has little effect on the scattering of the photons, with the coupling being the more important parameter.

Adding detunings or interactions, however, the position of the atoms can have very pronounced effects on the transmission properties of the system. In all cases, though, when $g^2\sigma_t$ is large or small it is most likely that both photons will remain in their original modes.

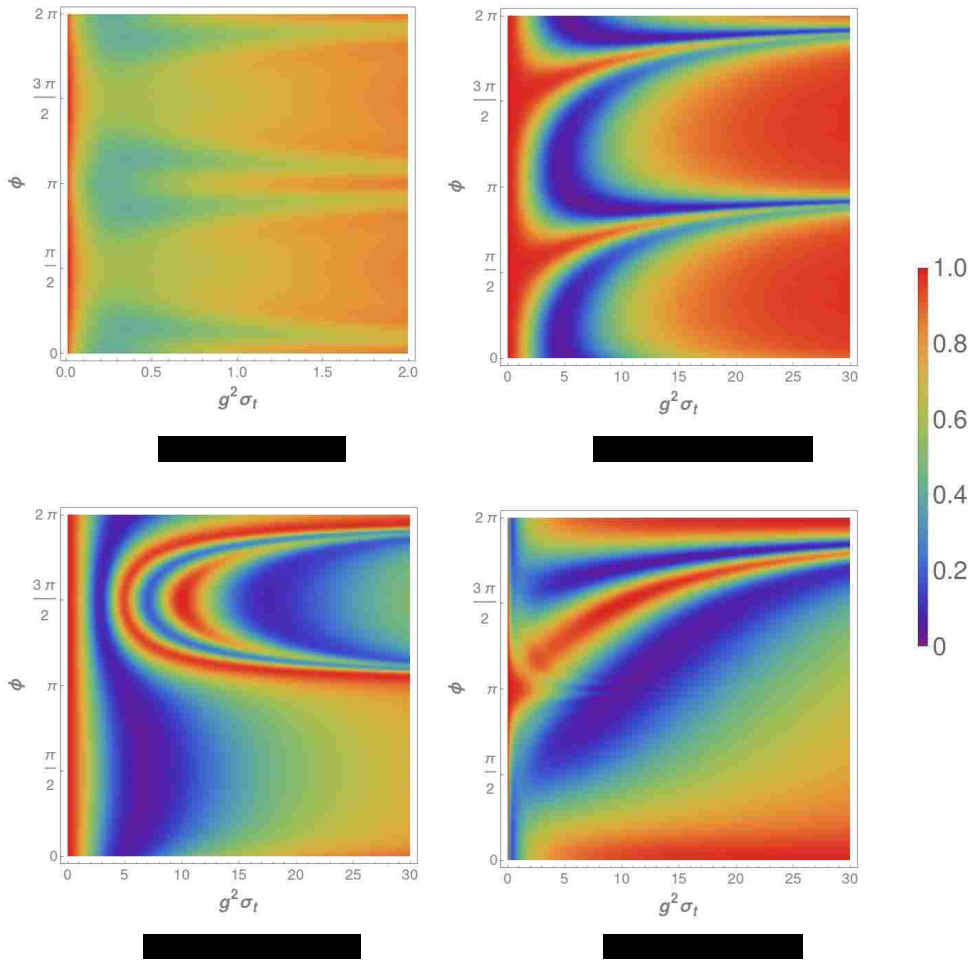

Figure 4.5: The probability that the photons are scattered into different modes as a function of $g^2\sigma_t$ and ϕ. For all plots $\beta = 0$ and the other parameters are a) $\delta = \Delta = 0$, b) $\delta = 10\sigma_t$, $\Delta = 0$, c) $\Delta = 10\sigma_t$, $\delta = 0$.

We will start with the most interesting result; when $\phi = 3\pi/2$, $\delta = 0$, and $\Delta = g^2$, both counter-propagating photons will be transmitted with unit probability regardless of the pulse shape. From our analysis of the single photon case, we have shown that when these two conditions have been met $\rho(t) = 0$ and thus the linear components of f_{aa} and f_{bb} vanish, while the linear component of f_{ab} is proportional to just $\tau(t)$. To understand what happens

to the entangled component, recall that for these parameters $\Gamma_+ = \Gamma_- = \Gamma_c = \Gamma_s = g^2$. As a result, the function $f^+_{ent,ab}$ will always be zero, and thus $f_{aa} = f_{bb} = 0$. This leads to the remarkable result that, while the photons will transmit with unit probability (which we show in Fig. 4.6), the nonlinear contribution to the wavepacket is nonzero and the final state will be at least partially entangled. With the aforementioned choices of ϕ, δ, and Δ we have that the only nonzero component of the wavefunction is given by

$$f_{ab}(t_1, t_2) = (f(t_1) - 2g^2 G_{g^2}(t_1))(f(t_2) - 2g^2 G_{g^2}(t_2)) - 4g^2 e^{-g^2|t_1 - t_2|} G_{g^2}(t_<)^2 \qquad (4.57)$$

This is identical to the single atom, unidirectional (or standing wave) result given in Eq. 3.30, provided that $\Gamma \to g^2$. The fact that this result is the same is highly nontrivial, as here the modification appears in a bidirectional geometry. Because the photons are travelling in opposite directions they can easily be routed before and after interacting with the atoms. Additionally, considering this state in the frequency domain shows that this is the same transformation that would be experienced by a two-photon wavepacket incident on a three-level atom in the "V" configuration where each photon couples to one of the two transitions (for examples, see [28, 30, 64]). This itself is not surprising, as a V system has a level structure that is isomorphic to the levels presented here, specifically the transitions between $|gg\rangle$ and $|\pm\rangle$), provided that the state $|ee\rangle$ is not accessed. This appears to be the case here, as the scattered state does not contain any entanglement due to interacting with $|ee\rangle$. This is also a very important result for this work, as we will show in Chapter 6 that this scattering process can be used to create a conditional-phase (CPHASE) gate between the two photons that would, in principle, enable quantum logic (see Section 1.3 for a description of a CPHASE gate).

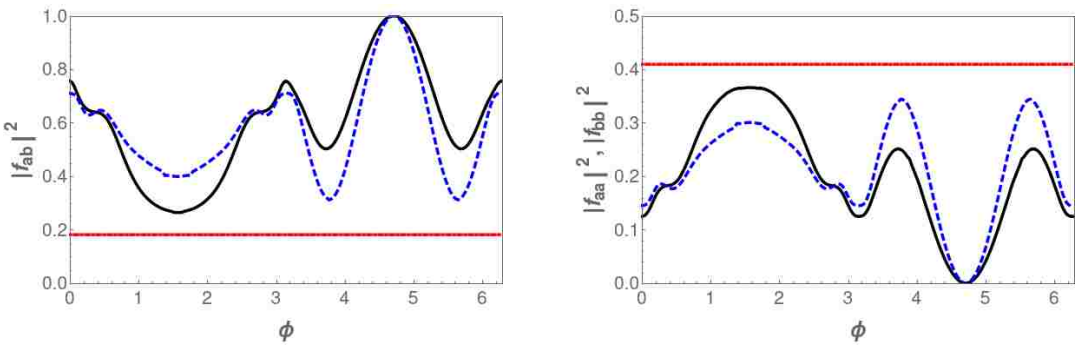

Figure 4.6: Probabilities of both photons leaving in the same direction (left) or in opposite directions (right), when the photons are initially counter-propagating. Values are calculated for a square pulse of duration $T = \sqrt{3}$, for the parameters $\Delta = g^2|\sin(k_F a)|$, $\delta = \beta = 0$, and $g^2\sigma_t = 1$. The dotted (constant) line shows the corresponding probabilities for a single atom. The dashed line shows the result of including all the terms in the wavefunction, whereas the solid line shows only the contribution of the linear terms.

Realizing this interaction experimentally may be challenging, however; it clearly requires fairly large, precise interactions between the atoms ($\Delta = g^2$) and a particular separation ($\phi = 3\pi/2$). As such, we also analyze the other transmission window that occurs when $\Delta = 0$, namely the one seen in Fig. 4.5 when $\delta = -g^2 \tan\phi$. At this point one has

$$\Gamma_\pm = \frac{g^2}{\cos\phi} e^{i\phi}\,(1 \pm \cos\phi) \qquad\qquad \frac{\Gamma_c}{\Gamma_+} = \frac{\Gamma_s}{\Gamma_-} = e^{-i\phi}\cos\phi \tag{4.58}$$

The equivalence shown in the last line implies that under the adiabatic (or long-pulse) approximation made in Chapter 3 ($G_\pm \simeq f/\Gamma_\pm$) and above in Eq. 4.45, both the single-photon reflection coefficient $\rho(t)$ (Eq. 4.36) and the dobubly-excited state contribution to $f^+_{ent,ab}$ (Eq. 4.56) will approximately vanish. Note that this limit requires that both δ and g^2 be large so that each of Γ_+ and Γ_- will also be large. Under this approximation, the total scattered state from Eq. 4.55 reduces to

$$\begin{aligned} f_{aa}(t_1,t_2) &= f_{bb}(t_1,t_2) \\ &\simeq -\sqrt{2}\cos^2\phi\, e^{-2i\phi}\left(e^{-\Gamma_+|t_1-t_2|} - e^{-\Gamma_-|t_1-t_2|}\right) f^2(t_<) \\ f_{ab}(t_1,t_2) &\simeq e^{-4i\phi} f(t_1) f(t_2) \\ &\quad - 2\cos^2\phi\, e^{-2i\phi}\left(e^{-\Gamma_+|t_1-t_2|} + e^{-\Gamma_-|t_1-t_2|}\right) f^2(t_<) \end{aligned} \tag{4.59}$$

This demonstrates that in this limit the probability for the photons to leave in the same direction can become very small and, as such, the photons will pass through each other. We show this transmission window in Fig. 4.7. This term still has a nonvanishing nonlinear component, however, and is similar in form to that seen in Eq. 4.57. This suggests that one may also be able to exploit this transmission window to construct a CPHASE gate in the same style as the one proposed by Brod and Combes. We have already shown in Chapter 2 that for a single photon it is entirely possible to tune an array of atoms so that the photon will transmit with near-unit probability and experience a phase proportional to transmitting thorough a number of two-atom sites. In Chapter 5 we will explore how two photons transmit through multiple sites and in Chapter 6 we will combine everything to study how well one can build a phase gate using this transmission window.

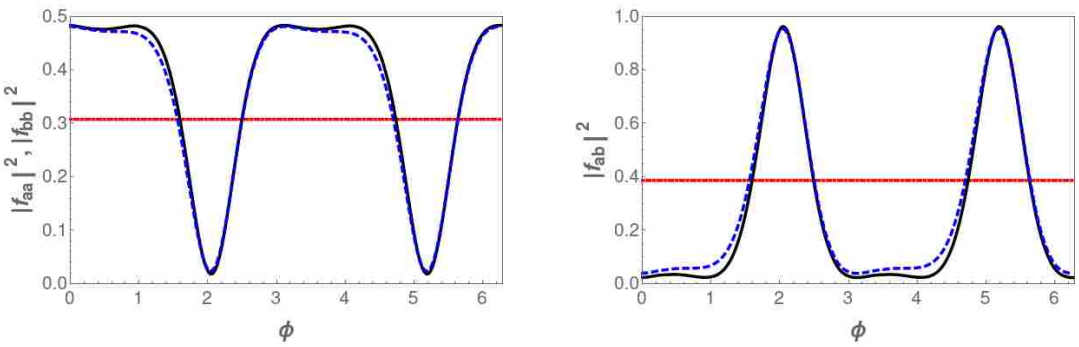

Figure 4.7: Probabilities of both photons leaving in the same direction (left) or in opposite directions (right), when the photons are initially counter-propagating. Values are calculated for a square pulse of duration $T = \sqrt{3}$, for the parameters $\delta\sigma_t = 10$, $\Delta\sigma_t = \beta\sigma_t = 0$, and $g^2\sigma_t = 5$. The dotted (constant) line shows the corresponding probabilities for a single atom. The dashed line shows the result of including all the terms in the wavefunction, whereas the solid line shows only the contribution of the linear terms.

4.4 Conclusions

In this chapter we extended the time-domain approach of Chapter 3 to two atoms and explored single- and two-photon scattering of photons from two level systems coupled to a lossless waveguide. We demonstrated how to apply the Markov approximation in the time domain. We analytically and numerically studied the photon transport properties and

nonlinear interactions and explored the effects of direct atom-atom interactions. Most importantly, we found that the transmission windows described in Chapter 2 for single photons are also present for two photons, though the agreement is especially good for photons coming from opposite directions. We explored these regions analytically and found that there is good reason to expect that they can be used to implement a CPHASE gate between two photons.

Chapter 5

Scattering of Two Photons From Many Atoms

5.1 Introduction

In Chapter 4 we found that two photons will transmit with high probability from a system consisting of two atoms. Here we will extend the time-domain solution first presented in Chapter 3 to deal with N, non-interacting atoms. We will use this to analyze whether the same atomic spacing presented in Chapter 2 enables high two-photon transmission. Additionally, we will ultimately use the solutions presented here in Chapter 6 to evaluate the effectiveness of a heuristic model of two photon transport.

5.1.1 Extending the syntax to many atoms and arbitrary positions

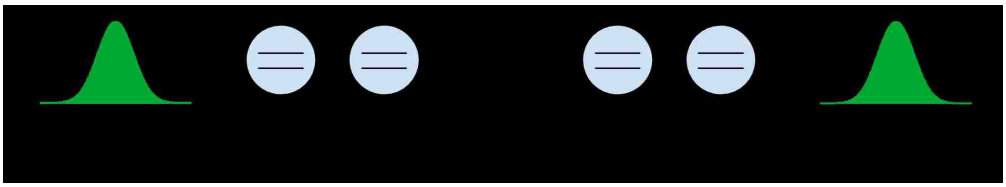

Figure 5.1: A diagram of the system being considered. All photons are constrained to move in 1-D in a waveguide that is coupled to an array of n atoms at arbitrary positions. z will denote the distance along a waveguide with z=0 being the location of the center of the atomic array.

In what follows we will be considering a system of the form as in Fig. 5.1 consisting of N, non-interacting atoms each with positions given by z_j. Due to the fact that we are allowing for arbitrary positions the symmetric atomic states $|\pm\rangle$ used in Chapter 4 will no longer couple to one standing wave mode. As such, there is no advantage in moving to the $|\pm\rangle$ basis. The Hamiltonian that describes this system is

$$H = \hbar g \sum_{j=1}^{N} \left[\hat{\phi}_j(t) e^{-i\delta t} \sigma_j^\dagger + \hat{\phi}_j^\dagger(t) e^{i\delta t} \sigma_j \right] \tag{5.1}$$

where the atomic operators $\sigma_j^\dagger$ and σ_j raise or lower the jth atom and and the field operators are identical to that used in Eq. 2.1. The field operator is reproduced below.

$$\hat{\phi}_j(t) = e^{ik_F z_j}\hat{A}\big(t - \frac{z_j}{c}\big) + e^{ik_F z_j}\hat{B}\big(t + \frac{z_j}{c}\big) \tag{5.2}$$

This operator commutes with relationship

$$[\hat{\phi}_j(t), \hat{\phi}_k^\dagger(t_1)] = e^{ik_F(z_j - z_k)}\delta\big(t - t_1 - \frac{z_j - z_k}{c}\big) + e^{-ik_F(z_j - z_k)}\delta\big(t - t_1 + \frac{z_j - z_k}{c}\big) \tag{5.3}$$

Before moving on to solving the equations, it is important to note how the Markovian approximation will play a role. Similar to what was seen in Chapter 4, the commutator of $\hat{\phi}_j$ will be found in the context of terms like

$$\int_{-\infty}^{t} dt_1 [\hat{\phi}_j(t), \hat{\phi}_k^\dagger(t_1)] e^{-i\delta t + i\delta t_1} |\psi(t_1)\rangle \tag{5.4}$$

Here, the limits of integration constrain the solution so that only the delta function coupled with the positive phase term will survive. Noting that in the Markovian approximation $|\psi(t - z_j/c)\rangle \approx |\psi(t)\rangle$ and that terms that go as $z_j\delta/c \approx 0$ we can approximate the above integral as

$$\int_{-\infty}^{t} dt_1 [\hat{\phi}_j(t), \hat{\phi}_k^\dagger(t_1)] e^{-i\delta t + i\delta t_1} |\psi(t1)\rangle \approx e^{ik_F|z_j - z_k|} |\psi(t)\rangle \tag{5.5}$$

For compactness, we will define $\theta_{j,k} = e^{ik_F|z_j - z_k|}$. This means that, within the Markovian approximation, the commutator for the field operators has the effective form of

$$[\hat{\phi}_j(t), \hat{\phi}_k^\dagger(t_1)] = 2\theta_{j,k}\delta(t - t_1) \tag{5.6}$$

The factor of 2 has been included to account for the fact that $\delta(t - t_1)$ will only be satisfied at the upper limit of integration (adding a factor of 1/2 when evaluated) whereas $\delta(t - t_1 - \epsilon)$ will be fully satisfied.

5.2 Solving the Schrödinger equation

To solve for the final scattered photon state, we will express the system's total state as

$$|\psi(t)\rangle = |\psi_{2,0}(t)\rangle + |\psi_{1,1}(t)\rangle + |\psi_{0,2}(t)\rangle \tag{5.7}$$

where the first index refers to the number of photons and the second refers to the number of excited atoms. Each of these terms contains both atom and photon states. In what follows we will use the same procedure developed in Chapter 3 where we normal order all photon operators to arrive at a truncated series solution in terms of photon number. Because of this, the number of photons matters more than the specific states that are excited.

We will also define the operator $\hat{h}(t) = \sum_{j=1}^{N} \hat{\phi}_j(t) e^{-i\delta t} \sigma_j^\dagger$ so that, from the above Hamiltonian (Eq. 5.1), the equations of motion have the compact form of

$$|\dot{\psi}_{2,0}\rangle = -ig\hat{h}^\dagger(t)|\psi_{1,1}(t)\rangle \tag{5.8a}$$

$$|\dot{\psi}_{1,1}\rangle = -ig\hat{h}(t)|\psi_{2,0}(t)\rangle - ig\hat{h}^\dagger(t)|\psi_{0,2}(t)\rangle \tag{5.8b}$$

$$|\dot{\psi}_{0,2}\rangle = -ig\hat{h}(t)|\psi_{1,1}(t)\rangle \tag{5.8c}$$

Following the method we integrate Eq. 5.8a and substitute it into Eq. 5.8b to get

$$|\dot{\psi}_{1,1}\rangle = -ig\hat{h}(t)|G\rangle|\psi_I\rangle - ig\hat{h}^\dagger(t)|\psi_{0,2}(t)\rangle - g^2 \int_{-\infty}^{t} dt_1 \hat{h}(t)\hat{h}^\dagger(t_1)|\psi_{1,1}(t_1)\rangle \tag{5.9}$$

Note we are assuming that the initial state contains two photons and no atomic excitations, expressed by $|\psi_I\rangle \otimes |G\rangle$ where $|G\rangle = |g_1\rangle \otimes |g_2\rangle .... \otimes |g_n\rangle$ and $|\psi_I\rangle$ is the initial photon state. At this point we normal order the photon operators in $\hat{h}(t)\hat{h}^\dagger(t_1)$. Commuting only the photon components gives the following expression.

$$\hat{h}(t)\hat{h}^\dagger(t_1) = \sum_{j,k=1}^{N} \Big(2\delta(t-t_1)\theta_{j,k} + \hat{\phi}_k^\dagger(t_1)\hat{\phi}_j(t)\Big)\sigma_j^\dagger\sigma_k e^{-i\delta t + i\delta t_1} \tag{5.10}$$

Placing this into the equation for $|\psi_{1,1}(t)\rangle$ and evaluating the delta function we get

$$\begin{aligned}|\dot{\psi}_{1,1}\rangle =& -g^2 \sum_{j,k=1}^{N} \theta_{j,k}\sigma_j^\dagger\sigma_k|\psi_{1,1}(t)\rangle - ig\hat{h}(t)|G\rangle|\psi_I\rangle - ig\hat{h}^\dagger(t)|\psi_{0,2}(t)\rangle \\ & - g^2\int_{-\infty}^{t} dt_1 \sum_{j,k=1}^{N} \hat{\phi}_k^\dagger(t_1)\hat{\phi}_j(t)\sigma_j^\dagger\sigma_k e^{-i\delta(t-t_1)}|\psi_{1,1}(t_1)\rangle \end{aligned} \tag{5.11}$$

From here, we define an integrating factor $\hat{\Gamma} = g^2\sum_{j,k=1}^{N}\theta_{j,k}\sigma_j^\dagger\sigma_k$. As there is no time dependence on the atomic operators, this can be used to arrive at the solution

$$\begin{aligned}|\psi_{1,1}\rangle =& -ig\int_{-\infty}^{t} dt_1 e^{-\hat{\Gamma}(t-t_1)}\hat{h}(t)|G\rangle|\psi_I\rangle - ig\int_{-\infty}^{t} dt_1 e^{-\hat{\Gamma}(t-t_1)}h^\dagger(t_1)|\psi_{0,2}(t_1)\rangle \\ & - g^2\int_{-\infty}^{t} dt_1 e^{-\hat{\Gamma}(t-t_1)}\int_{-\infty}^{t_1} dt_2 \sum_{j,k=1}^{N} \hat{\phi}_k^\dagger(t_2)\hat{\phi}_j(t_1)\sigma_j^\dagger\sigma_k e^{-i\delta(t_1-t_2)}|\psi_{1,1}(t_2)\rangle \end{aligned} \tag{5.12}$$

We now substitute $|\psi_{1,1}(t)\rangle$ into itself. While $e^{-\hat{\Gamma}(t-t_1)}$ is an operator, it consists of only atomic operators. Thus the photon components of all parts of the sums in $\hat{h}$ will commute with this element. In addition, due to the nature of the time ordering, photon operators with time indices that differ by more than one will commute. This is due to the Markov approximation made earlier and is justified more thoroughly in Section 4.2.1.

This will cause the component of the substituted term containing $|\psi_{0,2}(t)\rangle$ to vanish, as each component of the sum will contain a photon lowering operator of some form acting on a state with no photons. The term with $|\psi_{1,1}(t)\rangle$ will similarly vanish. This term will have operators (without the integrals) of the form

$$e^{-\hat{\Gamma}(t-t_1)}\hat{\phi}_j^\dagger(t_2)\hat{\phi}_j(t_1)e^{-\hat{\Gamma}(t_2-t_3)}\hat{\phi}_l^\dagger(t_4)\hat{\phi}_m(t_3)|\psi_{1,1}(t)\rangle \tag{5.13}$$

As the photon operators $\hat{\phi}_j(t_1)$ and $\hat{\phi}_l^\dagger(t_4)$ differ by more than one time index they will commute cleanly under the Markov approximation. Thus, every term will have two photon lowering operators acting on $|\psi_{1,1}(t_4)\rangle$, a state with only one photon, causing the term to vanish. The initial state has two photons so it will not vanish under iteration. Eq. 5.11

then becomes

$$|\psi_{1,1}(t)\rangle = -ig\int_{-\infty}^{t} dt_1 e^{-\hat{\Gamma}(t-t_1)}\hat{h}(t)|G\rangle|\psi_I\rangle - ig\int_{-\infty}^{t} dt_1 e^{-\hat{\Gamma}(t-t_1)}\hat{h}^\dagger(t_1)|\psi_{0,2}(t_1)\rangle$$
$$+ ig^3\int_{-\infty}^{t} dt_1\int_{-\infty}^{t_1} dt_2\int_{-\infty}^{t_2} dt_3 e^{-\hat{\Gamma}(t-t_1)}\sum_{j,k=1}^{N}\hat{\phi}_k^\dagger(t_2)\hat{\phi}_j(t_1)\sigma_j^\dagger\sigma_k e^{-i\delta(t_1-t_2)}e^{-\hat{\Gamma}(t_2-t_3)}\hat{h}(t_3)|G\rangle|\psi_I\rangle \tag{5.14}$$

As this is in terms of just the initial state and $|\psi_{0,2}(t)\rangle$ we can substitute it into Eq. 5.8c. Doing so will kill the triple integral term, as $\hat{h}(t)$ contains photon lowering operators that will commute with $\hat{\phi}^\dagger(t_2)$. The differential equation for the state when both photons have been absorbed is then

$$|\dot{\psi}_{0,2}\rangle = -g^2\int_{-\infty}^{t} dt_1\hat{h}(t)e^{-\hat{\Gamma}(t-t_1)}\hat{h}(t)|G\rangle|\psi_I\rangle - g^2\int_{-\infty}^{t} dt_1\hat{h}(t)e^{-\hat{\Gamma}(t-t_1)}\hat{h}^\dagger(t_1)|\psi_{0,2}(t_1)\rangle \tag{5.15}$$

When normal ordering the photon operators in $|\psi_{0,2}(t_1)\rangle$ one must be careful to remember that there is an exponential term between the two. Fortunately, the fact that photon operators commute to give a delta function removes the effect of the exponential, in part because evaluating the delta function of $\delta(t_i - t_j)$ from the commutator of the photon operators will lead to $e^{-\hat{\Gamma}(t_i-t_j)} \to e^0 = 1$. After working out the algebra by expanding each operator (including the matrix exponent) in terms of a sum and commuting the photon terms, it can be shown that the whole expression reduces to

$$|\dot{\psi}_{0,2}\rangle = -\hat{\gamma}|\psi_{0,2}(t)\rangle - g^2\int_{-\infty}^{t} dt_1\hat{h}(t)e^{-\hat{\Gamma}(t-t_1)}\hat{h}(t)|G\rangle|\psi_I\rangle \tag{5.16}$$

Where we have defined

$$\hat{\gamma} = g^2\sum_{j,k,l,m=1}^{N} e^{ik_F|z_j-z_k|}\delta_{l,m}(1-\delta_{j,l})(1-\delta_{k,m})\sigma_j^\dagger\sigma_l^\dagger\sigma_k\sigma_m \tag{5.17}$$

Using an integrating factor of $\hat{\gamma}$ Eq. 5.15 becomes

$$|\psi_{0,2}(t)\rangle = -g^2\int_{-\infty}^{t} dt_1\int_{-\infty}^{t_1} dt_2 e^{-\hat{\gamma}(t-t_1)}\hat{h}(t_1)e^{-\hat{\Gamma}(t_1-t_2)}\hat{h}(t_2)|G\rangle|\psi_I\rangle \tag{5.18}$$

Putting this all together we can finally write the ground state as a function of time by

substituting all these equations into the equation for $|\psi_{2,0}(t)\rangle$ and multiplying both sides by $\langle G|$ to obtain states with no atoms excited. Doing so yields

$$\begin{aligned}|\psi_g(t)\rangle =&|\psi_I\rangle - g^2\int_{-\infty}^{t} dt_1 \int_{-\infty}^{t_1} dt_2 \langle G|\hat{h}^\dagger(t_1)e^{-\hat{\Gamma}(t_1-t_2)}\hat{h}(t_2)|G\rangle|\psi_I\rangle \\ &+ g^4\int_{-\infty}^{t} dt_1 \int_{-\infty}^{t_1} dt_2 \int_{-\infty}^{t_2} dt_3 \int_{-\infty}^{t_2} dt_4 \Bigg[\\ &\langle G|\hat{h}^\dagger(t_1)e^{-\hat{\Gamma}(t_1-t_2)} \sum_{j,k=1}^{N} \hat{\phi}_k^\dagger(t_3)\hat{\phi}_j(t_2)\sigma_j^\dagger\sigma_k e^{-\hat{\Gamma}(t_3-t_4)}\hat{h}(t_4)|G\rangle|\psi_I\rangle \\ &+ \langle G|\hat{h}^\dagger(t_1)e^{-\hat{\Gamma}(t_1-t_2)}\hat{h}^\dagger(t_2)e^{-\hat{\gamma}(t_2-t_3)}\hat{h}(t_3)e^{-\hat{\Gamma}(t_3-t_4)}\hat{h}(t_4)|G\rangle|\psi_I\rangle\Bigg] \end{aligned} \tag{5.19}$$

While certainly unwieldy and more complicated than the previous solutions for a single atom (Eq. 3.26) and for two atoms (Eq. 4.30), it has a similar physical structure that describes all the different possible scattering events. Each term deals with a different possibility for photon scattering and mirrors the process described in Section 4.2.1. The first term in Eq. 5.19 represents the probability that no interaction occurs. The second (the double-integral term) represents the probability that only one of the two photons will interact with any atoms. The process here is that one photon is absorbed at any time ($\hat{h}_1(t_2)$), may be instantly emitted and re-absorbed by any number of atoms ($e^{-\hat{\Gamma}(t_1-t_2)}$), and then is emitted back into the waveguide at a later time ($\hat{h}_1^\dagger(t_1)$). The third term (first quadruple-integral term) involves a photon being absorbed at one time, (possibly) transferring to another atom, then being re-emitted at a time before a second photon is absorbed. This second photon can then be transferred to any other atom and then be emitted back into the waveguide. Finally, the last term (second quadruple-integral term) involves a photon being absorbed and (potentially) hopping to a different atom. A second photon is then absorbed. After this, one of the two photons may move to a different atom ($e^{-\hat{\gamma}(t_2-t_3)}$) and then they are both emitted.

As before, we note that this solution is time-dependent and, in principle, can be used to obtain the evolution of the field state and atomic populations as a function of time. We

will explain how to evaluate the operators in the exponents in the scattering limit of $t \to \infty$. Ultimately, normal ordering the atomic operators will lead to a closed form that sums over all possible scattering terms and is relatively straightforward to evaluate.

5.3 Simplifying the general expression

5.3.1 Single photon term

Equation 5.19 can be converted into a computable form by re-writing the exponential terms $e^{-\hat{\Gamma}(t_i - t_j)}$ as a matrix. As given, such terms are an exponential of atomic operators and effectively describe all the possible paths that a photon could take after being absorbed at once site to be emitted at a separate site, along with all the possible phases that will be accrued from this hopping. Unfortunately, the number of possible paths to go from one atom to another is virtually infinite, as the Markovian approximation allows for instantaneous transfer of photons. Casting this infinite sum of possible events as a matrix and diagonalizing it provides a numerically tractable way to calculate the final scattered state.

To accomplish this, we define an atomic identity operator over all single-atom excited states as

$$N_1 = \sum_{j=1}^{N} |j\rangle\langle j| \tag{5.20}$$

This can be re-written as a unitary operator $N_1 = U_1^\dagger U_1$, with

$$U_1 = \begin{bmatrix} \langle 1| \\ \vdots \\ \langle N| \end{bmatrix} \tag{5.21}$$

While this is not a true identity, when acting on any state with only a single atomic excitation it will preserve the state. As each $e^{-\hat{\Gamma}(t_i - t_j)}$ will act on the space of single atom excitations, the $\hat{N}_1$ operator will thus preserve the state of the system. The point of

defining such an operator is that we can express the exponential as

$$e^{-\hat{\Gamma}(t_1-t_2)} = U_1^\dagger e^{-U_1\hat{\Gamma}U_1^\dagger(t_1-t_2)}U_1 \tag{5.22}$$

where the matrix product $A = U\hat{\Gamma}U_1^\dagger$ contains no operators, only the $\theta_{j,k}$ phase factors and g^2. The matrix product gives

$$U\Gamma U^\dagger = g^2 \begin{bmatrix} \langle 1| \\ \vdots \\ \langle N| \end{bmatrix} \cdot \sum_{j,k=1} \theta_{j,k}\sigma_j^\dagger\sigma_k \cdot [|1\rangle \quad \cdots \quad |N\rangle] = g^2 M \tag{5.23}$$

From the above, it is clear that each element of M will be simply

$$M_{i,j} = \langle i| \sum_{m,n=1} \theta_{m,n}\sigma_m^\dagger\sigma_n|j\rangle = g^2\theta_{i,j} \tag{5.24}$$

This matrix can then be diagonalized as $M = PDP^{-1}$ and the exponent can finally be written without operators as

$$e^{-\hat{\Gamma}(t_1-t_2)} = U_1^\dagger P e^{-g^2 D_1(t_1-t_2)}P^{-1}U_1 \tag{5.25}$$

While this process is certainly unwieldy, it is easy to develop code to automatically calculate U_1, P, and D_1 for an arbitrary number of atomic pairs. Unfortunately, matrix diagonalization is not a problem with a tractable solution for an arbitrary $n \times n$ matrix. As such, the specifics of D_1 will depend on the parameters of the system and the number of pairs being considered and a numerical approach is required.

Regardless of the computational complexity of diagonalizing M, the final matrix exponential must have the (effective) form

$$e^{-\hat{\Gamma}(t_1-t_2)} = \sum_{j,k=1}^{N} C_{j,k}(t_1-t_2)|j\rangle\langle k| \tag{5.26}$$

We can further specify the coefficients $C_{j,k}(t_1 - t_2)$ by noting that this can be written as

$$C_{j,k}(t_1-t_2) = \sum_{i=1}^{N} P_{j,i}P_{i,k}^{-1}e^{-g^2\lambda_i(t_1-t_2)} \tag{5.27}$$

where each λ_i is an eigenvalue of M. The notation $P_{j,i}$ refers to the j,ith matrix element of

P. The advantage of writing the coefficients this way is that is draws out the exponents that define the different effective couplings and detunings for the system, allowing for the final state to be written in terms of $f(t)$, $G_\Gamma(t)$, and $\mathcal{E}_\Gamma(t)$ as defined in Eq. 3.23 and Eq. 4.39.

Using the above definitions we can begin writing the different components of Eq. 5.19 in terms of the eigenvalues of the exponentials. Starting with the single photon interaction term and defining $\Gamma_i = g^2\lambda_i - i\delta$;

$$\begin{aligned} &-g^2 \int_{-\infty}^{t} dt_1 \int_{-\infty}^{t_1} dt_2 \langle G|\hat{h}^\dagger(t_1) e^{-\hat{\Gamma}(t_1-t_2)} \hat{h}(t_2)|G\rangle|\psi_I\rangle \\ &= -g^2 \int_{-\infty}^{t} dt_1 \int_{-\infty}^{t_1} dt_2 \sum_{i=1}^{N}\sum_{j,k=1}^{N} P_{j,i}P^{-1}_{i,k} e^{-\Gamma_i(t_1-t_2)} \hat{\phi}_j^\dagger(t_1)\hat{\phi}_k(t_2)|\psi_I\rangle \end{aligned} \tag{5.28}$$

This has the same form as Eq. 2.19, where the transmitted and reflected spectra of a single photon can be written in terms of the eigenvalues of a matrix describing the phases accrued by transferring from one atom to another.

5.3.2 Two-photon term: successive atomic excitations

Using the same analysis as in the single photon term with U_1, the first two-photon term in Eq. 5.19 can be written in terms of the eigenvalues of M as

$$\begin{aligned} g^4 \int_{-\infty}^{\infty} dt_1 dt_2 dt_3 dt_4 \theta(t_1-t_2)\theta(t_2-t_3)\theta(t_3-t_4) &\sum_{p,q=1}^{N}\sum_{j,k=1}^{N} P_{j,p}P^{-1}_{p,k} e^{-\Gamma_p(t_1-t_2)} \\ &\times \sum_{l,m}^{N} P_{l,q}P^{-1}_{q,m} e^{-\Gamma_q(t_3-t_4)} \hat{\phi}_j^\dagger(t_1)\hat{\phi}_l^\dagger(t_3)\hat{\phi}_k(t_2)\hat{\phi}_m(t_4)|\psi_I\rangle \end{aligned} \tag{5.29}$$

Following the example given in Chapter 3, we integrate the t_2 integral by parts in order to separate the entangled and non-entangled components of the scattered state. This is done by defining $u = \theta(t_2 - t_3)$ and $v = \int_{-\infty}^{t_2} dt \theta(t_1 - t) e^{-\Gamma_p(t_1-t)}\hat{\phi}_k(t_2)$. Further defining an operator $\hat{\mathcal{G}}_{k,\Gamma_i}(t_1) = \int_{-\infty}^{t_1} dt_2 e^{-\Gamma_i(t_1-t_2)}\hat{\phi}_k(t_2)$ for compactness, we integrate one of the terms

in Eq. 5.29.

$$\int_{-\infty}^{\infty} dt_2 \theta(t_1-t_2)\theta(t_2-t_3)e^{-\Gamma_p(t_1-t_2)}\phi_k(t_2) = \theta(t_1-t_3)\Big[\hat{\mathcal{G}}_{k,\Gamma_P}(t_1) - e^{-\Gamma_p(t_1-t_3)}\hat{\mathcal{G}}_{k,\Gamma_p}(t_3)\Big] \quad (5.30)$$

Placing this into the entire sum of Eq. 5.29, we arrive at

$$g^4 \int_{-\infty}^{\infty} dt_1 dt_3 \theta(t_1-t_3) \sum_{p,q=1}^{N} \sum_{j,k,l,m=1}^{N} P_{j,p}P^{-1}_{p,k}P_{l,q}P^{-1}_{q,m}\hat{\phi}^{\dagger}_j(t_1)\hat{\phi}^{\dagger}_l(t_3)\Big[\hat{\mathcal{G}}_{k,\Gamma_p}(t_1) - e^{-\Gamma_p(t_1-t_3)}\hat{\mathcal{G}}_{k,\Gamma_p}(t_3)\Big]\hat{\mathcal{G}}_{m,\Gamma_q}(t_3)|\psi_I\rangle \quad (5.31)$$

This has the same structure as Eq. 3.29 (though presented in a different form here) and contains terms that describe the event where both photons are absorbed successively. It also contains the entanglement that arises from the fact that the two photons cannot excite the same atom at the same time.

5.3.3 Two-photon term: simultaneous atomic excitations

The remaining term is by far the most difficult to evaluate. This is due to the fact that for N atoms there are ${}_nC_2$ different possible ways for two photons to be absorbed. In order to keep track of these states (note that $|j\rangle|k\rangle = |k\rangle|j\rangle$), we will define an effective identity operator and matrix for γ, in a similar way to Γ. These are given by

$$N_2 = \sum_{j=1}^{N-1}\sum_{k=1+j}^{N}|j\rangle|k\rangle\langle j|\langle k| = \sum_{j=1}^{{}_nC_2}|2_j\rangle\langle 2_j| = U_2^{\dagger}U_2 \quad U_2 = \begin{bmatrix}\langle 1|\langle 2|\\ \vdots \\ \langle N-1|\langle N|\end{bmatrix} = \begin{bmatrix}\langle 2_1|\\ \vdots \\ \langle 2_{{}_nC_2}|\end{bmatrix} \quad (5.32)$$

We have introduced the notation $|2_j\rangle = |j[1]\rangle|j[2]\rangle$ to reduce the double sum to a single sum over all the possible unique combinations of states. Here, $j[1] = l$ and $j[2] = m$ represents the numbering of a unique atomic state of the form $|l\rangle|m\rangle$. The index j corresponds to the j^{th} element of a list containing all possible doubly excited states. In our code we have chosen to create this list by letting the l index run from 1 to $N-1$ and the m index run from l to N. With this labeling of the states, $U_2\hat{\gamma}U_2^{\dagger} = M_2$ will have elements

$$\langle l|\langle m|U_2\hat{\gamma}U_2^{\dagger}|r\rangle|s\rangle = \theta_{l,s}\delta_{m,r} + \theta_{l,r}\delta_{m,s} + \theta_{m,s}\delta_{l,r} + \theta_{m,r}\delta_{l,s} \quad (5.33)$$

This allows us to express the exponential in terms of this manifold of states. We will also define the operator

$$\hat{\mathcal{E}}_{j,k,\gamma_r,\Gamma_q,}(t_2) = \int_{-\infty}^{t_2} dt_3 e^{-\gamma_r(t_2-t_3)} \hat{\phi}_j(t_3) \hat{\mathcal{G}}_{k,\Gamma_q}(t_3) \tag{5.34}$$

and define $M_2 = QD_2Q^{-1}$ so that $\langle 2_j|U_2 e^{-\gamma(t_2-t_3)}U_2^{-1}|2_k\rangle = \sum_{i=1}^{{}^nC_2} e^{-\gamma_i(t_2-t_3)}Q_{j,i}Q^{-1}_{i,k}$, where each $\gamma_i = g^2\lambda_i - 2i\delta$ and λ_i is an eigenvalue of M_2. This leads to a sum of the form

$$\begin{aligned} g^4 \int_{-\infty}^{\infty} dt_1 dt_2 \sum_{p,q=1}^{N} \sum_{r=1}^{{}^nC_2} \sum_{k,l=1}^{{}^nC_2} \sum_{j,m=1}^{N} \theta(t_1-t_2) e^{-\Gamma_p(t_1-t_2)} Q_{k,r} Q^{-1}_{r,l} \hat{\phi}^\dagger_j(t_1) \\ \times \Big(P_{j,p} P^{-1}_{p,k[1]} \hat{\phi}^\dagger_{k[2]}(t_2) + P_{j,p} P^{-1}_{p,k[2]} \hat{\phi}^\dagger_{k[1]}(t_2) \Big) \\ \times \Big(P_{l[1],q} P^{-1}_{q,m} \hat{\mathcal{E}}_{l[2],m,\gamma_r,\Gamma_q,}(t_2) + P_{l[2],q} P^{-1}_{q,m} \hat{\mathcal{E}}_{l[1],m,\gamma_r,\Gamma_q,}(t_2) \Big) |\psi_I\rangle \end{aligned} \tag{5.35}$$

This expression contains all possible ways that two photons may be simultaneously absorbed before being re-emitted.

5.3.4 Final state

With the above general forms it is possible to write the overall scattered state in terms of computable matrices. This has the form

$$\begin{aligned} |\psi_g(\infty)\rangle = |\psi_I\rangle - g^2 \int_{-\infty}^{\infty} dt_1 \sum_{i=1}^{N} \sum_{j,k=1}^{N} P_{j,i} P^{-1}_{i,k} \hat{\phi}^\dagger_j(t_1) \hat{\mathcal{G}}_{k,\Gamma_i}(t_1) |\psi_I\rangle \\ + g^4 \int_{-\infty}^{\infty} dt_1 dt_2 \theta(t_1-t_2) \sum_{p,q=1}^{N} \sum_{j,k,l,m=1}^{N} P_{j,p} P^{-1}_{p,k} P_{l,q} P^{-1}_{q,m} \hat{\phi}^\dagger_j(t_1) \hat{\phi}^\dagger_l(t_3) \Big[\hat{\mathcal{G}}_{k,\Gamma_p}(t_1) - e^{-\Gamma_p(t_1-t_2)} \hat{\mathcal{G}}_{k,\Gamma_p}(t_2) \Big] \hat{\mathcal{G}}_{m,\Gamma_q}(t_2) |\psi_I\rangle \\ + g^4 \int_{-\infty}^{\infty} dt_1 dt_2 \theta(t_1-t_2) \sum_{p,q=1}^{N} \sum_{r=1}^{{}^nC_2} \sum_{k,l=1}^{{}^nC_2} \sum_{j,m=1}^{N} e^{-\Gamma_p(t_1-t_2)} Q_{k,r} Q^{-1}_{r,l} \hat{\phi}^\dagger_j(t_1) \Big(P_{j,p} P^{-1}_{p,k[1]} \hat{\phi}^\dagger_{k[2]}(t_2) + P_{j,p} P^{-1}_{p,k[2]} \hat{\phi}^\dagger_{k[1]}(t_2) \Big) \\ \times \Big(P_{l[1],q} P^{-1}_{q,m} \hat{\mathcal{E}}_{l[2],m,\gamma_r,\Gamma_q,}(t_2) + P_{l[2],q} P^{-1}_{q,m} \hat{\mathcal{E}}_{l[1],m,\gamma_r,\Gamma_q,}(t_2) \Big) |\psi_I\rangle \end{aligned} \tag{5.36}$$

This again has the same effective structure as the scattered state derived in Chapter 4 for two atoms. There is one term describing the possibility where neither photon interacts with the atoms, one that describes a single photon interaction, one that describes two photons interacting successively, and one that describes both photons being absorbed simultaneously. The primary advantage of this expression over Eq. 5.19 is that here, the

state is written exclusively in terms of photon operators and that $\hat{\mathcal{G}}$ and $\hat{\mathcal{E}}$ will reproduce Eq. 3.23 ($G_\Gamma(t)$) and Eq. 4.39 ($\mathcal{E}_\Gamma(t)$) for an initially unentangled state.

5.4 Two unentangled counter-propagating photons

At this point we will finally specify the form of $|\psi_I\rangle$. We will assume that the two photons are identical, unentangled, and counter-propagating so that the initial state is given by

$$|\psi_I\rangle = \int dt_1 dt_2 f(t_1) f(t_2) \hat{A}^\dagger(t_1) \hat{B}^\dagger(t_2) |0\rangle \tag{5.37}$$

In terms of the different possible modes, the final scattered state is given by

$$\begin{aligned} |\psi_g(\infty)\rangle = \int dt_1 dt_2 \Big(& \frac{1}{\sqrt{2}} f_{aa}(t_1, t_2) \hat{A}^\dagger(t_1) \hat{A}^\dagger(t_2) |0\rangle \\ & + \frac{1}{\sqrt{2}} f_{bb}(t_1, t_2) \hat{B}^\dagger(t_1) \hat{B}^\dagger(t_2) |0\rangle + f_{ab}(t_1, t_2) \hat{A}^\dagger(t_1) \hat{B}^\dagger(t_2) |0\rangle \Big) \end{aligned} \tag{5.38}$$

As explained in Chapter 3 as well, when equating this to the scattered photon solution there is an ambiguity as to which variable corresponds to which in the co-propagating case. For example, the term containing only two A photons will have the form of

$$\int dt_1 dt_2 f_{A,A}(t_1, t_2) \hat{A}^\dagger(t_1) \hat{A}^\dagger(t_2) |0\rangle = \int dt_a dt_b f_{Scattered}(t_a, t_b) \hat{A}^\dagger(t_a) \hat{A}^\dagger(t_b) |0\rangle \tag{5.39}$$

As both functions are integrating over both variables, it is impossible to say whether $t_a \to t_1$ or $t_a \to t_2$. Thus, the scattered state derived above must be made to be symmetric in its time variables by $f_{Scattered}(t_a, t_b) = \frac{1}{2}\big(f_{Scattered}(t_a, t_b) + f_{Scattered}(t_b, t_a)\big)$ to account for this.

To simplify the final expression we will define the sums

$$\Sigma_i^{\pm_a, \pm_b} = \sum_{j,k=1}^{N} P_{j,i} P^{-1}_{i,k} e^{ik_F(\pm_a z_j \pm_b z_k)} \tag{5.40}$$

$$\chi^{\pm_a,\pm_b}_{p,q,r} = \sum_{k,l=1}^{{}^{n}C_2}\sum_{j,m=1}^{N} Q_{k,r}Q^{-1}_{r,l}\hat{e}^{\pm_a ik_F z_j}\Big(P_{j,p}P^{-1}_{p,k[1]}e^{\pm_b ik_F z_{k[2]}} + P_{j,p}P^{-1}_{p,k[2]}e^{\pm_b ik_F z_{k[1]}}\Big)$$
$$\times\Big(P_{l[1],q}P^{-1}_{q,m}\big(e^{ik_F(-z_{l[2]}+z_m)} + e^{ik_F(z_{l[2]}-z_m)}\big) + P_{l[2],q}P^{-1}_{q,m}\big(e^{ik_F(-z_{l[1]}+z_m)} + e^{ik_F(z_{l[1]}-z_m)}\big)\Big) \tag{5.41}$$

and note also that, as explained in more detail in Chapter 4, in the Markovian approximation when no longer commuting, the $\hat{\phi}$ operators take the form

$$\hat{\phi}_j = \Big(e^{ik_F z_j}\hat{A}(t) + e^{-ik_F z_j}\hat{B}(t)\Big) \tag{5.42}$$

Putting all this together for the co-propagating scattered photons leads to the temporal profiles of

$$f_{a,a}(t_1,t_2) = 1/\sqrt{2}\Big\{ -g^2\sum_{i=1}^{N}\Sigma_i^{-,-}\Big(G_{\Gamma_i}(t_1)f(t_2) + G_{\Gamma_i}(t_2)f(t_1)\Big) + g^4\sum_{p,q=1}^{N}\Big(\Sigma_p^{-,+}\Sigma_q^{-,-} + \Sigma_p^{-,-}\Sigma_q^{-,+}\Big)G_{\Gamma_p}(t_1)G_{\Gamma_q}(t_2)$$
$$-g^4\sum_{p,q=1}^{N}\Big(\Sigma_p^{-,+}\Sigma_q^{-,-} + \Sigma_p^{-,-}\Sigma_q^{-,+}\Big)\Big[\theta(t_1-t_2)e^{-\Gamma_p(t_1-t_2)}G_{\Gamma_p}(t_2)G_{\Gamma_q}(t_2) + \theta(t_2-t_1)e^{-\Gamma_p(t_2-t_1)}G_{\Gamma_p}(t_1)G_{\Gamma_q}(t_1)\Big]$$
$$+g^4\sum_{p,q=1}^{N}\sum_{r=1}^{{}^{n}C_2}\chi^{-,-}_{p,q,r}\Big[\theta(t_1-t_2)e^{-\Gamma_p(t_1-t_2)}E_{\gamma_r,\Gamma_q}(t_2) + \theta(t_2-t_1)e^{-\Gamma_p(t_2-t_1)}E_{\gamma_r,\Gamma_q}(t_1)\Big]\Big\} \tag{5.43}$$

$$f_{b,b}(t_1,t_2) = 1/\sqrt{2}\Big\{ -g^2\sum_{i=1}^{N}\Sigma_i^{+,+}\Big(G_{\Gamma_i}(t_1)f(t_2) + G_{\Gamma_i}(t_2)f(t_1)\Big) + g^4\sum_{p,q=1}^{N}\Big(\Sigma_p^{+,-}\Sigma_q^{+,+} + \Sigma_p^{+,+}\Sigma_q^{+,-}\Big)G_{\Gamma_p}(t_1)G_{\Gamma_q}(t_2)$$
$$-g^4\sum_{p,q=1}^{N}\Big(\Sigma_p^{+,-}\Sigma_q^{+,+} + \Sigma_p^{+,+}\Sigma_q^{+,-}\Big)\Big[\theta(t_1-t_2)e^{-\Gamma_p(t_1-t_2)}G_{\Gamma_p}(t_2)G_{\Gamma_q}(t_2) + \theta(t_2-t_1)e^{-\Gamma_p(t_2-t_1)}G_{\Gamma_p}(t_1)G_{\Gamma_q}(t_1)\Big]$$
$$+g^4\sum_{p,q=1}^{N}\sum_{r=1}^{{}^{n}C_2}\chi^{+,+}_{p,q,r}\Big[\theta(t_1-t_2)e^{-\Gamma_p(t_1-t_2)}E_{\gamma_r,\Gamma_q}(t_2) + \theta(t_2-t_1)e^{-\Gamma_p(t_2-t_1)}E_{\gamma_r,\Gamma_q}(t_1)\Big]\Big\} \tag{5.44}$$

In order to write down the split mode, as detailed in Chapter 3, the time indices must be dealt with in a different way. Instead of symmetrizing the state, we match the indices that go with each mode. In the scattered state, there are terms that go as $\hat{\phi}^\dagger_j(t_1)\hat{\phi}^\dagger_k(t_2)$ which will contain operators with indices $\hat{A}^\dagger(t_1)\hat{B}^\dagger(t_2)$ and $\hat{A}^\dagger(t_2)\hat{B}^\dagger(t_1)$. The final form of the scattered state only maps t_1 to the $\hat{A}$ mode and t_2 to the $\hat{B}$ mode, however. As such, we must flip time indices so that the final state maps t_1 and t_2 to the correct modes. Doing

so give the final state of

$$
\begin{aligned}
f_{a,b}(t_1,t_2) = f(t_1)f(t_2) - g^2\sum_{i=1}^{N}\left(\Sigma_i^{-,+}G_{\Gamma_i}(t_1)f(t_2) + \Sigma_i^{+,-}G_{\Gamma_i}(t_2)f(t_1)\right) \\
+g^4\sum_{p,q=1}^{N}\left(\Sigma_p^{-,+}\Sigma_q^{+,-} + \Sigma_p^{-,-}\Sigma_q^{+,+}\right)\left[\theta(t_1-t_2)G_{\Gamma_p}(t_1)G_{\Gamma_q}(t_2) + \theta(t_2-t_1)G_{\Gamma_p}(t_2)G_{\Gamma_q}(t_1)\right] \\
-g^4\sum_{p,q=1}^{N}\left(\Sigma_p^{-,+}\Sigma_q^{+,-} + \Sigma_p^{-,-}\Sigma_q^{+,+}\right)\left[\theta(t_1-t_2)e^{-\Gamma_p(t_1-t_2)}G_{\Gamma_p}(t_2)G_{\Gamma_q}(t_2) + \theta(t_2-t_1)e^{-\Gamma_p(t_2-t_1)}G_{\Gamma_p}(t_1)G_{\Gamma_q}(t_1)\right] \\
+g^4\sum_{p,q=1}^{N}\sum_{r=1}^{{}_nC_2}\left[\chi_{p,q,r}^{-,+}\theta(t_1-t_2)e^{-\Gamma_p(t_1-t_2)}E_{\gamma_r,\Gamma_q}(t_2) + \chi_{p,q,r}^{+,-}\theta(t_2-t_1)e^{-\Gamma_p(t_2-t_1)}E_{\gamma_r,\Gamma_q}(t_1)\right] \quad (5.45)
\end{aligned}
$$

While these expressions are incredibly complicated, because the functions are related to eigenvalues of two matrices is is possible to write code that can calculate all the necessary coefficients. Doing so, in Fig. 5.2 we present a plot of the probability that two counter-propagating photons will either remain in their respective mode or will end up in the same mode. In this calculation we have used an initially unentangled state where both photons have a space-time profile of a square pulse, given in Eq. 4.37. Additionally, the atoms are positioned to take advantage of the optimal spacing condition presented in Chapter 2 and shown in Fig. 2.12. With this, it is clear that two photons will still transmit through the system with high probability, just as was found in Chapter 4 for two counter-propagating photons.

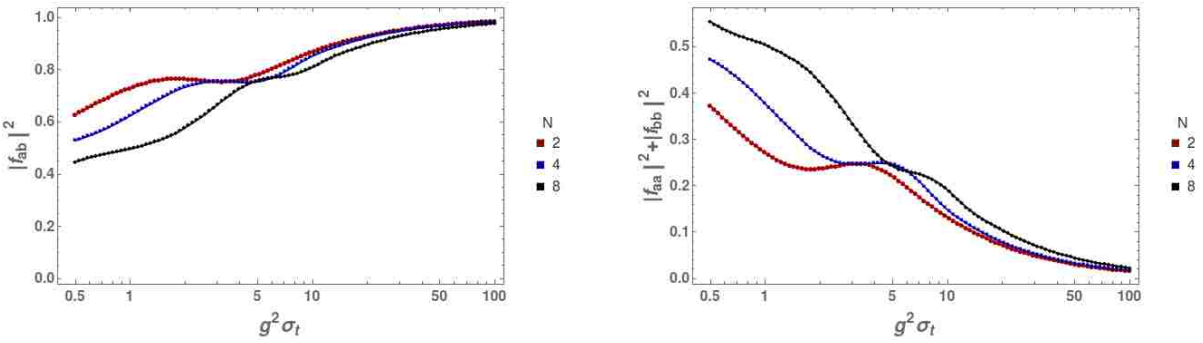

Figure 5.2: The norm of the spectral components $f_{a,a}$ and the sum of $f_{a,a} + f_{b,b}$ as a function of $g^2\sigma_t$ for N=2, 4, and 8 atoms. Here we have set the spacing to match the optimal position found in Chapter 2 to maximize single photon transmission. Additionally, we have set $\delta/g^2 = 1$.

This result is encouraging, as it suggests that an array of non-interacting atoms may be

able to perform quantum logical tasks between two photons. We will explore this possibility further in Chapter 6, leaving the extension of the time domain result of Chapter 3 to an arbitrary number of atoms as the main point here.

5.5 Conclusions

In this chapter we extended the time-domain solution presented in Chapter 3 to deal with an array of N non-interacting atoms placed at arbitrary positions along a 1-D waveguide. We demonstrated how the general solution has the same basic form as Eq. 3.18 and Eq. 4.30 where the terms that appear correspond to each possible scattering process. We converted the general solution of Eq. 5.19 into a form that lends itself to efficient computation and found the probability amplitudes for the scattered state of two counter-propagating photons. Finally, using the parameters derived in Chapter 2 for optimal photon transmission in the absence of direct atom-atom interactions, we plotted the probability that the photons will remain in their respective mode or be scattered in the same mode. We found that a transmission window does indeed exist for two counter-propagating photons and multiple atoms in the adiabatic limit with positions optimized as in Chapter 2, and that as the system approaches this limit of $g^2\sigma_t \gg 1$ the probability that the photons will be in the same mode decreases dramatically. This conclusion is important for Chapter 6, where we will use the solution presented in Eq. 5.45 to analyze whether this transmission window can be used to construct a CPHASE gate.

Chapter 6

Conditional Quantum Logic With Photons

6.1 Introduction

In this chapter we will analyze how well the transmission windows explored in Chapter 4 for two photons can be used to construct a CPHASE gate for conditional quantum logic using the same general structure described by Brod and Combes in [30]. In their work, Brod and Combes consider an array of atomic sites given by Fig. 6.1. Each site consists of a two level system coupled to a 1-D waveguide, where the direction of propagation is enforced by a mirror at the end of the waveguide and circulators separate photons entering and exiting the waveguide to enforce unidirectional photon propagation. This ad hoc structure was chosen to model an effective Kerr nonlinearity, which was the focus of their companion paper with Gea-Banacloche in [64]. What they discovered was that, as two counter-propagating photons transmitted through the system, they acquired a phase shift of π and, for a large number of sites, they left the system spectrally unentangled. This is exactly what would be required for a passive, deterministic CPHASE gate between two photons. As detailed in [64], this spontaneous disentanglement is a consequence of the fact that the system conserves both energy (in that the photons do not change their frequency) and momentum (in part because they continue in the same direction after the interaction).

This interaction does not leave the photons untouched, however; their spectra will still be modified as though they had both independently transmitted through the system. To mitigate this, Brod and Combes assume that in any quantum computation all photons undergo this same distortion so that any unique phase imparted by a gate due to the presence of two photons may be detected. We will adopt this same convention as well, comparing the spectrum of two counter-propagating photons to the wavefunction that would result if the two photons interacted with the system completely independently of one another.

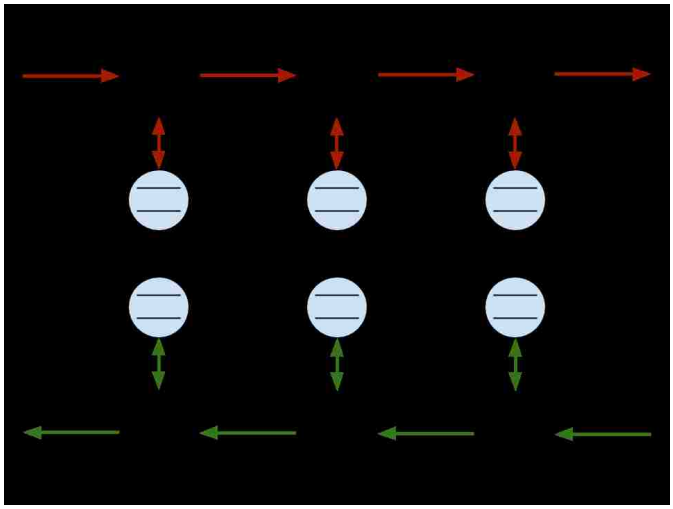

Figure 6.1: A diagram of the structure proposed in [64] to create a CPHASE gate between two photons. In their proposal, photons are routed between pairs of interacting atoms. Circulators and half waveguides ensure that photons will always travel in the same direction.

The gate proposed in [30] works best in the limit that the Kerr interaction strength becomes infinite. In this limit, each pair of closely spaced atoms in Fig. 6.1 reduces to a two level system, as only one atom can be excited at a given time. We will show how networking an array of pairs of two level systems leads to the same effect, that spectral entanglement between counter-propagating photons is reduced and that a nontrivial phase shift can be acquired between the photons. In section 6.2 we will show that the transmission window that occurs when atomic pairs are able to interact, detailed in sections 2.5 and 4.3.3, can be used to construct a passive, deterministic CPHASE gate that matches the operating parameters presented in [30]. In the second section, we will explore how one can alternatively use the non-interacting transmission windows (Sections 2.42 and 5.4), when $\tan(k_F d) = -\delta/g^2$, to preform conditional quantum logic with counter-propagating photons.

6.2 Constructing a phase gate using interacting atomic pairs

6.2.1 Introduction and setup

In Chapter 4 we demonstrated that two counter-propagating photons scattering from a pair of interacting atoms are able to be absorbed by the atoms, and thus indirectly interact with one another, while being re-emitted into their respective modes. This requires that the condition $\sin(k_F d) = -\Delta/g^2$ is satisfied. Such effective unidirectional behavior, in principle, allows for an ideal realization of the gate proposed by Brod and Combes [30, 64]. There is one other complication to address, however; in Chapter 4, the behavior of the photons was derived for a pair of atoms centered at the origin. If the atoms are not centered at the origin the situation changes somewhat. In this case, the operators $\hat{\phi}_\pm(t)$ from Eq. 4.4 become

$$\hat{\phi}_\pm(t) \to \hat{\Phi}_\pm(t) = \frac{1}{\sqrt{2}}\Big(e^{ik_F(z_0-d/2)}\hat{A}\big(t-\frac{z_0-d/2}{c}\big) + e^{ik_F(z_j+d/2)}\hat{A}\big(t-\frac{z_0+d/2}{c}\big) + e^{-ik_F(z_0-d/2)}\hat{B}\big(t+\frac{z_0-d/2}{c}\big) + e^{-ik_F(z_0+d/2)}\hat{B}\big(t+\frac{z_0+d/2}{c}\big)\Big) \tag{6.1}$$

It turns out that even when the atoms are off center, the commutation relationship presented in Eq. 4.5 still holds; that is

$$\big[\hat{\Phi}_\pm(t_i), \hat{\Phi}^\dagger_\pm(t_j)\big] = 2\delta\big(t_i - t_j\big) \pm e^{ik_F d}\delta\big(t_i - t_j - d/c\big) \pm e^{-ik_F d}\delta\big(t_i - t_j + d/c\big) \tag{6.2}$$

As a result of this, if the atomic pair is not centered at the origin we can follow the same process and approximations made in Chapter 4 to derive the scattered state of two photons from the system of two atoms. Eq. 4.24 will still describe the scattering, except with $\hat{\phi}_\pm \to \hat{\Phi}_\pm$. If we make the same Markovian approximation for the operators $\hat{\Phi}_\pm$ with respect to the separation between the atoms in the pair, that is $t \pm d/c \approx t$, and we use the fact that to achieve unit transmission for counter propagating photons with atomic interactions (Eq. 4.57) it must be true that $\Delta/g^2 = 1$, $\delta = 0$, and $k_F d = 3\pi/2$, the

operators will take the form

$$\hat{\Phi}_+ = -\Big(e^{ik_F z_0}\hat{A}\big(t - z_0/c\big) + e^{-ik_F z_0}\hat{B}\big(t + z_0/c\big)\Big)$$
$$\hat{\Phi}_- = -i\Big(e^{ik_F z_0}\hat{A}\big(t - z_0/c\big) - e^{-ik_F z_0}\hat{B}\big(t + z_0/c\big)\Big) \tag{6.3}$$

Further using the fact that when the system has been tuned to this transmission window $\Gamma_+ = \Gamma_- = g^2$ (as $k_F d = 3\pi/2$ and $\Delta = g^2$) we end up with a final scattered state of two counter-propagating photons from two interacting atoms centered at position z_0 of

$$\begin{aligned}
|\psi_g(t)\rangle &= |\psi_I\rangle \\
&-2g^2 \int_{-\infty}^{t} dt_1 \int_{-\infty}^{t_1} dt_2 e^{-g^2(t_1-t_2)}\Big(\hat{A}^\dagger\big(t_1 - z_0/c\big)\hat{A}\big(t_2 - z_0/c\big) + \hat{B}^\dagger\big(t_1 + z_0/c\big)\hat{B}\big(t_2 + z_0/c\big)\Big)|\psi_I\rangle \\
&+4g^4 \int_{-\infty}^{t} dt_1 \int_{-\infty}^{t_1} dt_2 \int_{-\infty}^{t_2} dt_3 \int_{-\infty}^{t_3} dt_4 e^{-g^2(t_1-t_2)} e^{-g^2(t_3-t_4)} \\
&\qquad \Bigg[\hat{A}^\dagger\big(t_1 - z_0/c\big)\hat{B}^\dagger\big(t_3 + z_0/c\big)\hat{A}\big(t_2 - z_0/c\big)\hat{B}\big(t_4 - z_0/c\big) \\
&\qquad + \hat{B}^\dagger\big(t_1 - z_0/c\big)\hat{A}^\dagger\big(t_3 + z_0/c\big)\hat{B}\big(t_2 - z_0/c\big)\hat{A}\big(t_4 - z_0/c\big)\Bigg]|\psi_I\rangle
\end{aligned} \tag{6.4}$$

Note that the contribution from the doubly excited state has vanished. This is a consequence of the form of $\hat{\Phi}_\pm$ given in Eq. 6.3. With these choices of parameters, the doubly excited component of the wavefunction will only contain lowering operators of the form $\hat{A}\big(t_3 - z_0/c\big)\hat{A}\big(t_4 - z_0/c\big)$ and $\hat{B}\big(t_3 + z_0/c\big)\hat{B}\big(t_4 + z_0/c\big)$. When acting on an initial state containing counter-propagating photons this will yield zero.

Next, we transform the time variables in Eq. 6.4 from t_i to $\tau_i \pm z_0/c$, where the sign of the position is determined by the sign of the time shift in the operators. For example, if $\hat{A}^\dagger\big(t_1 - z_0/c\big)$, $t_1 \to \tau_1 + z_0/c$ so that the time component in the operators will simply be

one of τ_i. Performing this transformation for all the variables yields

$$
\begin{aligned}
|\psi_g(t)\rangle = |\psi_I\rangle &- 2g^2 \int_{-\infty}^{t-z_0/c} d\tau_1 \int_{-\infty}^{\tau_1} d\tau_2 e^{-g^2(\tau_1-\tau_2)} \hat{A}^\dagger(\tau_1)\hat{A}(\tau_2)|\psi_I\rangle \\
&- 2g^2 \int_{-\infty}^{t+z_0/c} d\tau_1 \int_{-\infty}^{\tau_1} d\tau_2 e^{-g^2(\tau_1-\tau_2)} \hat{B}^\dagger(\tau_1)\hat{B}(\tau_2)|\psi_I\rangle \\
&+ 4g^4 \int_{-\infty}^{t-z_0/c} d\tau_1 \int_{-\infty}^{\tau_1} d\tau_2 \int_{-\infty}^{\tau_2+2z_0/c} d\tau_3 \int_{-\infty}^{\tau_3} d\tau_4 e^{-g^2(\tau_1-\tau_2)} e^{-g^2(\tau_3-\tau_4)} \hat{A}^\dagger(\tau_1)\hat{B}^\dagger(\tau_3)\hat{A}(\tau_2)\hat{B}(\tau_4)|\psi_I\rangle \\
&+ 4g^4 \int_{-\infty}^{t+z_0/c} d\tau_1 \int_{-\infty}^{\tau_1} d\tau_2 \int_{-\infty}^{\tau_2-2z_0/c} d\tau_3 \int_{-\infty}^{\tau_3} d\tau_4 e^{-g^2(\tau_1-\tau_2)} e^{-g^2(\tau_3-\tau_4)} \hat{B}^\dagger(\tau_1)\hat{A}^\dagger(\tau_3)\hat{B}(\tau_2)\hat{A}(\tau_4)|\psi_I\rangle
\end{aligned}
\tag{6.5}
$$

We now consider the final state of the photons if the initial state has the form

$$
|\psi_I\rangle = \int dt_a dt_b f_A(t_a) f_B(t_b) \hat{A}^\dagger(t_a)\hat{B}^\dagger(t_b)|0\rangle \tag{6.6}
$$

where the photons are initially unentangled (meaning the space-time wavefunction can be written as a product of the A and B modes separately) but they may have different pulse shapes. In this case, we can follow the same process as before to obtain the final scattered state ($t \to \infty$) of

$$
\begin{aligned}
\tilde{f}_g(t_1,t_2) = &\Big(f_A(t_1) - 2g^2 G^A_{g^2}(t_1)\Big)\Big(f_B(t_2) - 2g^2 G^B_{g^2}(t_2)\Big) \\
&-4g^4 \Bigg[\theta\big(t1 - t_2 + 2z_0/c\big) e^{-2g^2(t_1-t_2+2z_0/c)} G^A_{g^2}(t_2 - 2z_0/c) G^B_{g^2}(t_2) \\
&\qquad + \theta\big(t2 - t_1 - 2z_0/c\big) e^{-2g^2(t_2-t_1-2z_0/c)} G^A_{g^2}(t_1) G^B_{g^2}(t_1 + 2z_0/c)\Bigg]
\end{aligned}
\tag{6.7}
$$

where we have defined $G^A_{g^2}(t) = \int_{-\infty}^{t} dt' e^{-g^2(t-t')} f_A(t')$ and $G^B_{g^2}(t) = \int_{-\infty}^{t} dt' e^{-g^2(t-t')} f_B(t')$.

In the limit where $z_0 \to 0$ we recover exactly the form presented in Eq. 3.30 for two photons scattering from a single two level emitter in a unidirectional geometry. If, on the other hand, $z_0/c \gg \sigma_t$ the terms $G^A_\Gamma(t_2 - 2z_0/c)G^B_\Gamma(t_2)$ and $G^A_\Gamma(t_1)G^B_\Gamma(t_1 + 2z_0/c)$ will vanish, as the overlap between the two functions will be effectively zero (which is opposite of what we are trying to achieve). This makes physical sense; the term describes entanglement generated by the limitation that a two level system can only absorb one photon at a time. Such an effect only occurs when the two photons *can* interact with the

atom at the same time. If the system is off center (defined as the point where the two photons maximally overlap) one photon may interact before the other. If this off-center distance is large enough that one photon has a chance to complete its interaction with the atom before the second one arrives, then this term should go to zero, as there is no opportunity for the photons to become entangled. In this case the scattering process consists only of two independent scattering events, and this is exactly what is described above for $z_0/c \to \infty$. Regardless of the strength of the interaction or the placement of the system, it is true that no matter where the two-atom system is located it will preserve photon number in each mode for two counter-propagating photons.

6.2.2 Phase gate design and operation

We will now consider what happens if one couples N of these interacting pairs to a single waveguide. In this analysis we assume that each pair couples identically to the waveguide and that they have all been tuned to the transmission window $\sin(\phi) = -\Delta/g^2$. We are further assuming that the pairs of atoms are separated sufficiently far so that the dipole-dipole interaction is negligible between atoms in different pairs. The functional form of such an interaction is given in [36] and, to a good approximation goes as $\frac{1}{z^3}$. Thus, a separation between atoms in nearby pairs of around 10 times the spacing between atoms within a pair would lead to an inter-pair interaction strength that is 1000 times less than the strength between atoms within the same pair. Thus this inter-pair separation can safely be ignored.

In order to describe this system of N pairs of atoms, we will work in the frequency domain. We choose to make this shift as it is much easier to describe the transmission of a single photon through many scatterers in this domain, since each successive interaction merely multiplies the pulse by $t(\omega)$, the single photon transmission coefficient. The frequency spectrum of the two-photon wavefunction given in Eq. 6.7 representing the

scattering of two photons from a single pair of atoms is

$$\tilde{f}_g(\omega_1,\omega_2) = \left(\frac{g^2+i\omega_1}{g^2-i\omega_1}\right)\tilde{f}_A(\omega_1)\left(\frac{g^2+i\omega_2}{g^2-i\omega_2}\right)\tilde{f}_B(\omega_2) - \frac{2g^2}{\pi}\int_{-\infty}^{\infty} d\omega_a d\omega_b \left(\frac{e^{2i(\omega_a-\omega_1)z_0/c}}{g^2-i\omega_1} + \frac{e^{-2i(\omega_b-\omega_2)z_0/c}}{g^2-i\omega_2}\right)\frac{\delta(\omega_1+\omega_2-\omega_a-\omega_b)\tilde{f}_A(\omega_a)\tilde{f}_B(\omega_b)}{(g^2-i\omega_a)(g^2-i\omega_b)} \tag{6.8}$$

In the end, the state of two photons scattering through an array of pairs of atoms, as with everything in quantum mechanics, will be a sum of all the possible events. Because the two photons will always remain in their respective modes they can only both interact at one of the pairs in the system. When passing through the other pairs, the spectrum of each photon will be modified independently. The final state will thus be a sum over the interaction at each of the pairs in the system.

To derive this, we first consider how the spectrum of the photons would be modified if they only interacted with the j^{th} pair in an array consisting of N pairs. The rightmost pair is numbered as 1 and the leftmost pair is numbered as N. Prior to reaching the j^{th} pair, the right-propagating ($\hat{a}_{\omega_1}$) photon will have transmitted through $j-1$ sites and the left-propagating photon ($\hat{b}_{\omega_2}$) will have transmitted through $N-j$ sites. From the expression given in Eq. 2.42 this will lead to an initial spectrum of $\tilde{f}_A(\omega) = t(\omega)^{j-1}\tilde{f}(\omega)$ and $\tilde{f}_B(\omega) = t(\omega)^{N-j}\tilde{f}(\omega)$, as the reflection coefficient for each pair is zero. After the two photons interact at the j^{th} site, their combined spectrum will be given by Eq. 6.8, except with $\tilde{f}_A$ and $\tilde{f}_B$ replaced by the expressions given. After they interact, the right-going photon will continue on to transmit through $N-j$ sites and the left-going photon will transmit through $j-1$ sites. Each site will cause the spectrum to be multiplied by $t(\omega)$ again so that the spectrum after the interaction will become $\tilde{f}_g(\omega-1,\omega_2) \rightarrow t(\omega_1)^{N-j}t(\omega_2)^{j-1}\tilde{f}_g(\omega_1,\omega_2)$. If we add up all the interactions at each

possible site, the total spectrum of the two photons will be given by

$$\tilde{f}_g(\omega_1,\omega_2) = t(\omega_1)^N t(\omega_2)^N \tilde{f}(\omega_1)\tilde{f}(\omega_2) - \frac{2g^2}{\pi}\int_{-\infty}^{\infty} d\omega_a d\omega_b \sum_{j=1}^{N} t(\omega_1)^{N-j} t(\omega_2)^{j-1} t(\omega_a)^{j-1} t(\omega_b)^{N-j} \times \left(\frac{e^{2i(\omega_a-\omega_1)z_j/c}}{g^2 - i\omega_1} + \frac{e^{-2i(\omega_b-\omega_2)z_j/c}}{g^2 - i\omega_2}\right) \frac{\delta(\omega_1+\omega_2-\omega_a-\omega_b)\tilde{f}(\omega_a)\tilde{f}(\omega_b)}{(g^2 - i\omega_a)(g^2 - i\omega_b)} \tag{6.9}$$

This is identical in form to the scattered spectrum presented by Brod and Combes in [64] for two counter-propagating photons in the limit that the interaction they propose is infinitely strong. This suggests that we should arrive at virtually the same results as presented in Fig. 3 a) of [64], albeit presented in a different form, that a state containing two photons will experience a phase shift of π with unit fidelity.

In studying the fidelity of the CPHASE operation with this system we adopt a slightly different definition of fidelity than that presented in [30] and [64]. In their papers, Brod and Combes use an 'average gate fidelity' that, as its name suggests, provides the probability that the proposed gate will function as desired for any arbitrary input state. From a computational standpoint this is a very good measure of a gate's performance. We are, however, interested in a more stringent condition; measuring how much the pulse is distorted, as this is the physical cause of the failure of many CPHASE gate proposals. Due to this, we quantify fidelity as the overlap between the final scattered state and a target two photon state. This is defined as

$$\sqrt{\mathcal{F}}e^{i\phi} = \langle \text{Target}|\psi_g(\infty)\rangle \tag{6.10}$$

where the quantity $\mathcal{F}$ provides insight into the extent to which the two pulses have the same shape and the phase ϕ is the useful phase for computation described in Chapter 1.

Using this definition, in Fig. 6.2 we plot the fidelity of a Gaussian pulse (defined by the Fourier transform of the spectrum given in Eq. 3.41) in the limit where any $\omega z_j/c \approx 0$ (i.e. the sites are close enough that we can ignore any time delays between the sites). In effect we are assuming the system is Markovian. The target state for these plots is the spectrum

that would result if two photons transmitted through the system and did not interact with one another, but acquired a phase shift of π, given by

$$|\text{Target}\rangle = -\int d\omega_1 d\omega_2 t(\omega_1)^N t(\omega_2)^N \tilde{f}(\omega_1)\tilde{f}(\omega_2)\hat{a}^\dagger_{\omega_1}\hat{b}^\dagger_{\omega_2}|0\rangle \tag{6.11}$$

As can be seen from Fig. 6.2, as the number of sites increases the fidelity of the operation approaches one, which corresponds to a useful computational phase of π and a two-photon pulse shape that exactly matches $|\text{Target}\rangle$. This is what is required for a passive, deterministic CPHASE gate and is virtually the same result as presented in Fig. 3 a) of [64] as expected.

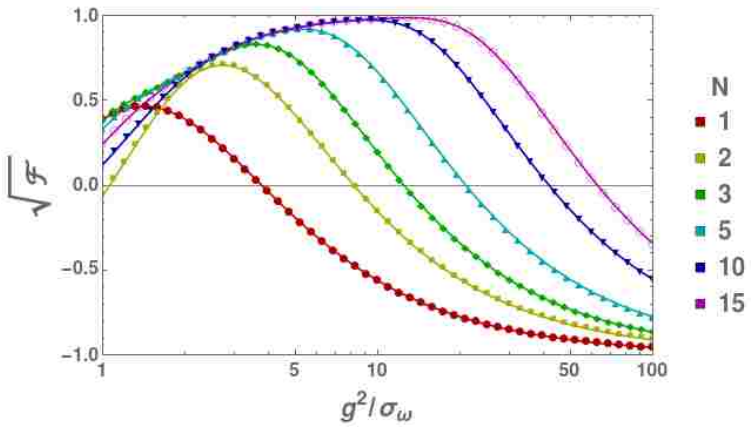

Figure 6.2: The fidelity of the proposed CPHASE gate for various N pairs of atoms as a function of g^2/σ_ω. A value of 1 corresponds to ideal gate operation.

In Fig. 6.3 we plot the infidelity ($|1-\sqrt{\mathcal{F}}|$) of our proposal to realize a CPHASE gate and compare it to the infidelity predicted by Brod and Combes in [64] (black dots) using their definition of average fidelity. Their number is always lower, implying a better gate operation. This difference arises from the definitions of fidelity. In the gate design presented here and in [30], the logical state states $|0,0\rangle$, $|1,0\rangle$, and $|0,1\rangle$ will always transform perfectly as we are both assuming that *all* photons are forced to undergo the same single-photon distortion at each computational step. Thus, the *average* gate fidelity will be higher than what is being measured here, the fidelity of just the operation $|1,1\rangle \rightarrow -|1,1\rangle$.

We find that the fidelity of the operation scales at the same rate to that presented in [64]. In their work, Brod and Combes found that, for a unidirectional waveguide and a coupling constant of $g^2 = 1$ (γ in their paper), the maximum fidelity occurs when the spectral pulse width σ_ω is approximately $\sigma_\omega = .350N^{-.81}$, with N being the number of sites (the pairs of atoms in our case). In order to relate this to the dimensionless parameter g^2/σ_ω used in our work, we note that, because we are working in a bidirectional geometry, our coupling constant relates to theirs by $g^2 = \frac{\gamma}{2}$. With this, we have that for our system, the optimal fidelity should occur when $g^2/\sigma_\omega = 1.43N^{.81}$. This is represented in Fig. 6.3 by the dashed vertical lines. As can be seen from the plot, this fit does match the points of maximum fidelity very well.

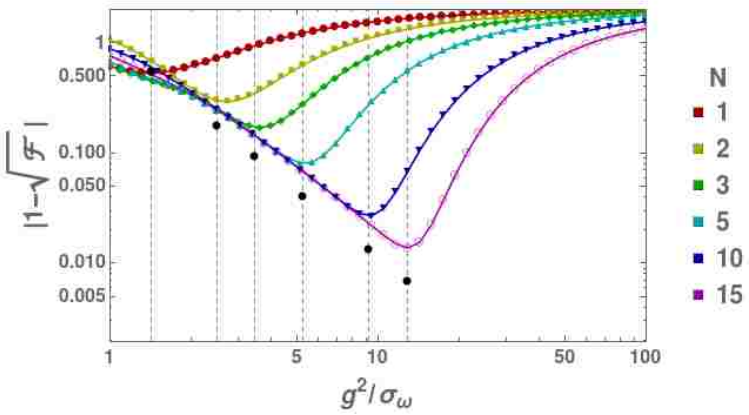

Figure 6.3: The infidelity of the proposed CPHASE gate for various N pairs of atoms as a function of g^2/σ_ω. The dashed lines represent the optimum system parameters predicted by the fit of $\sigma_{\max}$ in Fig. 3 b) of [30] and the black dots represent the infidelity calculated in [30] for the parameters which maximize the fidelity of their gate.

Next, in Fig. 6.4 we consider the effect of including a nonzero separation between the pairs of atoms for $N = 12$ sites. Here, $\sigma_\omega z/c$ represents the scaling of the phase factors appearing in Eq. 6.9 and is related to the time required to travel between pairs of atoms. As one would expect, when the separation between each site becomes close to the order of the pulse width (i.e. $\sigma_\omega z_0/c \approx 1$) the fidelity of the operation decreases dramatically. This has an intuitive physical explanation, for if the sites become separated on the order of a

pulse width the photons will only interact at a some of the sites. In this limit, the array will act like a system containing fewer pairs of atoms. Additionally, there is virtually no difference between the case when $\sigma_\omega z/c = 0$ and when $\sigma_\omega z/c = 10^{-5}$. This is also consistent with the rest of the work here, as this parameter effectively determines whether the system is Markovian or not. If $\sigma_\omega z/c \approx 10^{-5}$, a pulse width $\sigma_\omega \approx 1$ GHz requires a spacing between pairs of $z \approx 10\mu m$. For a more narrow band photon, $\sigma_\omega \approx 1$ MHz, for $\sigma_\omega z/c$ to be on the order of 10^{-5} the atomic pairs can be separated by about a centimeter. This suggests that, at least for spectrally narrow photons, the proposed CPHASE gate can have a relatively large length.

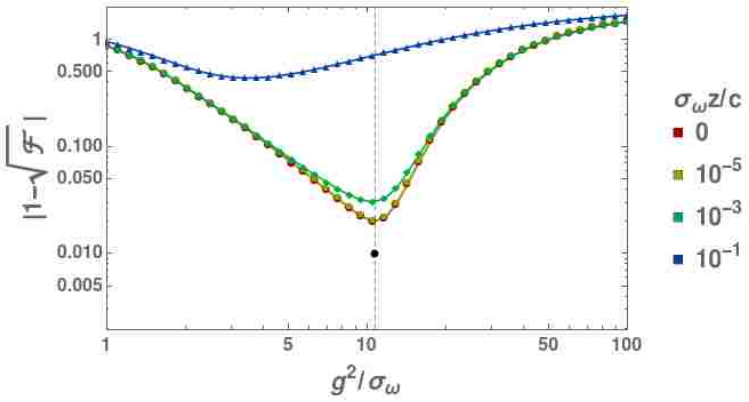

Figure 6.4: The difference between the calculated fidelity and the expected fidelity for a Gaussian pulse with various values of separation between atoms $z_0/c/\sigma_t$. $N = 12$ for all curves.

6.2.3 Visualization of the spectra and explanation of operation

It is also useful to visualize how the entanglement generated by the atom is reduced as the number of sites in the phase gate increases. In Figs. 6.5-6.8 we present the full spectrum of the scattered two photon pulse given by Eq. 6.9 for an initially unentangled two photon state where each photon begins with a Gaussian wavepacket. We also plot the spectrum of an 'ideal' pulse, that is a two photon wavepacket given by $|\text{Target}\rangle$, as defined in Eq. 6.11.

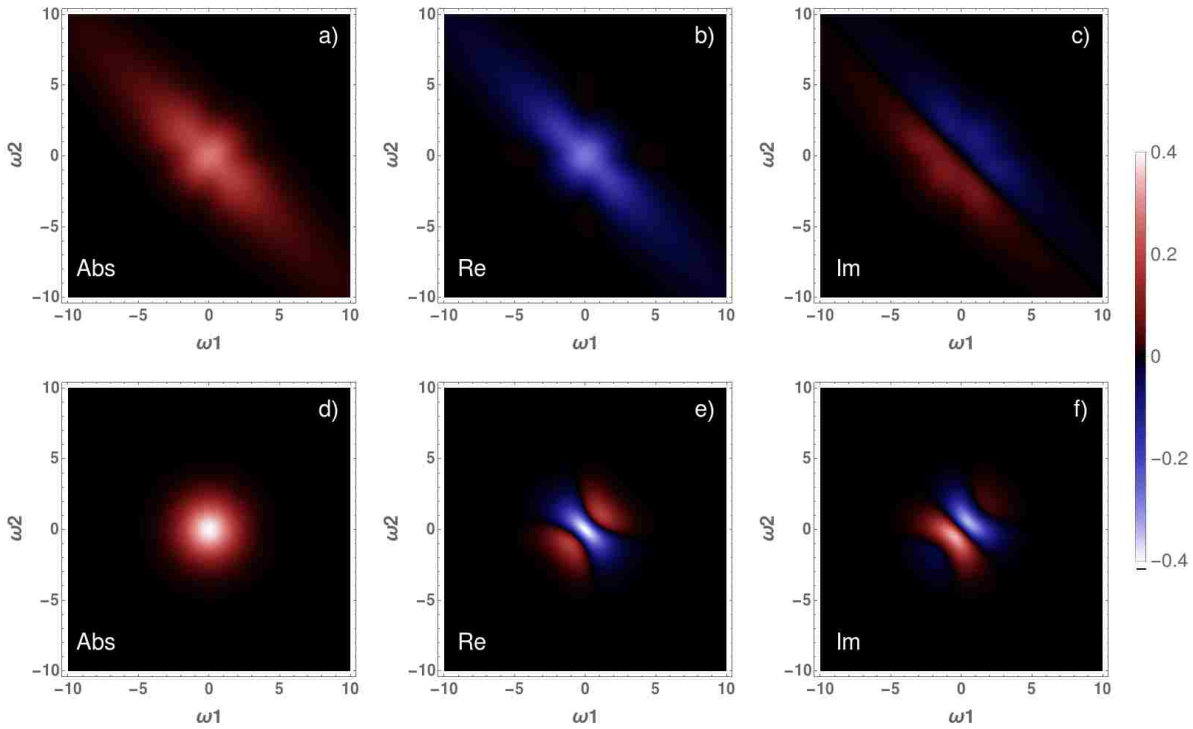

Figure 6.5: The spectrum of the pulse for N=1 site. The top row represents the full spectrum of the pulse from Eq. 6.9 and the bottom row represents the ideal pulse. The columns correspond to the absolute value of the spectrum, the real part, and the imaginary part respectively.

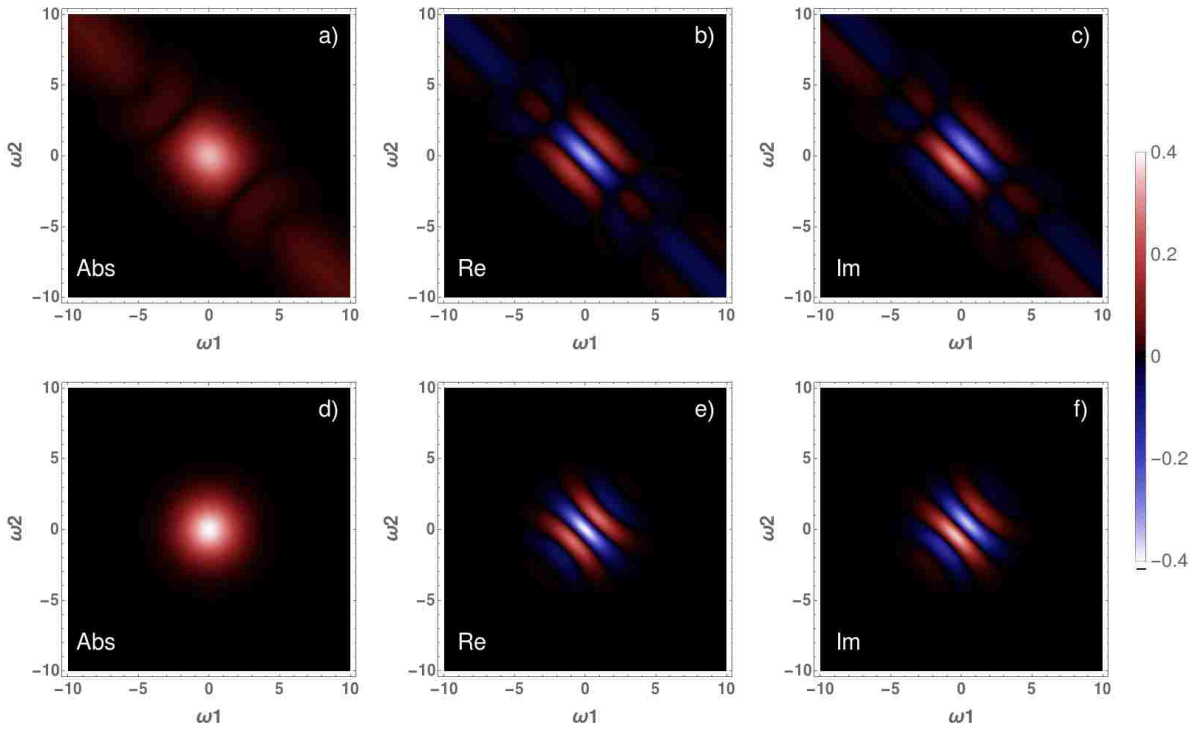

Figure 6.6: The same figure as Fig. 6.5 for N=3 sites.

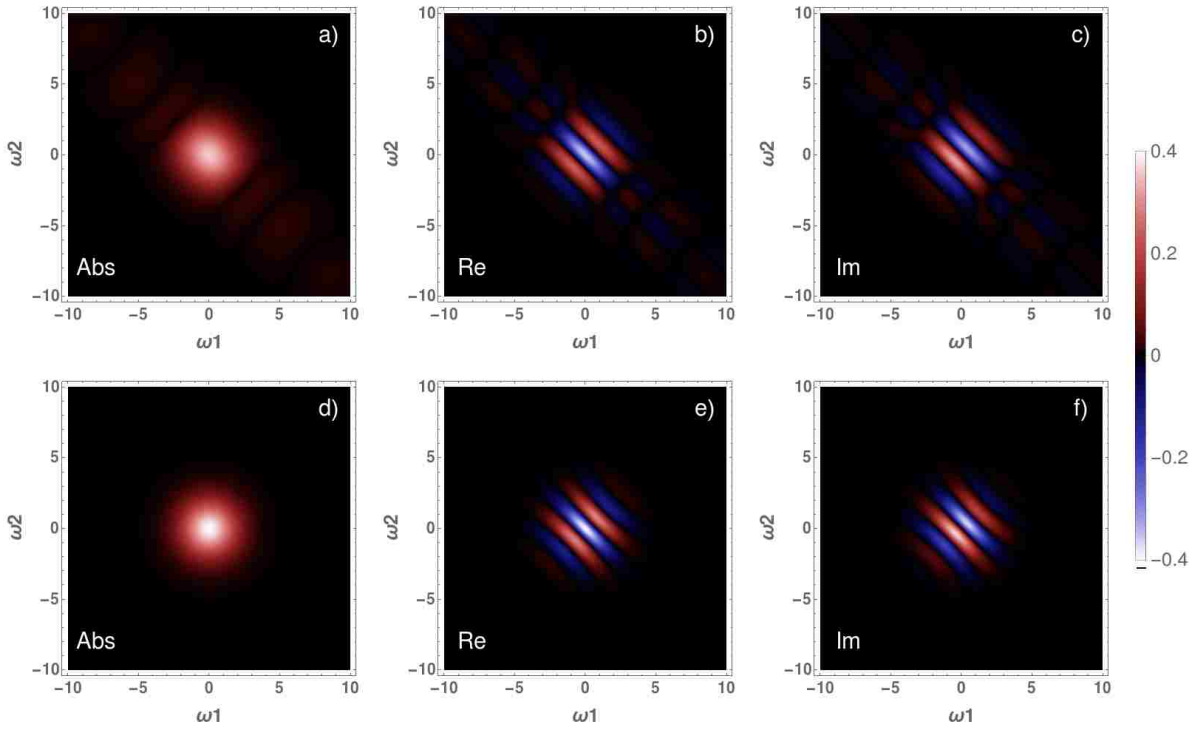

Figure 6.7: The same figure as Fig. 6.5 for N=5 sites.

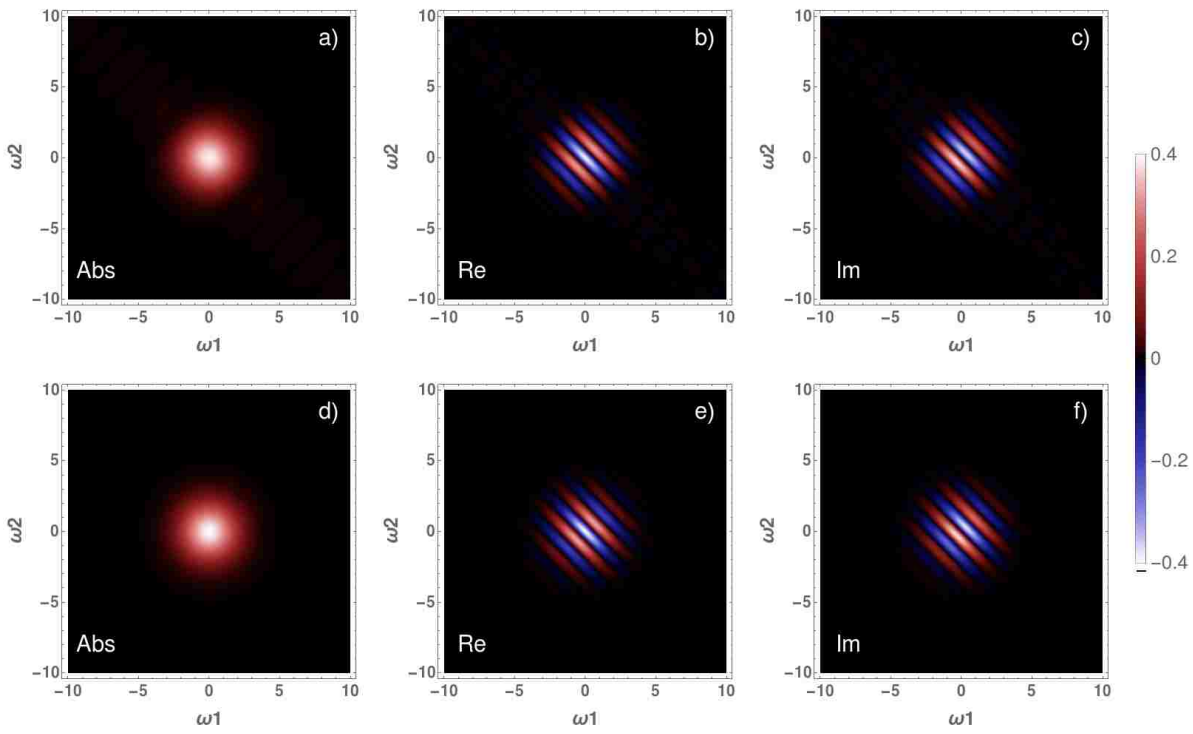

Figure 6.8: The same figure as Fig. 6.5 for N=20 sites.

In these plots, the effect of the entangling term can be observed in the broadening that appears along the line $\omega_1 = -\omega_2$. Clearly, for a single site this is a highly nontrivial effect that significantly distorts the shape of the scattered photons and thus leads to a poor fidelity with respect to the ideal pulse. Interestingly, however, the scattered photons already have acquired a phase of π, evidenced by the fact that the general shape of the real and imaginary components match the ideal state. As the number of sites (pairs of atoms) increases, however, this spectral broadening decreases. By the time $N = 20$ the exact and ideal pulses look nearly identical and numerically the fidelity is very close to 1, though there is still some residual entanglement present (seen in the faint features along $\omega_1 = -\omega_2$).

This also clearly demonstrates a limit on the operation of this particular phase gate; a single photon will have its spectrum modified by a nontrivial phase. In the ideal case, the absolute value of the pulse in frequency space is the same regardless of the number of interaction sites in the gate. The phase changes significantly, however, as seen in the

oscillations of the real and imaginary components of the spectrum. As mentioned previously, this issue can easily be rectified by ensuring that at each step of the computation all photons have passed through the same number of these arrays of atoms. Ensuring this happens does increase the number of waveguide-atom structures that must be built; for example, as seen in Fig. 6.9, if one were to use the usual dual-rail scheme for quantum computation (where a qubit is encoded into one of two spatial modes) a CPHASE gate would require three of such atom-waveguide systems in order to modify all photons correctly.

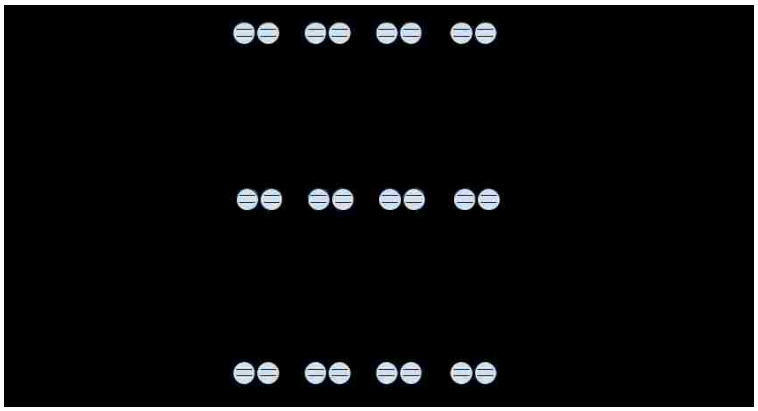

Figure 6.9: A simple schematic of how one would be able to construct a CPHASE gate between two photons using a series of interacting atoms coupled to a one-dimensional waveguide. Here the spatial mode and direction of the photons encodes the logical values of $|0\rangle$ and $|1\rangle$. Note that a nonreciprocal element would need to be placed on each side of the central waveguide to ensure that photons going in different directions can be correctly routed.

This requirement does not detract from the fact that the gate works, however, and that it is possible for two photons to interact and effectively remain unentangled after the interaction. Additionally, our proposed system should be significantly easier to scale and build on a chip than the somewhat ad hoc system proposed by Brod and Combes in [64]. Moreover, we have shown that the desired gate operation is robust with respect to a realistic separation of nanoscale structures. This success also leads to a second important conclusion; *any* array of two level systems in which the scatterers couple to the guided modes in such a way that photons travelling in either direction will remain in their

respective modes can function as a passive, deterministic quantum logic gate for counter-propagating photons. This is especially encouraging given the recent experimental work in creating chiral coupling of two level systems to waveguide modes (such as detailed in [21]), as such systems are isomorphic to the atomic chain presented here, but typically have the added benefit of marking photons moving in different directions with different polarizations. Because polarization allows for easier routing and separation of photons, such systems seem to be ideal candidates to realize quantum logic with photons and create interesting, nonclassical photon-photon interactions.

Finally, we present why the entanglement generated by the nonlineary of each individual two level system vanishes when two photons pass through an array of atoms. As pointed out by Gea-Banacloche in [64], the reason for the reduction in entanglement seen in Fig. 6.5 is that, in the limit of large N and large $g^2\sigma_t$, the sum in 6.9 approximates a delta function. Using the same approximations presented in Section VII of [64] this comes about as follows.

In the adiabatic limit it will be true that $g^2\sigma_t = g^2/\sigma_\omega \gg 1$. Thus we can follow the approximation given in Eq. 63 of [64] to write

$$t(\omega) \approx e^{2i\frac{\omega}{g^2}} \tag{6.12}$$

With this, the sum over all transmission coefficients in 6.9 will, in the limit of large N become a delta function of the form

$$\sum_{j=1}^{N} t(\omega_1)^{N-j} t(\omega_2)^{j-1} t(\omega_a)^{j-1} t(\omega_b)^{N-j} \approx g^2\pi\delta(\omega_a - \omega_b - \omega_1 + \omega_2) \sum_{j=1}^{N} e^{i\frac{N-1}{g^2}(\omega_1+\omega_2+\omega_a+\omega_b)} \tag{6.13}$$

As discussed in [30], this delta function represents momentum conservation and arises from the fact that the photons are moving in opposite directions and must remain moving in opposite directions. In a sense, the two photons are measuring one another by the fact that they must interact at only one site. The combination of all these measurements ensures that momentum is conserved. We then combine the delta function in Eq. 6.13 with

the delta function in Eq. 6.9 to arrive at

$$\delta(\omega_a - \omega_b - \omega_1 + \omega_2)\delta(\omega_a + \omega_b - \omega_1 - \omega_2) = \frac{1}{2}\delta(\omega_a - \omega_1)\delta(\omega_b - \omega_2) \tag{6.14}$$

Integrating over ω_a and ω_b the final, total spectrum becomes

$$\tilde{f}_g(\omega_1, \omega_2) = t(\omega_1)^N t(\omega_2)^N \tilde{f}_A(\omega_1)\tilde{f}_B(\omega_2)\left(1 - \frac{g^6 e^{-\frac{2i}{g^2}(\omega_1+\omega_2)}}{(g^2 - i\omega_1)(g^2 - i\omega_2)}\left[\frac{1}{g^2 - i\omega_1} + \frac{1}{g^2 - i\omega_2}\right]\right) \tag{6.15}$$

Similar to Eq. 66 of [64] this state is a linear superposition of separable (i.e. spectrally unentangled) states such as described in Section 1.4. It is still an entangled state, but the non-separable term primarily responsible for the distortion in the wavefunction (related to f_{ent} of Eq. 3.31) has vanished. From here, it is easy to show that in the adiabatic limit of a spectrally narrow pulse (i.e. a long duration) this reduces to a completely unentangled product state of the two photons. To see this, we assume the bandwidth of the pulse is sufficiently small so that the terms $g^2 - i\omega \approx g^2$. Then Eq. 6.15 becomes

$$\tilde{f}_g(\omega_1, \omega_2) = -t(\omega_1)^N t(\omega_2)^N \tilde{f}_A(\omega_1)\tilde{f}_B(\omega_2) \tag{6.16}$$

which is exactly the ideal pulse shape with a phase shift of π as desired. This is the same result seen in [64] and thus our proposal to realize the gate designed by Brod and Combes behaves the same in the adiabatic and large N limit. Moreover, the gate operation is similarly independent of the shape of the incoming photons.

6.3 Constructing a phase gate with non-interacting atomic pairs

6.3.1 Phase gate design and operation

We now turn our attention to the transmission window described in Chapters 2, 4 and 5 for an array of non-interacting atoms coupled to a waveguide. In Chapter 2, and particularly in Fig. 2.13, we demonstrated that in the large g^2/σ_ω limit, when a system of atoms is tuned so that the separation between atoms in a given pair is given by

$k_F d = \pi - \arctan(\delta/g^2)$ and the spacing between pairs is chosen appropriately, a single photon will transmit through the system with virtually unit probability and acquire a phase proportional to the number of pairs. This phase is given by Eq. 2.36 and is reproduced below.

$$t(\omega) = \mathrm{Exp}\left\{ i\mathrm{Arg}\left[-\frac{(\omega+\delta)^2}{(g^2 - i(\omega+\delta))^2 - g^4 e^{-2i\arctan(\delta/g^2)}} \right] \right\} \tag{6.17}$$

We have also shown in Fig. 5.2 that in the same large $g^2\sigma_t = g^2/\sigma_\omega$ limit, two photons will transmit through an array of atoms with high probability. With this, we posit that the final, scattered state of two photons will have the same form as Eq. 6.9, but with $t(\omega)$ replaced by Eq. 6.17 and the interaction when both photons are at the same site being described by $f_{a,b}(t_1, t_2)$ from Eq. 4.55. Just as in the previous section, we will transform Eq. 4.55 to the frequency domain to more easily add up all the possible scattering events. Using this heuristic model, the final scattered spectrum of two, counter-propagating photons from an array of N pairs of non-interacting atoms positioned using the optimal spacing defined in Chapter 2 should be approximately

$$\begin{aligned}
\tilde{f}_{a,b}(\omega_1,\omega_2) &= t(\omega_1)^N t(\omega_2)^N \tilde{f}(\omega_1)\tilde{f}(\omega_2) \\
&+ \cos(\phi)^2 e^{-2i\phi} \int d\omega_a d\omega_b \delta(\omega_1+\omega_2-\omega_a-\omega_b) \sum_{j=1}^{N} t(\omega_1)^{N-j} t(\omega_b)^{N-j} t(\omega_2)^{j-1} t(\omega_a)^{j-1} \tilde{f}(\omega_a)\tilde{f}(\omega_b) \\
&\left\{ \frac{\Gamma_+}{\pi}\Big(\frac{1}{\Gamma_+ - i\omega_1} + \frac{1}{\Gamma_+ - i\omega_2}\Big)\left[\Big(\frac{\Gamma_+}{\Gamma_+ - i\omega_b} - \frac{\Gamma_-}{\Gamma_- - i\omega_b}\Big)\frac{1}{\gamma - i(\omega_a+\omega_b)} - \frac{\Gamma_+}{(\Gamma_+ - i\omega_a)(\Gamma_+ - i\omega_b)}\right] \right. \\
&\left. + \frac{\Gamma_-}{\pi}\Big(\frac{1}{\Gamma_- - i\omega_1} + \frac{1}{\Gamma_- - i\omega_2}\Big)\left[\Big(\frac{\Gamma_-}{\Gamma_- - i\omega_b} - \frac{\Gamma_+}{\Gamma_+ - i\omega_b}\Big)\frac{1}{\gamma - i(\omega_a+\omega_b)} - \frac{\Gamma_-}{(\Gamma_- - i\omega_a)(\Gamma_- - i\omega_b)}\right] \right\}
\end{aligned} \tag{6.18}$$

where the terms Γ_+, Γ_-, and γ are defined in Eq. 4.23.

In fact, the terms related to the doubly excited state (the ones multiplying terms with γ) do not contribute to the overall result. This is due to the term $\left(\frac{\Gamma_+}{\Gamma_+ - i\omega_b} - \frac{\Gamma_-}{\Gamma_- - i\omega_b}\right)$ which, as $\Gamma_\pm$ is large, will be approximately zero. Because of this we will remove this term and use

Eq. 6.19 to model the final, scattered state of two counter-propagating photons.

$$\begin{aligned}\tilde{f}_{a,b}(\omega_1,\omega_2) &= t(\omega_1)^N t(\omega_2)^N \tilde{f}(\omega_1)\tilde{f}(\omega_2) \\ &-\frac{\cos(\phi)^2}{\pi}e^{-2i\phi}\int d\omega_a d\omega_b \delta(\omega_1+\omega_2-\omega_a-\omega_b)\sum_{j=1}^{N} t(\omega_1)^{N-j}t(\omega_b)^{N-j}t(\omega_2)^{j-1}t(\omega_a)^{j-1}\tilde{f}(\omega_a)\tilde{f}(\omega_b) \\ &\times\left[\Big(\frac{1}{\Gamma_+-i\omega_1}+\frac{1}{\Gamma_+-i\omega_2}\Big)\frac{\Gamma_+^2}{(\Gamma_+-i\omega_a)(\Gamma_+-i\omega_b)}+\Big(\frac{1}{\Gamma_--i\omega_1}+\frac{1}{\Gamma_--i\omega_2}\Big)\frac{\Gamma_-^2}{(\Gamma_--i\omega_a)(\Gamma_--i\omega_b)}\right]\end{aligned} \tag{6.19}$$

We first demonstrate that this approximation is valid in the adiabatic limit for a Gaussian pulse for up to $N = 4$ pairs of atoms. We have chosen to use a Gaussian pulse as it is the same pulse used to calculate reflection and transmission probabilities in Chapter 2 and is commonly used in other works (such as [64]). In Fig. 6.10 we plot the fidelity for a pulse with time and frequency profiles given by

$$f(t) = \frac{e^{-t^2/4\sigma_t}}{\sqrt{\sigma_t\sqrt{2\pi}}} \qquad\qquad \tilde{f}(\omega) = \frac{e^{-\omega^2/4\sigma_\omega}}{\sqrt{\sigma_\omega\sqrt{2\pi}}} \tag{6.20}$$

Fidelity is compared to the target state

$$|\text{Target}\rangle = \int d\omega_1 d\omega_2 t(\omega_1)^N t(\omega_2)^N \tilde{f}(\omega_1)\tilde{f}(\omega_2)\hat{a}^\dagger_{\omega_1}\hat{b}^\dagger_{\omega_2}|0\rangle \tag{6.21}$$

where the transmission coefficients are given by Eq. 6.17, N refers to the number of pairs of atoms, and the target differs from Eq. 6.11 in that we have not included any phase. As we will see later, the phase that arises from using the optimal position spacing from Chapter 2 and setting $\delta/g^2 = 1$ is not π but rather $\pi/2$. Looking at Fig. 6.10, it is clear that in the adiabatic limit the calculated fidelity and phase is virtually identical, regardless of whether the full solution of Eq. 5.45 or the heuristic approximation of Eq. 6.19 is used. Note that, due to the nature of the Fourier transform, when relating the frequency and time results the parameters have been re-scaled so that $\sigma_t = \frac{1}{2\sigma_\omega}$. Additionally, in calculating the solution from Eq. 6.19 we used a third order adiabatic approximation of G_Γ (as $g^2\sigma_t > 30$), given by the k=3 solution to Eq. 3.48, to derive an analytic form of $\mathcal{E}_\Gamma$ for the Gaussian pulse to more efficiently compute the solution.

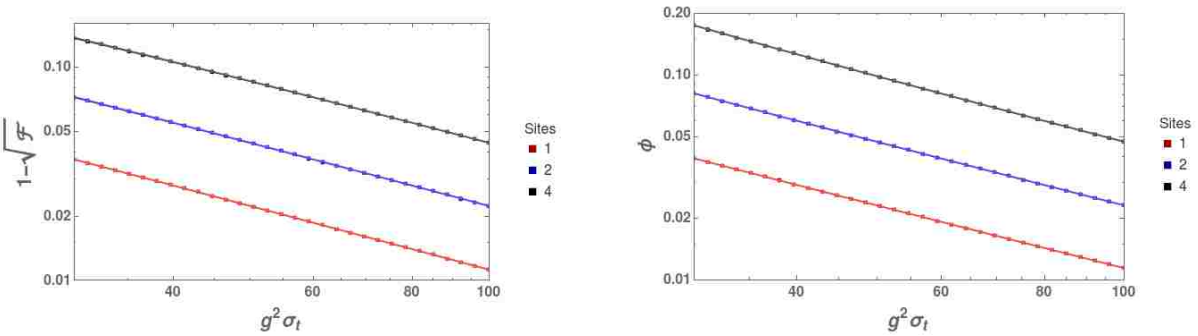

Figure 6.10: The infidelity (left) and the useful phase shift (right) predicted by the Markovian solution presented in Eq. 5.45 (light color, circle marker) and the heuristic solution presented in Eq. 6.19 (dark color, square marker) for 1, 2 and 4 pairs of atoms for two counter-propagating photons with initial pulse shapes defined by Eq. 6.20. Note that the two curves are directly on top of each other due to the high numerical agreement. We have set $\delta/g^2 = 1$ in this calculation and in the Markovian calculation used the optimized spacing derived in Chapter 2.

While it would be nice continue to show that the approximation of the scattered state continues to be valid for larger numbers of atoms, the computational time required to go past 4 sites in the Markovian solution of Eq. 5.45 becomes prohibitively expensive. There is, however, no reason to expect that the approximation ceases to be valid for a larger system. As was seen in Fig. 2.10, the reflection probability is always very small for large g^2/σ_ω. As such, the magnitude of any terms that are left out of the heuristic solution should be incredibly small and contribute little to the overall scattered state. To stay within a regime that this high single- and two-photon transmission should hold true we will restrict ourselves to exploring how the gate functions in the region of $g^2/\sigma_\omega \in [30, 200]$. The upper limit here is chosen to limit the total number of sites needed to achieve unit fidelity, as will be shown soon.

We now begin to study how an array of N pairs of non-interacting atoms, spaced as described in Fig. 2.12, can function as a CPHASE gate. Following the previous analysis of the array of interacting atoms, in Fig. 6.11 we first plot the fidelity and useful phase of the final scattered state as compared to the target state in Eq. 6.21.

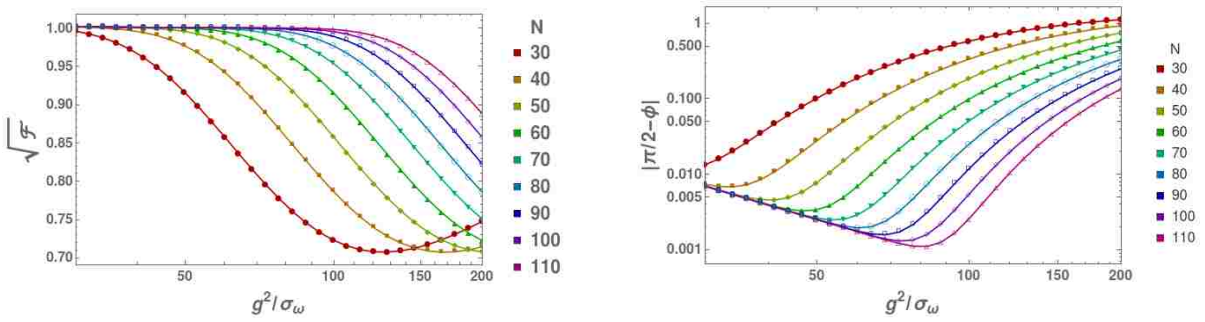

Figure 6.11: The fidelity and phase difference between ϕ and $\pi/2$ of Eq. 6.19 compared to Eq. 6.21 for various N pairs of atoms and g^2/σ_ω.

Immediately, one notices that the gate functions; it is possible for two photons to acquire a phase shift of $\pi/2$ with near-unit fidelity. While this is not the ideal phase of π, due to the difference in the structure of the atom-photon interaction, it represents a nontrivial phase that would enable universal quantum computation. The maximum phase in Fig. 6.11 occurs when $g^2/\sigma_\omega = 1.34N^{.871}$. These points of maximum phase also correspond to high fidelity, though in actuality the fidelity calculated around these points is slightly greater than 1, with a maximum of 1.002. A fidelity larger than one implies that the norm of the state is also greater than one. This is perhaps not surprising; the approximation of the single photon transmission coefficient in Eq. 6.17 assumes unit transmission, but, as was shown in Chapter 2, there is still a small probability of reflection. The fact that we are ignoring this is most likely is causing fidelity to be greater than one, but as it is a small deviation there is no reason to suspect that removing the assumption of unit single-photon transmission would significantly affect the gate operation. It would seem, then, that for this gate to function two conditions must be satisfied; the system must be in the adiabatic limit of $g^2/\sigma_\omega \gg 1$ and the number of sites must be approximately $N = g^2/\sigma_\omega$.

6.3.2 Visualization of the spectra and limits on operation

As a result of the fact that the approximation required to use Eq. 6.19 requires g^2/σ_ω to be large it is difficult to make a one-to-one comparison with the previous gate design using interacting pairs of atoms. In section 6.2, the system works exactly; that is, there is no probability that the two photons will be reflected. As such, we were able to consider all values of g^2/σ_ω and explore small numbers of sites in which the gate functions well.

For the array of non-interacting atoms being considered here, we cannot explore this transition, as it would require computing the fidelity from Eq. 5.45 for large numbers of atoms, a task that would take far too long and that would undercut the utility of making the approximations in Eq. 6.19. Instead, we will consider what happens as the number of pairs of atoms is varied for $g^2/\sigma_\omega = 50$ when $\delta/g^2 = 1$. These values have been chosen to ensure that the system can be considered to be adiabatic and so that the useful phase will be approximately $\pi/2$.

In Fig. 6.12 we plot the phase and fidelity of the proposed CPHASE gate as a function of N. For this gate, as the number of sites increases the fidelity is initially high, decreases around $N = 12$, and recovers in the limit when $g^2/\sigma_\omega \approx N$. The phase begins low and, as the number of pairs increases, it climbs to eventually reach the ideal phase of $\pi/2$. Moreover, we find that as the number of pairs of atoms continues to increase the phase and fidelity saturates, just as shown in Fig. 4 of [30].

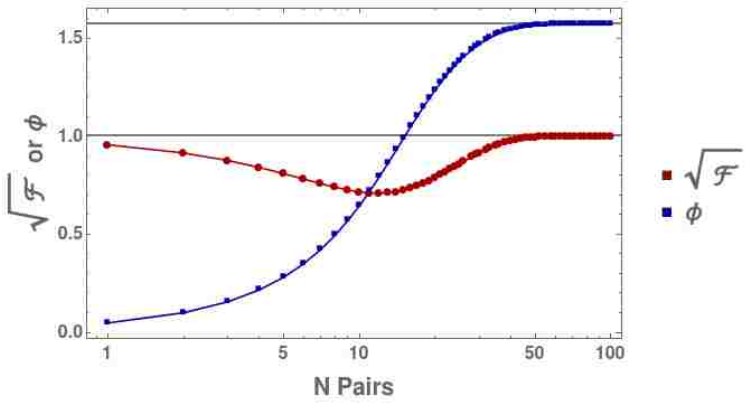

Figure 6.12: This figure shows how for a fixed $g^2/\sigma_\omega = 50$ the phase (blue squares) and fidelity (red circles) of the gate as a function of the number of pairs of atoms, N.

We can explore the shape of the spectrum as we did in 6.2.3. In Figs. 6.13-6.16 we plot the spectrum of the scattered photons, given by Eq. 6.19, and the spectrum of the target state $e^{i\pi/2}|\text{Target}\rangle$ where again $|\text{Target}\rangle$ is given by Eq. 6.21.

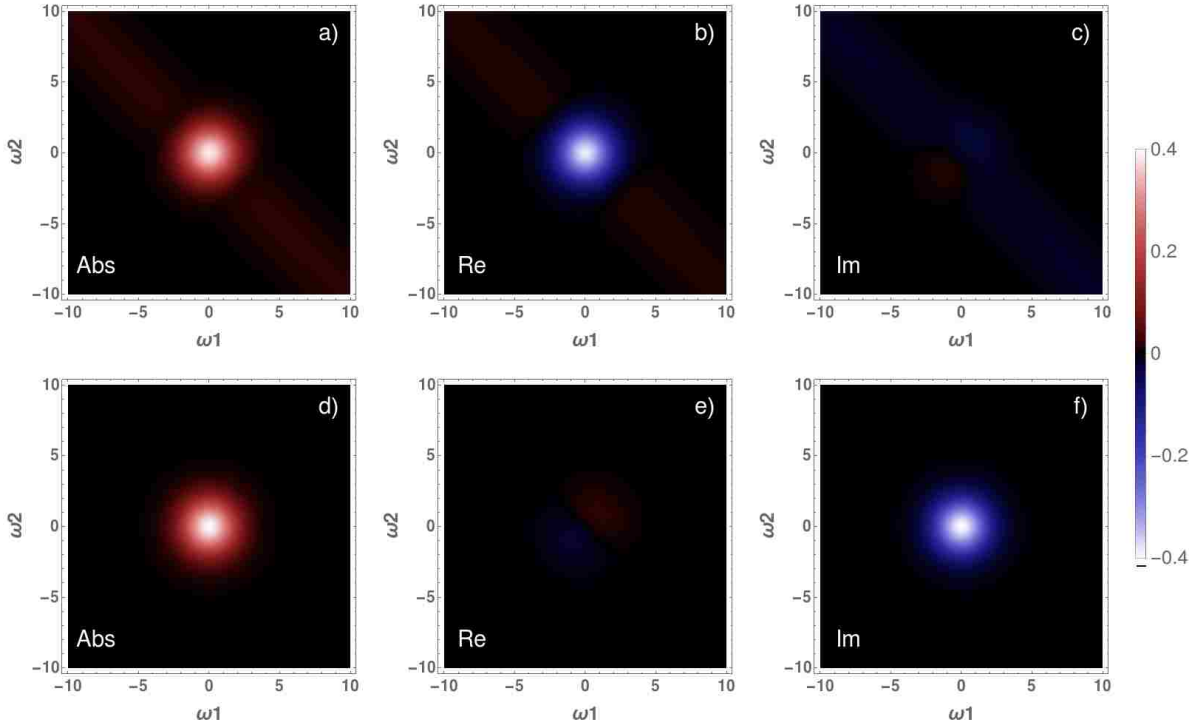

Figure 6.13: The spectrum of the pulse for N=1 site when $g^2/\sigma_\omega = 50$. The top row represents the full spectrum of the pulse from Eq. 6.19 and the bottom row represents the ideal pulse described in the text. The columns correspond to the absolute value of the spectrum, the real part, and the imaginary part respectively.

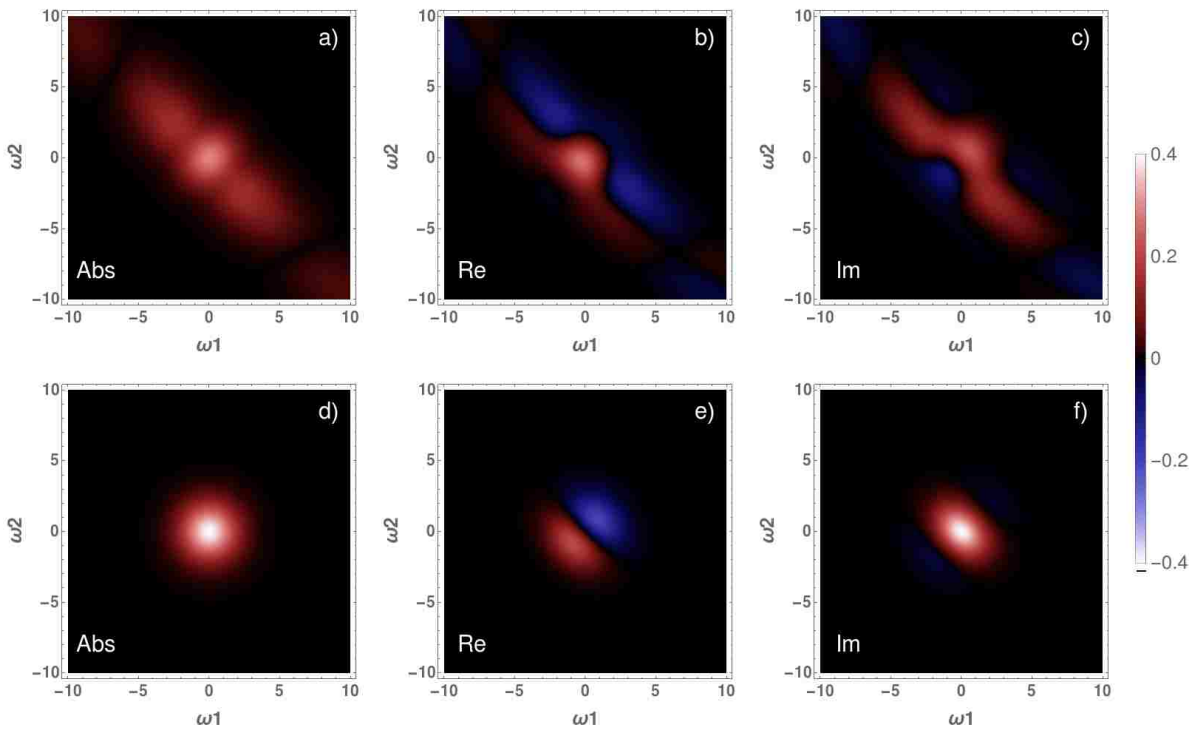

Figure 6.14: The same figure as Fig. 6.13 for N=12 sites where fidelity is minimized in Fig. 6.12

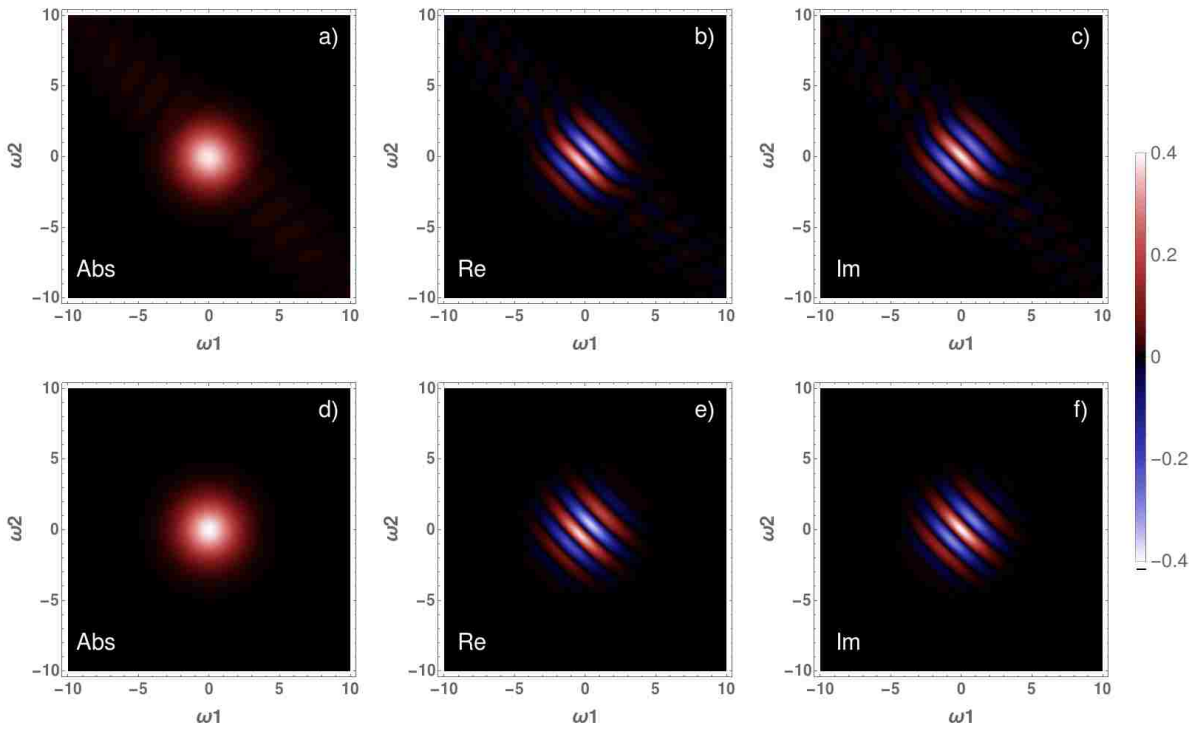

Figure 6.15: The same figure as Fig. 6.13 for N=50 sites.

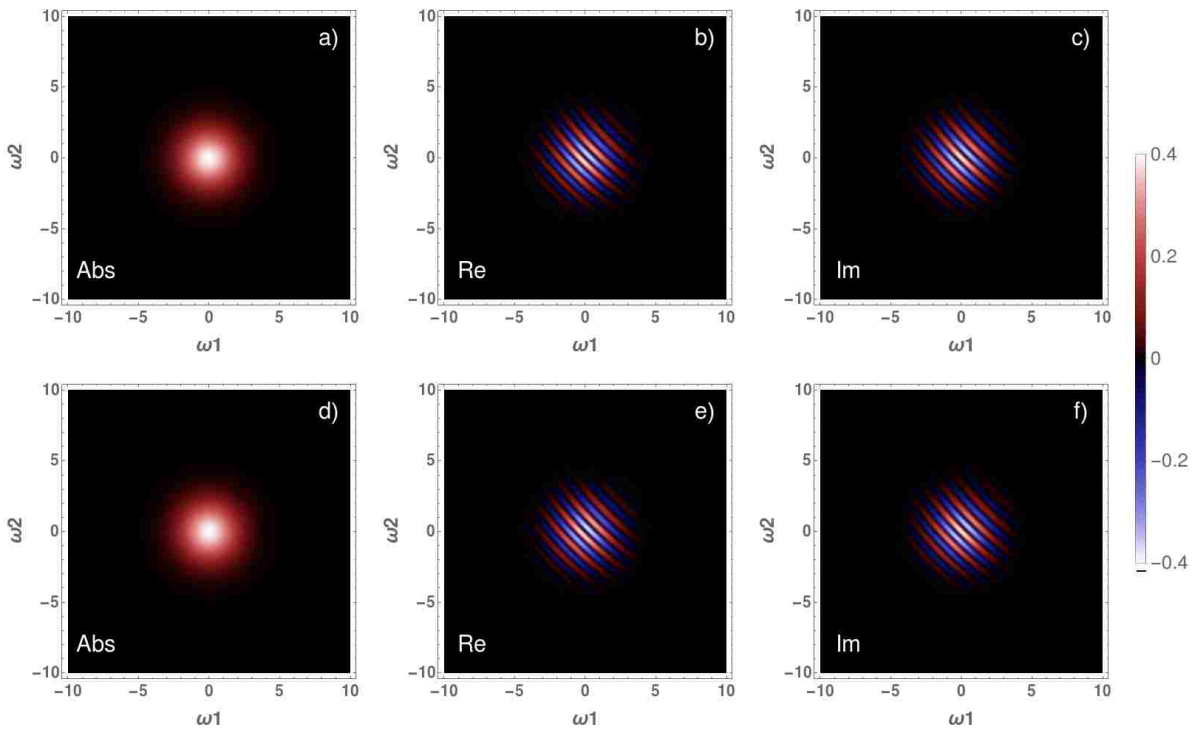

Figure 6.16: The same figure as Fig. 6.13 for N=100 sites.

Here, with one site it is clear that the fidelity is good because the photons are transmitted and have virtually the same shape as the ideal state. The phase is low, however, as can be seen by the fact that the real and imaginary components of the full and ideal states are swapped. This makes sense; from Fig. 6.10 it is clear that a single site provides a very low phase shift and allows photons to transmit with high probability. As the number of sites increases, the entangled component actually becomes larger. At $N = 12$ sites in Fig. 6.14, where the fidelity in Fig. 6.12 is minimized, it is clear that the photons are highly entangled as it is likely to find them along the line $\omega_1 = -\omega_2$. Only when the number of sites becomes larger does this entanglement vanish, similar to the process seen in 6.2.3.

From all this it is clear that an array of non-interacting atoms should be able to function as a passive, deterministic CPHASE gate between two photons in a similar manner as an array of interacting atoms. This gate design has one further complication not

present in the design of [64]; the incoming photons must be spectrally narrow enough that they reside entirely inside the transmission windows presented in Fig. 2.15. If the spectrum of the photons is Gaussian this is not a problem, as the Gaussian function decays very rapidly. If the spectrum is something broader, such as a Lorentzian, a significant amount of the pulse may be outside the transmission window and could be reflected. As the number of pairs required for the gate to function well is large (on the order of 30) this translates into a potentially catastrophic error. Indeed, comparing the phase and fidelity of a Lorentzian pulse in the same way as Fig. 6.10 reveals that as the number of sites increases the difference between the approximate spectrum of Eq. 6.19 and the full solution of Eq. 5.45 becomes significantly greater, to the point where it is not possible to achieve a near-perfect CPHASE operation.

The reason this happens can be seen in Figs. 6.17 and 6.18. Here we have plotted the folded cumulative distribution of a Gaussian spectrum, given by Eq. 6.20, and a Lorentzian spectrum, given by

$$\tilde{f}(\omega) = \frac{\sqrt{\Omega}}{\sqrt{2\pi}(\Omega/2 - i\omega)} \tag{6.22}$$

where Ω is the width of the Lorentzian (as a Lorentzian does not truly have a standard deviation) and is related to the standard deviation of the temporal shape of the pulse (which is a decreasing exponential function) by $\Omega = \frac{1}{\sqrt{2\sigma_t}}$. This pulse has a very physical origin; it is the frequency representation of a single two level system decaying.

For the spectral functions defined here the folded cumulative distribution is given by

$$FCDF(\omega) = \Theta(-\omega)\int_{-\infty}^{\omega} d\omega |\tilde{f}(\omega)|^2 + \Theta(\omega)\int_{\omega}^{\infty} d\omega |\tilde{f}(\omega)|^2 \tag{6.23}$$

When $\omega < 0$ it gives the probability that the photon will be found at a frequency less than ω and when $\omega > 0$ it gives the probability that the photon will be found at a frequency greater than ω. This is a useful figure of merit because it provides a sense of how much of the photon resides outside of the transmission window. As can be seen in Fig. 6.17 when

the system is in the adiabatic regime ($g^2/\sigma_\omega > 30$) if the photon has a Gaussian distribution virtually all of the photon will be contained within the transmission window. When $g^2/\sigma_\omega = 30$ the probability of finding the photon beyond the transmission window ($\omega/g^2 < .2$) is on the order of 10^{-9}. As this parameter increases, the probability of reflection becomes vanishingly small.

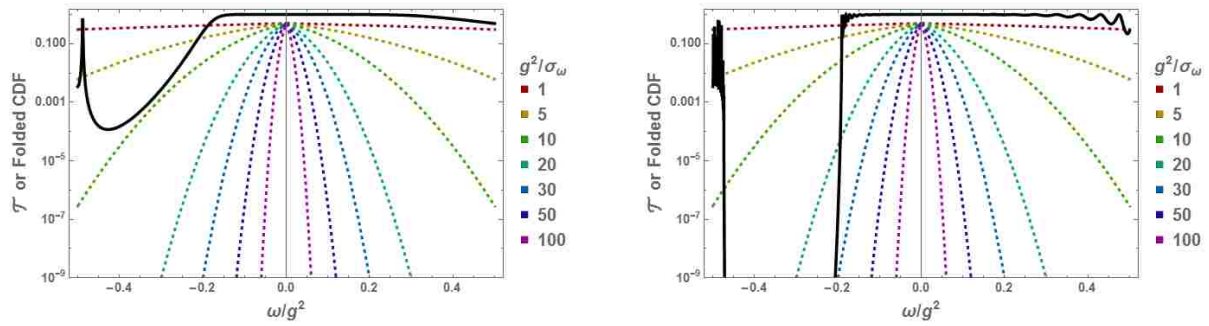

Figure 6.17: A comparison of the folded cumulative distribution of an incoming Gaussian pulse to the transmission coefficient for $N = 6$ pairs (right) and $N = 50$ pairs (left). The solid black line is the intensity transmission coefficient calculated from Eq. 2.20 for $2N$ atoms. Note that the choice of N pairs gives the same transmission coefficient presented in Fig. 2.15 using the optimal spacing presented in Chapter 2.

This does not hold true for a Lorentzian, however. Even when the system is in the adiabatic regime there is still a significant probability that the photon will be found outside the transmission window. At $\omega/g^2 = .2$ and with $g^2/\Omega = 30$, the probability of finding the photon outside the transmission window (i.e. at a frequency of $\omega/g^2 < .2$) is about .0265. While this represents only 2% of the overall photon, this error compounds with two photons as they have a large chance to interact at multiple sites, leading to the ultimate failure of the gate and the breakdown of the approximation given in Eq. 6.19.

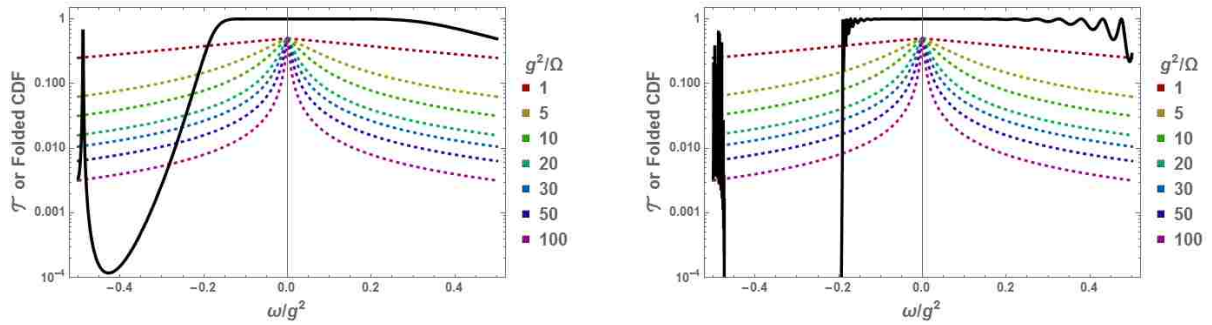

Figure 6.18: The same as Fig. 6.17 but with a Lorentzian incoming pulse.

Thus if one were to construct a CPHASE gate using a series of non-interacting atoms coupled to a 1-D waveguide one would need to ensure that the photons are narrow enough in frequency to properly transmit through the system. This represents a departure from the gate designed using the interacting transmission window where, similar to [30], the gate operates regardless of the distribution of the incoming pulse. This departure is a consequence of the fact that the transmission in Eq. 6.19 is only approximately one for a narrow range of frequencies. Any incoming photon pulse may have a component outside this window, however, and thus for two photons to transmit they both must be made to fit inside this narrow feature. On the other hand, Eq. 6.9 has a theoretically infinite bandwidth; thus there is no chance that a photon of any frequency, no matter how far detuned or whatever shape, will be reflected.

There are several ways to circumvent this complication. Different processes of creating narrow-band single photons will produce different spectral distributions. Choosing an appropriate source would be one way to ensure that the photons fit within the transmission window of the system. It would also be possible to add a band-pass filter to select only the frequencies that will transmit with near unit probability. This would add undesirable losses into the system and make any computation dependent on the final detection of a photon. These errors should be relatively small, though, as for the Lorentzian only about 2% of the pulse would be lost, and this would be a one-time event occurring at the beginning of a computation. Finally it may be possible to use pulse-shaping techniques (such as in [65]) to

force the incoming photons to be narrow in frequency or have a Gaussian shape. Again, this would add in extra losses, especially since pulse shaping typically requires nonlinear elements, but once the photons have been appropriately shaped they will transmit through the system and not experience further errors.

6.4 Conclusions

In this chapter we combined elements from all the previous chapters to demonstrate that the nonlinearity present in arrays of two level systems is able to be used for quantum computation. We have successfully shown that an array of such emitters coupled losslessly to a one-dimensional waveguide can successfully perform a passive, deterministic CPHASE operation between two photons. This is significant, as it shows that there is not a theoretical roadblock to performing quantum logic with photonic qubits. That is not to say, of course, that the systems proposed to perform a CPHASE operation would be easy to build; both transmission windows used to build a gate in this chapter require precise alignment of the emitters and a large number (on the order of 20 or more) to be successfully coupled losslessly to a waveguide. Additionally, the better performing design requires that the emitters be placed close enough that there is a strong, direct dipole-dipole interaction.

We also demonstrated that the design presented in Section 6.2 functions identically to the gate proposed by Brod and Combes in [30] and [64]. We extended our model to consider the effect of travel time between sites and were able to show that if the system is small enough that the Markovian approximation holds the distance between sites matters little. The fact that our proposal works in the same way as the Brod and Combes proposal also suggests that *any* array of two level systems that preserve photon number for counter-propagating pulses will be able to function as a CPHASE gate, including chiral waveguides or systems that can take advantage of different polarizations. Finally, we presented results that suggest an array of non-interacting atoms should also be able to perform a passive, deterministic CPHASE operation between two photons. This design is

limited by the fact that the photons must be spectrally narrow enough, but may be significantly easier to construct as it does not rely on enforcing unidirectional behavior by ensuring strong, finely-tuned interactions between two level systems.

Chapter 7

Conclusions and Future Work

In this text we studied in depth an array of two level systems coupled losslessly to a one-dimensional waveguide structure. In doing so, we accomplished three main tasks; we developed an approach to photon scattering in the time domain that allows for efficient computation of the scattered state of multiphoton pulses, identified and explored transmission windows that appear due to quantum interference between the scattering of photons from multiple atoms, and demonstrated that the nonlinearity present in arrays of two level systems is able to be used for quantum computation.

Using the approach demonstrated in [32], in Chapter 2 we explored the exact scattered state of a single photon from an array of arbitrarily positioned two level systems coupled to a waveguide. In agreement with other authors, we found that the final frequency distribution of the photon scattered by a single atom is accurately described by a frequency-dependent transmission and reflection coefficient and that this description allows one to treat the system of atoms as an array of cavities. Using techniques from quantum optics we derived the same transmission and reflection coefficients. We also found, again in agreement with other works, that the scattering of a single photon is modified significantly by the number of two level emitters coupled to the waveguide. By increasing the number of atoms we explored two different transmission windows, appearing either when the atoms are able to interact via a direct dipole-dipole energy transfer or when they are not able to interact but are placed so that quantum interference preferentially favors transmission over reflection. In Chapters 4 and 5 we continued to explore the non-interacting transmission window and were able to demonstrate that two counter-propagating photons will transmit through (i.e remain in their respective modes) an array of atoms with near-unit probability.

In dealing with the multiphoton wavefunction, we developed a novel, time-domain approach to multiphoton scattering, identical to that published in [11] concurrently with our publication [12]. In this approach, the normal ordering of photon creation and

annihilation operators ensures that one can write a final expression for the scattered state of the photons in terms of a finite series, given in Eq. 3.18. In using this solution to study the scattering of two photons from a single two level system, we explored the origin of entanglement between the photons and were able to show that, due to the fact that a single emitter can only absorb one photon at a time, the arrival times of photons, as measured by a photo-detector, will be correlated. In Chapter 4 we extended this approach to describe the scattered state of two photons from two atoms, where the atoms can be placed an arbitrary distance apart. We explored how control of the atomic position changes the transport properties for co-propagating, counter-propagating, and standing wave mode photons. We found that the addition of a second atom leads to interesting possibilities of isolating entangled terms, reducing the overall entanglement between the photons, and in creating regions of very high transmission. We also demonstrated that the same transmission windows studied in Chapter 2 for a single photon are also present for two atoms. Finally, in Chapter 5 we considered the case of two photons scattering from an array of N atoms and arrived at a solution for two counter-propagating photons scattering from an array of N atoms. We used this solution to show that the non-interacting transmission window studied in Section 2.4.2 is also present for two photons transmitting through up to 8 atoms.

The generality of the solution presented in Eq. 5.19 immediately suggests a direction for future work; exploring how multiple atoms modify the transport and entanglement properties of two photons. In Chapter 4 we demonstrated that the addition of a second atom dramatically changes the properties of the scattered photons; it is likely that adding more atoms will similarly create new nonclassical states of light and provide even greater control over the properties of the scattered photons. Additionally, using the process in Eq. 3.18, we can in principle extend the solutions in Eq. 4.30 and Eq. 5.19 to deal with initial states that contain more than two photons. This is a largely-unexplored area of photon scattering and this approach provides an intuitive, analytic way to study entanglement and

photon transport of multiphoton pulses.

Finally, we applied the results and methods developed in Chapters 2 through 5 to design and evaluate a conditional phase gate between two counter-propagating photons inspired by the gate presented in [30]. We were able to demonstrate in Section 6.1 that pairs of interacting two level systems coupled to a waveguide are indeed able to function as a CPHASE gate between two counter-propagating photons, and that the gate operates in the same manner as that proposed in [30]. By creating a heuristic model and demonstrating numerical agreement with the full solution of Chapter 5, we argued that an array of non-interacting atoms should also be able to function as a conditional logic gate between two photons, provided that the frequency distribution of the photons is sufficiently narrow and the system is tuned to the non-interacting transmission windows studied in Chapters 2, 4 and 5.

It is significant that the nonlinearity present in two level systems coupled to a waveguide can be used to perform quantum information processing tasks. Our study suggests an experimental way to realize a passive, deterministic quantum logic gate between photonic qubits that does not suffer from the theoretical limitations of many gate proposals. Additionally, the general nature of the equations implies that any array of two level systems losslessly coupled to a waveguide would be capable of producing the desired effect. The downside, of course, is that constructing the arrays of atoms proposed in this work would require incredibly precise engineering of either dipole-dipole interactions or placement of the emitters. Additionally, achieving true, lossless operation is difficult. If the losses at each site were of the order of 1%, with 15 sites (as was shown to be needed for achieving a fidelity of around .01 in Fig. 6.3) the total photon loss could be on the order of 15% at each step of the computation. This suggests a direction for further work; quantifying the effect of losses in the system and finding ways to mitigate them from a fundamental perspective, without resorting to post-selecting events where photons are detected. Another direction for future work is to better evaluate the numerical agreement

between the heuristic model of Eq. 6.19 and the full solution of Eq. 5.45. While the results presented here suggest that the approximate form given in Eq. 6.19 is good, more work can be done to demonstrate that this agreement holds for a larger number of atoms than was presented in Fig. 6.10. Finally, in studying the ability of an array of non-interacting atoms to function as a CPHASE gate, we assumed that $\delta/g^2 = 1$. Changing this parameter should enable one to change the value of the phase imparted by the gate and characterizing this effect would provide insight into the gate's functionality.

Bibliography

[1] D. D. Sukachev M. J. Burek J. Borregaard M. K. Bhaskar C. T. Nguyen J. L. Pacheco H. A. Atikian C. Meuwly R. M. Camacho F. Jelezko E. Bielejec H. Park M. Lonar M. D. Lukin A. Sipahigil, R. E. Evans. An integrated diamond nanophotonics platform for quantum-optical networks. *Science*, 13, 2016.

[2] M. Arcari S. Lindskov Hansen L. Midolo S. Mahmoodian G. Kirsanskė T. Pregnolato E.H. Lee J.D. Song S. Stobbe A. Javadi, I. Sollner and P. Lodahl. Single-photon non-linear optics with a quantum dot in a waveguide. *Nature Communications*, (Article 8655), 2015.

[3] B. Peropadre J.-L. Orgiazzi1 M. A. Yurtalan R. Belyansky C. M. Wilson P. Forn-Daz1, J. J. Garca-Ripoll and A. Lupascu. Ultrastrong coupling of a single artificial atom to an electromagnetic continuum in the nonperturbative regime. *Nature Physics*, 13, 2016.

[4] A. Javadi-S. Lindskov Hansen S. Mahmoodian J. Liu H. Thyrrestrup E. H. Lee J. D. Song S. Stobbe M. Arcari, I. Söllner and P. Lodahl. Near-unity coupling efficiency of a quantum emitter to a photonic crystal waveguide. *Phys. Rev. Lett.*, 113(093603), 2014.

[5] J. T. Shen and S. Fan. Strongly correlated two-photon transport in a one-dimensional waveguide coupled to a two-level system. *Phys. Rev. Lett.*, 98(153003), 2007.

[6] J. T. Shen and S. Fan. Coherent photon transport from spontaneous emission in one-dimensional waveguides. *Optics Letters*, 30(2001), 2005.

[7] S. Kocabas E. Rephaeli and S. Fan. Few-photon transport in a waveguide coupled to a pair of colocated two-level atoms. *Phys. Rev. A*, 84(063832), 2005.

[8] D. J. Gauthier H. Zheng and H. U. Baranger. Waveguide qed: Many-body bound-state effects in coherent and fock-state scattering from a two-level system. *Phys. Rev. A*, 82(063816), 2010.

[9] V. Noh T. Feng See and D. G. Angelakis. Diagrammatic approach to multiphoton scattering. *Phys. Rev. A*, 95(053845), 2017.

[10] M. Pletyukhov1 and V. Gritsev. Scattering of massless particles in one-dimensional chiral channel. *New J. Phys.*, 14(095028), 2012.

[11] A. Roulet and V. Scarani. Solving the scattering of n photons on a two-level atom without computation. *New J. Phys.*, 18(093035), 2016.

[12] W. Konyk and J. Gea-Banacloche. Quantum multimode treatment of light scattering by an atom in a waveguide. *Phys. Rev. A*, 93(063807), 2016.

[13] D. P. S. McCutcheon A. Nysteen and J. Mrk. Strong nonlinearity-induced correlations for counterpropagating photons scattering on a two-level emitter. *Phys Rev. A*, 91(063823), 2015.

[14] S. Kocabas. Effects of modal dispersion on few-photonqubit scattering in one-dimensional waveguides. *Phys Rev. A*, 93(033829), 2016.

[15] H. Zheng and Baranger. Persistent quantum beats and long-distance entanglement from waveguide-mediated interactions. *Phys Rev. Lett.*, 110(113601), 2013.

[16] E.T. Jaynes and F. Cummings. Comparison of quantum and semiclassical radiation theories with application to the beam maser. *Proceedings of the IEEE*, 51:89–109, 1963.

[17] Girish S. Agarwal. *Quantum Optics*. Cambridge University Press, 2012.

[18] J. H. Shapiro. Single-photon kerr nonlinearities do not help quantum computation. *Phys Rev. A*, 73(062305), 2006.

[19] J. Gea-Banacloche. Impossibility of large phase shifts via the giant kerr effect with single-photon wave packets. *Phys Rev. A*, 81(043823), 2010.

[20] Robert Purdy Nicholas Furtak-Wells, Lewis A. Clark and Almut Beige. Quantizing the electromagnetic field near two-sided semitransparent mirrors. *Phys. Rev. A*, 97(043827), 2018.

[21] S. Stobbe P. Schneeweiss J. Volz A. Rauschenbeutel H. Pichler P. Zoller P. Lodahl, S. Mahmoodian. Chiral quantum optics. *Nature*, 541:473–480, 2017.

[22] Michael A. Nielsen and Isaac L. Chuang. *Quantum Computation and Quantum Information*. Cambridge University Press, 2011.

[23] Mark M. Wilde. *Quantum Information Theory*. Cambridge University Press, 2017.

[24] S. Mahmoodian A. G. White T. Ralph, I. S olner and P. Lodahl. Photon sorting, efficient bell measurements, and a deterministic controlled-z gate using a passive two-level nonlinearity. *Phys. Rev. Lett.*, 114(173603), 2015.

[25] L.-M. Duan and H. J. Kimble. Scalable photonic quantum computation through cavity-assisted interactions. *Phys Rev. Lett.*, 92(127902), 2004.

[26] G. Rempe B. Hacker, S. Welte and S. Ritter. A photon-photon quantum gate based on a single atom in an optical resonator. *Nature*, 536, 2016.

[27] G. Milburn E. Knill, R. Laflamme. A scheme for efficient quantum computation with linear optics. *Nature*, 409(6816), 2001.

[28] I. L. Chuang C. Chudzicki and J. H. Shapiro. Deterministic and cascadable conditional phase gate for photonic qubits. *Phys. Rev. A*, 87(042325), 2013.

[29] M. Heuck J. Mrk A. Nysteen, D. McCutcheon and D. Englund. Limitations of two-level emitters as nonlinearities in two-photon controlled-phase gates. *Phys Rev. A*, 95(062304), 2017.

[30] D. J. Brod and J. Combes. Passive cphase gate via cross-kerr nonlinearities. *Phys. Rev. Lett.*, 117(080502), 2016.

[31] A. F. van Loo A. Fedorov A. Wallraff K. Lalumiere, B. C. Sanders and A. Blais. Input-output theory for waveguide qed with an ensemble of inhomogeneous atoms. *Phys Rev A*, 88(043806), 2013.

[32] Shi-Yao Zhu Zeyang Liao, Xiaodong Zeng and M. Suhail Zubairy. Single-photon transport through an atomic chain coupled to a one-dimensional nanophotonic waveguide. *Phys Rev A*, 92(023806), 2015.

[33] T. S. Tsoi and C. K. Law. Quantum interference effects of a single photon interacting with an atomic chain inside a one-dimensional waveguide. *Phys Rev A*, 78(063832), 2008.

[34] H. Nha Z. Liao and M. S Zubairy. Dynamical theory of single-photon transport in a one-dimensional waveguide coupled to identical and nonidentical emitters. *Phys. Rev. A*, 94(053842), 2016.

[35] J. Ruostekoski and J. Javanainen. Arrays of strongly coupled atoms in a one-dimensional waveguide. *Phys Rev A*, 96(033857), 2017.

[36] J. Xu M.-T. Cheng and G. S. Agarwal. Waveguide transport mediated by strong coupling with atoms. *Phys. Rev. A*, 95(053807), 2017.

[37] J. Gea-Banacloche W. Konyk. One- and two-photon scattering by two atoms in a waveguide. *Phys. Rev. A.*, 96(063826), 2017.

[38] A. V. Gorshkov D. E. Chang, L. Jiang and H. J. Kimble. Cavity qed with atomic mirrors. *New J. Phys.*, 14(063003), 2012.

[39] H. Nguyen Le V Scarani P. Guimond, A. Roulet. Rabi oscillation in a quantum cavity: Markovian and non-markovian dynamics. *Phys. Rev. A*, 93(023808), 2016.

[40] H. Nha Z. Liao and M. S. Zubairy. Single-photon frequency-comb generation in a one-dimensional waveguide coupled to two atomic arrays. *Phys. Rev. A*, 93(033851), 2016.

[41] F. J. Garcia-Vidal C. Gonzalez-Ballestero and E. Moreno. Non-markovian effects in waveguide-mediated entanglement. *New J. Phys.*, 15(073015), 2013.

[42] A. M. Bra´ nczyk B. Q. Baragiola, R. L. Cook and J. Combes. N-photon wave packets interacting with an arbitrary quantum system. *Phys. Rev. A*, 86(013811), 2012.

[43] H. Nguyen Le A. Roulet, C. Teo and V. Scarani. Proposal for monitoring and heralding position states of atoms in a one-dimensional waveguide. *Phys. Rev. A*, 90(053821), 2014.

[44] A. Nazir B. W. Lovett, J. H. Reina and G. A. D. Briggs. Optical schemes for quantum computation in quantum dot molecules. *Phys. Rev. B*, 68(205319), 2003.

[45] I. H. Deutsch G. K. Brennen and P. S. Jessen. Entangling dipole-dipole interactions for quantum logic with neutral atoms. *Phys. Rev. A*, 61(062309), 2000.

[46] M. S Zubairy Z. Liao M. Al-Amri. Resonance-fluorescence-localization microscopy with subwavelength resolution. *Phys. Rev. A*, 85(023810), 2012.

[47] J. Pan Y. Li J.P. Draayer F. Pan, T. Wang. Exact solutions of an extended dicke model. *Physics Letters A*, 341(94–100), 2005.

[48] A. W. Elshaari E. E. Hach III and S. F. Preble. Fully quantum-mechanical dynamic analysis of single-photon transport in a single-mode waveguide coupled to a traveling-wave resonator. *Phys. Rev. A*, 82(063839), 2010.

[49] S. E. Kocabas S. Fan and J. T. Shen. Input-output formalism for few-photon transport in one-dimensional nanophotonic waveguides coupled to a qubit. *Phys. Rev. A*, 82(063821), 2010.

[50] S. Takeuchi K. Kojima, H. F. Hofmann and K. Sasaki. Nonlinear interaction of two photons with a one-dimensional atom: Spatiotemporal quantum coherence in the emitted field. *Phys. Rev. A*, 68(013803), 2003.

[51] M. A. Bouchene S. Derouault. One-photon wavepacket interacting with a two-level atom in a waveguide: Constraint on the pulse shape. *Phys. Lett. A*, 376(3491–3494), 2012.

[52] *See, for example, M. O. Scully and M. S. Zubairy,* Quantum Optics*, Section 4.2 (Cambridge University Press, 1997.*

[53] P. L. Kelley and W. H. Kleiner. Theory of electromagnetic field measurement and photoelectron counting. *Phys. Rev.*, 136(A316), 1964.

[54] Z. Cheng and G. Kurizki. Optical multiexcitons: quantum gap solitons in nonlinear bragg reflectors. *Phys. Rev. Lett.*, 75(3430), 1995.

[55] E. A. Demler D. E. Chang, A. S. Sø rensen and M. D. Lukin. A single-photon transistor using nanoscale surface plasmons. *Nature Phys.*, 3(807), 2007.

[56] Q.-Y. Liang A. V. Gorshkov M. D. Lukin O. Firstenberg, T. Peyronel and V. Vuletić. A single-photon transistor using nanoscale surface plasmons. *Nature*, 502(71), 2013.

[57] J. D. Franson. Bell inequality for position and time. *Phys. Rev. Lett.*, 62(2205), 1989.

[58] B. Podolsky A. Einstein and N. Rosen. Can quantum-mechanical description of physical reality be considered complete? *Phys. Rev.*, 47(777), 1935.

[59] Z. Y. Ou C. K. Hong and L. Mandel. Measurement of subpicosecond time intervals between two photons by interference. *Phys. Rev. Lett.*, 59(2044–2046), 1987.

[60] H. N. Le A. Roulet and V. Scarani. Two photons on an atomic beam splitter: Nonlinear scattering and induced correlations. *Phys. Rev. A*, 93(033838), 2016.

[61] T. Henage L. Isenhower D. D. Yavuz T. G. Walker E. Urban, T. A. Johnson and M. Saffman. Observation of rydberg blockade between two atoms. *Nature Letters*, 5(110-114), 2009.

[62] Tatjana Wilk Amodsen Chotia Matthieu Viteau Daniel Comparat Pierre Pillet Antoine Browaeys Alpha Gatan, Yevhen Miroshnychenko and Philippe Grangie. Observation of collective excitation of two individual atoms in the rydberg blockade regime. *Nature Letters*, 5(115-118), 2009.

[63] M. D. Lukin D. Witthaut and A. S. Sørensen. Photon sorters and qnd detectors using single photon emitters. *Europhys. Lett.*, 97(50007), 2012.

[64] J. Combes D. J. Brod and J. Gea-Banacloche. Two photons co- and counterpropagating through n cross-kerr sites. *Phys. Rev. A*, 94(023833), 2016.

[65] Shengwang Du G. Y. Yin P. Kolchin, C. Belthangady and S. E. Harris. Electro-optic modulation of single photons. *Phys Rev. Lett.*, 101(103601), 2008.

[66] V. Gritsev G. Blatter D. Oehri, M. Pletyukhov and S. Schmidt. Tunable, nonlinear hong-ou-mandel interferometer. *Phys Rev. A*, 91(033816), 2015.

[67] L. Pedrotti J. Gea-Banacloche. Single-photon, cavity-mediated gates: Detuning, losses, and nonadiabatic effects. *Phys Rev. A*, 86(052133), 2011.

[68] N. Nemet J. Gea-Banacloche. Conditional phase gate using an optomechanical resonator. *Phys Rev. A*, 89(052327), 2014.

Appendix A

Dynamics of the Single-Photon, Two-Atom Interaction

As was mentioned in previous chapters, the solutions presented in the time domain for the interaction between photons and atoms are not restricted to the scattering limit. Here we show how to consider the dynamics of the system by modifying the solution for the scattering of a single photon from two atoms, given in Eq. 4.36, to instead explore the spacetime profile of the pulse during the interaction. To do so, we first assume the interaction begins at $t = 0$ rather than $t = -\infty$. The photon state as a function of time is then given by

$$\begin{aligned} |\psi_g(t)\rangle = |\psi_0\rangle &- 2\Gamma_c \int_0^t dt_1 \int_0^{t_1} dt_2 e^{-\Gamma_+(t_1-t_2)} \hat{C}^\dagger(t_1)\hat{C}(t_2)|\psi_0\rangle \\ &- 2\Gamma_s \int_0^t dt_1 \int_0^{t_1} dt_2 e^{-\Gamma_-(t_1-t_2)} \hat{D}^\dagger(t_1)\hat{D}(t_2)|\psi_0\rangle \end{aligned} \tag{A.1}$$

From here integrals of the form $\int_0^{t_1} dt_2 e^{-\Gamma_i(t_1-t_2)} f(t_2 - \tau_0)$ must be evaluated, where τ_0 represents the initial spacetime position of the pulse. The solution to this is nearly identical to that of $G_{\Gamma_i}(t)$ provided that τ_0 is sufficiently far away from the origin. To show this, consider that with the change of variables $\tau = t_2 - \tau_0$ we can express G as

$$\begin{aligned} G_\Gamma(t_1) =& e^{-\Gamma t_1} \int_0^{t_1} dt_2 e^{\Gamma t_2} f(t_2 - \tau_0) \\ =& e^{-\Gamma t_1} \int_0^{t_1-\tau_0} d\tau e^{\Gamma(\tau+\tau_0)} f(\tau) \\ \approx& e^{-\Gamma(t_1-\tau_0)} \int_{-\infty}^{t_1-\tau_0} d\tau e^{\Gamma\tau} f(\tau) = G(t_1 - \tau_0) \end{aligned} \tag{A.2}$$

Using this and writing the $\hat{C}$ and $\hat{D}$ standing-wave mode operators in terms of travelling wave operators yields the following time-dependent pulse. Note that the definitions of f_A and f_B are slightly different than given in Eq. 4.36, as the limits of

integration on the initial state will be different than the interaction components.

$$
\begin{aligned}
|\psi_g(t)\rangle &= |\psi_0\rangle + \int_0^t dt_1 \big[f_A(t_1)A^\dagger(t_1) + f_B(t_1)B^\dagger(t_1)\big]|0\rangle \\
f_A(t_1) &= -\Gamma_c G_{\Gamma_+}(t_1-\tau_0) - \Gamma_s G_{\Gamma_-}(t_1-\tau_0) \\
f_B(t_1) &= -\Gamma_c G_{\Gamma_+}(t_1-\tau_0) + \Gamma_s G_{\Gamma_-}(t_1-\tau_0)
\end{aligned} \tag{A.3}
$$

To explore the intensity of the field as a function of position and time we introduce the field operator $E^{(+)}(z,t)$

$$
\begin{aligned}
E^{(+)}(z,t) &= \int d_\omega \Big[e^{-i\omega(t-z/c)+ik_F(z-ct)}a_\omega + e^{-i\omega(t+z/c)-ik_F(z+ct)}b_\omega\Big] \\
&= \sqrt{2\pi}\big[e^{ik_F(z-ct)}A(t-z/c) + e^{-ik_F(z+ct)}B(t+z/c)\big]
\end{aligned} \tag{A.4}
$$

The intensity is given by $\langle\psi_g|E^{(-)}(z,t)E^{(+)}(z,t)|\psi_g\rangle$, with $E^{(-)}(z,t)$ being the complex conjugate of $E^{(+)}(z,t)$. To evaluate this, first the action of $E^{(+)}(z,t)|\psi_g\rangle$ must be found. Commuting all the operators, this becomes

$$
\begin{aligned}
E^{(+)}(z,t)|\psi_g(t)\rangle = E^{(+)}(z,t)|\psi_0\rangle + \sqrt{2\pi}\int_0^t dt_1 \big[e^{ik_F(z-ct)}A(t-z/c) + e^{-ik_F(z+ct)}B(t+z/c)\big] \\
\big[f_A(t_1)A^\dagger(t_1) + f_B(t_1)B^\dagger(t_1)\big]|0\rangle \\
= \sqrt{2\pi}\int_{-\infty}^{\infty} dt_1 f(t_1)e^{ik_F(z-ct)}\delta\big(t_1-(t-z/c)\big) \\
+\sqrt{2\pi}\int_0^t dt_1\big[f_A(t_1)e^{ik_F(z-ct)}\delta\big(t_1-(t-z/c)\big) + f_B(t_1)e^{-ik_F(z+ct)}\delta\big(t_1-(t+z/c)\big)\big]|0\rangle \\
= \sqrt{2\pi}\big[f(t-z/c)e^{ik_F(z-ct)}\Theta(t-z/c) \\
+f_A(t-z/c)e^{ik_F(z-ct)}\Theta(t-z/c)\Theta(z/c) + f_B(t+z/c)e^{-ik_F(z+ct)}\Theta(t+z/c)\Theta(-z/c)\big]|0\rangle
\end{aligned} \tag{A.5}
$$

As $\langle\psi_g|E^{(-)}(z,t)$ will simply be the complex conjugate of the above function, and there

are no remaining operators, the intensity as a function of position and time is

$$\langle\psi_g|E^{(-)}(z,t)E^{(+)}(z,t)|\psi_g\rangle = \\ 2\pi\Big|e^{ik_F(z-ct)}\big(f(t-z/c)\Theta(t-z/c)+f_A(t-z/c)\Theta(t-z/c)\Theta(z/c)\big) \\ +e^{-ik_F(z+ct)}f_B(t+z/c)\Theta(t+z/c)\Theta(-z/c)\Big|^2 \tag{A.6}$$

In order to ensure that the interaction will happen after time $t=0$, the initial state is centered around the position $-5\sigma_t$ to ensure that it is sufficiently far away from the atoms.

Before plotting the pulse as a function of position, we also solve the excitation probability of the $|\psi_\pm\rangle$ states. These are given from Eqs. 4.22a and 4.22b, after using the fact that the initial state has only one photon and applying the Markovian approximation to the operators, by the functions below.

$$|\psi_+(t)\rangle = -i\sqrt{2\Gamma_c}\int_0^t dt_1 e^{-\Gamma_+(t-t_1)}\hat{C}(t_1)|\psi_I\rangle = -i\sqrt{\Gamma_c}G_{\Gamma_+}(t-\tau_0) \tag{A.7}$$

$$|\psi_-(t)\rangle = -\sqrt{2\Gamma_s}\int_0^t dt_1 e^{-\Gamma_-(t-t_1)}\hat{D}(t_1)|\psi_g(t_1)\rangle = -\sqrt{\Gamma_s}G_{\Gamma_-}(t-\tau_0) \tag{A.8}$$

This makes sense physically, as we have shown previously that the function G_Γ is related to the atomic excitation probability. With this, the probability to find the atoms in either of the superposition states becomes

$$\langle\psi_+|\psi_+\rangle = \Gamma_c\Big|G_{\Gamma_+}(t-\tau_0)\Big|^2 \qquad\qquad \langle\psi_-|\psi_-\rangle = \Gamma_s\Big|G_{\Gamma_-}(t-\tau_0)\Big|^2 \tag{A.9}$$

We also desire the probability for the photon to be in the field state. This is given as

$$\langle\psi_g|\psi_g\rangle = 1-\Gamma_c\Big|G_{\Gamma_+}(t-\tau_0)\Big|^2-\Gamma_s\Big|G_{\Gamma_-}(t-\tau_0)\Big|^2 \tag{A.10}$$

Below are figures for the position and respective probabilities as a function of time for the case when the photon is on resonance ($\delta=0$) and there are no atomic interactions ($\Delta=0$). For these figures, k_F has been set to 10^{14} to model what would happen for an optical photon and the initial pulse shape has been chosen to be Gaussian.

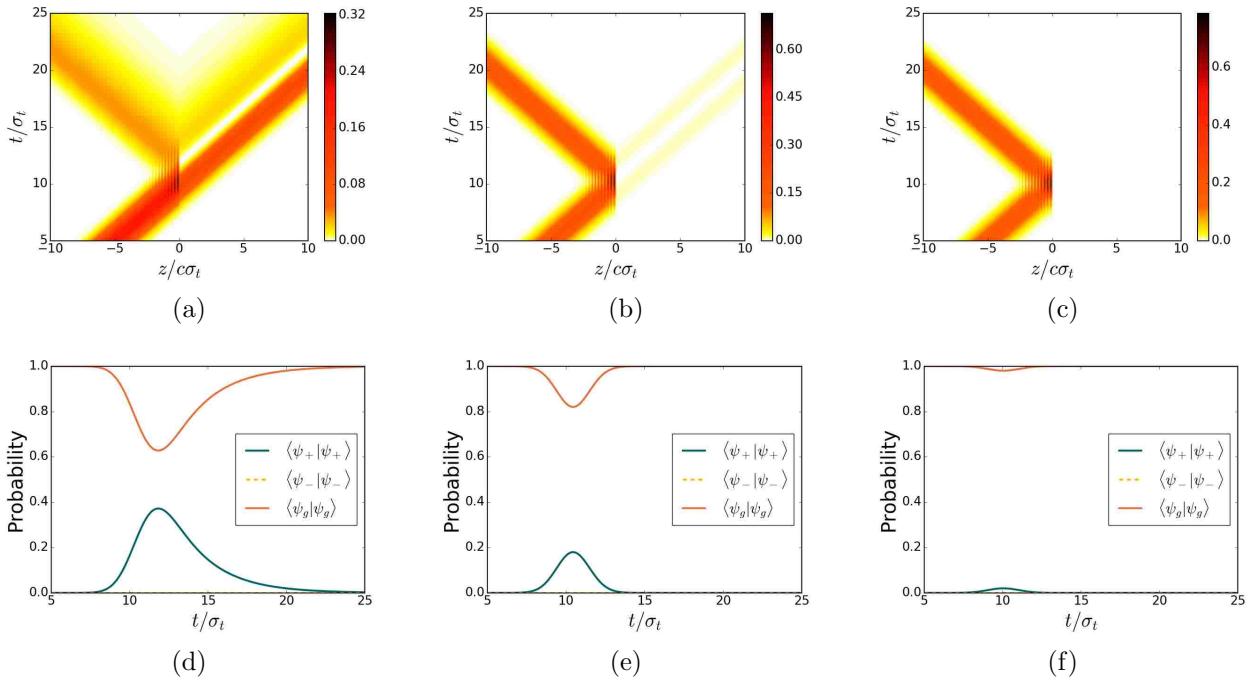

Figure A.1: The position of the photons and excitation probabilities of the atoms as a function of time. Here $\delta = \Delta = 0$ and $k_F z = 2\pi$ for all plots. The rightmost column corresponds to $g^2\sigma_t = .1$, the middle column to $g^2\sigma_t = 1$, and the leftmost column to $g^2\sigma_t = 10$. In the bottom plots, the blue curve is the excitation probability of the $|+\rangle$ state, the yellow dashed curve is the excitation probability of the $|-\rangle$ state, that the red curve is the probability that neither atom is excited.

The first set of figures in Fig. A.1 correspond to the case where the atoms are positioned so that only the $|+\rangle$ state is coupled to the waveguide. As can be seen, as the coupling increases the pair of atoms acts more like a mirror, as was seen for a single photon interacting with a single atom. Additionally, the probability that the atomic state $|+\rangle$ is excited is generally small.

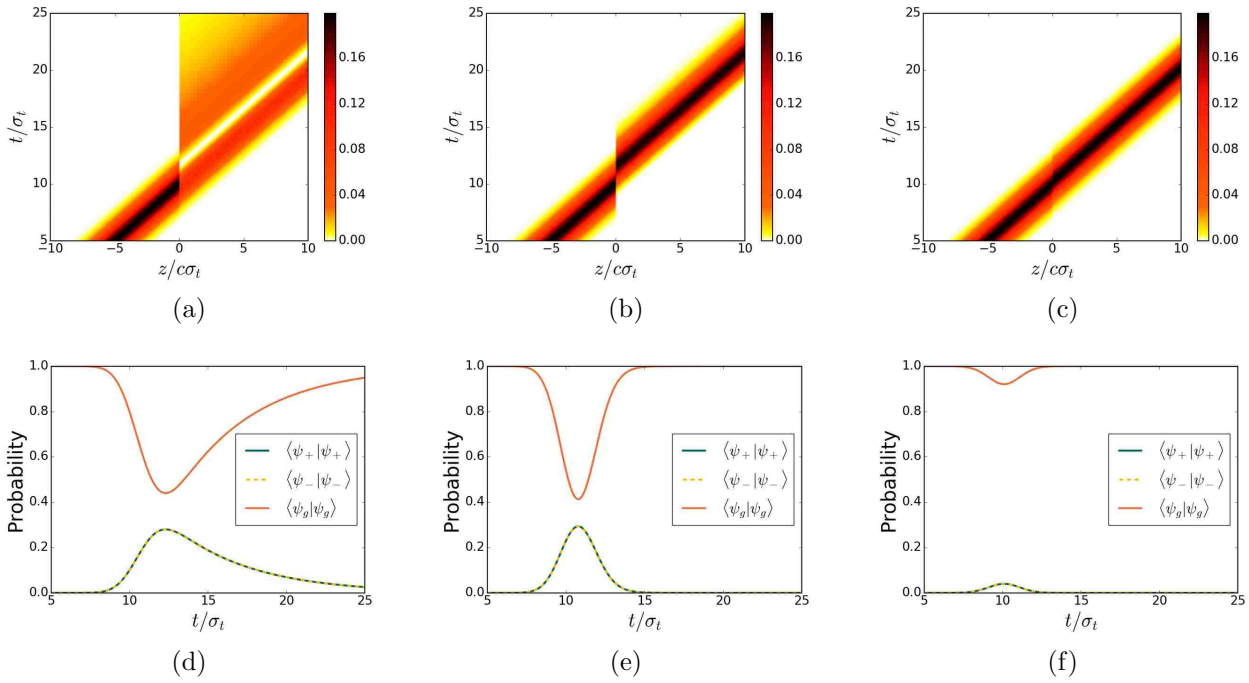

Figure A.2: The position of the photons and excitation probabilities of the atoms as a function of time. Here $\delta = 0$, $\Delta = g^2$ and $k_F z = 3\pi/2$ for all plots. The rightmost column corresponds to $g^2\sigma_t = .1$, the middle column to $g^2\sigma_t = 1$, and the leftmost column to $g^2\sigma_t = 10$. In the bottom plots, the blue curve is the excitation probability of the $|+\rangle$ state, the yellow dashed curve is the excitation probability of the $|-\rangle$ state, that the red curve is the probability that neither atom is excited.

When the atoms are able to interact by a dipole-dipole interaction (given by Eq. 2.37) and the system is tuned to the transmission window described in Section 2.5, the entire photon is transmitted with unit probability. This can be seen in Fig. A.2, where the photon pulse is always found to transmit. For low couplings, however, the photon may be significantly delayed with respect to its original path. Additionally, as $\Gamma_+ = \Gamma_-$ when the system is tuned to this particular transmission window, both the $|+\rangle$ and $|-\rangle$ states experience the same probability to be excited, and in the case when $g^2\sigma_t = 1$ it becomes significantly more likely that the photon will be absorbed when compared to Fig. A.1.

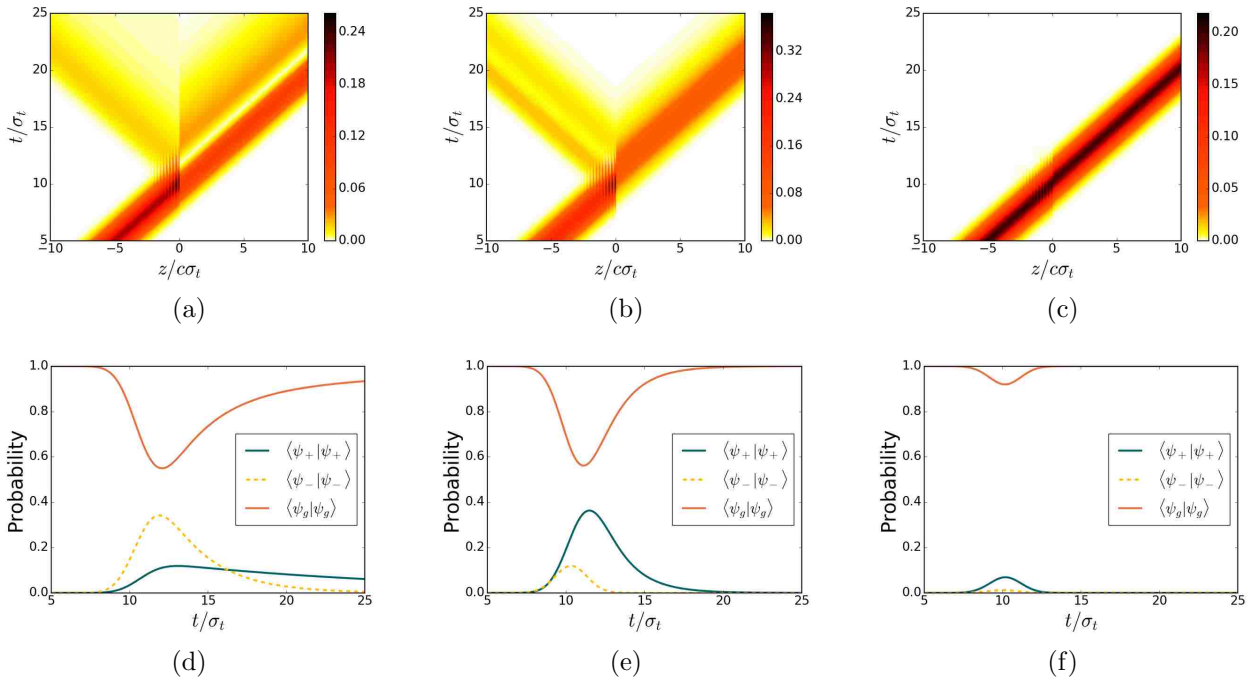

Figure A.3: The position of the photons and excitation probabilities of the atoms as a function of time. Here $\delta = g^2$, $\Delta = 0$ and $k_F z = 3\pi/4$ for all plots. The rightmost column corresponds to $g^2\sigma_t = .1$, the middle column to $g^2\sigma_t = 1$, and the leftmost column to $g^2\sigma_t = 10$. In the bottom plots, the blue curve is the excitation probability of the $|+\rangle$ state, the yellow dashed curve is the excitation probability of the $|-\rangle$ state, that the red curve is the probability that neither atom is excited.

Finally, we present results for a system tuned to the non-interacting transmission window that occurs when $\tan(k_F z) = -\delta/g^2$. Here, the photon is generally transmitted, but the pulse remains distorted for higher values of $g^2\sigma_t$ than compared to the final pulse in Fig. A.2. Each of the states $|\pm\rangle$ now couple differently to the photon modes, and as such the excitation probability of the two is also different.

In summary, we presented how to modify the time domain approach to explore system dynamics. We used this to present visualizations of the single photon transmission windows shown in Section 4.3.1.

Appendix B

Operation of a Single Site Atom-Cavity Phase Gate

B.1 Introduction

In this appendix we explore a related question to the main topic of photon scattering from an array of two level systems in a waveguide; how well can a single site function as a CPHASE gate? In exploring this, we will specifically consider a single three-level atom in the V configuration, contained within a cavity, where each level of the atom is accessed by photons with different polarizations. The motivation for studying this particular system is threefold; first, the addition of the cavity, in principle, allows the two photons to interact multiple times with the atom which could reduce the number of sites required to build a logic gate in the style of Brod and Combes [30]. Second, in the appropriate limit, this system behaves identically to a single two level emitter coupled to a waveguide. Thus, in studying the atom-cavity system we can also show that a single emitter cannot be used to construct a high-fidelity, passive CPHASE gate. Finally, it provides a different method of approaching the scattering problem and gives some background on how to quantize field modes. Rather than using the time domain and looking for commuting operators we will use the Laplace transform to directly solve the scattered state of a multiphoton pulse. The work in this appendix was presented in the summer of 2017 at DAMOP in Sacramento. Note also that [66] similarly solves for the scattering of two photons from a cavity.

B.2 Solving for the scattered state

B.2.1 Hamiltonian and operator action

As mentioned in the introduction, in this appendix we will be studying the scattering of two counter-propagating photons with different polarizations from a three-level system inside a cavity. A diagram of this system is given in Fig. B.1, where as before $\hat{a}$ and $\hat{b}$ modes represent right and left travelling wave photons and the subscripts h or v denote the

polarization of the photon.

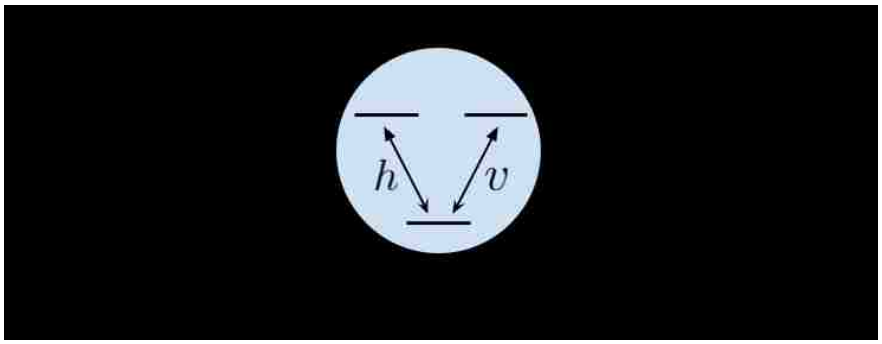

Figure B.1: A diagram of the atom-cavity system being considered here, where a three level V system, with the levels accessed by different polarizations, is embedded inside a cavity which itself is in some structure that only allows photons to travel in one dimension outside the cavity.

In order to appropriately describe the photon inside the cavity, we use the cavity quasimode operator derived in [67]. This operator describes the quantized field inside a cavity of length l embedded in a much larger cavity of length L. We will ultimately let $L \to \infty$ to model the field modes in free space. In all this, we will be assuming that photons outside the cavity may only transmit in one dimension, enforced by a waveguide, fiber, or other structure. For a cavity with mirrors M_1 and M_2 with corresponding transmission (t_i) and reflection (r_i) coefficients, the field that the atom experiences is given by

$$\cos(k_0 z) \sum_k \frac{\sqrt{\frac{2\kappa c}{L}}}{\kappa - i(ck + \Delta)} \left(\tau_1 a_k + \tau_2 b_k\right) \tag{B.1}$$

In this equation, k_0 is the wavenumber of the atomic transition, $ck = \Omega_k - \Omega_0$ (where $\Omega_k = ck$) is the frequency spacing from the center of the incoming wavepacket Ω_0, $\Delta = \Omega_0 - \Omega_c$ is the detuning between the center of the pulse and the cavity frequency, κ is the cavity loss rate (given by $\kappa = \frac{t_1+t_2}{4}\frac{c}{l}$), l is the length of the cavity, and L the quantization length. $\tau_i = \frac{t_i}{\sqrt{t_1^2+t_2^2}}$ is a factor that determines the coupling to each of the modes based on the mirrors involved, and it has the property that $\tau_1^2 + \tau_2^2 = 1$. In deriving this equation, we make the usual quantum optics assumptions that the reflectivity of the mirrors is close to 1, that the quantity c/l is on the order of optical wavelengths, and that

detunings are sufficiently small.

With these modes, the Hamiltonian describing the interaction between the atom and cavity is

$$H = \hbar g \cos(k_0 z)\sqrt{\frac{2\kappa c}{L}}\Big[\sum_k e^{-i(ck+\delta_h)t}\frac{\tau_1 a_{k,h} + \tau_2 b_{k,h}}{\kappa - i(ck+\Delta)}|H\rangle\langle g| + \sum_k e^{-i(ck+\delta_v)t}\frac{\tau_1 a_{k,v} + \tau_2 b_{k,v}}{\kappa - i(ck+\Delta)}|V\rangle\langle g|\Big] + H.C. \quad \text{(B.2)}$$

Here $\delta_{h,v}$ represents the detuning of the photon pulse from one of the atomic transitions, g is the coupling constant to the atom, $|H\rangle$ is the excited state arising from interacting with the horizontally polarized light, $|V\rangle$ is the the excited state from the vertically polarized light, and $|g\rangle$ is the ground state. The general solution to this equation is rather complicated, as various combinations of $a_{k,i}$ and $b_{k,i}$ lead to many terms corresponding to all the possible scattering channels. In addition, the two standing wave mode operators defined by $\frac{1}{\sqrt{2}}(\tau_1 a_{k,i} \pm \tau_2 b_{k,i})$ are not orthogonal, but rather commute with $\frac{\tau_1^2-\tau_2^2}{2}\delta(k-k')$. In order to make the problem more tractable, we further assume that the mirrors are identical ($\tau_1 = \tau_2 = \tau$). This allows us to write the Hamiltonian in terms of standing wave operators $\hat{c}_{k,i} = \frac{1}{\sqrt{2}}(a_{k,i} + b_{k,i})$.

Lastly, the general wavefunction for the system as a function of time is

$$|\psi(t)\rangle = \sum_{k_1} f_{k_1,h}(t)\hat{c}^\dagger_{k_1,v}|0\rangle|H\rangle + \sum_{k_2} f_{k_2,v}(t)\hat{c}^\dagger_{k_2,h}|0\rangle|V\rangle + \sum_{k_1,k_2} f_{k_1,k_2,g}(t)\hat{c}^\dagger_{k_1,h}\hat{c}^\dagger_{k_2,v}|0\rangle|g\rangle \quad \text{(B.3)}$$

B.3 General two photon solution

Unlike in previous chapters, before solving the Schrödinger equation we will assume that the initial state only contains two photons, one in each of the standing wave polarizations $\hat{c}_{k,h}$ and $\hat{c}_{k,v}$. We make this assumption because, using the beamsplitter arrangement of Fig. 1.1, the two photons will leave the same port they enter the beamsplitter with unit probability. Thus they can be routed in different directions after the scattering event. As we are considering the system's ability to function as a quantum logic

gate, it is very useful to study a configuration that preserves photon number. Moreover, as the $\hat{d}$ standing wave modes do not interact with the atom-cavity system (since they do not appear in Eq. B.2 when $\tau_1 = \tau_2$), a solution of the $\hat{c}$ modes will ultimately allow one to find the solution for travelling wave photons in a similar manner as described in Section 3.3.

Solving the Schrödinger equation with such an input state gives the following series of differential equations for the photon coefficients.

$$\sum_{k_1} \dot{f}_{k_1,h}(t)\hat{c}^\dagger_{k_1,v}|0\rangle = -2ig\tau\cos(k_0 z)\sqrt{\frac{\kappa c}{L}}\sum_k \frac{\hat{c}_{k,h}}{\kappa - i(ck+\Delta_h)}e^{-i(ck+\delta_h)t}\sum_{k_1,k_2} f_{k_1,k_2,g}(t)\hat{c}^\dagger_{k_1,v}\hat{c}^\dagger_{k_2,h}|0\rangle \tag{B.4a}$$

$$\sum_{k_2} \dot{f}_{k_2,v}(t)\hat{c}^\dagger_{k_2,h}|0\rangle = -2ig\tau\cos(k_0 z)\sqrt{\frac{\kappa c}{L}}\sum_k \frac{\hat{c}_{k,v}}{\kappa - i(ck+\Delta_v)}e^{-i(ck+\delta_v)t}\sum_{k_1,k_2} f_{k_1,k_2,g}(t)\hat{c}^\dagger_{k_1,v}\hat{c}^\dagger_{k_2,h}|0\rangle \tag{B.4b}$$

$$\begin{aligned}\sum_{k_1,k_2} \dot{f}_{k_1,k_2,g}(t)\hat{c}^\dagger_{k_1,v}\hat{c}^\dagger_{k_2,h}|0\rangle = -2ig\tau\cos(k_0 z)\sqrt{\frac{\kappa c}{L}}\sum_k \Bigg[&\frac{\hat{c}^\dagger_{k,h}}{\kappa + i(ck+\Delta_h)}e^{i(ck+\delta_h)t}\sum_{k_1} f_{k_1,h}(t)\hat{c}^\dagger_{k_1,v}|0\rangle \\ &+\frac{\hat{c}^\dagger_{k,v}}{\kappa + i(ck+\Delta_v)}e^{i(ck+\delta_v)t}\sum_{k_2} f_{k_2,v}(t)\hat{c}^\dagger_{k_2,h}|0\rangle\Bigg]\end{aligned} \tag{B.4c}$$

In order to describe photons leaving the cavity into free space (or a continuum of guided modes), we assume that the quantization length L is infinite. This transforms the sums over k to integrals in ω by the transformation $\sum_k \to \frac{L}{2\pi c}\int d\omega$. Each of the coefficients in front of $\tau_1 a_{k,h} + \tau_2 b_{k,h}$ in Eq. B.2 will go as $f_k \to f_\omega\sqrt{2\pi c/L}$. The net effect of this transformation is to remove the dependence on L in the equations and leave behind

a factor of 2π. The transformed versions of the differential equations are

$$\int d\omega_1 \dot{f}_h(\omega_1,t)\hat{c}^\dagger_{\omega_1,v}|0\rangle = -2ig\tau\cos(k_0 z)\sqrt{\frac{\kappa}{2\pi}}\int d\omega \frac{\hat{c}_{\omega,h}}{\kappa - i(\omega+\Delta_h)}e^{-i(\omega+\delta_h)t} \int d\omega_1 d\omega_2 f_g(\omega_1,\omega_2,t)\hat{c}^\dagger_{\omega_1,v}\hat{c}^\dagger_{\omega_2,h}|0\rangle \tag{B.5a}$$

$$\int d\omega_2 \dot{f}_v(\omega_2,t)\hat{c}^\dagger_{\omega_2,h}|0\rangle = -2ig\tau\cos(k_0 z)\sqrt{\frac{\kappa}{2\pi}}\int d\omega \frac{\hat{c}_{\omega,v}}{\kappa - i(\omega+\Delta_v)}e^{-i(\omega+\delta_v)t} \int d\omega_1 d\omega_2 f_g(\omega_1,\omega_2,t)\hat{c}^\dagger_{\omega_1,v}\hat{c}^\dagger_{\omega_2,h}|0\rangle \tag{B.5b}$$

$$\begin{aligned}\int d\omega_1 d\omega_2 \dot{f}_g(\omega_1,\omega_2,t)\hat{c}^\dagger_{\omega_1,v}\hat{c}^\dagger_{\omega_2,h}|0\rangle &= -2ig\tau\cos(k_0 z)\sqrt{\frac{\kappa}{2\pi}} \\ &\int d\omega \left[\frac{\hat{c}^\dagger_{\omega,h}}{\kappa + i(\omega+\Delta_h)}e^{i(\omega+\delta_h)t}\int d\omega_1 f_h(\omega_1,t)\hat{c}^\dagger_{\omega_1,v}|0\rangle \right. \\ &\left. + \frac{\hat{c}^\dagger_{\omega,v}}{\kappa + i(\omega+\Delta_v)}e^{i(\omega+\delta_v)t}\int d\omega_2 f_v(\omega_2,t)\hat{c}^\dagger_{\omega_2,h}|0\rangle\right]\end{aligned} \tag{B.5c}$$

The $\hat{c}$ operators commute between the horizontal and vertical polarizations, and have commutation relations $[\hat{c}_{\omega_i,h/v}, \hat{c}^\dagger_{\omega_j,h/v}] = \delta(\omega_i - \omega_j)$. Normal ordering the equations and matching coefficients for each $\hat{c}_{\omega,h/v}$ operator give the main differential equations for the same spectral components of the wavefunction as described in Section 3.4 for a single atom.

$$\dot{f}_h(\omega_1,t) = -2ig\tau\cos(k_0 z)\sqrt{\frac{\kappa}{2\pi}}\int d\omega \frac{e^{-i(\omega+\delta_h)t}}{\kappa - i(\omega+\Delta_h)}f_g(\omega_1,\omega,t) \tag{B.6a}$$

$$\dot{f}_v(\omega_2,t) = -2ig\tau\cos(k_0 z)\sqrt{\frac{\kappa}{2\pi}}\int d\omega \frac{e^{-i(\omega+\delta_v)t}}{\kappa - i(\omega+\Delta_v)}f_g(\omega,\omega_2,t) \tag{B.6b}$$

$$\dot{f}_g(\omega_1,\omega_2,t) = -2ig\tau\cos(k_0 z)\sqrt{\frac{\kappa}{2\pi}}\left[\frac{e^{i(\omega_2+\delta_h)t}}{\kappa + i(\omega_2+\Delta_h)}f_h(\omega_1,t) + \frac{e^{i(\omega_1+\delta_v)t}}{\kappa + i(\omega_1+\Delta_v)}f_v(\omega_2,t)\right] \tag{B.6c}$$

In order to obtain a solution for the long time limit of $f_g(\omega_1,\omega_2,\infty)$, we choose to use the Laplace transform to remove the derivative. The Laplace transform is also advantageous because the scattering limit ($t\to\infty$) is equivalent to the limit $s\to 0$. The useful relations for the Laplace transform we will use are

$$\begin{aligned}\mathcal{L}[\dot{f}(t)] &= sF(s) - f(0) & \lim_{t\to\infty} f_{gg}(\omega_1,t) &= \lim_{s\to 0} sF(\omega_1,s) \\ \mathcal{L}[\int_0^t dt' f(t')] &= \frac{F(s)}{s} & \mathcal{L}[e^{at}f(t)] &= F(s-a)\end{aligned} \tag{B.7}$$

These transformations are defined for the traditional Laplace transform

($\mathcal{L} = \int_0^\infty dt e^{-st}$) and the bilateral Laplace transform ($\mathcal{L} = \int_{-\infty}^\infty dt e^{-st}$), meaning that the initial state can either be defined with $t_0 = 0$ or $t_0 = -\infty$, though, as will be shown, an initial state of $t_0 = 0$ is necessary to obtain an analytic solution.

After applying the Laplace transform to Eqs. B.6a-B.6c, we get, with $\gamma \equiv 2g\tau \cos(k_0 z)\sqrt{\frac{\kappa}{2\pi}}$,

$$sF_h(\omega_1, s) = f_h(\omega_1, t_0) - i\gamma \int d\omega \frac{F_g(\omega_1, \omega, s + i(\omega + \delta_h)}{\kappa - i(\omega + \Delta_h)} \tag{B.8a}$$

$$sF_v(\omega_2, s) = f_v(\omega_2, t_0) - i\gamma \int d\omega \frac{F_g(\omega, \omega_2, s + i(\omega + \delta_v)}{\kappa - i(\omega + \Delta_v)} \tag{B.8b}$$

$$sF_g(\omega_1, \omega_2, s) = f_g(\omega_1, \omega_2, t_0) - i\gamma \left[\frac{F_h(\omega_1, s - i(\omega_2 + \delta_h)}{\kappa + i(\omega_2 + \Delta_h)} + \frac{F_v(\omega_2, s - i(\omega_1 + \delta_v))}{\kappa + i(\omega_1 + \Delta_v)} \right] \tag{B.8c}$$

Provided that the atom is initially in the ground state $f_h(\omega_1, t_0) = f_v(\omega_2, t_0) = 0$. From here, we may either substitute the excited states into the ground state, or substitute the ground state into the excited states. The advantage of substituting the excited states into the ground state is that the system of equations reduces to one integral equation of F_g. The advantage of substituting the ground state into the excited state is that when solving for the ground state, terms such as $\alpha + i(\omega + \beta)$ will appear more quickly in the $s \to \infty$ limit. Both cases lead to the same integral equation, however, and as such we choose to substitute into the ground state as it is perhaps a more natural path to obtaining a solution.

We also introduce the further assumptions that the detunings between the cavity and atomic transitions are equal ($\Delta_h = \Delta_v = \Delta$), that the photons are detuned symmetrically ($\delta_h = \delta_v = \delta$), and that the initial photon pulse contains two identically shaped, uncorrelated photons so that $f_g(\omega_1, \omega_2, t_0) = f_g(\omega_2, \omega_1, t_0) = f(\omega_1)f(\omega_2)$. This is not a necessary assumption to solve the problem but it will simplify the solution from a series of two coupled equations to a single integral equation, as the entire system is symmetric. Additionally, we are ultimately looking to quantify how much the system distorts just such an input state. With these assumptions, the excited state functions are substituted into

the ground state, leading to

$$sF_g(\omega_1,\omega_2,s) = f_g(\omega_1,\omega_2,t_0) - \gamma^2 \int \frac{d\omega}{\big(\kappa - i(\omega+\Delta)\big)} \Bigg[\frac{F_g(\omega_1,\omega,s+i(\omega-\omega_2)}{\big(s-i(\omega_2+\delta)\big)\big(\kappa+i(\omega_2+\Delta)\big)} + \frac{F_g(\omega,\omega_2,s+i(\omega-\omega_1)}{\big(s-i(\omega_1+\delta)\big)\big(\kappa+i(\omega_1+\Delta)\big)} \Bigg] \tag{B.9}$$

To ensure that the variables in F_g are consistent, it is convenient to make the transformation of $\omega_1 \to \omega_a$ and $\omega_2 \to \omega_b$, along with the transformation $s \to s + i(\omega_a + \omega_b - \omega_1 - \omega_2)$. This relegates ω_1 and ω_2 to being dummy variables that do not contribute to the integral and preserves the form of the terms in the s component of F_g. The new equation is then

$$\begin{aligned} \big(s+i(\omega_a+\omega_b-\omega_1-\omega_2)\big)F_g\big(\omega_a,\omega_b,s+i(\omega_a+\omega_b-\omega_1-\omega_b)\big) &= f_g(\omega_a,\omega_b,t_0) \\ -\gamma^2 \int \frac{d\omega}{\big(\kappa-i(\omega+\Delta)\big)} \Bigg[& \frac{F_g\big(\omega_a,\omega,s+i(\omega+\omega_a-\omega_1-\omega_2)\big)}{\big(s+i(\omega_a-\omega_1-\omega_2-\delta)\big)\big(\kappa+i(\omega_b+\Delta)\big)} \\ & + \frac{F_g\big(\omega,\omega_b,s+i(\omega+\omega_b-\omega_1-\omega_2)\big)}{\big(s-i(\omega_b-\omega_1-\omega_2-\delta)\big)\big(\kappa+i(\omega_a+\Delta)\big)} \Bigg] \end{aligned} \tag{B.10}$$

It is clear that the function $F_g\big(\omega_a,\omega_b,s+i(\omega_a+\omega_b-\omega_1-\omega_b)\big)$ appears on both sides of the equation with one of its indices integrated. From here, to simplify the expression, we define several functions

$$d_0(\omega',\omega'') = \frac{1}{s+i(\omega'+\omega''-\omega_1-\omega_2)} \tag{B.11a}$$

$$d_\delta(\omega') = \frac{-\gamma^2}{s+i(\omega'-\omega_1-\omega_2-\delta)} \tag{B.11b}$$

$$K(\omega') = \frac{1}{\kappa - i(\omega'+\Delta)} \tag{B.11c}$$

$$\alpha(\omega') = \int d\omega K(\omega) F_g\big(\omega',\omega,s+i(\omega+\omega'-\omega_1-\omega_2)\big) \tag{B.11d}$$

and write the integral as

$$F_g\big(\omega_a, \omega_b, s + i(\omega_a + \omega_b - \omega_1 - \omega_b)\big) =$$

$$d_0(\omega_a, \omega_b) f_g(\omega_a, \omega_b, t_0) + d_0(\omega_a, \omega_b) d_\delta(\omega_a) K^*(\omega_b) \alpha(\omega_a) + d_0(\omega_a, \omega_b) d_\delta(\omega_b) K^*(\omega_a) \alpha(\omega_b) \tag{B.12}$$

By substituting Eq. B.12 into Eq. B.11d one obtains an integral expression for α of the form

$$\begin{aligned} \alpha(\omega_a) = &\int d\omega K(\omega) d_0(\omega_a, \omega) f_g(\omega_a, \omega, t_0) \\ &+ \alpha(\omega_a) d_\delta(\omega_a) \int d\omega K(\omega) K^*(\omega) d_0(\omega_a, \omega) + K^*(\omega_a) \int d\omega K(\omega) d_0(\omega_a, \omega) d_\delta(\omega) \alpha(\omega) \end{aligned} \tag{B.13}$$

The term $K(\omega)K^*(\omega)$ will effectively act as a delta function for $\omega \to -\Delta - i\kappa$ when being integrated along with functions that contain poles in only the upper half plane. This is due to the residue theorem, as $\oint f(\xi) d\xi = 2\pi i \sum_k Res(f, z_k)$ and the residue of a simple pole is given by $\lim_{z \to z_k}(z - z_k) f(z)$ for a curve that has a winding number of -1 (counterclockwise). If integrating over a curve in the lower half plane, one must take care to flip the limits of integration of the real component so that it corresponds to the desired part. Terms that go as $\beta - i\omega$ (with $Re[\beta] > 0$) will have a pole in the lower half plane, whereas terms that go as $\beta + i\omega$ will have poles in the upper half plane. This reduces the third term to

$$\alpha(\omega_a) d_\delta(\omega_a) \int d\omega K(\omega) K^*(\omega) d_0(\omega_a, \omega) = \frac{\pi}{\kappa} \alpha(\omega_a) d_\delta(\omega_a) d_0(\omega_a, -\Delta - i\kappa) \tag{B.14}$$

Moving this term to the left side and solving for $\alpha(\omega_a)$ again gives

$$\alpha(\omega_a) = H(\omega_a) F_0(\omega_a) + H(\omega_a) K^*(\omega_a) \int d\omega K(\omega) d_0(\omega_a, \omega) d_\delta(\omega) \alpha(\omega) \tag{B.15}$$

where we define

$$H(\omega_a) = \frac{\kappa\big(s + i(\omega_a - \omega_1 - \omega_2 - \delta)\big)\big(s + \kappa + i(\omega_a - \omega_1 - \omega_2 - \Delta)\big)}{\pi\gamma^2 + \kappa\big(s + i(\omega_a - \omega_1 - \omega_2 - \delta)\big)\big(s + \kappa + i(\omega_a - \omega_1 - \omega_2 - \Delta)} \tag{B.16a}$$

$$F_0(\omega_a) = \int d\omega K(\omega) d_0(\omega_a, \omega) f_g(\omega_a, \omega, t_0) \tag{B.16b}$$

The presence of the ω_a index in the kernel of the integral on the left side of Eq. B.15 significantly complicates the solution. A closed form can be obtained, however, by multiplying both sides by $K(\omega_a)d_0(\omega', \omega_a)d_\delta(\omega_a)$ and integrating over ω_a. This will lead to an integral of $\int d\omega_a K(\omega_a)K^*(\omega_a)H(\omega_a)d_0(\omega', \omega_a)d_\delta(\omega_a)$. Again, the $K(\omega_a)K^*(\omega_a)$ term will act as a delta function, provided that none of the other functions involved in the integral have poles in the lower half plane. This is obviously true for d_δ and d_0, but demonstrating it analytically for $H(\omega)$ is very challenging due to the presence of a square root term with complex components. It is, however, very easy to check numerically: running over one million random combinations of the parameters in question (with $s = 0$ in anticipation of the final solution), there were no poles found in the lower half plane or on the real axis. It would appear, then, that this function also has only poles in the upper half plane. In the case where $\delta = \Delta = 0$ this condition is trivially satisfied.

Now, evaluating the integral so that $\omega_a \to -\Delta - i\kappa$, we get

$$\int d\omega_a K(\omega_a) d_0(\omega', \omega_a) d_\delta(\omega_a)\alpha(\omega_a) = \int d\omega_a K(\omega_a) d_0(\omega', \omega_a) d_\delta(\omega_a) H(\omega_a) F_0(\omega_a)$$
$$+\frac{\pi}{\kappa} d_0(\omega', -\Delta - i\kappa) H(-\Delta - i\kappa) d_\delta(-\Delta - i\kappa) \int d\omega K(\omega) d_0(-\Delta - i\kappa, \omega) d_\delta(\omega)\alpha(\omega) \tag{B.17}$$

As ω' is unbound, we can set it to equal $-\Delta - i\kappa$. In this way it is possible to obtain a closed form for $\int d\omega K(\omega) d_0(-\Delta - i\kappa, \omega) d_\delta(\omega)\alpha(\omega)$. Solving such an expression gives

$$\int d\omega K(\omega) d_0(-\Delta - i\kappa, \omega) d_\delta(\omega)\alpha(\omega) =$$
$$\Big[1 - \frac{\pi}{\kappa} d_0(-\Delta - i\kappa, -\Delta - i\kappa) H(-\Delta - i\kappa) d_\delta(-\Delta - i\kappa)\Big]^{-1}$$
$$\times \int d\omega_a K(\omega_a) d_0(-\Delta - i\kappa, \omega_a) d_\delta(\omega_a) H(\omega_a) F_0(\omega_a) \tag{B.18}$$

This can then be substituted into B.17 which in turn can be substituted back into B.15

to arrive at the form of α.

$$\alpha(\omega_a) = H(\omega_a)F_0(\omega_a) + H(\omega_a)K^*(\omega_a)\int d\omega K(\omega)d_0(\omega_a,\omega)d_\delta(\omega)H(\omega)F_0(\omega)$$
$$+\frac{\pi\chi}{\kappa}H(\omega_a)K^*(\omega_a)d_0(\omega_a,-\Delta-i\kappa)H(-\Delta-i\kappa)d_\delta(-\Delta-i\kappa)\int d\omega K(\omega)d_0(-\Delta-i\kappa,\omega)d_\delta(\omega)H(\omega)F_0(\omega) \tag{B.19}$$

With

$$\chi = \left[1-\frac{\pi}{\kappa}d_0(-\Delta-i\kappa,-\Delta-i\kappa)H(-\Delta-i\kappa)d_\delta(-\Delta-i\kappa)\right]^{-1} \tag{B.20}$$

While complicated, α is completely written in terms of the initial ground state and a number of integral functions.

To more explicitly evaluate the integrals in the scattering limit we let $s \to 0$. In order to do this, we make two assumptions regarding the initial state following the procedure in [68]. First, that $f_g(\omega_1,\omega_2,0)$ is analytic everywhere in the upper half of the complex plane, which is true of most probability distributions. Second, that the pulse vanishes for times $t<0$. This is mathematically impossible to achieve for any smooth pulse (though it is certainly possible for a square pulse). Physically, however, the long tails of pulses such as a Gaussian do not contribute significantly to the overall interaction and they can be safely ignored. Recall that we have also assumed that the initial photon state is separable. As long as the pulse is peaked sufficiently far to the right of $t=0$ (for example 3 standard deviations) we can safely define the initial state for a single photon as

$$f_0(\omega) = f_g(\omega,0) = \int_0^\infty e^{i\omega t}\tilde{f}_g(t-\mu,0) \tag{B.21}$$

where μ is the time offset and $\mu >> \sigma$ for the pulse. When cast in this form it is clear that any complex $\omega = R(\cos\phi + i\sin\phi)$ will vanish for $\phi \in [0,\pi]$ as $R\to\infty$, as the real component of the exponential will go as $e^{-R\sin\phi}$, ensuring that the function $f_0(\omega)$ will vanish exponentially fast in the upper half plane (as $\sin(\phi)\in[0,1]$ for $\phi\in[0,\pi]$).

With this in hand, an integral of the form found in F_0 becomes

$$\begin{aligned} F_0(\omega_a) &= f_0(\omega_a)\int d\omega \frac{f_0(\omega)}{\big(\kappa - i(\omega+\Delta)\big)\big(s + i(\omega+\omega_a-\omega_1-\omega-2)\big)} \\ &= \frac{2\pi f_0(\omega_a) f_0(\omega_1+\omega_2-\omega_a+is)}{\kappa - i(\omega_1+\omega_2-\omega_a+\Delta+is)} \end{aligned} \tag{B.22}$$

by use of the residue theorem. The term $\big(\kappa - i(\omega+\Delta)\big)^{-1}$ will have a pole in the lower half plane and the term $\big(s + i(\omega+\omega_a-\omega_1-\omega-2)\big)^{-1}$ a pole in the upper. Again, the above solution is valid provided that f_0 is analytic everywhere in the upper half plane (has no poles).

Unfortunately, it is not possible to solve the two photon interaction term exactly via the previous method due to the presence of a $-\omega$ in the numerator. This term, after simplifying, is given as

$$\begin{aligned} &\int d\omega K(\omega) d_0(\omega_a,\omega) d_\delta(\omega) H(\omega) F_0(\omega) = \\ &-2\gamma^2\kappa\pi \int d\omega \frac{f_0(\omega_1+\omega_2-\omega+is) f_0(\omega)}{(\omega+\omega_a-\omega_1-\omega_2-is)(\omega+\Delta+i\kappa)\big(\pi\gamma^2+\kappa(s-i(\delta+\omega_1+\omega_2-\omega))(s+\kappa-i(\omega_1+\omega_2-\omega+\Delta))\big)} \end{aligned} \tag{B.23}$$

Defining $x = \eta - \omega$ with $\eta = \frac{\omega_1+\omega_2}{2}$ and $\lambda_\pm$ as the roots of $\pi\gamma^2 + \kappa(s - i(\delta+\omega_1+\omega_2-\omega))(s+\kappa-i(\omega_1+\omega_2-\omega+\Delta))$, so that this term can be expressed as $-\kappa(\omega - 2\eta - \lambda_-)(\omega - 2\eta - \lambda_+)$, we can use a partial fraction decomposition to rewrite the integral as a sum of four integrals given by $2\pi\gamma^2(I_1(\omega_a) + I_2(\omega_a) + I_3(\omega_a) + I_4(\omega_a))$. Each of the $I_j(\omega_a)$ functions are given as

$$I_1(\omega_a) = \int_{-\infty}^{\infty} dx \frac{f_0(\eta-x) f_0(\eta+x+is)}{(x-\Delta-\eta+i\kappa)(\Delta+2\eta+\lambda_-+i\kappa)(\Delta+2\eta+\lambda_++i\kappa)(\Delta+2\eta+i\kappa-\omega_a+is)} \tag{B.24a}$$

$$I_2(\omega_a) = -\int_{-\infty}^{\infty} dx \frac{f_0(\eta-x) f_0(\eta+x+is)}{(x+\eta-\omega_a+is)(\Delta+2\eta+i\kappa-\omega_a+is)(-\lambda_--\omega_a+is)(-\lambda_+-\omega_a+is)} \tag{B.24b}$$

$$I_3(\omega_a) = -\int_{-\infty}^{\infty} dx \frac{f_0(\eta-x) f_0(\eta+x+is)}{(x+\eta+\lambda_-)(\Delta+2\eta+\lambda_-+i\kappa)(\lambda_--\lambda_+)(\lambda_-+\omega_a-is)} \tag{B.24c}$$

$$I_4(\omega_a) = -\int_{-\infty}^{\infty} dx \frac{f_0(\eta-x) f_0(\eta+x+is)}{(x+\eta+\lambda_+)(\Delta+2\eta+\lambda_++i\kappa)(\lambda_+-\lambda_-)(\lambda_++\omega_a-is)} \tag{B.24d}$$

In the $s \to 0$ limit I_2 will have a pole on the real axis for real ω_a. This integral can be

written in terms of a Cauchy principal value integral using the identity

$$\lim_{\epsilon\to 0}\frac{1}{x-y-i\epsilon} = PV\frac{1}{x-y} + i\pi\delta(x-y) \tag{B.25}$$

Combining all these things, letting $s \to 0$, transforming to the original variables, and simplifying everything greatly using mathematica, the total solution for the scattered state of the two photons (from Eq. B.12) can be written as follows in Eq. B.27. In writing this, we also introduced the effective coupling to the atom Γ, defined by $\gamma^2 = \Gamma\kappa/\pi$, so that $\Gamma = 2\tau^2\cos^2(k_0 z)g^2$. This is to more clearly show the effect of κ independent of the coupling strength of the atom. The presence of τ in the coupling constant is still related to the transmission coefficients of the mirrors.

$$\tilde{h}(\omega) = \Gamma - i(\delta+\omega)\big(\kappa - i(\omega+\Delta)\big) \tag{B.26a}$$

$$\tilde{h}_2(\omega_1,\omega_2) = \tilde{h}(\omega_1) + \tilde{h}(\omega_2) + 2\big(\kappa - i(\omega_1+\Delta)\big)\big(\kappa - i(\omega_2+\Delta)\big) \tag{B.26b}$$

$$\begin{aligned} f_g(\omega_1,\omega_2,\infty) = {} & \left[f_0(\omega_1) - 2\Gamma\kappa\frac{f_0(\omega_1)}{(\kappa+i(\omega_1+\Delta))\tilde{h}(\omega_1)}\right]\left[f_0(\omega_2) - 2\Gamma\kappa\frac{f_0(\omega_2)}{(\kappa+i(\omega_2+\Delta))\tilde{h}(\omega_2)}\right] \\ & + \frac{2\Gamma^3\kappa^2\left[\tilde{h}(\omega_1)+\tilde{h}(\omega_2)\right]\left[\kappa - i(\omega_1+\Delta) + \kappa - i(\omega_2+\Delta)\right]}{\pi\big(\kappa+i(\omega_1+\Delta)\big)\big(\kappa+i(\omega_2+\Delta)\big)\tilde{h}(\omega_1)\tilde{h}(\omega_2)\tilde{h}_2(\omega_1,\omega_2)}\Big[I_1(-\Delta-i\kappa) + I_2(-\Delta-i\kappa) + I_3(-\Delta-i\kappa) + I_4(-\Delta-i\kappa)\Big] \\ & - \frac{2\Gamma^2\kappa^2}{\pi\big(\kappa+i(\omega_1+\Delta)\big)\big(\kappa+i(\omega_2+\Delta)\big)\tilde{h}(\omega_1)\tilde{h}(\omega_2)}\Big[\tilde{h}(\omega_1)\big(\kappa - i(\omega_2+\Delta)\big)\Big(I_1(\omega_1) + PV\big[I_2(\omega_1)\big] + I_3(\omega_1) + I_4(\omega_1)\Big) \\ & + \tilde{h}(\omega_2)\big(\kappa - i(\omega_1+\Delta)\big)\Big(I_1(\omega_2) + PV\big[I_2(\omega_2)\big] + I_3(\omega_2) + I_4(\omega_2)\Big)\Big] \end{aligned} \tag{B.27}$$

After all the transformations, $\lambda_\pm$ found in the integrals becomes

$$\lambda_\pm = \frac{1}{2}\Big[\delta + \Delta + i\kappa \pm \sqrt{4\Gamma + (\Delta - \delta + i\kappa)^2}\Big] \tag{B.28}$$

Finally, there is one remaining element to this solution. As given, Eq. B.27 describes the pulse in terms of the modes inside the cavity. Translating to the modes outside the cavity requires multiplying the solution by $\frac{\left(\kappa+i(\omega_1+\Delta)\right)\left(\kappa+i(\omega_1+\Delta)\right)}{\left(\kappa-i(\omega_1+\Delta)\right)\left(\kappa-i(\omega_1+\Delta)\right)}$, as given in Eq. 36 and 45 in Ref. [67]. For clarity of notation we will write the integral sums as $I_{Total}(\omega_a) = I_1(\omega_a) + I_2(\omega_a) + I_3(\omega_a) + I_4(\omega_a)$ and $PV[I_{Total}(\omega_a)] = I_1(\omega_a) + PV\big[I_2(\omega_a)\big] + I_3(\omega_a) + I_4(\omega_a)$. Any value of ω_a in I_{Total} will be a

function of ω_1 and ω_2. Adding this term and simplifying we arrive at the following concise expression (with $\tilde{k}(\omega) = \kappa - i(\omega + \Delta)$):

$$f_g(\omega_1, \omega_2, \infty) = f_0(\omega_1)\frac{h^*(\omega_1)}{h(\omega_1)} f_0(\omega_2)\frac{h^*(\omega_2)}{h(\omega_2)} - \frac{2\Gamma^2\kappa^2}{\pi}\left[\frac{PV[I_{Total}(\omega_1)]}{\tilde{h}(\omega_2)\tilde{k}(\omega_1)} + \frac{PV[I_{Total}(\omega_2)]}{\tilde{h}(\omega_1)\tilde{k}(\omega_2)}\right]$$
$$+\frac{2\Gamma^3\kappa^2}{\pi\big(\tilde{h}(\omega_1) + \tilde{h}(\omega_2) + 2\tilde{k}(\omega_1)\tilde{k}(\omega_2)\big)}\Big[\frac{1}{\tilde{h}(\omega_1)} + \frac{1}{\tilde{h}(\omega_2)}\Big]\Big[\frac{1}{\tilde{k}(\omega_1)} + \frac{1}{\tilde{k}(\omega_2)}\Big] I_{Total}(-\Delta - i\kappa) \tag{B.29}$$

From here, solutions can be obtained for specific pulse shapes by evaluating the various components of I_{Total} with $s \to 0$. This has a similar form to Eq. 3.56 in that it consists of a separable component and a (rather complicated) spectral entanglement term that is a function of $\omega_1 + \omega_2$.

B.3.1 General single photon solution

Before describing the solution of the final state for different initial wavepackets, it is useful to determine the single photon solution for comparison with previous works and to explain the structure of Eq. B.29. Due to the nature of the level structure considered here, it is impossible for a photon to swap polarizations by interacting with the atom-cavity system. As such, the system reduces to a single two level atom for each of the polarizations. Starting from Eqs. B.5a-B.5c we note that a single photon will have the same differential equations, with the exception of there being only one frequency argument in the ground state and no frequency arguments in the excited state. Taking into account that only one of the polarization states will contribute we can write

$$\dot{f}_{h,v}(t) = -i\gamma \int d\omega \frac{f_g(\omega, t)e^{-i(\omega+\delta)t}}{\kappa - i(\omega + \Delta)} \tag{B.30a}$$

$$\dot{f}_g(\omega, t) = -i\gamma \frac{f_{h,v}(t)e^{i(\omega+\delta)t}}{\kappa + i(\omega + \Delta)} \tag{B.30b}$$

Performing the Laplace transform as before yields

$$sF_{h,v}(t) = -i\gamma \int d\omega \frac{F_g\big(\omega, s + i(\omega + \delta)\big)}{\kappa - i(\omega + \Delta)} \tag{B.31a}$$

$$sF_g(\omega, s) = f_g(\omega, t_0) - i\gamma \frac{F_{h,v}\big(s - i(\omega + \delta)\big)}{\kappa + i(\omega + \Delta)} \tag{B.31b}$$

Substituting the excited state into the ground state yields an integral equation of

$$sF_g(\omega, s) = f_g(\omega, t_0) - \gamma^2 \frac{\int d\omega' \frac{F_g\left(\omega', s + i\omega'\right)}{\kappa - i(\omega' + \Delta)}}{\big(\kappa + i(\omega + \Delta)\big)\big(s - i(\omega + \delta)\big)} \tag{B.32}$$

Using the transformation of $\omega \to \omega_a$ and $s \to s + i(\omega_a - \omega)$ gives a closed form for F_g.

$$F_g\big(\omega_a, s + i(\omega_a - \omega)\big) = \frac{f_g(\omega_a, t_0)}{s + i(\omega_a - \omega)} - \gamma^2 \frac{\int d\omega' \frac{F_g\left(\omega', s + i(\omega' - \omega)\right)}{\kappa - i(\omega' + \Delta)}}{\big(\kappa + i(\omega_a + \Delta)\big)\big(s - i(\omega + \delta)\big)\big(s + i(\omega_a - \omega)\big)} \tag{B.33}$$

As can be seen, this is now an integral equation for $F_g\big(\omega_a, s + i(\omega_a - \omega)\big)$. From here we define $\beta = \int d\omega' \frac{F_g\left(\omega', s + i(\omega' - \omega)\right)}{\kappa - i(\omega' + \Delta)}$. This is constant in ω_a and thus a direct solution of the integral equation is readily achievable. We can write

$$\begin{aligned} \beta = \int d\omega' \frac{f_g(\omega', t_0)}{\big(\kappa - i(\omega' + \Delta)\big)\big(s + i(\omega' - \omega)\big)} \\ -\gamma^2 \int d\omega' \frac{\beta}{\big(\kappa + i(\omega' + \Delta)\big)\big(\kappa - i(\omega' + \Delta)\big)\big(s - i(\omega + \delta)\big)\big(s + i(\omega' - \omega)\big)} \end{aligned} \tag{B.34}$$

Defining $F_0(\omega) = \int d\omega' \frac{f_g(\omega', t_0)}{\big(\kappa - i(\omega' + \Delta)\big)\big(s + i(\omega' - \omega)\big)}$ the solution for β is

$$\beta = \frac{\kappa\big(s - i(\omega + \delta)\big)\big(s + \kappa - i(\omega + \Delta)\big)F_0(\omega)}{\pi\gamma^2 + \kappa\big(s - i(\omega + \delta)\big)\big(s + \kappa - i(\omega + \Delta)\big)} \tag{B.35}$$

Transforming back to the original variables, the overall solution for the single photon's scattered state is

$$sF_g(\omega, s) = f_g(\omega, t_0) - \gamma^2\kappa \frac{\big(s + \kappa - i(\omega + \Delta)\big)F_0(\omega)}{\big(\kappa + i(\omega + \Delta)\big)\big(\pi\gamma^2 + \kappa\big(s - i(\omega + \delta)\big)\big(s + \kappa - i(\omega + \Delta)\big)\big)} \tag{B.36}$$

By noting that this has effectively the same form as the term $d_\delta(\omega_a)K^*(\omega_b)H(\omega_a)F_0(\omega_a)$

found in the two photon solution we can see that this will take the form of

$$f_g(\omega,\infty) = -f_0(\omega)\frac{\tilde{h}^*(\omega)}{\tilde{h}(\omega)} = -\frac{\Gamma + i(\omega+\delta)\big(\kappa + i(\omega+\Delta)\big)}{\Gamma - i(\omega+\delta)\big(\kappa - i(\omega+\Delta)\big)} \tag{B.37}$$

after making the same transformations back to the original variables, to Γ, and to the field modes outside of the cavity. This solution is identical in form to Eq. 46 in [67] which also describes the interaction between a single photon pulse and an atom in a cavity.

B.3.2 Resonances and limiting cases

The fact that the first term in Eq. B.29 represents two, independent single photon interactions suggests that the roots of the function $\tilde{h}(\omega)$ may provide insight into the system's behavior and possible limits of interest. This function describes each photon's interaction with a combined atom-cavity system. As given in Eq. B.26a, $\tilde{h}(\omega)$ has roots

$$\lambda_\pm = \frac{1}{2}\Big[\delta + \Delta + i\kappa \pm \sqrt{4\Gamma + (\Delta - \delta + i\kappa)^2}\Big] \tag{B.38}$$

The real and imaginary components of these roots are rather complicated, but they amount to two couplings and detunings just as was found for the real and imaginary eigenvalues of Eq. 2.18. The imaginary component will correspond to the strength of the interaction and the real component will correspond to the detuning of the interaction. This can be seen from comparing $(\omega - Re[\lambda_\pm] - iIm[\lambda_\pm]) = -i\big(Im[\lambda_\pm] + i(\omega - Re[\lambda_\pm])\big)$ to the form for a single photon interaction in Eq. 2.27.

In the case where $\delta = \Delta = 0$ (the atom and cavity are at the same resonance and the pulse is tuned to this resonance) this reduces to

$$\lambda_\pm = -\frac{i\kappa}{2} \pm \sqrt{\Gamma - \frac{\kappa^2}{4}} \tag{B.39}$$

If $\Gamma > \kappa^2/4$, the square root will be real and the system will effectively consist of two interactions with strength $\kappa/2$ and detunings $\pm\sqrt{\Gamma - \frac{\kappa^2}{4}}$. If $\Gamma < \kappa^2/4$ the term will become imaginary and it will lead to two on-resonance interactions with different coupling strengths. Here κ governs the strength of the overall interaction and Γ the amount the

photons interact with each resonance. This can be seen in in Fig. B.2 where we plot how the coupling and detuning change with both κ and Γ.

Another interesting case occurs when $\delta = \Delta$, i.e. the photons are detuned from the atom by the same amount they are detuned from the cavity. Then the two roots in Eq. B.38 reduce to

$$\lambda_{\pm} = -\frac{i\kappa}{2} + \delta \pm \sqrt{\Gamma - \frac{\kappa^2}{4}} \tag{B.40}$$

If the system is further tuned so that $\delta = \sqrt{\Gamma - \frac{\kappa^2}{4}}$, the two roots have the same coupling strength of $\frac{\kappa}{2}$ but one root will be detuned off resonance (provided that $\Gamma - \frac{\kappa^2}{4} > 0$ so that δ is real). This can also be seen in Fig. B.2. Both behaviors lead to two limiting cases when the atom-cavity system reduces to a single two level system, the 'bad cavity' and 'good cavity' limits.

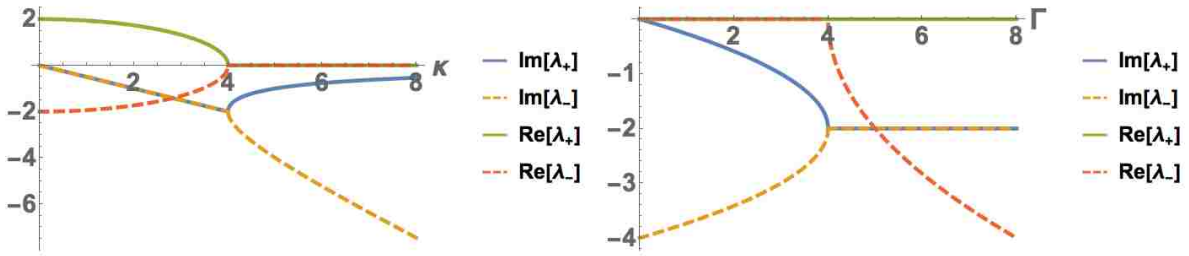

(a) (b)

Figure B.2: a)The real and imaginary components of the coupling of the two atom-cavity resonances as a function of κ with $\Gamma = 4$ and $\delta = \Delta = 0$. This corresponds to the 'bad cavity limit' where one of the two couplings (imaginary component) becomes so large its corresponding process occurs too quickly to contribute to the scattering process. b) The same components of $\lambda_{\pm}$ as a) when $\delta = \Delta = \sqrt{\Gamma - \kappa^2/4}$. This corresponds to the 'good cavity limit' when one of the two resonances becomes too far detuned (real component) to contribute.

Bad cavity limit

The first limit occurs when the photons are on resonance and $\kappa >> \Gamma$ and $\kappa >> 1/\sigma_t$ (with σ_t representing the temporal width of the pulse) while the ratio Γ/κ remains on the order of $1/\sigma_t$. This limit corresponds to an incredibly leaky cavity and thus is the 'bad cavity' limit, as when $\kappa \to \infty$ the cavity should vanish, leaving only the bare atom.

Provided that $\kappa >> \Gamma$ and $\kappa >> 1/\sigma_t$, we can write the square root in Eq. B.38 as $i\kappa\sqrt{1-4\Gamma/\kappa^2}$. The two roots are then $\lambda_1 = i\gamma'$ and $\lambda_2 = i(\kappa - \gamma') \approx i\kappa$. In the limit of large κ (or alternatively a very long pulse) the interaction time of this first resonance will be so short it will not affect the shape of the photons. Mathematically, the bad cavity limit consists of the case where $\kappa \to \infty$ while Γ/κ remains finite. Defining $\gamma' = \Gamma/\kappa$ the single photon term becomes

$$f_g(\omega, \infty) = -f_0(\omega)\frac{\gamma' + i\omega}{\gamma' - i\omega} \tag{B.41}$$

This has the same form as the single photon scattering off of a unidirectional waveguide and also agrees with Eq. 48 in [67].

The two photon state similarly reproduces the solution for an atom in a waveguide. The term appearing in Eq. B.29 given by $+\frac{2\Gamma^3\kappa^2}{\pi\left(\tilde{h}(\omega_1)+\tilde{h}(\omega_2)+2\tilde{k}(\omega_1)\tilde{k}(\omega_2)\right)}\left[\frac{1}{\tilde{h}(\omega_1)}+\frac{1}{\tilde{h}(\omega_2)}\right]\left[\frac{1}{\tilde{k}(\omega_1)}+\frac{1}{\tilde{k}(\omega_2)}\right]I_{Total}(-\Delta - i\kappa)$ will vanish. This can be easily seen by the fact that the term goes as $\Gamma'^3 O(\kappa) I_{Total}(-\Delta - i\kappa)$. Expressing I_{Total} in its original form we have

$$I_{Total} = \lim_{s\to 0} -\kappa \frac{f_0(\omega_1+\omega_2-\omega+is)f_0(\omega)}{(\omega+\omega_a-\omega_1-\omega_2-is)(\omega+\Delta+i\kappa)\big(\pi\gamma^2+\kappa(s-i(\delta+\omega_1+\omega_2-\omega))(s+\kappa-i(\omega_1+\omega_2-\omega+\Delta))\big)} \tag{B.42}$$

From this it is clear that I_{Total} goes as $O(\kappa^{-2})$. When $\omega_a = -\Delta - i\kappa$ this will add another order of κ to the denominator. As the entire term goes as $O(\kappa^{-1})$, when $\kappa \to \infty$ this will certainly vanish. This has been confirmed by formally taking the limit as well.

The other two photon term will be preserved. This can again be seen by considering the

orders of κ present in the calculation. The factors $\frac{\Gamma^2\kappa^2}{\tilde{h}(\omega_i)\tilde{\kappa}(\omega_j)}$ go as $\Gamma'^2 O(\kappa^2)$. For $\omega_a = \omega_{1,2}$ I_{Total} will go as $O(\kappa^{-2})$ and the overall order is $O(\kappa^0)$. In order to solve this, we apply the given limit to each of the integral terms present in $PV[I_{Total}(\omega)]$ and simplify. The only surviving terms come from the integral of I_2 and I_3. The solution from I_2 is

$$PV\int dx \frac{2i\gamma^2 f_0(\eta+x)f_0(\eta-x)}{\pi(\gamma'-i\omega_1)(\gamma'-i\omega_2)}\Big(\frac{1}{x+\eta-\omega_1}+\frac{1}{x+\eta-\omega_2}\Big) \tag{B.43}$$

The first integral term will vanish, however, because $\eta = (\omega_1+\omega_2)/2$. Rewriting the terms with x we get $f_0(\eta-x)f_0(\eta+x)\Big(\frac{1}{x+(\omega_1+\omega_2)/2}-\frac{1}{-x+(\omega_1+\omega_2)/2}\Big)$. The integral is symmetric over a transformation of $x \to -x$, and making this transformation will lead to these terms canceling out. The solution from I_3 is then

$$-\int d\omega \frac{4i\gamma'^2 f_0(\eta+x)f_0(\eta-x)}{\pi(\gamma'-i\omega_1)(x+\eta+i\gamma')(\gamma'-i\omega_2)} \tag{B.44}$$

It is not immediately obvious that this represents the same integral as found in Eq. 3.56, but it can be shown to be equivalent. Writing Eq. 3.56 in terms of x and η we have

$$-\frac{2\gamma'^2}{\pi}\Big(\frac{1}{\gamma'-i\omega_1}+\frac{1}{\gamma'-i\omega_2}\Big)\int dx\Big(\frac{if_0(\eta-x)f_0(\eta+x)}{2(\gamma'-i\eta)(i\gamma'+x+\eta)}+\frac{if_0(\eta-x)f_0(\eta+x)}{2(\gamma'-i\eta)(i\gamma'+\eta-x)}\Big) \tag{B.45}$$

Again the integrals are identical with respect to the transformation $x \to -x$. Making this transformation to the second term and finding a common denominator gives the exact same result as the cavity solution presented above.

Good cavity limit

The other limit of interest is the 'good cavity' limit. When $\delta = \sqrt{\Gamma - \frac{\kappa^2}{4}}$, the two roots become $\lambda_+ = -\frac{i\kappa}{2} + 2\delta$ and $\lambda_- = -i\kappa/2$. With $\Gamma >> \kappa^2$ and $\Gamma >> 1/T$ the interaction corresponding to λ_+ will not affect the photons as it will be too far detuned. When this happens, the entire system also behaves as a single two level atom.

Formally this limit consists of setting $\delta = \Delta = \sqrt{\Gamma - \kappa^2/4}$ and $\Gamma \to \infty$. Then the single

photon term transforms to

$$f_g(\omega, \infty) = -f_0(\omega)\frac{\kappa' + i\omega}{\kappa' - i\omega} \tag{B.46}$$

with $\kappa' = \kappa/2$. Taking the same limit for the two photon state we arrive at the exact same integral solutions as given in the bad cavity limit, except with γ' substituted with κ'.

B.4 Phase gate operation

B.4.1 Maximum phase and fidelity

As in Chapter 6 we are primarily concerned with evaluating whether two counter-propagating photons will be able to transmit through this system and interact in such a way that they acquire a nontrivial phase of π between them. In order to evaluate this, we will again measure fidelity as in Eq. 6.10, where the fidelity of the two photon scattering event is compared to two, independent single photon scattering events. We will plot the fidelity for an initial two photon state where the photons either have a Lorentzian (Eq. 6.22) or a Gaussian (Eq. 6.20) distribution and are initially uncorrelated.

We will also use the definition of average gate fidelity given in the supplementary material of [30] for comparison with their results. The average gate fidelity in some respects gives a better picture of the operation of the gate, although it does tend to artificially increase the numerical value of the fidelity because, as described in Chapter 6, it includes operations that will always succeed (such as $|0\rangle \otimes |0\rangle \rightarrow |0\rangle \otimes |0\rangle$). This measure of fidelity quantifies, on average, how likely it is that a particular gate will succeed.

When both photons are guaranteed to be found in a particular spatial mode (like in this case here where the photons are initially in standing wave modes) the average fidelity for a gate to impart a phase of θ is given by

$$F(\theta) = \frac{1}{10}\big(6 + 3Re[e^{i\theta}\sqrt{\mathcal{F}}e^{i\phi}] + |\sqrt{\mathcal{F}}e^{i\phi}|^2\big) \tag{B.47}$$

where $\sqrt{\mathcal{F}}$ and ϕ are the fidelity and phase given by Eq. 6.10. Note that an average fidelity

of .4 corresponds to a pulse that remains unchanged with no phase shift ($\mathcal{F} = 1$) and an average fidelity of .6 corresponds to no overlap whatsoever. The useful regime is anything above .6, which corresponds to a state with a nonzero fidelity for the two photon operation and some amount of useful phase for computation.

In Figs. B.3 and B.4 we plot the fidelity (Eq. 6.10) and average gate fidelity (Eq. B.47) for random values of the pulse width, γ, Γ, κ, Δ, and δ. We chose to plot random values rather than scan over parameters because the parameter space is large. Plotting the phase and fidelity in this way provides insight into what is possible with the gate.

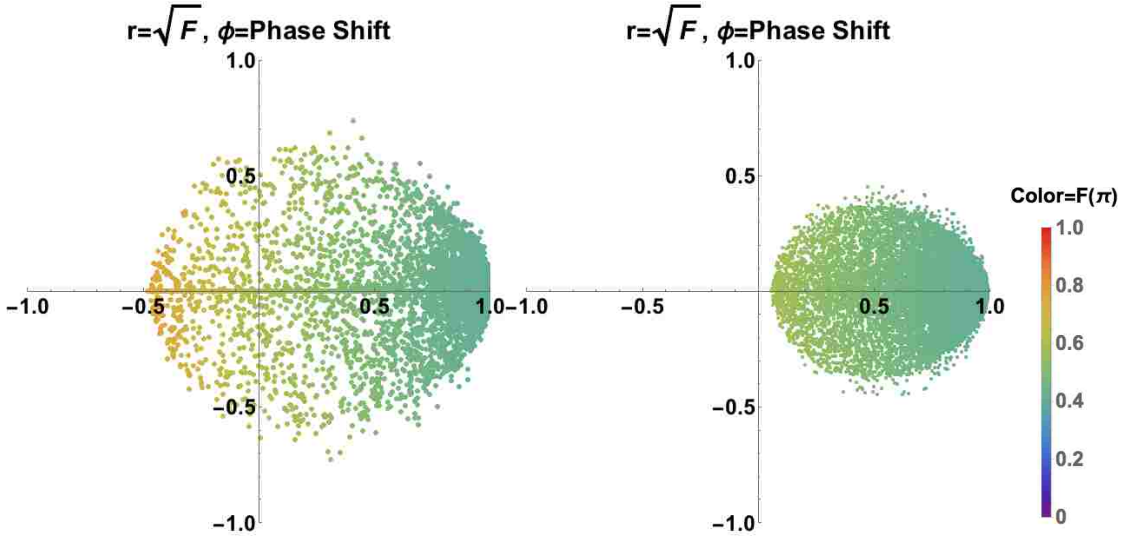

(a) (b)

Figure B.3: The fidelity and phase of the two photon scattered state compared to two single photon interactions. In both plots, the distance from the origin represents the fidelity, the phase is given by the polar angle, color represents the corresponding average gate fidelity, and random values have been chosen for all physical parameters. a) represents a state where the photons are initially Gaussian and b) represents a state where the photons are initially Lorentzian.

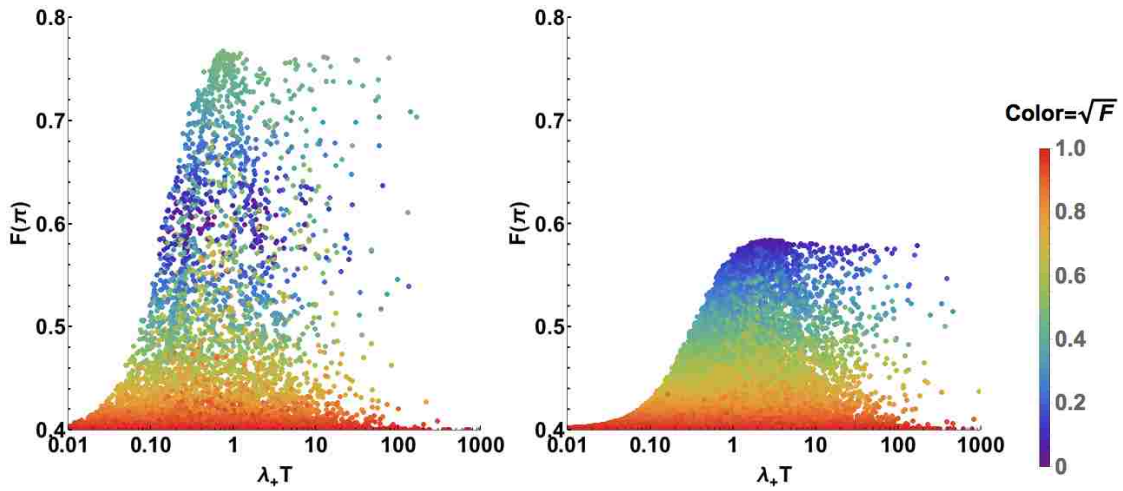

(a) (b)

Figure B.4: The average gate fidelity of the two photon scattered state compared to two single photon interactions. In both plots color represents the fidelity ($\sqrt{\mathcal{F}}$) of the two photon operation, and random values have been chosen for all physical parameters. a) represents a state where the photons are initially Gaussian and b) represents a state where the photons are initially Lorentzian.

As can be seen in these plots, if the photons initially have a Gaussian profile the atom-cavity system (and thus also a single two level atom) is able to impart some useful phase with a nonzero fidelity. It is possible to achieve an average gate fidelity of around .785, which very closely matches the maximum obtained by [30] of .781 for a single interaction site. If the photons initially have a Lorentzian profile, however, the single-pass fidelity and phase is effectively zero. It is possible for two photons to interact and maintain high fidelity (Fig. B.3 b) but no useful phase shift is produced. It is actually impossible in a single pass for these photons to pick up a phase of π; in Fig. B.3 b no combination of parameters provides a phase of π and in Fig. B.4 b the average fidelity never rises above .6.

It is also curious that the envelope of the average fidelity plot is effectively the same between the Gaussian and Lorentzian distributions but with a different peak and width. This suggests that there may be some sort of scaling law at work between different initial pulse shapes. Additionally, the fact that this behaves better for a Gaussian implies that it may be possible to use pulse shaping techniques to create an initial state that would

further maximize fidelity.

With the exception of a very particular pulse, then, it would seem that it is impossible to build a phase gate with just one two or three-level system, unless one is willing to accept significant errors in the computation. As this three-level system encompasses a single two level system, the results presented here also show that a single site is unable to function well as a CPHASE gate. This agrees with the data shown in Fig. 6.3, and the calculated fidelities are on the order of that presented in the analysis of [29] for a single two level system's ability to function as a CPHASE gate.

B.5 Conclusions

In this appendix we demonstrated how to find the scattered state of two counter-propagating photons scattering from a single three-level system in a cavity. In doing so, we provided an illustration of a different means of solving for the scattered state, working entirely in the frequency domain and using complex integration with the Laplace transform to arrive at a solution. We explored different limits of the system and were able to show that in two particular cases it approximates a single, two level system. We also demonstrated that the final solution in Eq. B.29 has a similar form to Eq. 3.56 where the final scattered wavefunction of two photons is a sum of an entangling process and two, independent interactions with the system. Finally, we explored the system's ability to function as a quantum CPHASE gate. We found that it performs essentially the same as a single two level system (though it is slightly better) and is on its own unable to impart a phase of π with high fidelity. We also demonstrated that the shape of the pulse considered can have a dramatic affect on the functioning of a phase gate, a point that has not been adequately addressed in the literature on the subject.